DOCTOR OF PHILOSOPHY

Biaxial Cyclic Plastic Bending

Toor, Amrit Pal Singh

Award date:
1986

Awarding institution:
Lanchester Polytechnic
Coventry University

BIAXIAL CYCLIC PLASTIC BENDING

A Thesis Submitted to the Council for National Academic Awards in Partial Fulfilment for the Degree of Doctor of Philosophy

by

AMRIT PAL SINGH TOOR BSc

Department of Combined Engineering

Coventry (Lanchester) Polytechnic

APRIL 1986

ABSTRACT

BI-AXIAL CYCLIC PLASTIC BENDING

A P TOOR

The problem of bi-axial bending and cyclic bi-axial bending has been examined analytically and experimentally. The specific problem of a cantilever subjected to cycles of horizontal deflection with a sustained vertical load was investigated for circular and square cross-section beams. The stress-strain curves representing initial and cyclic material properties were modelled mathematically and incorporated in a "finite element" analysis computer program. A research rig was developed together with a data acquisition system which enabled the loads and deflection to be monitored throughout the cyclic process.

The validity of simplifying assumptions such as using the simplified curvature equations and ignoring any rotation of the neutral surface was evaluated together with the movement of the neutral surface for non-circular sections in bi-axial plastic bending.

The changing material properties resulting from the cyclic process was modelled and the computer program was able to follow the loading history of each elemental fibre in the beam, update the material properties within each cycle and from cycle to cycle. A comparison of experimental results and theoretical predictions showed that accurate modelling of the material properties was necessary for good results in the first quarter cycle when the plastic strains are small. It was easier to model cyclic material behaviour due to the absence of elastic behaviour on stress reversal, and the theoretical predictions of deflections and loads in the steady state cyclic condition were good. The computer program identified elements which unloaded during bending due to rotation of the neutral surface. It was shown that their effect was small for the range of strains examined but if the strain range was increased the unloading process should be included in any analysis. The method of analysis adopted also allowed the strain distribution throughout the beam to be evaluated at all stages of loading.

ACKNOWLEDGEMENTS

THe author wishes to express his gratitude to Dr S J Harvey and Dr P J Hancell of the Department of Combined Engineering, Coventry (Lanchester) Polytechnic for their helpful discussions and advice during the course of this work.

Thanks are also due to:-

The Technical Staff of the Department of Combined Engineering, Coventry (Lanchester) Polytechnic for their assistance in rig design and construction.

Mrs J Collingwood for her sterling efforts in typing this thesis.

CONTENTS

CHAPTER 1

INTRODUCTION

CHAPTER ONE

1.0 INTRODUCTION

1.1 GENERAL

A traditional engineering approach to many problems in design has been to design for infinite life and the procedure involved in engineering analysis has often been based on elastic theory and empirical data. Inevitably this approach extracts a penalty, especially in weight, when only finite fatigue life is required.

With the rapidly changing technology a considerable amount of engineering components become obsolete long before their possible working life, eg components of space vehicles. In such cases, especially where weight is critical, as is the case in space vehicles, it is necessary to relax the infinite life concept. These demands have encouraged engineers to devote more attention to the finite life approach.

In certain cases where the nominal stress remains elastic, the concept of how fatigue damage accumulates has led to theories which enable prediction of failure under random loads, such theories are now widely used in aircraft design. On the other hand where stress and strain are in the plastic range, attention has been directed towards what is called 'high strain' or 'low cycle' fatigue and theories have been developed which purport to predict fatigue life as a function of strain range.

Another aspect associated with inelastic stress and strain is the problem of large and permanent deflections or strains, especially where tolerance of components is critical. In addition, many large components are subjected to loads, which results in the co-existence of elastic and plastic regions side by side. This gives rise to large stress and strain gradients and possibly local concentration of strain. Analytically these problems are very difficult to deal with.

Examples of strain concentration and high strain fatigue can be found in many prime movers. Consider, for example, steam turbines. Steam turbines can be subjected to two common types of start-up and shut-down cycles.

a) Weekly cycle, in which the turbine starts up at the beginning of the week, runs for about 120 hours and is then shut down over the weekend.

b) Daily cycle, in which the turbine starts up each morning runs for about 16 hours and is shut down.

Design procedures have been established for 'high strain' fatigue operation and many are detailed in ASME codes. Essentially the main problem is to identify the areas of strain concentration and predict the inelastic strain occurring within each cycle of plastic strain. A knowledge of these strains, together with materials data in the form of Manson-Coffin plots and an appropriate cumulative damage law enables a life prediction estimate to be made.

However, this process poses formidable problems. Predicting the plastic strains requires an appropriate yield criterion, a flow rule, and a hardening law. Generally the material properties change within a cycle of plastic strain and from cycle to cycle. Cyclic material data is usually obtained from push-pull tests. Many materials are shown to cyclically harden or soften to a stable state, (Fig 1.1a) and Fig 1.1b), and Manson-Coffin plots can be obtained from the cycles to failure data. Although widely used, the push-pull tests are of limited value. Firstly, the strain range is restricted by buckling problems in the compressive cycle and secondly the uni-axial stress condition is not often encountered in practice, where initial cracks usually have to propagate through a stress gradient. To overcome some of these problems high-strain bending tests are carried out. Much higher cyclic strain can be obtained and the cycles to crack initiation can be directly compared to push-pull data on the assumption that elemental fibres in the beam undergo cycles of push-pull strain. However the cycles to complete failure are much greater in bending due to the time required to propagate the crack through the depth of the beam.

A problem closely associated with high strain fatigue is that of incremental collapse or cyclic strain induced creep. If a component undergoes cycles of plastic strain and at the same time is subjected to a sustained "follow-up" load in a conjugate direction, then an irrecoverable plastic strain increment will occur in the direction of the follow up load.

The effect is cumulative and can lead to failure of the component by gross deformation before fatigue failure. There are many examples of this deformation mechanism, also known as ratchetting, eg a pressure vessel subjected to cycles of push-pull with a steady internal pressure and a cantilever subjected to cycles of horizontal deflections whilst supporting a steady vertical load.

Most of the research investigations related to the prediction of plastic strains and the development of appropriate yield criteria and flow rule have concentrated on plane stress conditions, ie thin walled tubes subjected to different combinations of torsion, push-pull and internal pressure. However, even for these simple loading conditions it has not yet been possible to develop a unified plasticity approach which can adequately predict the plastic strains and the mode of deformation within the cycle of plastic strain. Very little attention has been given to the more complex problems where strain gradients exist and elastic-plastic zones are present. Since it is the strain gradient problem which is more likely to arise in practice it is felt that it is worthy of investigation, whilst at the same time acknowledging that many simplifying assumptions may have to be made to make the problem tractable. Many of the practically important problems arise due to bending, ie discontinuity stresses at junctions in pressure vessels and in structural applications. However, in order to test any theoretical approach against experimental results it was decided that the problem of a cantilever subjected to cyclic horizontal deflection with a sustained steady vertical load should be investigated.

This appears at first sight to be a simple problem, but the complications soon become apparent when attempting to predict the downward, cumulative deflection at the end of the cantilever. These are:-

a) The strain gradient through the depth of the beam and along the beam.

b) The loading configuration constitutes one of bi-axial bending and there is little published literature on this problem in the plastic range.

c) The problem is made more difficult because it is not radial or proportional loading and the neutral surface is continually changing.

d) The material properties are cyclic dependent and the strain hardening characteristics will vary throughout the depth and length of the beam.

1.2 GENERAL APPROACH TO THE PROBLEM

The problem lends itself to a form of finite element analysis. If we assume that plane sections remain plane during elastic and plastic bending, then the beam can be considered as being made up of elemental fibres undergoing push-pull cycles.

If the cyclic material behaviour can be modelled mathematically then an attempt can be made to predict the cyclic load deflection characteristics of the cantilever in unidirectional cyclic bending, ie, without a sustained follow up load. The analysis could then be extended to include the additional load, which then results in a bi-axial bending condition. The subsequent rotating neutral surface creates a particular problem of changing geometrical properties, Fig (1.2) and in order to over come this the analytical and experimental work will concentrate on beams of circular cross-section and square sections. The action of the rotating neutral surface creates further problems in that individual elemental fibres will "unload" during the general loading process (Fig 1.3) ie some elements will unload from tension and go into compression, or vice versa, with consequent changes in material properties such as Bauschinger effects. This phenomena has not previously been examined and one of the objectives of this research will be to determine if this effect is important or not in determining the cantilever deflections. This will be done by comparing results obtained by ignoring the effect of elements unloading with those obtained when taking the unloading process into account.

Although yield surfaces have not received much consideration with regards to bending they have proved useful in other loading conditions. Their use for this particular problem will be examined and evaluated.

In order to test the validity of the theoretical approach a comprehensive test program is planned. A cantilever bi-axial bending test rig will be designed and developed, which will enable cantilever force - deflection characteristics to be obtained together with incremental collapse deflections throughout the cyclic process, and particularly the mode of deformation within any cycle.

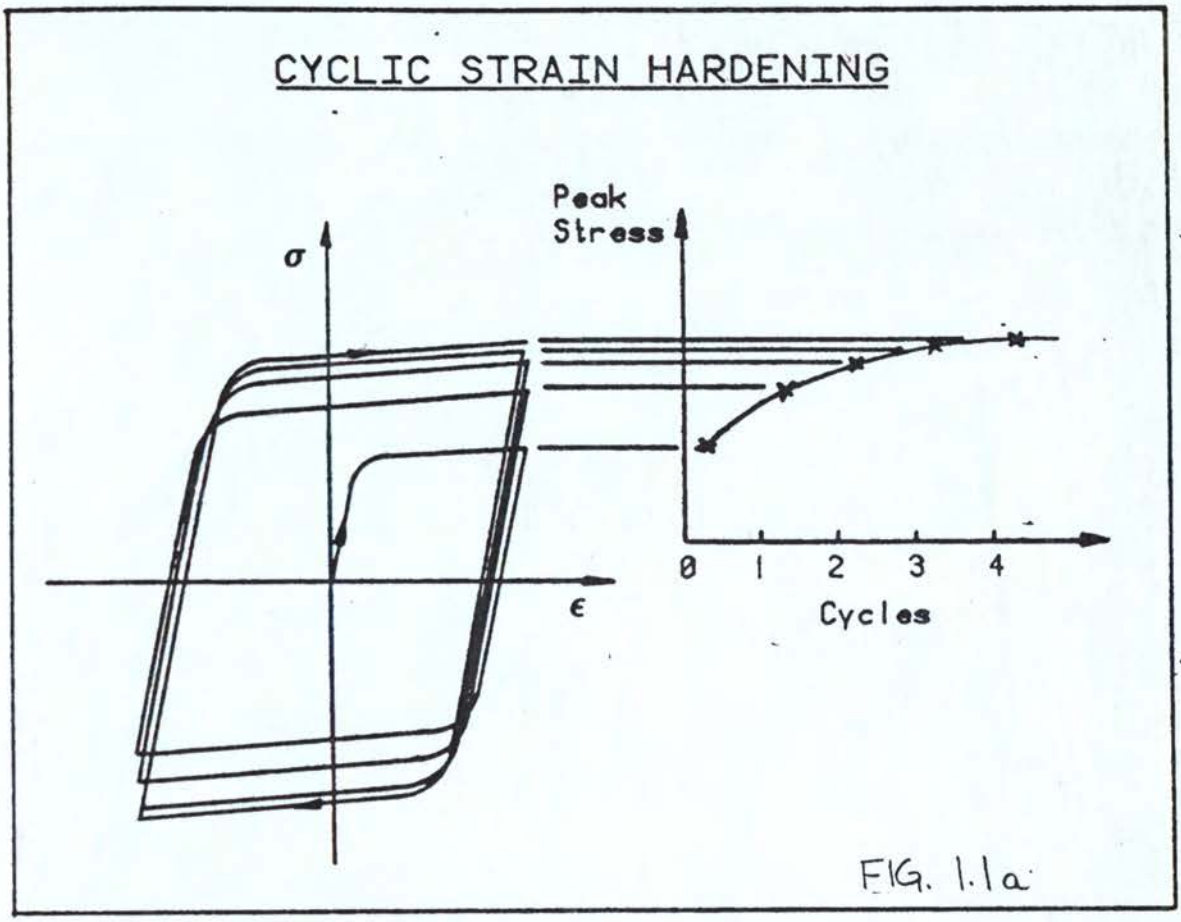

FIG. 1.1a

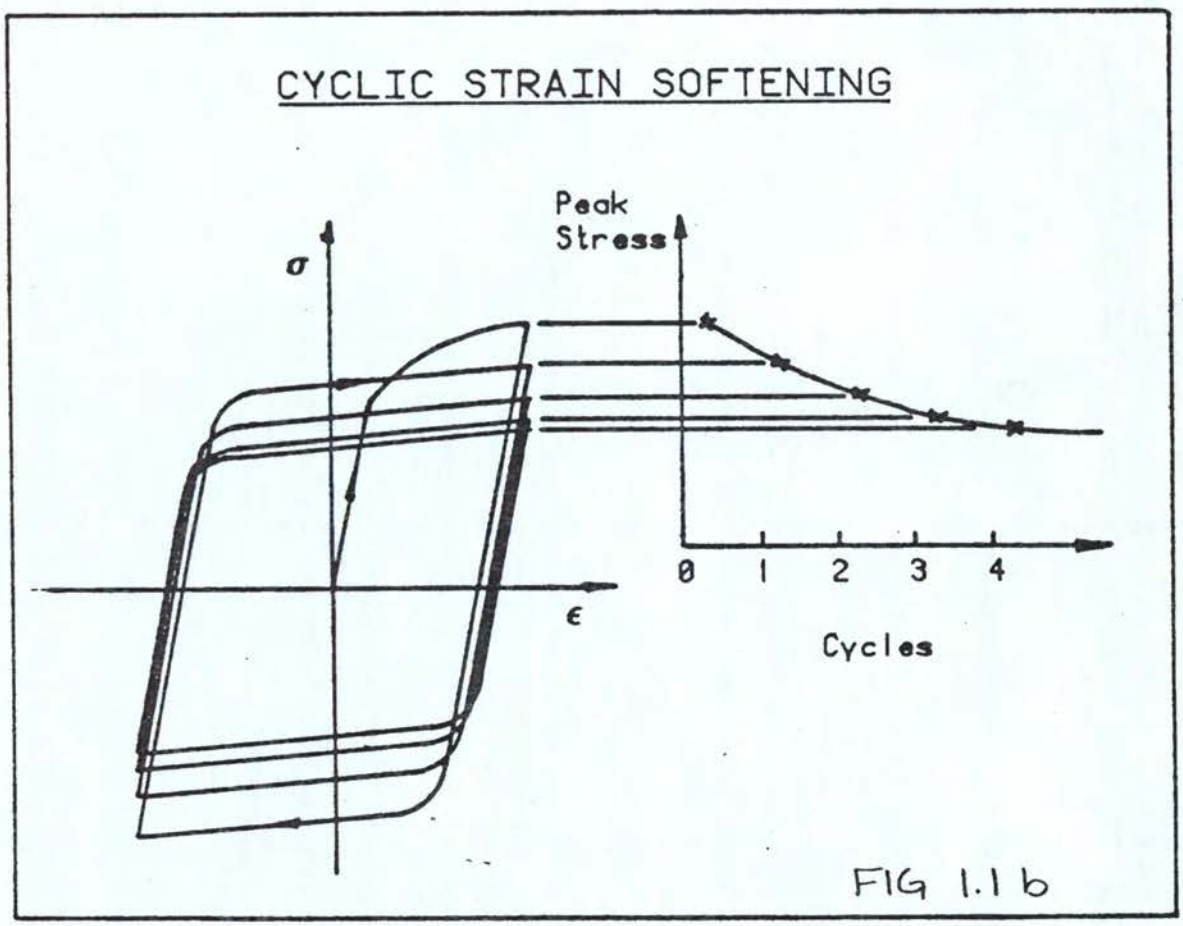

FIG 1.1 b

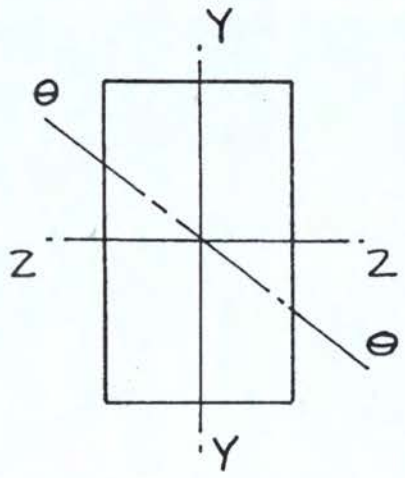

$I_{\theta\theta} \neq I_{zz} \neq I_{yy}$

FIG. 1.2

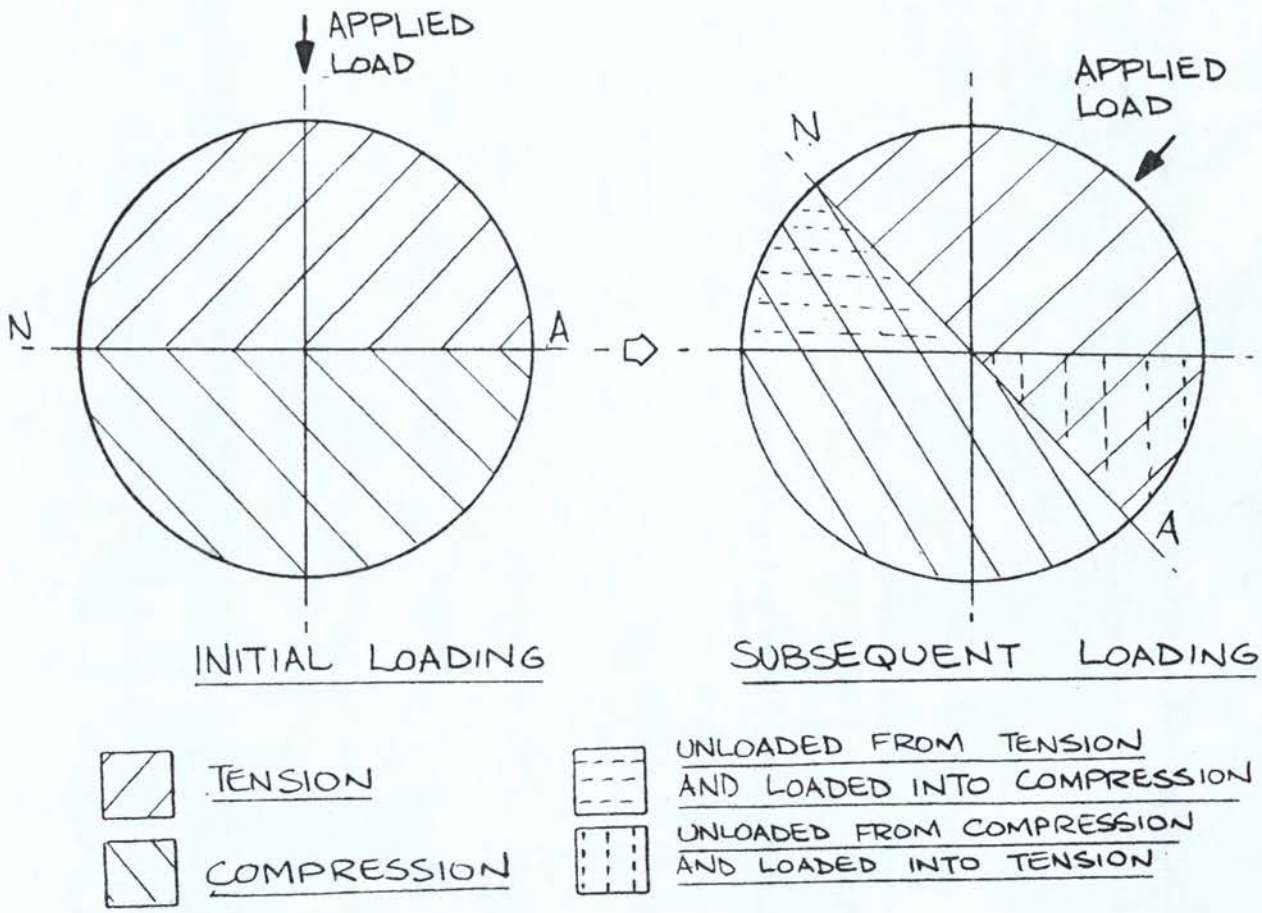

FIG. 1.3

CHAPTER 2

LITERATURE REVIEW

CHAPTER TWO

2.0 LITERATURE REVIEW

2.1 INTRODUCTION

The 1950's and 1960's saw a tremendous development in the plasticity research generally and there are several books (1) (5) (8) (16) and reviews (10) (11) which cover the many aspects of plasticity. The problem of plastic bending received wide attention, particularly with regard to limit analysis in the design of structures, and slip line field methods were developed extensively and plastic hinge solutions have been proposed to a wide range of beam geometries (14) (34). Much of the research was of a fundamental nature, the determination of yield surfaces, flow rules, crystal slip, anisotropy etc and therefore not directly useful to the designer. Considerable interest was generated into cyclic plasticity in the 1960's when it was realised that many components were undergoing cycles of sometimes large plastic strains during their lifetime and this work was extensively reviewed by Manson (13) and more recently by Miller (15).

The complete solution to even simple plasticity problems is very difficult and simplifying assumptions have generally been made with regards to material properties. However, it is the material properties which are the most important parameter in the cyclic plasticity process and if a realistic solution is to be obtained then these properties must be modelled realistically.

In this investigation there are several aspects of plasticity which bear directly on the problem. These are

a) Plastic bending

b) Unsymmetrical and biaxial loading

c) Cyclic loading

d) Cyclic material properties

e) Yield surfaces.

In this review therefore it is these aspects which are examined, in order to attempt to bring them together so that the complexities of the problem can be better understood.

2.2 SIMPLE PLASTIC BENDING

The solution to the simple plastic bending problem was first proposed by Saint Venant (see references 2, 3 and 6). Saint Venant in order to facilitate a solution assumed plane sections remained plane and neglected any transverse stresses. Von-Bach in 1905, provided the argument on the validity of the Saint Venant's assumption, that plane sections remained plane, was valid for materials which do not obey Hooke's law. Meyer in 1907 provided some experimental evidence from tests above the yield point on wrought iron.

In the book by Phillips (7) there is a chapter dedicated to moment-curvature relationships above the yield point. These relationships have been found for various cross-sections. The stress-strain characteristics being represented for three idealised materials.

(i) for elastic-perfectly elastic plastic material

(ii) when $\sigma = \sigma_o \varepsilon^n$ - 2.1

(iii) when stress-strain curve is represented by a series of tangents to the real stress-strain curve.

Johnson and Mellor (8) developed an analysis similar to Phillips, for a rectangular cross sectioned beam and used the material of type (ii) above.

Work relating to the deflection of cantilevers is limited, generally simplified by considering that the deflections are small relative to the length and therefore using a simplified expression for the curvature. Using the full curvature equation is usually considered not necessary or too complicated. Certainly there are not many engineering design structures where large plastic deformation or deflections can be tolerated, but a method of solution using the full curvature equation was developed by Das (9).

2.3 UNSYMMETRICAL AND BIAXIAL PLASTIC BENDING

These two forms of bending have many similar features. The analysis of unsymmetrical sections under the action of simple bending appears to have posed some difficulties. Even the standard text on the plastic theories of bending, Prager and Hodge (12), Baker et al (51), Neal (17) and Phillips (7) do little more than mention the unsymmetrical problem. Clearly the more complex the shape of the cross-section the more difficult the problem becomes.

Heyman (18) (23) studied the problem of unequal angle section cantilever and defined the "strong" and "weak" axis of bending. It can be appreciated that the analysis of a simple rectangular beam creates problems when the line of action of the bending force is at an angle to the principal axis of the cross section. There appears to be only two papers of any significance which investigate this problem and even in these the direction of the applied moment is assumed to be fixed.

Barrett (19) considered the plastic bending of a rectangular beam subjected to a pure bending moment acting in a plane other than one of symmetry Fig (2.1). He expressed the stress-strain curve in the form

$$\varepsilon = A \frac{f}{f_2} + B \left(\frac{f}{f_2} \right)^n \qquad - 2.1$$

Where A and B are material constants
f is stress
f_2 is stress at 2% strain.

In order to avoid, he claimed, the tedious arithmetical summations which would have been necessary had he used the actual stress-strain curves. The results were presented in the terms of form factors, ie aspect ratios. These were in the form which related the inclination of the neutral surface in elastic (θ_E) and plastic (θ) bending with the line of the bending moment, fig (2.2). The analysis showed that

$$\left(\frac{M_z}{M_y} \right)_{plastic} > \left(\frac{M_z}{M_y} \right)_{elastic}$$

and therefore for a given angle of the plane of loading the neutral surface for a non elastic distribution of stress is rotated further than it would be if the stress distribution were elastic.

Although the analysis led to complex mathematical functions it was felt that the form of material data was applicable to a wide range of ductile materials. Brown (20) considered the unsymmetrical section as a general topic and established the concept of "centroidal locus", Fig (2.3). The term centroidal locus refers to the plot of a curve traced out by the centroids of the two areas of the cross-section divided equally by the neutral axis, as the neutral axis is rotated through 180°. Brown gave no specific solutions but noted that the principal axis of elastic and plastic bending need not coincide. This was shown also to be the property of a section having only one axis symmetry Fig (2.4), and that principal axes in plastic bending are not necessarily orthogonal. Brown also developed a graphical method for locating the principal zero stress axis from the centroidal locus.

Heyman (18) (23)' applied Brown's concept to establish the "strong" and "weak" axis in plastic bending, corresponding to the major and minor axis in elastic bending. It is interesting to note that the properties of convexity of the centroidal locus and the tangency of the neutral axis direction appears to have similarities to the properties of 'yield' surfaces.

Harrison (21) investigated the collapse of rectangular beam sections carrying bending moments in both principal planes, and showed that how collapse is influenced by both behaviour of the section under inclined bending and also compatibility of deformations in both principal planes.

Brooks (22) extended Barrett's work by relating the bending moments acting in the principal planes, the direction of the plane of the resultant moment, the curvature and the direction of the plane of curvature Fig (2.5). In order to simplify the problem he considered the material to be elastic - perfectly plastic.

In all the papers referred to the line of action of the bending moment remained constant. When the moments about the principal planes are varied independently then there can be large rotation of the neutral surface. This would pose no problems as long as the material remains elastic, but could create many problems if the material becomes plastic. Rotation of the neutral surface would result in some elements unloading and possibly re-loading. It would appear that this particular problem has not been researched. The difference in the two loading cases, ie moments fixed in direction and moments of varying direction would appear to have similarities with the condition of radial and non-radial loading paths in plasticity.

2.4 CYCLIC BENDING

Research in cyclic plastic bending was promoted by two major developments. Firstly the development of plastic methods of structural design with limit analysis and minimum weight design resulted in the acceptance that some elements in a structure would be subjected to plastic strains and that the loads on some structures would be cyclic, ie wind loads. As a result it was realised that structural members could fail by incremental collapse or ratchetting.

This phenomena has been observed and reported by many researchers often as the result of investigations into pressure vessel behaviour. Weil and Rapasky (24) showed that repeated thermal stresses caused progressive distortion. Coffin (25) in his work on fatigue under repeated loading of uniaxial specimens also observed incremental growth under combined steady and cyclic loads. Morton and Moffat (26) reported persistent cyclic strain increments in stainless steel pressure vessel components when repeated pressure loads exceeded the shakedown pressure. The shakedown problem has been extensively investigated and shakedown theorems developed by Neal (27) Leckie (28). It was shown that in many cases, although there might be initial plasticity , structural members would often shakedown under cyclic loads and eventually produce an elastic response. Parks (29) was probably the first to identify the various modes of deformation of components subjected to cyclic loading. Several problems of incremental collapse have been also examined by Edmunds and Beer (30) and Bree (31).

The other interest in cyclic bending arose when it was realised that to design for limited life was not necessary for many components and that many components were undergoing cyclic plastic strains in critical areas. During the start up and shut down of steam turbines plastic cyclic strains were shown to occur. However these cycles were often less than 1000 per year and therefore a 30 year life would only produce 30,000 cycles. Considerable research was undertaken to determine cyclic material properties. This work has been extensively covered by Manson et al (32) and Coffin (33).

The cyclic data was often obtained from push-pull tests, usually strain controlled. However this mode of testing was limited due to the buckling of specimens during the compression cycle even for small plastic strains. It was realised that a beam in bending could be considered as being made up of elemental fibres undergoing push-pull cycles. Therefore the fatigue life of a component in a tension-compression test would be the same as the outer fibre of a beam in cyclic bending at the same strain level. Failure in this sense refers to crack initiation in the outer fibre of the beam. It was thus possible to use the bending mode to generate quite large plastic cyclic strains. Conversely it was shown that the cyclic moment - curvature relationship could be predicted from cyclic push-pull data. Das (9) examined the problem of a strain concentration in bending by predicting the failure of a beam in 3 point bending using cyclic push-pull data. He then showed that the strains in the areas of the strain concentration could be predicted from the cyclic moment curvature relationship. Using these strains and a cumulative damage law he was able to predict the cycles to failure quite accurately. On the other hand, Royals (35) (36) carried out uniform bending fatigue tests to determine the "mid-life" moment - curvature relationship and fatigue resistance data for mild steel. On the basis of this work he proposed a design procedure which allows the deduction of strain and allowable bending for a given fatigue life. Topper (37) described a moment - curvature behaviour corresponding to different cyclic stages. Another model (38) describes the same relationship under load control, thus incorporating creep.

2.5 CYCLIC MATERIAL PROPERTIES

Cyclic material properties are usually characterised by development of cyclic stress-strain hysteresis curve, Fig (2.6), and materials are observed to cyclically harden of soften (39) (40). Annealed materials will usually show cyclic softening characteristics while work hardening materials and others, hardened by heat-treatment, will cyclically soften. The cyclic strain hardening or softening is usually rapid in the early cycles and many materials then settle down to a steady state cyclic condition. Dugdale (40) has shown the same steady state hysteresis curve is developed for a particular strain level, irrespective of prior load history.

An obvious material characteristic is the Bauschinger effect ie a reduced yield stress in compression following a tensile strain and vice versa. Some simple models have been proposed which attempt to predict the development and the shape of the hysteresis curve (41) (42). However these models are of limited use and provide little guidance to the material behaviour under more complex loading conditions. This is a general problem in the low cycle fatigue work, with material data obtained from simple uniaxial tests whilst in practice many of the engineering components are subject to changing 2D and 3D stress systems.

Sidebothom and Chan (43) investigated the influence of the Bauschinger effect on the load deformation characteristics of inelastically strained structural members.

They concluded that the load carrying capacity of beams were appreciably lower than the theoretical values derived on the assumption of no Bauschinger effect.

Clearly, if any beam can be considered to be made up of individual elemental fibres then the cyclic moment curvature response of the beam can be developed from cyclic push-pull data.

2.6 YIELD SURFACES

The concept of a plastic potential in plasticity work can be extended to many problems. Prager (44) has shown that for problems in bending

$$dk = d\lambda \frac{df}{dM}$$

where f is the yield function in terms of the bending moment. For a circular beam the yield surface with radial loading is shown in Fig (2.7)

The normality rule applies and Heyman (18) and Neal (17) have proposed yield surfaces for rectangular and circular beam sections for elastic - perfectly plastic materials. These simple models have not been further developed and there appears to be no published work relating to any experimental verification of the yield surface concept for beam problems. The simple models cited, have only considered the very simple case of radial loading, ie no rotation of the principal planes and perhaps a realistic model would be too complex to be of any value to the design engineer.

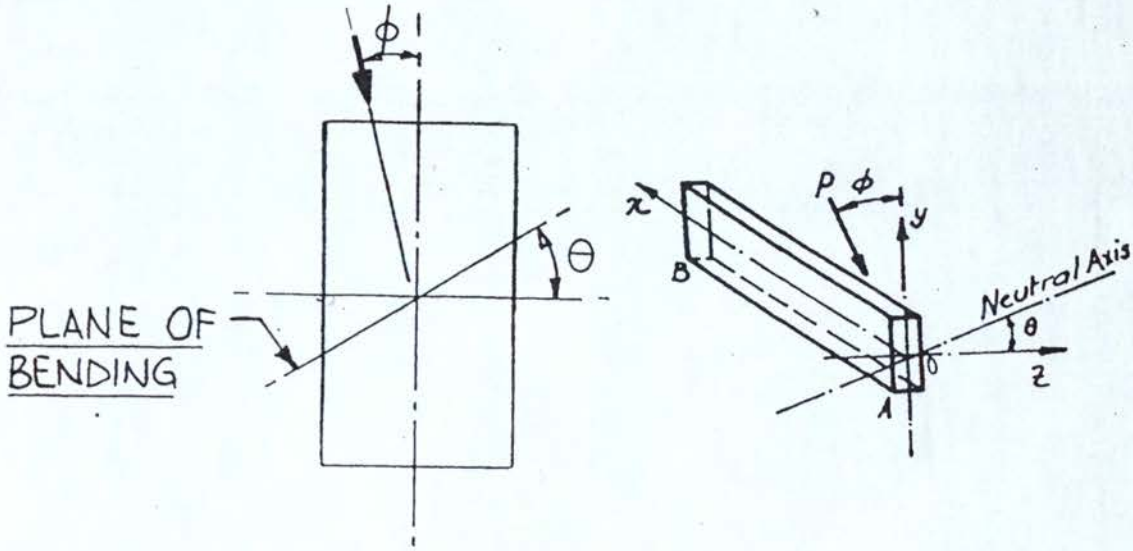

UNSYMMETRICAL BENDING

FIG 2.1

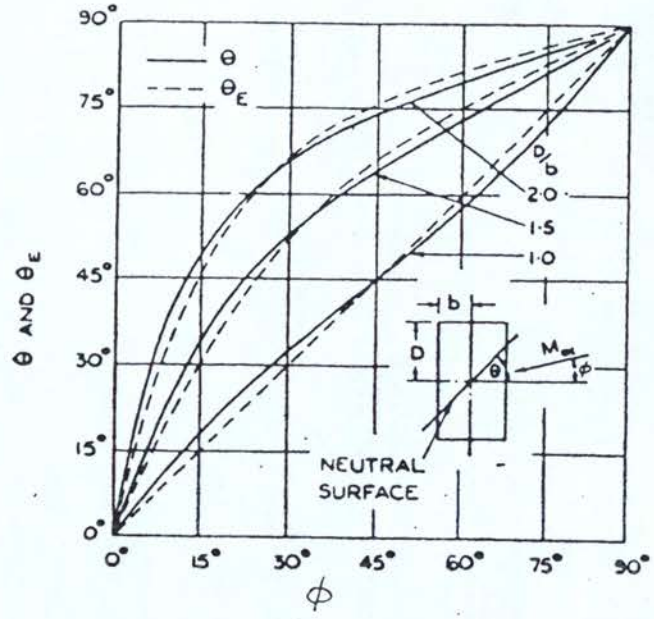

ROTATION OF PRINCIPAL PLANE - AFTER BARRETT

FIG 2.2

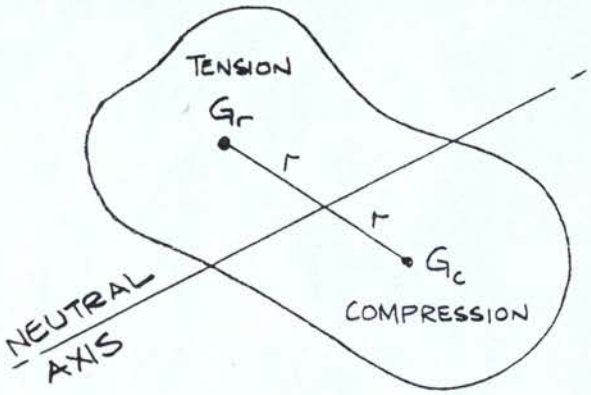

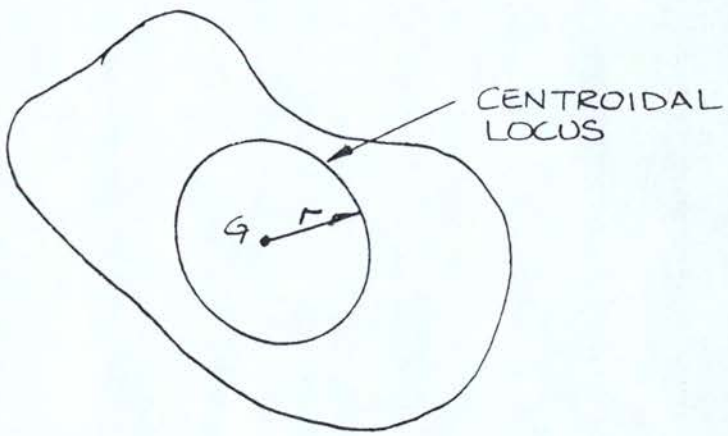

THE CONCEPT OF CENTROIDAL LOCUS
— AFTER BROWN

FIG 2.3

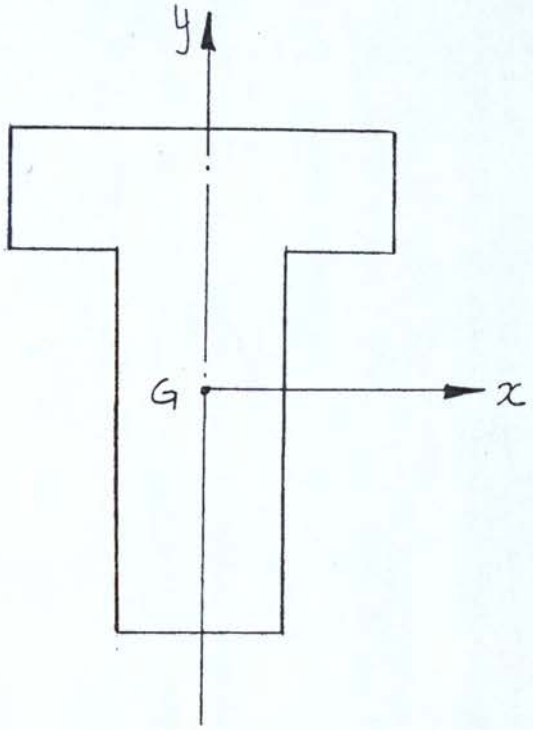

SECTION WITH ONLY ONE AXIS OF SYMMETRY

FIG. 2.4

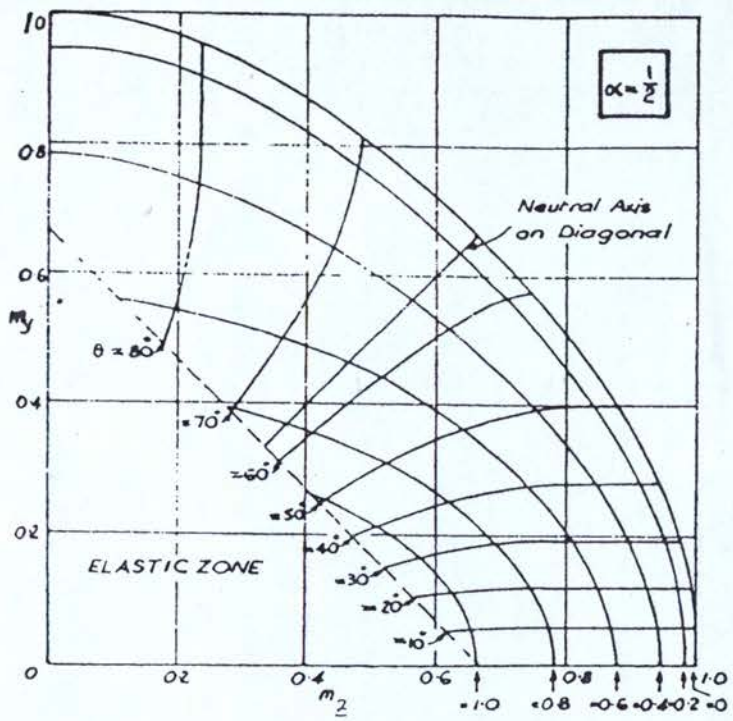

TYPICAL PLOT OF M_y Vs M_z FOR BEAM OF ASPECT RATIO OF 0.5 IN TERMS OF PARMETERS α & θ

– AFTER BROWN

FIG 2.5

TYPICAL HYSTERESIS LOOP

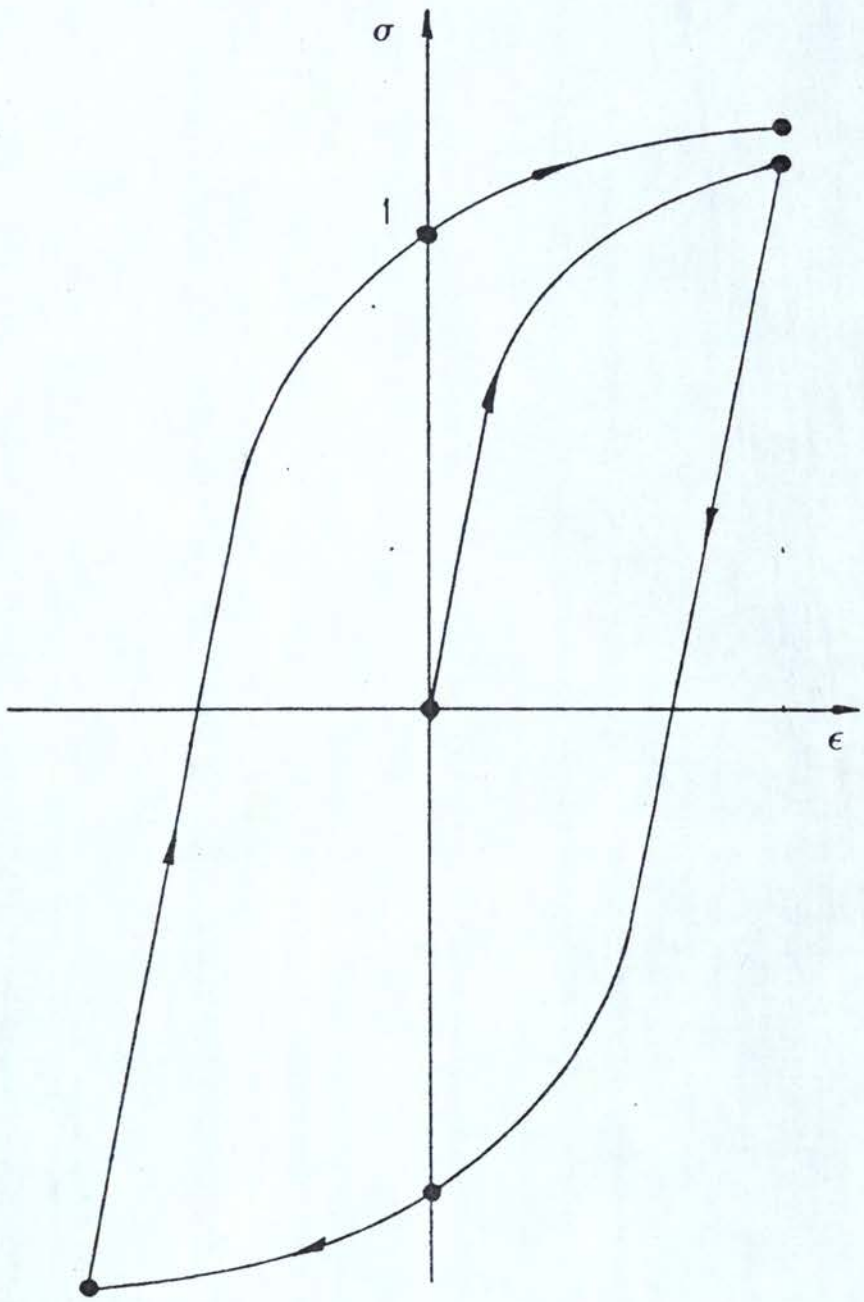

FIG 2.6

YIELD SURFACE IN TERMS OF BENDING

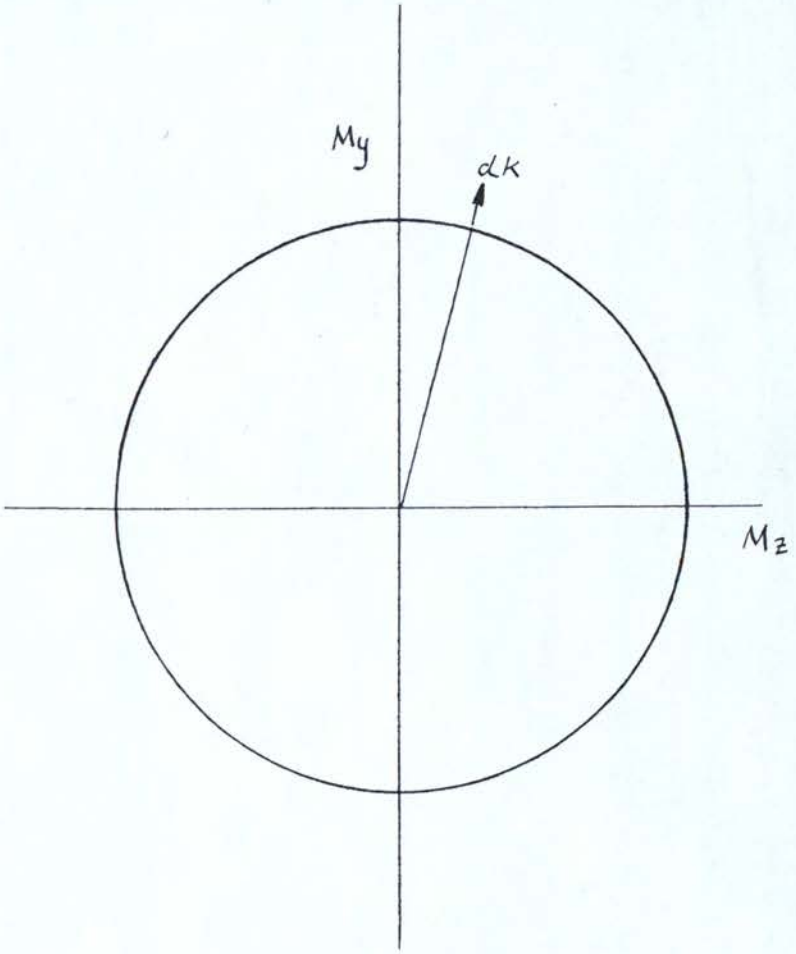

FIG 2.7

CHAPTER 3

EXPERIMENTAL APPROACH

CHAPTER THREE

EXPERIMENTAL APPROACH

3.1 DESIGN OF TEST RIG AND DATA ACQUISITION SYSTEM

3.1.1 INTRODUCTION

The main requirements of the test rig are that it

a) Be capable of bending a cantilever about two planes without introducing any unwanted additional forces. Longitudinal forces can be induced by the changing geometry of the specimen unless freedom of movement of the load applying and reacting members is achieved.

b) Be rigidly constructed in order to reduce rig deformation effects to a minimum and therefore allow the true deflection of the cantilever to be measured. These rig effects would generally arise due to lack of rigidity at the fixed end and to unwanted movement with the loading device at the end of the cantilever.

c) Be capable of accepting adequate instrumentation to monitor all the required deflections and forces and that the instrumentation should be suitable for computerised data acquisition and control of the cyclic bending process.

3.1.2 PROBLEM DEFINITION

Based on the conditions described above the problem could be defined as follows.

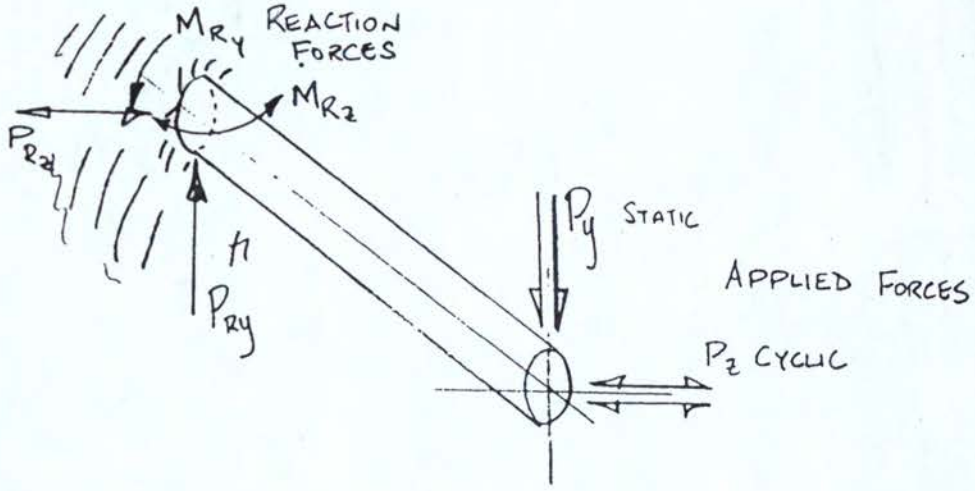

Consider a beam length l subjected to the forces and moments as shown above. If the beam was rigidly "built in" at one end then application of forces will cause strain in the axial direction, due to length l changing very slightly as the free end is displaced. This effect could be removed by allowing the beam freedom in the X-direction.

On the other hand if it is rigidly clamped at the free end (already allowing for freedoms in X, Y and Z direction) then the beam could be subjected to double curvature as shown below.

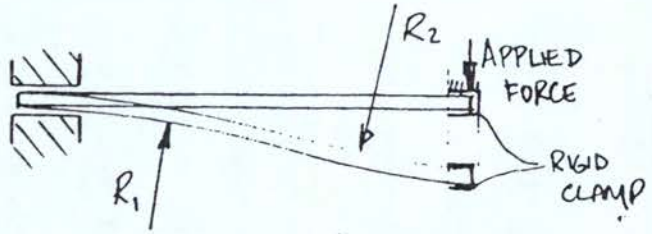

To eliminate this effect the free end of the beam, when clamped, must have all six (X, Y, Z, θ_X θ_Y θ_Z) degrees of freedom.

3.1.3 DESIGN OF BI-AXIAL BENDING RIG

3.1.3.1 FIXED END LOCKING MECHANISM

The design of fixed end clamp is shown in Fig (3.1). The structure is designed to be sufficiently rigid such that deflections are negligible when the beam is loaded at the opposite end.

The beam is clamped between hardened and tempered steel jaws as indicated on the diagram. The complete clamp assembly is allowed to slide on linear roller bearings, hence allowing that freedom in the 'X' direction referred to earlier.

3.1.3.2 LOADED END MECHANISM

Fig (3.2) shows the load carriage. Both the horizontal and vertical freedoms are achieved through linear bearings. The rotational freedoms are facilitated by means of a spherical bearing. The vertical rods which transmit cyclic loads to the beam are hardened steel and ground to be within specified tolerance to avoid any friction effects.

3.1.3.3 CYCLIC LOADING MECHANISM

The cyclic load is applied by means of 1/8 horse power electric motor. Transmission from the motor to the lead-screw is through gear box and belt drive. The reason for using both belt and gearbox is so that the system could be sufficiently slowed to accommodate a data acquisition system.

3.1.4 DATA MONITORING SYSTEM AND CALIBRATION

3.1.4.1 LINEAR VARIABLE DISPLACEMENT TRANSDUCERS (HORIZONTAL AND VERTICAL

The vertical and horizontal tip deflections of the beam were monitored by means of linear variable displacement transducers (LVDT).

The horizontal LVDT (type: SEALABS No 373/15) was attached to the bed of the rig and its armature was attached to the load carriage as shown in Fig (3.4.6). The transducer was coupled to a signal conditioner and power supply unit, the output of which was fed to a multiplexer.

The vertical transducer (type: Sangamo AC/15) was attached to the frame of the load carriage and the armature to the vertical slider mechanism. Fig (3.4a). The output from the signal conditioner was connected in a similar way, to the horizontal LVDT.

Both transducers, along with associated power supply units, were calibrated against a micro-meter load, and output displayed on a digital voltmeter. Calibration graphs (output voltage Vs displacement) are shown in Figs (3.5) and Fig (3.6) for horizontal and vertical transducers respectively.

3.1.4 DATA MONITORING SYSTEM AND CALIBRATION

3.1.4.1 LINEAR VARIABLE DISPLACEMENT TRANSDUCERS (HORIZONTAL AND VERTICAL

The vertical and horizontal tip deflections of the beam were monitored by means of linear variable displacement transducers (LVDT).

The horizontal LVDT (type: SEALABS No 373/15) was attached to the bed of the rig and its armature was attached to the load carriage as shown in Fig (3.4.6). The transducer was coupled to a signal conditioner and power supply unit, the output of which was fed to a multiplexer.

The vertical transducer (type: Sangamo AC/15) was attached to the frame of the load carriage and the armature to the vertical slider mechanism. Fig (3.4a). The output from the signal conditioner was connected in a similar way, to the horizontal LVDT.

Both transducers, along with associated power supply units, were calibrated against a micro-meter load, and output displayed on a digital voltmeter. Calibration graphs (output voltage Vs displacement) are shown in Figs (3.5) and Fig (3.6) for horizontal and vertical transducers respectively.

3.1.4.2 THE LOAD CELL

The load cell shown in Fig (3.7a) was used to monitor horizontal, cyclic load. The load cell was made from mild steel and was designed for ± 2500N direct in tension and compression.

Four strain gauges were mounted on the load cell. The four gauges were connected in a standard Wheatstone bridge configuration. Fig (3.7b). The strain gauge bridge was connected to a Sangamo Western Gemini transducer meter, the output of which was fed into a DVM.

The overall system was calibrated against a "face load transducer" (Hollinger Boldwin Messtechnic Model U2). This transducer was used to monitor loads in a push-pull test rig, see reference (48). Special mounting brackets were designed to substitute the load cell with the push-pull specimen.

The calibration graph Fig (3.8). (Applied load Vs DVM reading) shows a linear behaviour over the range of load for which it was designed.

3.1.4.3 THE DATA ACQUISITION AND CONTROL SYSTEM Fig (3.9).

The measurement system consisted of three different transducers LVDT 1, LVDT 2 and the Load Cell connected to a 4 input differential read-relay multiplexer.

The output of the multiplexer was connected to a 5½ digit "Racal Dama" digital voltmeter fitted with a IEEE general purpose interface port.

The drive was through a single 3-phase motor connected to two mechanically interlocking connectors. The following table gives the different combination of the connecters and the corresponding motor action.

CONNECTER 1	CONNECTER 2	MOTOR ACTION
ON	OFF	START
OFF	OFF	STOP
OFF	ON	REVERSE
ON	ON	STOP

A CBM PET microcomputer was used to control both connecters and the multiplexer via an eight bit output port peripherial box, fitted with individual switches to provide manual override facility. In simple terms a port consists of eight communication lines, each line can be designated to act as input or output. Associated with each line is a "pigeon hole" in the data register. When '1' is stored in the pigeon hole the corresponding line becomes an output and when '0' is stored the line will behave as an input.

The digital voltmeter is connected to the PET IEEE port. The controlling input is the horizontal transducer.

3.1.4.4 CONTROL PROGRAM

A computer program "CONTROL" was written to control the load cycle and collect experimental data and subsequently store it on a magnetic disc. The listing of the program is given in Appendix 3.

Program Description

The expected load/deflection (horizontal) hysteresis curve is divided into 7 elements as shown Fig (3.10).

Element	0	Loading "Forward direction" (first 1/4 cycle)
	1	Unloading
	2-3	Loading in "Reverse direction"
	4	Unloading from "Reverse direction"
	5-6	Subsequent "Forward Loading".

Element 0 only occurs once during the course of the test. Elements 1 to 6 occurs once for each cycle.

The program is instructed to record a number of data sets during each element and the number of cycles for which the test is to run. The maximum limit is dictated by the computer memory, in this case approximately 1000 sets of data.

The program is also given the limits of the cyclic deflection, in mm. These limits are dictated by the range of the horizontal transducer limits (ie ±15 mm).

3.1.5 TEST PROCEDURE

The loading carriage was manually moved (using the manual override facility on the PET 'peripherial box') to a zero position. Both ends of the specimen were loaded and clamped into appropriate end clamps. The computer program "CONTROL" was loaded into the computer memory and executed. After responding to various prompts and the zero had been monitored by the computer, the end load (to apply constant moment 'M_y') is applied to the load carriage. The final response to computer prompts was made (ie 'GO' entered to start the cyclic loading process).

At this point all operator activity was complete. After completion of the test all data is automatically stored on a magnetic disc.

3.2 DATA PROCESSING

The experimental data was then transferred to Tektronix 4052A desk top computer. The reason for this is that the Tektronix computer had graphics capability.

The transfer of data takes place by means of an interface box () and two programs TEKLINK (for the PET) and PETLINK (for the Tektronix) were written for this purpose. The listing of these programs are in Appendix 3.

The output from the Tektronix computer (using 'GRAPHPLOT' program reference (46)) is in the graphical form.

Typical Load/Deflection and Deflection/Deflection graphs are shown in Figs (3.11) and (3.12)

3.3 MATERIAL AND SPECIMENS

Two materials were selected for this investigation ie EN32B (C115) mild steel and stainless steel 321-S21 (see table for compositions). The choice of mild steel was made due to its wide use in Engineering. On the other hand the stainless steel was chosen because it has different mechanical properties and cyclic stress-strain characteristics than mild steel and is used extensively in high strain fatigue situations.

Two types of specimen were used in this investigation

(i) Square beam, Fig (3.13a)

(ii) Circular beam, Fig (3.13b).

Both test materials were supplied in the form of 12 mm x 12 mm square cross-sectional bars. The bars were cut to convenient lengths and the specimens were machined.

The square specimens were only machined to suit clamping mechanism on the load carriage and on the circular specimen the gauge length was also machined.

Additional specimens were machined for

(i) Uniaxial tensile test, Fig (3.14a)

(ii) Cyclic push-pull tests, Fig (3.14b)

The standard tensile test specimens were machined from the bars described above. The push-pull specimens were machined from 30 mm diameter rods. The specimens were hollow tubes and designed to suit a push-pull test rig developed by Adkin (4).

All mild steel specimens were fully annealed after machining at 920°C for 1 hour and furnace cooled. The stainless-steel specimens were left untreated.

3.4 STATIC STRENGTH PROPERTIES

The mechanical properties of the materials were obtained from monotonic tensile tests using a Hounsfield Tensometer. The specimen Fig (3.14a) was axially pulled to destruction and load-deflection data recorded. This was subsequently converted to stress-strain. The stress-strain curves for stainless steel and mild steel are shown in Figs (5.1) and (5.2) respectively.

Three specimens of each material were tested and insignificant difference was detected between results from different specimens of the same material.

3.5 PUSH-PULL TESTS

The procedure and specimen grips are described elsewhere (4).

The cyclic load-extension data was recorded and again this was converted to stress-strain. The tests in this case were strain controlled. The maximum strain used was ±2%, above which buckling was causing results to deteriorate. A selection of strain rates up to and including 2% were performed. The typical cyclic stress-strain curves obtained are shown in Figs (5.5) to (5.10) and (5.13) to (5.20) for mild steel and stainless steel respectively. These curves are 'steady state' cyclic curves.

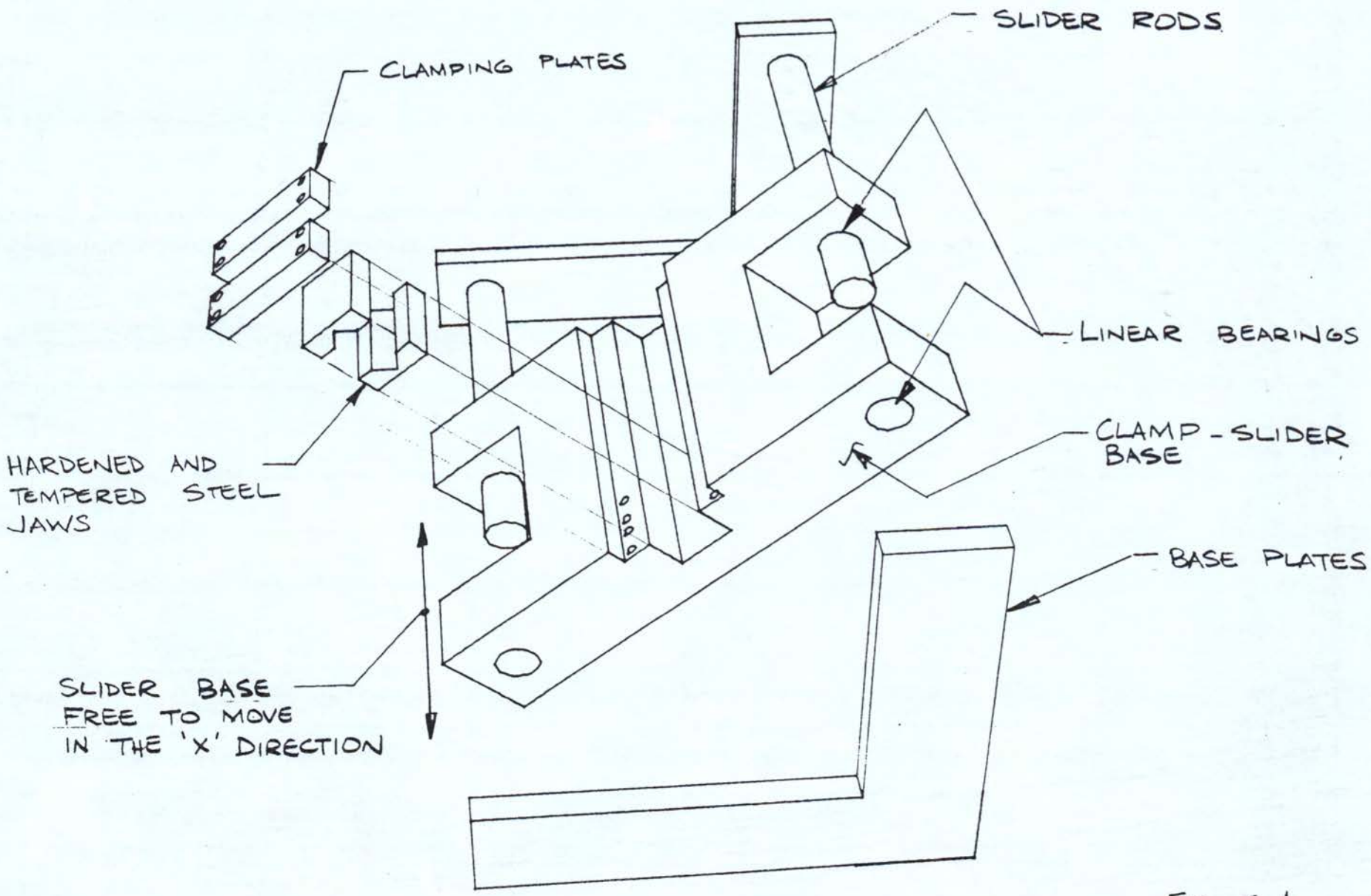
SLIDER RODS
CLAMPING PLATES
LINEAR BEARINGS
CLAMP - SLIDER BASE
HARDENED AND TEMPERED STEEL JAWS
BASE PLATES
SLIDER BASE FREE TO MOVE IN THE 'X' DIRECTION

FIG 3 1

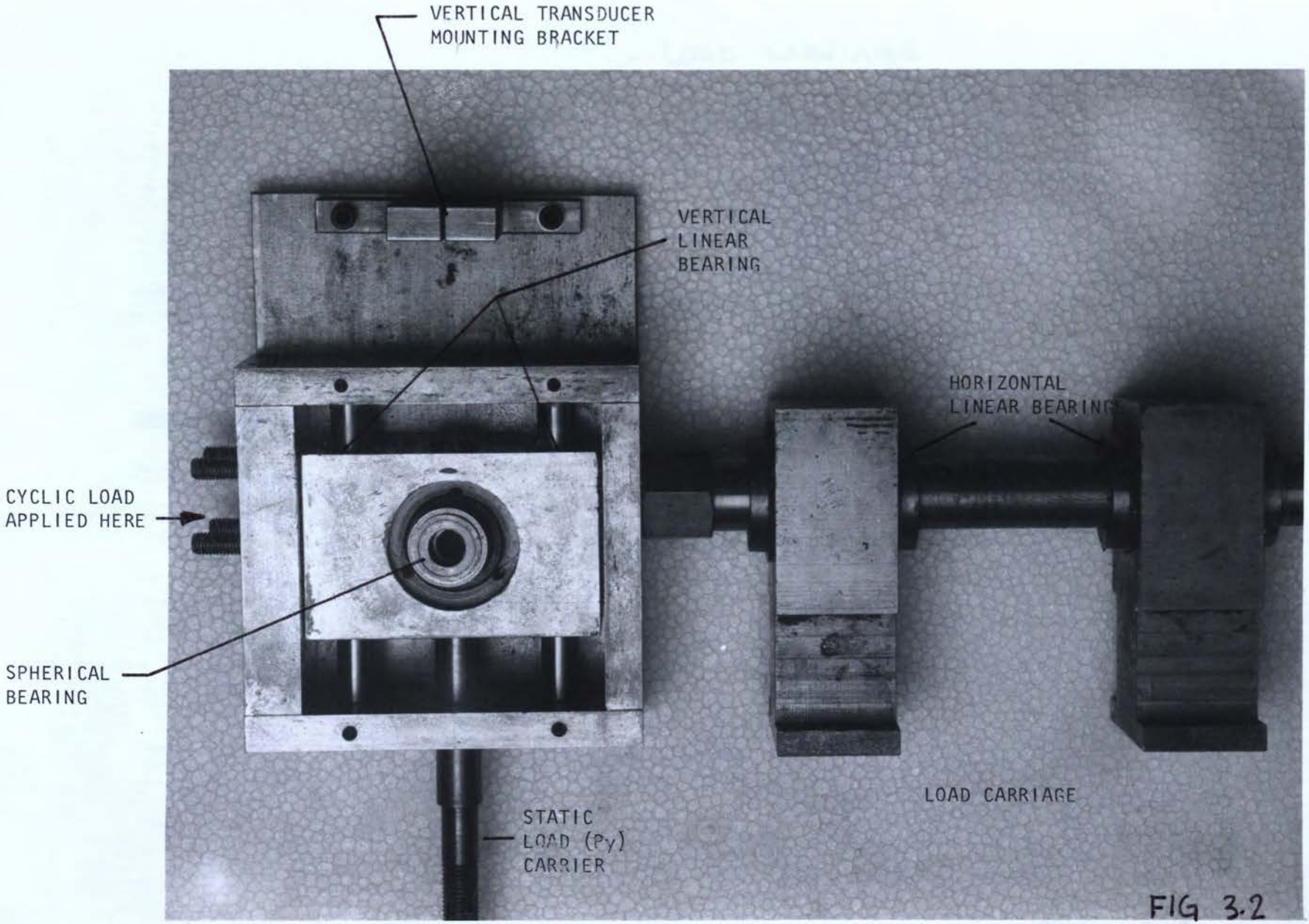
VERTICAL TRANSDUCER MOUNTING BRACKET
VERTICAL LINEAR BEARING
HORIZONTAL LINEAR BEARING
CYCLIC LOAD APPLIED HERE
SPHERICAL BEARING
LOAD CARRIAGE
STATIC LOAD (Py) CARRIER

FIG 3.2

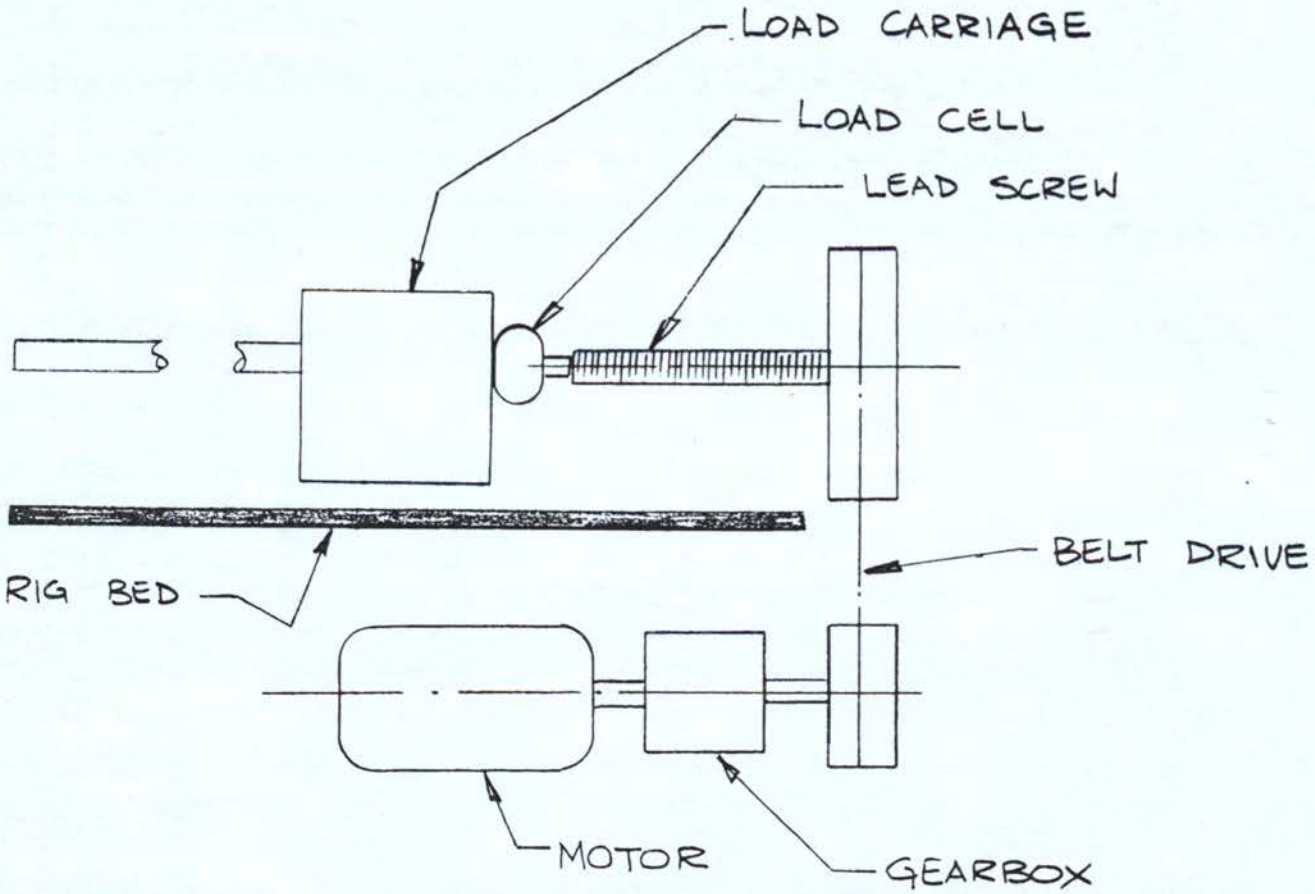

RIG - DRIVE CONFIGERATION

FIG 3.3

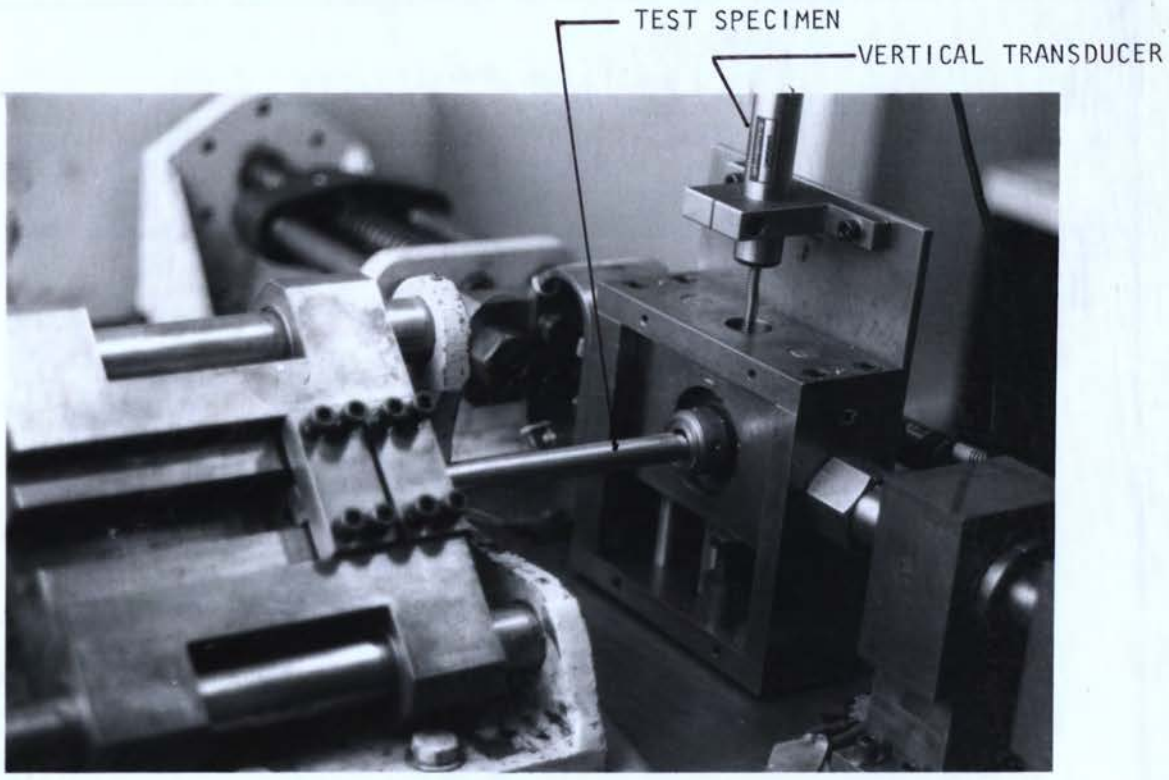

FIG. 3.4a

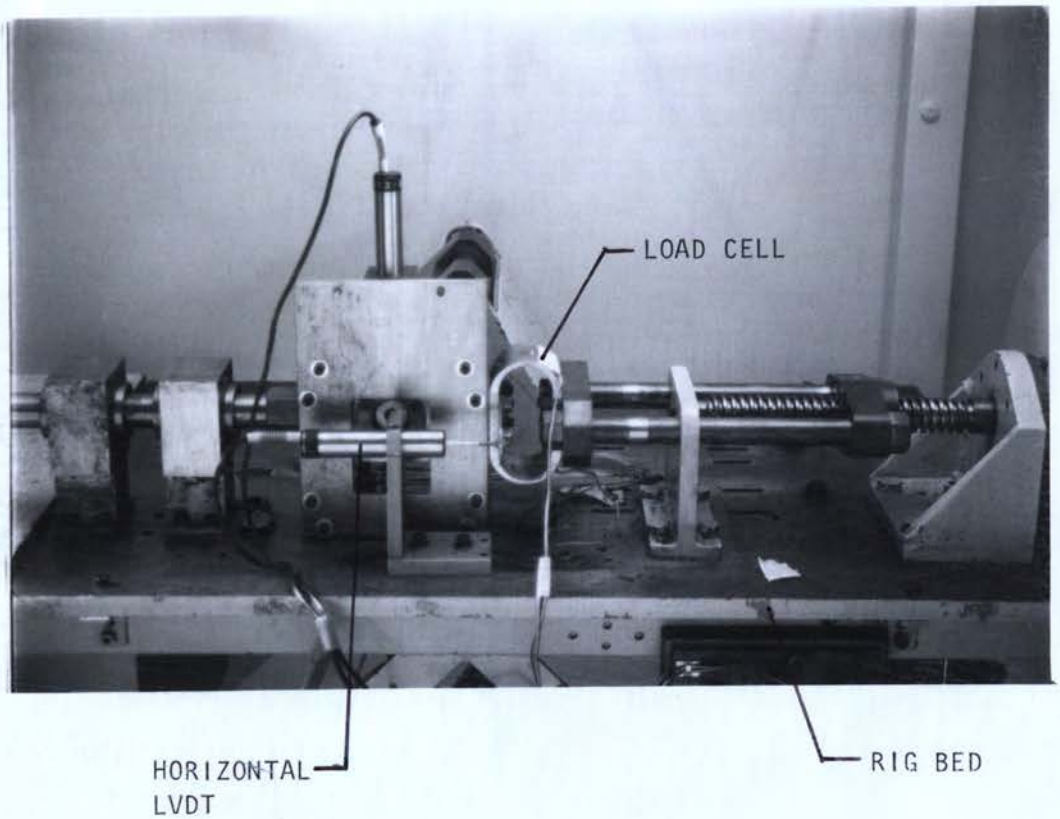

FIG. 3.4b

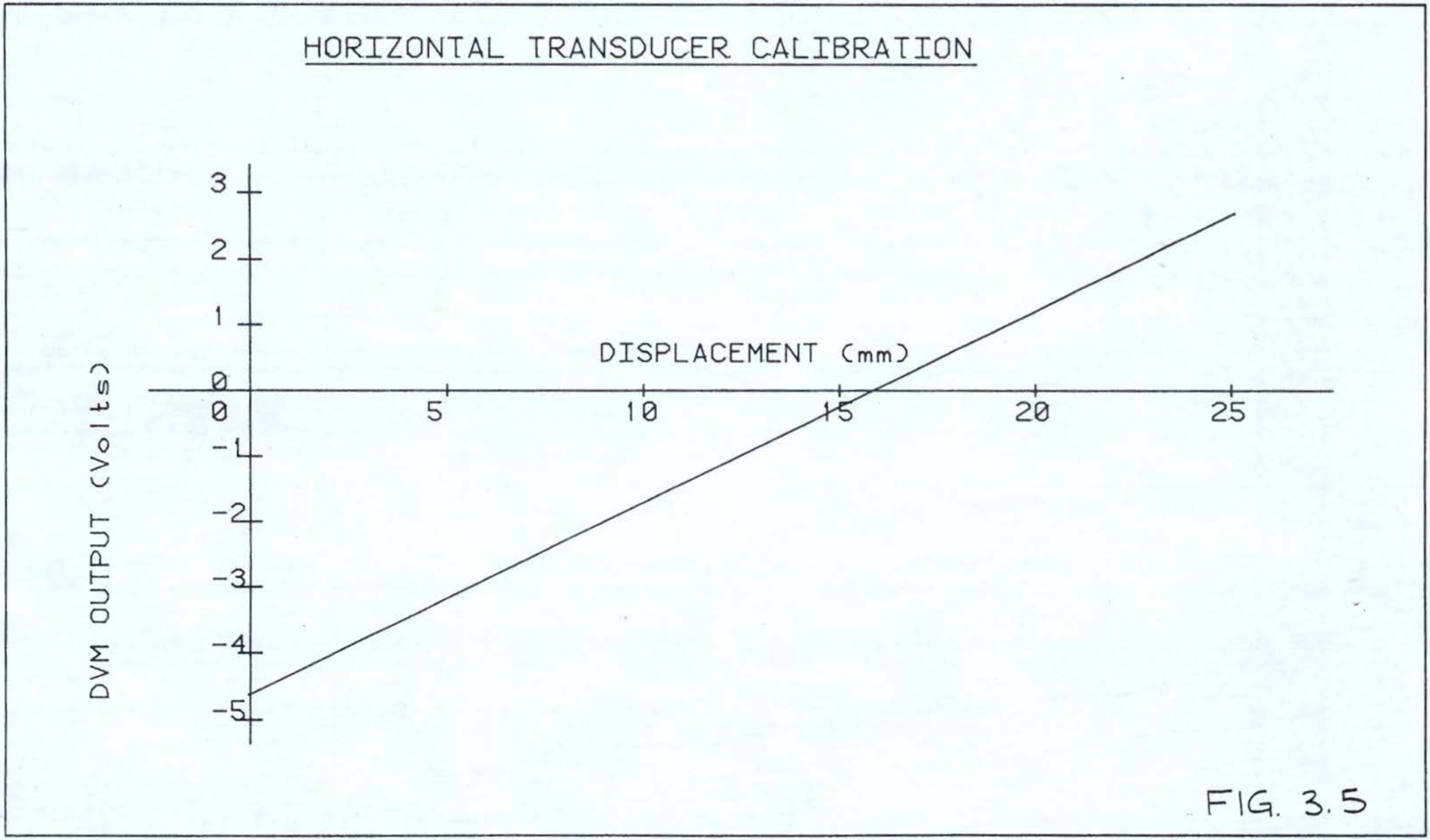
HORIZONTAL TRANSDUCER CALIBRATION
DVM OUTPUT (Volts)
3
2
1
0
-1
-2
-3
-4
-5
DISPLACEMENT (mm)
0
5
10
15
20
25

FIG. 3.5

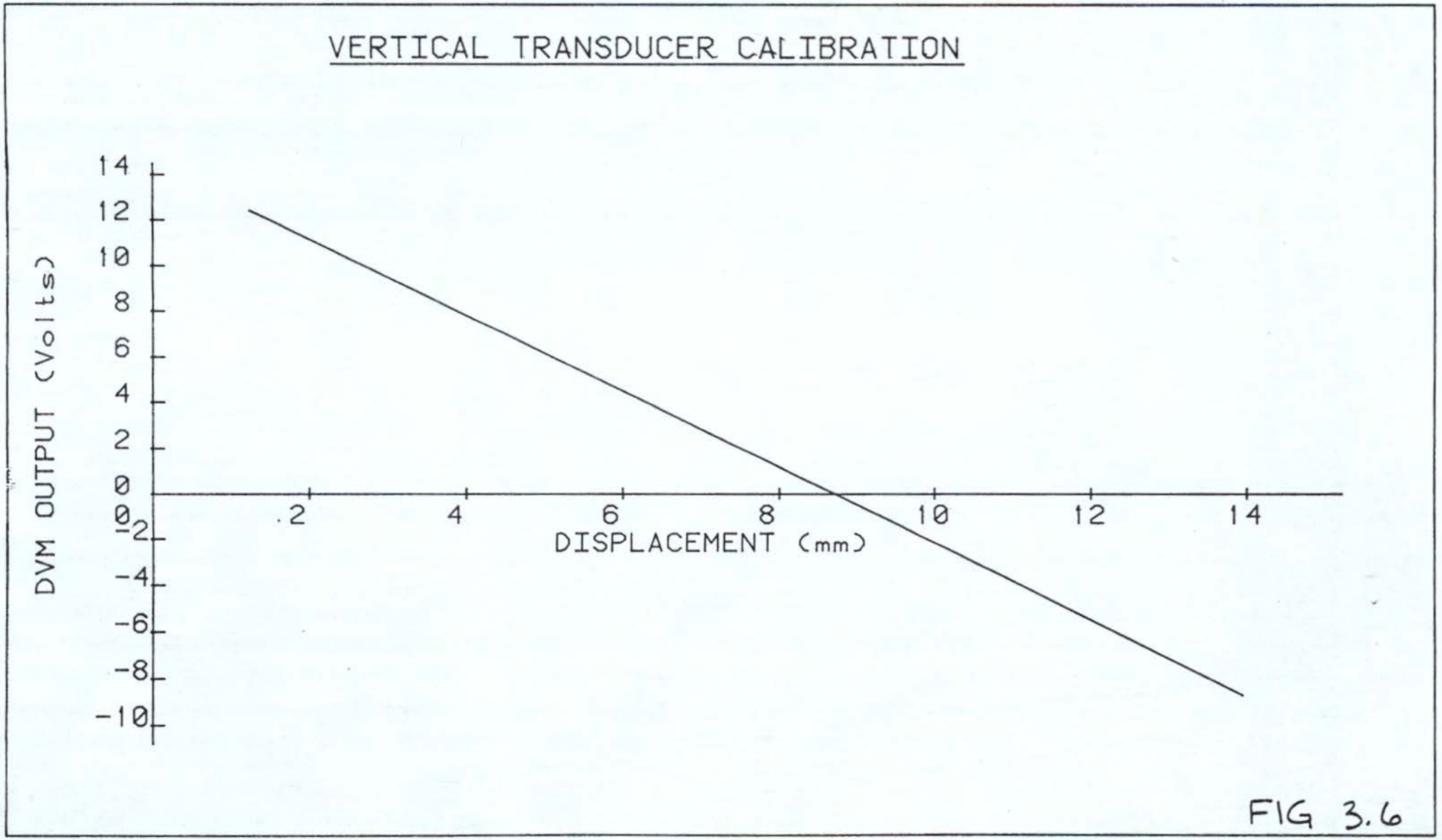
VERTICAL TRANSDUCER CALIBRATION
DVM OUTPUT (Volts)
14
12
10
8
6
4
2
0
-2
-4
-6
-8
-10
.2
4
6
8
10
12
14
DISPLACEMENT (mm)

FIG 3.6

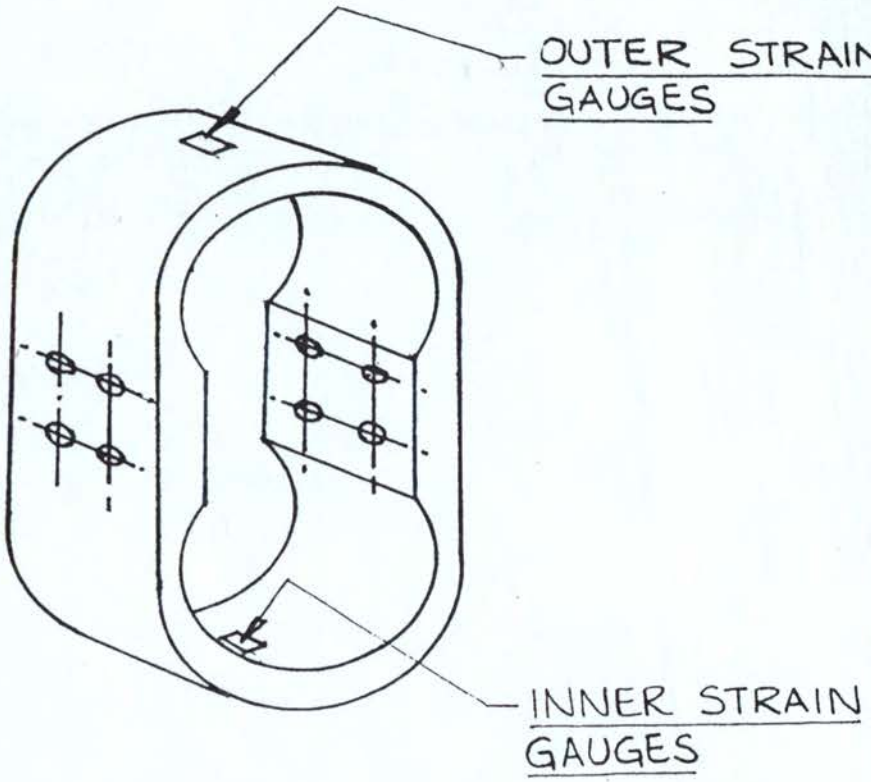

FIG 3.7a -LOAD CELL

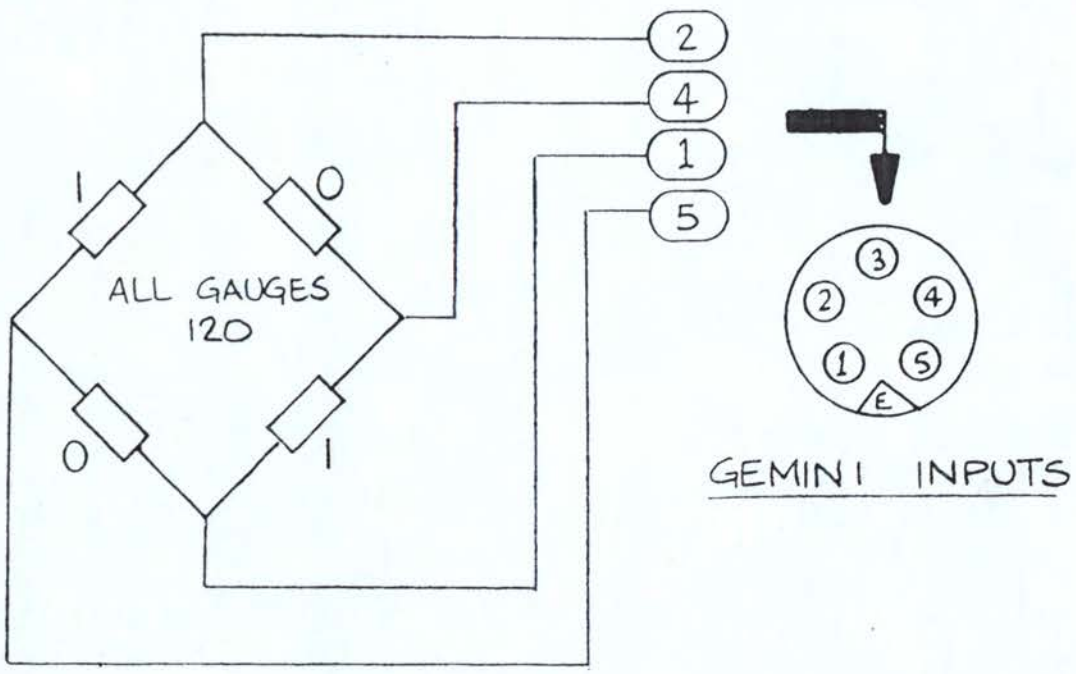

FIG 3.7b STRAIN GAUGE CIRCUIT

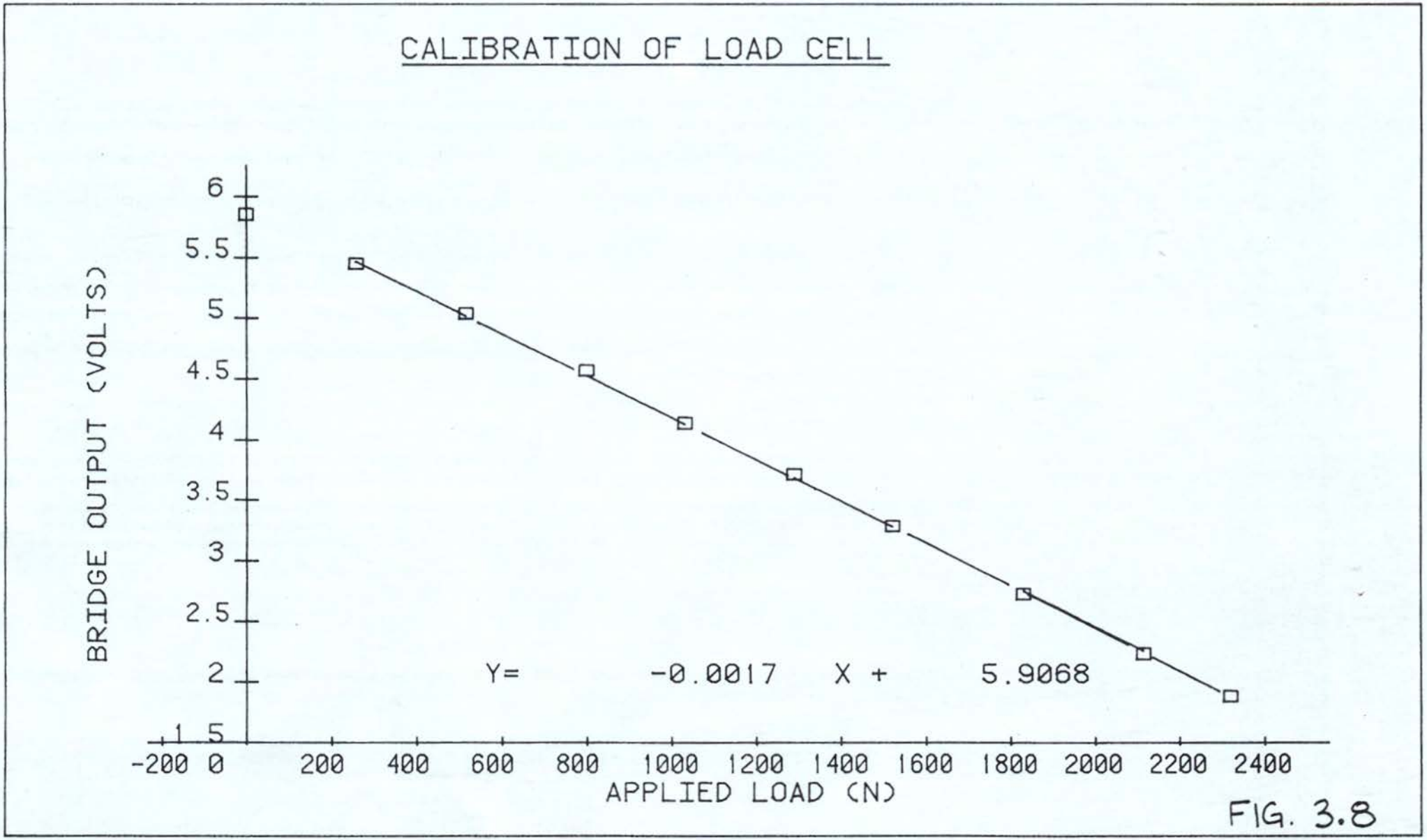
CALIBRATION OF LOAD CELL
BRIDGE OUTPUT (VOLTS)
6
5.5
5
4.5
4
3.5
3
2.5
2
1.5
Y= -0.0017 X + 5.9068
-200 0 200 400 600 800 1000 1200 1400 1600 1800 2000 2200 2400
APPLIED LOAD (N)

FIG. 3.8

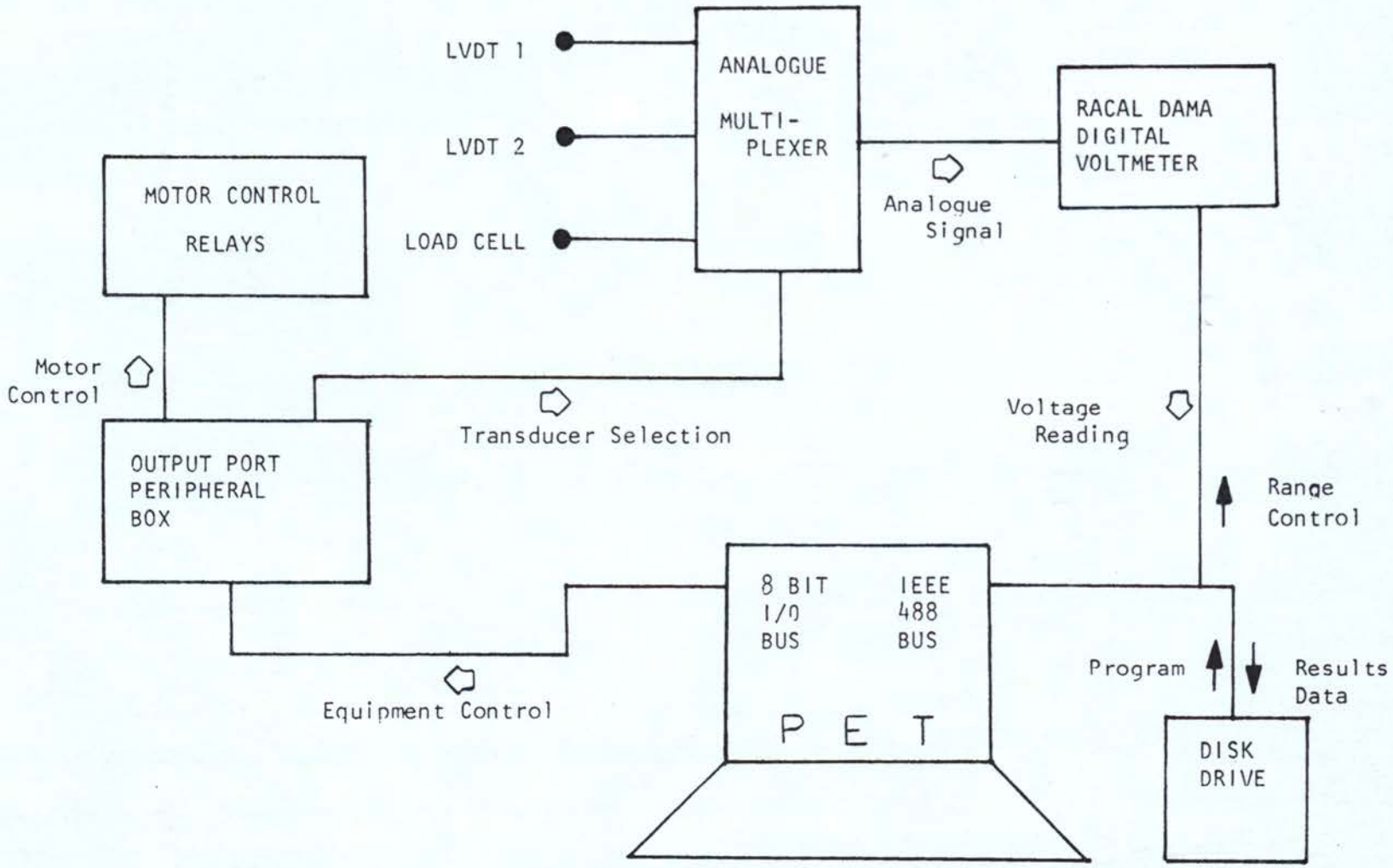

FIG 3.9 THE DATA ACQUISITION AND CONTROL SYSTEM

HYSTERESIS CURVE DIVISIONS

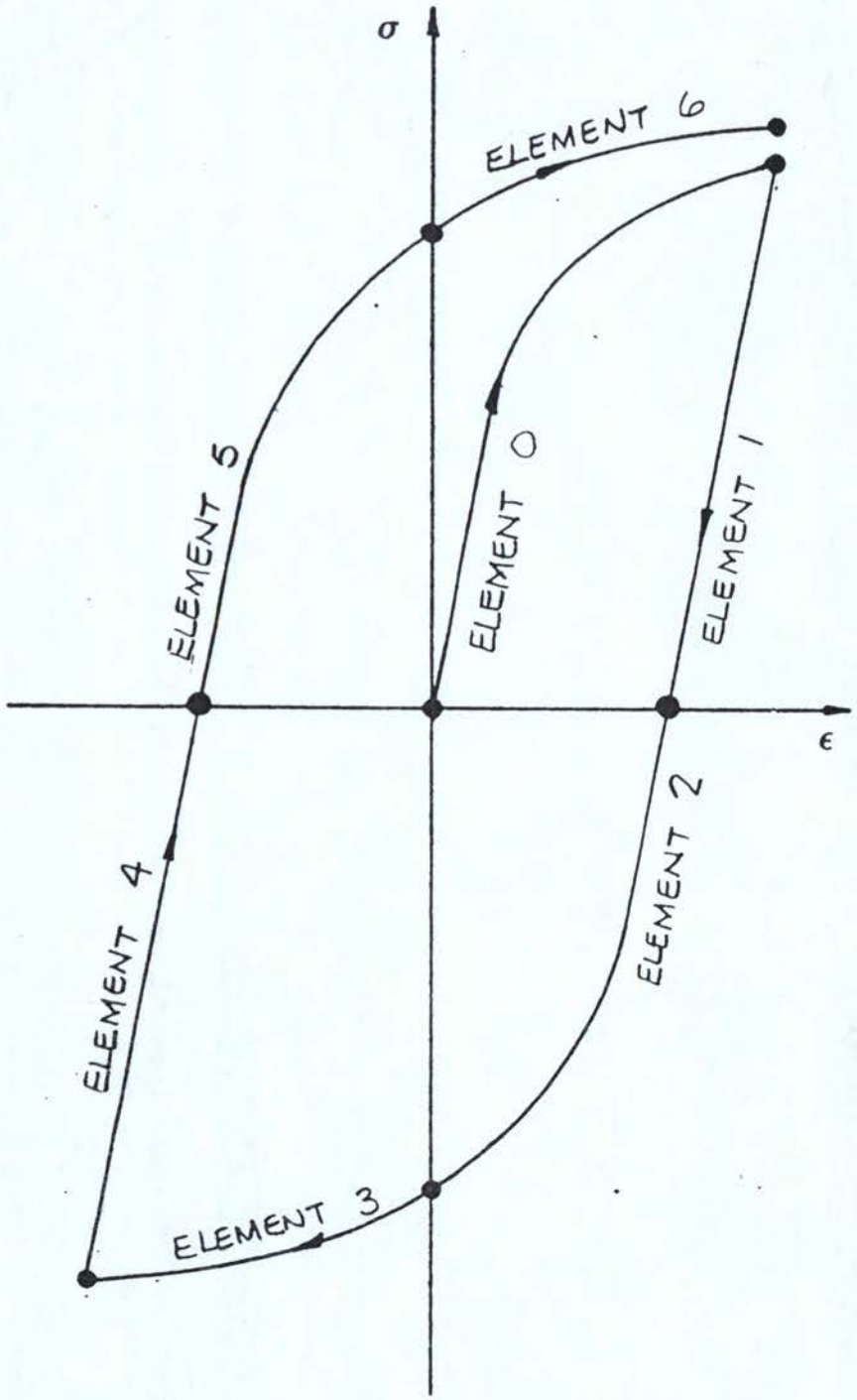

FIG 3.10

LOAD / DEFLECTION CHARACTERISTICS (Py=325 N)

MATERIAL : STAINLESS STEEL -SQUARE BEAM-

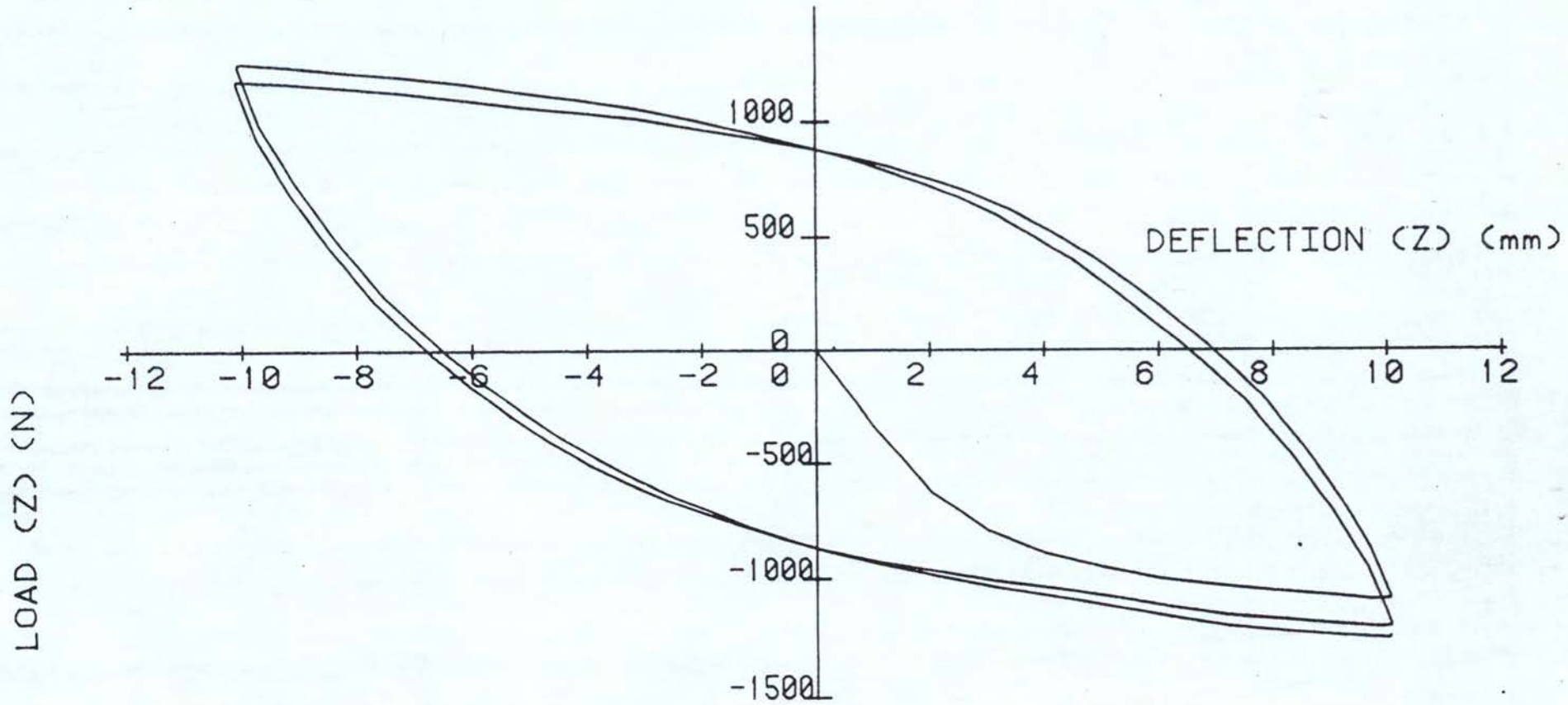

FIG. 3.11

SS I BAR

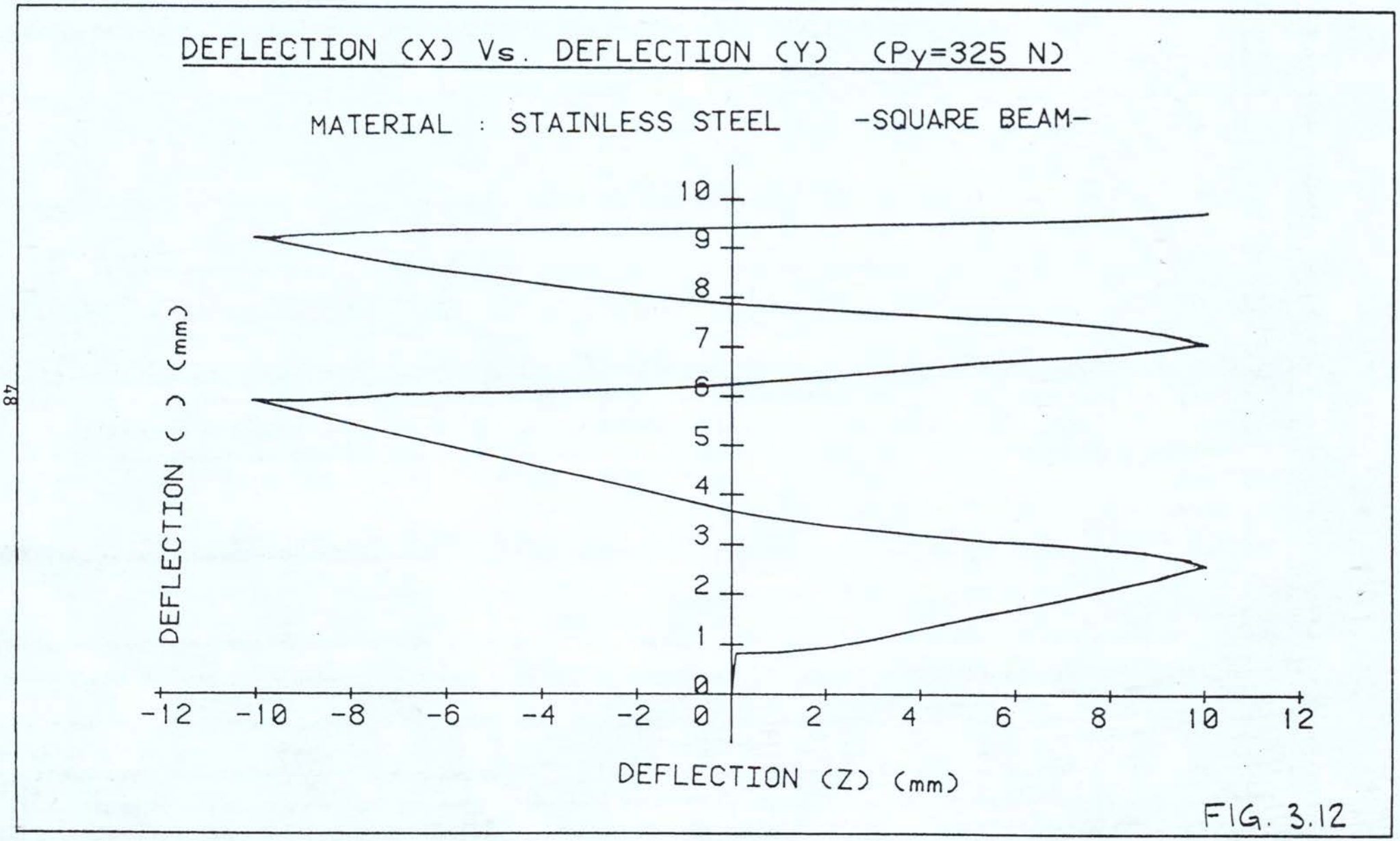

FIG. 3.12

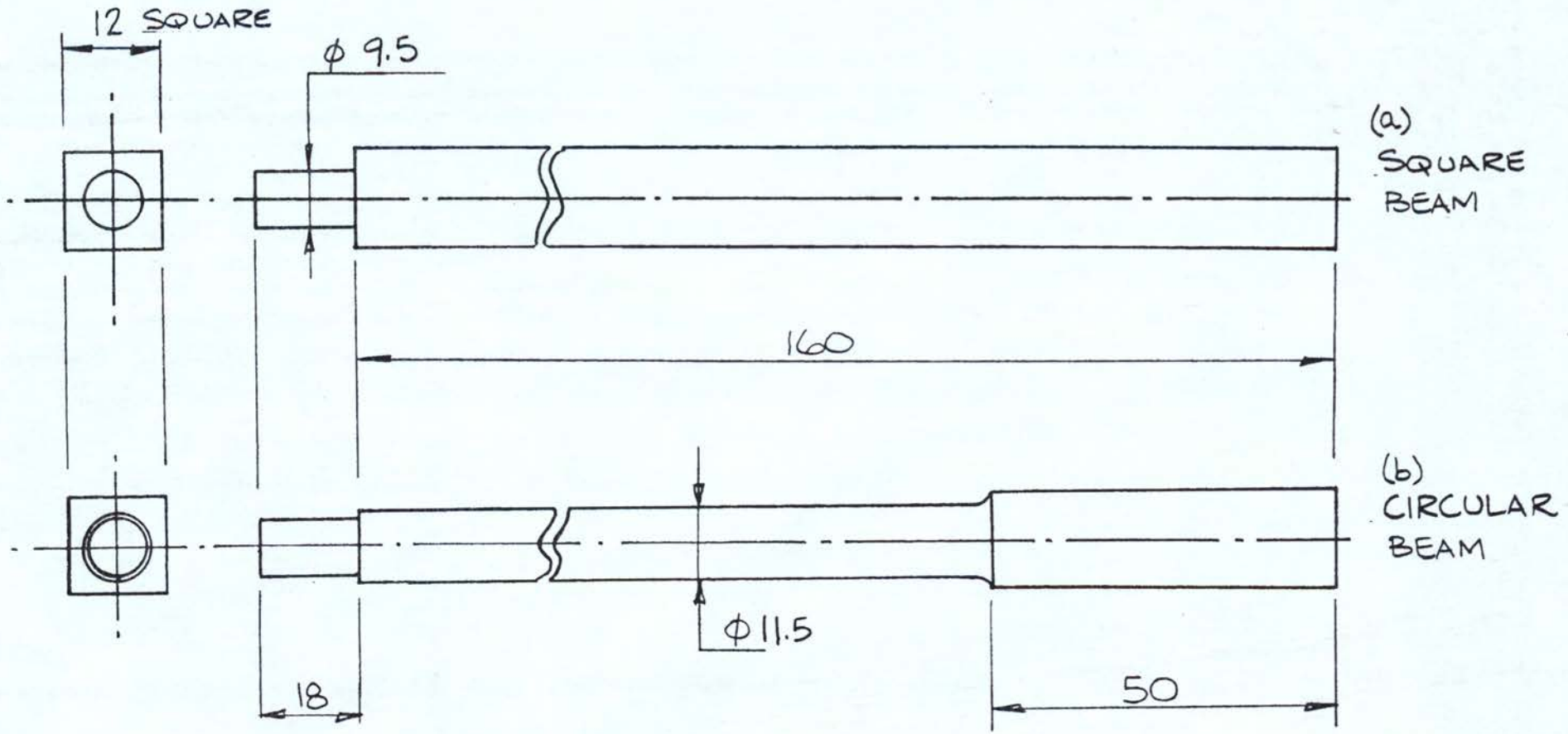

TEST SPECIMEN

FIG. 3.13

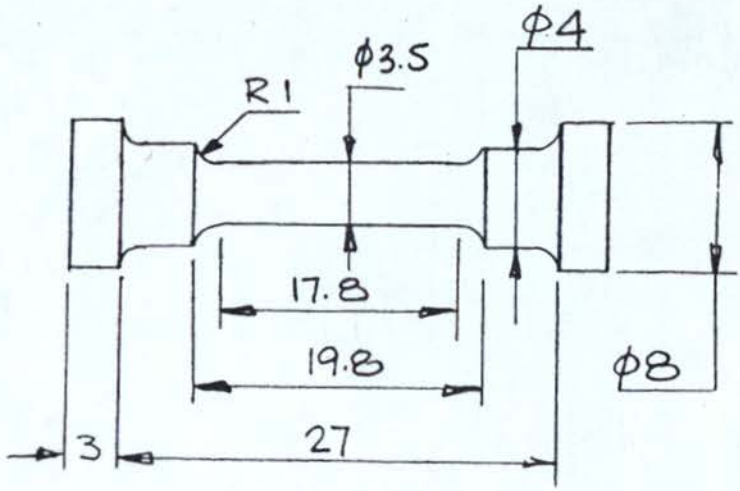

(a) TENSILE TEST SPECIMEN

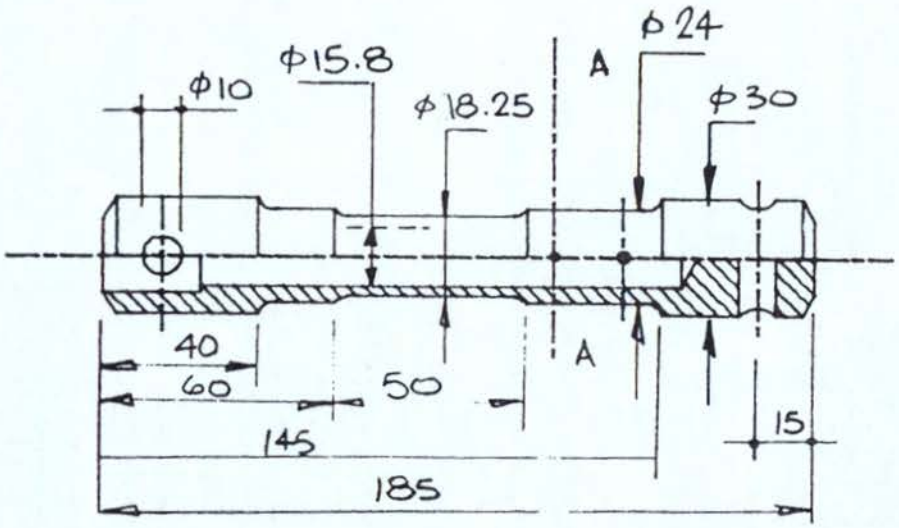

SECTION A-A

HALF SECTION ON CENTRE LINE

(b) CYCLIC TEST SPECIMEN

FIG. 3.14

CHAPTER 4

THEORETICAL CONSIDERATIONS

CHAPTER FOUR

4.0 THEORETICAL CONSIDERATIONS

4.1 INTRODUCTION

In developing an analytical method, the problem of simple bending of a cantilever beam is first considered and the simplifying assumptions made with regards to secondary stresses and the curvature equation are examined. The mathematical modelling of the stress-strain material properties is introduced in order to determine expressions for cantilever deflections. Rectangular and circular beams are analysed and it is shown that although they possess a high degree of symmetry of geometry and similar solutions for simple bending, the geometry becomes critical when bi-axial bending is considered. The problem of large plastic deflection is considered and a solution using the full curvature equation is developed and evaluated.

The biaxial bending problem is then analysed in detail in three parts.

a) Ignoring any movement of the neutral surface ie proportional loading (M_z/M_y = Constant).

b) Non-radial loading, but ignoring any unloading of elements as the neutral surface rotates.

c Non-radial loading with account being taken of elemental fibres unloading and re-loading as the neutral surface rotates.

These three approaches are undertaken in order to evaluate the effect of non-radial loading and rotating plane elements in order to ascertain their importance. Clearly if their influence is of no great significance in determining the incremental deflections it can lead to a simplification in the analysis.

Finally the cyclic loading - unloading aspect of the problem is considered by developing mathematical models of material behaviour, identifying the stress-strain history of the elemental fibres and incorporating this data into the analysis.

4.2 ASSUMPTIONS

Unless otherwise specified, in all analyses it will be assumed that

1) the plane sections remain plane;
2) the material is homogeneous;
3) the cross-sectional dimensions are small relative to the length of the beam, so that deformation due to shear may be neglected;
4) the initial residual stresses are negligible.

Based on the first two assumptions, the neutral surface lies in the middle of the cross-section and the strain ε in any fibre distance v from the neutral axis will be given by

$$\varepsilon = vK \qquad 4.1$$

where K is the curvature.

4.3 GENERAL CURVATURE EXPRESSION

Whether the problem of elastic or plastic deflection is being considered, the general curvature equation is of the form

$$K = \frac{\frac{d^2y}{dx^2}}{\left[1 + \left(\frac{dy}{dx}\right)^2\right]^{3/2}} \qquad 4.2$$

where y is the deflection at distance x from the origin.

In the elastic problem curvature is proportional to the applied bending moment and the solution leads to the well known Bernoulli-Euler law

$$K = \frac{M}{EI} \qquad 4.3$$

Combining equations 4.2 and 4.3 leads to a non-linear differential equation

$$\frac{\frac{d^2y}{dx^2}}{\left[1 + \left(\frac{dy}{dx}\right)^2\right]^{3/2}} = \frac{M}{EI} \qquad 4.4$$

For small deflections this reduces to

$$\frac{d^2y}{dx^2} = \frac{M}{EI} \qquad 4.5$$

In order to examine the problem of large deflections it is necessary to solve equation 4.4. The study of large amplitude bending of slender beams has engaged the attention of many research workers in the past. This work is well covered in Frisch-Fay (49), and solutions to a wide range of problems are provided in the form of elliptical integrals. However, the solutions are of little practical interest and relevance to real engineering problems.

4.4 PLASTIC BENDING

4.4.1 MATERIAL PROPERTIES

Once the beam is inelastically or plastically deformed, the stress-strain behaviour can no longer be assumed linear.

It is possible to use two or more straight lines with decreasing slopes Fig (4.1) to describe the stress strain relationship. Usually, however, it is preferable to describe the σ-ε curve mathematically, which simplifies the task of solving problems. Straight lines also imply discontinuties which in practice do not usually occur. In the case of bending there is a gradual transition of the intial yield moment to the fully plastic moment even for materials which do not work harden.

One of the simplest relationships representing the stress-strain curve in the plastic region is the power law.

$$\sigma = \sigma_o \varepsilon^n \qquad 4.6$$

where σ_o and n are material constants which adequately describe many materials. The amount of strain hardening is represented by the index n.

A more general stress-strain curve expression was defined by Ramberg and Osgood (50). The expression

$$\sigma = E\varepsilon + \sigma_o \varepsilon^n \qquad 4.7$$

allows the curve to be specified in both elastic and plastic regions. As n tended to infinity, the expression approximated to the behaviour of an elastically perferctly plastic material.

In this investigation material behaviour will be assumed to be that described by equation (4.6) because the cyclic material stress strain curves, show very small elastic regions.

4.4.2 SIMPLE PLASTIC BENDING

4.4.2.1 RECTANGULAR SECTIONED BEAM

Consider, for example, the rectangular cross sectioned beam Fig (4.2) and assuming each elemental fibre to be in tension or compression, then for system equilbrium

$$M = \int_{-h/2}^{h/2} \sigma b \, v \, dv \qquad 4.8$$

substituting for σ and integrating leads to

$$\frac{M}{I_n} = \frac{\sigma_o}{R_a^n} \qquad 4.9$$

or $$K = \left(\frac{M\sigma_o}{I_n} \right)^{\frac{1}{n}} \qquad 4.10$$

where $$I_n = \frac{bh^{n+2}}{2^{n+1}(n+2)} \qquad 4.11$$

and Ra = radius of curvature

These equations are slightly more general than the conventional trinity of equations used by engineers to solve elastic problems. For details of derivations of equations 4,8, 4.9, 4.10, 4.11 can be found in Johnson and Mellor (8).

4.4.2.2 CIRCULAR SECTIONED BEAM

Similarly if we consider a circular cross sectioned beam (Appendix 1), it can be shown that

$$M = 2\int_0^R \sigma w \, v \, dv \qquad 4.12$$

leads to $$K = \left[\frac{M}{4\sigma_o R^{n+3} J} \right]^{\frac{1}{n}} \qquad 4.13$$

where $$J = \int_0^{\Pi/2} \text{Cos}^2\alpha \, \text{Sin}^{n+1}\alpha \, d\alpha \qquad 4.14$$

Derivation of equations 4.12, 4.13 and 4.14 is shown in Appendix 1.

If we let $I_n = 4R^{n+3}J$, then equation 4.13 reduces to that derived for rectangular sectioned beam except that I_n, in this case, will be for a circular beam.

4.4.3 PROBLEM OF SMALL PLASTIC DEFLECTIONS

In the small deflections problem it is permissible to neglect the second order terms in the curvature equation 4.2, such that

$$K = \frac{d^2y}{dx^2} \qquad 4.15$$

Equating this to general plastic moment curvature equation (4.10), gives

$$\frac{d^2y}{dx^2} = \left(\frac{M}{\sigma_o I_n}\right)^{\frac{1}{n}} \qquad 4.16$$

and integrating twice to yield deflections

$$\boxed{y = \iint \left(\frac{M}{\sigma_o I_n}\right)^{\frac{1}{n}} dx\, dx} \qquad 4.17$$

Applied to a cantilever of length l Fig (4.3) and let M = Px then integrating gives.

$$y = \left(\frac{P}{\sigma_o I_n}\right)^{\frac{1}{n}} \left[\frac{n^2\left(x^{\frac{2n+1}{n}} - l^{\frac{2n+1}{n}}\right)}{(n+1)(2n+1)} + \frac{nl\,(l-x)^{\frac{n+1}{n}}}{n+1} \right] \qquad 4.18$$

Tip deflection is given when x = 0, so

$$y = \left(\frac{P}{\sigma_o I_n}\right)^{\frac{1}{n}} \frac{nl^{\frac{2n+1}{n}}}{2n+1} \qquad 4.19$$

when n=1, then equation 4.19 reduces to that of the elastic case.

4.4.4 PROBLEM OF LARGE PLASTIC DEFLECTIONS

If the deflections are large then it may not be permissible to neglect the second order terms in the curvature equation. Hence it is necessary to solve the complete curvature equation.

Das (9) attempted to manipulate the curvature equation into a more tractable form in the following manner.

The slope at any point along the length of the beam Fig (4.4) is given by

$$u = \frac{dy}{dx} \qquad 4.20$$

Hence

$$u' = \frac{du}{dx} = y'' \qquad 4.21$$

substituting for dy/dx and d^2y/dx into the curvature equation, gives

$$K = \frac{u'}{(1+u^2)^{3/2}} \qquad 4.22$$

let

$$u = y' = \sinh\gamma \qquad 4.23$$

then

$$K = \frac{\frac{d}{dx}(\sinh\gamma)}{\cosh^3\gamma} \qquad 4.24$$

integrating

$$\int K dx = \tanh\gamma$$

hence

$$\gamma = \tanh^{-1}\left(\int K dx\right) \qquad 4.25$$

substituting for γ into equation 4.23

gives

$$u = y' = \sinh\left[\tanh^{-1}\left(\int K dx\right)\right]$$

$$= \frac{\int K dx}{\sqrt{1-\left(\int K dx\right)^2}} \qquad 4.26$$

Deflection y is given by integrating equation 4.26, hence

$$y = \int u\,dx = \int \frac{\int K\,dx}{\sqrt{1-(\int K\,dx)^2}}\,dx \qquad 4.27$$

Alternatively, the curvature equation can also be solved by considering

$$W = \frac{u}{\sqrt{1-u^2}} \qquad 4.28$$

then $$\frac{dw}{dx} = \frac{du}{dx} \cdot \frac{dw}{du}$$

$$= \frac{u'}{[1+u^2]^{3/2}} \qquad 4.29$$

and so from equation 4.22

$$\frac{dw}{dx} = K \qquad 4.30$$

Integrating

$$\int dw = \int K\,dx$$

$$\frac{u}{\sqrt{1+u^2}} = \int K\,dx \qquad 4.31$$

leading to

$$u = \frac{\int K\,dx}{\sqrt{1-(\int K\,dx)^2}} \qquad 4.32$$

now $$y = \int u\,dx$$

$$= \int \frac{\int K\,dx}{\sqrt{1-(\int K\,dx)^2}}\,dx \qquad 4.33$$

which is exactly the same equation as derived by Das.

from moment curvature equation 4.10

$$\int K\,dx = \int \left[\frac{M\sigma_0}{I_n}\right]^{\frac{1}{n}} dx \qquad 4.34$$

substitute back for Kdx into equation 4.33 gives

$$y = \int \frac{\iint \left[\frac{M\sigma_o}{I_n}\right]^{\frac{1}{n}} dx}{1 - \left[\iint \left[\frac{M\sigma_o}{I_n}\right]^{\frac{1}{n}} dx\right]^2} dx \qquad 4.35$$

Applying this to a cantilever problem of Fig (4.3)

$$\left[\frac{M\sigma_o}{I_n}\right]^{\frac{1}{n}} dx = \left[\frac{P}{\sigma_o I_n}\right]^{\frac{1}{n}} \frac{n}{n+1}\left[x^{\frac{n+1}{n}} - 1^{\frac{n+1}{n}}\right] \qquad 4.36$$

and substituting equation 4.36 into 4.35 gives

$$y = \int_0^1 \frac{\left[\frac{P}{\sigma_o I_n}\right]^{\frac{1}{n}} \frac{n}{n+1}\left[x^{\frac{n+1}{n}} - 1^{\frac{n+1}{n}}\right]}{\sqrt{1 - \left[\frac{P}{\sigma_o I_n}\right]^{\frac{2}{n}} \frac{n^2}{(n+1)^2}\left[(x^{\frac{n+1}{n}} - 1^{\frac{n+1}{n}})\right]^2}} dx \qquad 4.37$$

Clearly this equation can be solved given the material data. Das (9) showed how this could be done by a simple graphical method. It is easy to establish the moment - curvature relationship once the material properties are known. Therefore if we know the moment, we can find the curvature, and hence determine the deflections.

4.5 BIAXIAL BENDING - PROPORTIONAL LOADING

4.5.1 SYMMETRICAL PROBLEM - CIRCULAR BEAM

Consider now the problem of circular cross-section beam subjected to two moments, say M_y and M_z, Fig (4.5).

This is no different to the problem of simple plastic bending since $M^2 = M_{y^2} + M_{z^2}$ providing that My and Mz increase in proportions

ie $\frac{M_z}{M_y}$ = constant.

4.5.2 RECTANGULAR CROSS SECTION

In the theory of simple bending, it was assumed that the beam was bending about an axis of symmetry and that the resultant forces were acting in this plane. With this restriction, the neutral surface passes through the centroid of the section and is perpendicular to the plane of loading.

Consider the symmetrical beam, Fig(4.6), subjected to two mutually perpendicular moments My and Mz whose resultant is M inclined at angle α to the y axis. Hence

$$\left.\begin{aligned} M_y &= M \cos \alpha \\ M_z &= M \sin \alpha \end{aligned}\right\} \qquad 4.38$$

Within the material limit of proportionality it can be shown

$$\tan \theta = \frac{I_{zz}}{I_{yy}} \tan \alpha \qquad 4.39$$

When the maximum stress exceeds the limit of proportionality, for the beam material, then equation 4.39 is no longer valid.

It has been shown (19) (22) that there is a further rotation of the neutral surface as the material is loaded into the plastic region.

The analyses developed by both Barrett (19) and Brooks (22) are mathematically complex, even though they had used simplified material characteristics. Barrett used the non linear expression of the form

$$\varepsilon = \sigma_E \frac{\sigma}{\sigma_2} + \sigma_o \left(\frac{\sigma}{\sigma_2}\right)^n \qquad - \quad 4.40$$

to describe the material behaviour.

Where σ σ_o and n are material constants

σ_2 is the stress appropriate to 0.2% proof stress.

With reference to Fig (4.7), Barrett developed the following expressions

$$M_z = 4\sigma_2 t^2 d \frac{2}{(\varepsilon_5 - \varepsilon_B)^2}\left[\Phi_1 - \Phi_o + \frac{\varepsilon_5\Phi_3 + \varepsilon_5\Phi_2}{\varepsilon_5 + \varepsilon_B}\right] - \quad 4.41$$

$$M_y = 4\sigma_2 t d^2 \frac{2}{(\varepsilon_5 - \varepsilon_B)^2}\left[\Phi_0 + \Phi_1 + \frac{\varepsilon_B\Phi_3 - \varepsilon_5\Phi_2}{\varepsilon_5 - \varepsilon_B}\right] - \quad 4.42$$

and $$\frac{\varepsilon_B}{\varepsilon_5} = \frac{1 - (t/d)\tan\theta}{1 + (t/d)\tan\theta}$$

where suffix B refers to point B on Fig (4.7)

Where Φ_o, Φ_1, Φ_2 and Φ_3 are functions of σ_2, σ_5, σ_B and the material constants σ_E σ_o and n (see table 4.1)

..

Brooks on the other hand assumed an elastic - perfectly plastic material, with reference to Fig (4.8) obtained the following expressions

$$M_y = \frac{2t\,\sigma_y}{3\cos^2\theta}\left[v_A^2 + v_A v_B + v_B^2 - T^2 - b\sin\theta\,(v_A - v_B)\right] \quad - 4.44$$

$$M_z = \frac{\sigma_y}{\sin^2\theta\cos\theta}\left[\frac{v_A^2\, v_B}{2} - \frac{v_B v_A}{2} + \frac{v_A - v_B}{3}\right] \quad - 4.45$$

$$v_A = d\cos\theta + t\sin\theta \quad - 4.46$$

and $$v_B = d\cos\theta - t\sin\theta \quad - 4.47$$

In each case the analysis is of a complex nature. Both Barrett and Brooks assumed a value of θ (for given material properties and beam geometry) and calculated M_y and M_z and the corresponding α is calculated from equation

$$\alpha = \tan^{-1}\left(\frac{M_z}{M_y}\right) \quad - 4.48$$

A more tractable method of demonstrating the rotation of the neutral surface is to assume a perfectly plastic material. Then at full plasticity (reference to Fig(4.9))

$$M_z = M\sin\alpha = 2\sigma_y\, dt^2\, \frac{2}{3}\, p \quad - 4.49$$

$$M_y = M\cos\alpha = 2\sigma_y\, d^2 t\, (1 - \frac{1}{3}\, p^2) \quad - 4.50$$

where σ_y is the yield stress, d, t and p are dimensions of the beam as indicated on Fig (4.9).

dividing equation 4.99 by 4.50 gives

$$\tan\alpha = \frac{2pt}{d(3-p^2)} \quad -4.51$$

rearranging we have

$$p^2 (d\tan\alpha) + p(2t) - 3d\tan\alpha = 0$$

and solving this quadratic equation gives

$$p = \frac{-2t \pm \sqrt{4t^2 + 12d^2 \tan^2\alpha}}{2d \tan\alpha} \qquad - 4.52$$

and from the diagram, fig (4.9)

$$\theta = \tan^{-1}\left[\frac{pd}{t}\right] \qquad - 4.53$$

It is clear that $\theta \neq \alpha$ unless $p = 0$. Then at $p = 0$ we have the problem of symmetrical bending anyway.

Fig (4.10), (4.11) and (4.12) shows neutral surface rotation as predicted by the three methods discussed above, for three beams of different b/t ratios. We have considered two extremes of non-elastic analysis and it is clear that the material expression used by Barrett is closer to elastic analysis and predicts small rotations of the neutral surface. On the other extreme we have considered a totally plastic material and the predicted rotations are some what greater.

In the cyclic plasticity situation, the material charcteristic equation used by Barrett will require modification because the linear portion is small Fig (4.7). One method of doing this would be to let $\sigma_\varepsilon = 0$ and $\sigma z = 1$ then equation 4.40 will reduce to equation 4.6. We have a material characteristic which lies somewhere between Brook's (elastic-perfectly plastic) and Barrett's (non linear equation 4.40).

Therefore the corresponding rotation of the neutral surface must also lie between their predicted rotations.

For a square beam (b/t = 1) the maximum difference between the predicted rotations of neutral surface by the three methods is small (about 3° see Fig (4.12)). In such a case it would be justified to use the simplest method to evaluate the position of the neutral surface. In practice the design engineer will not always know what value of θ to assume, but he will always know the applied moments. Using Brook's or Barrett's method could prove to be tedious. On the other hand θ could be calculated directly from equations 4.52 and 4.53.

4.6 BIAXIAL BENDING - NON-PROPORTIONAL LOADING

4.6.1 SYMMETRICAL BEAM

Consider the beam in Fig (4.5), once more. This time let the moments M_y and M_z vary independently. Due to the beam's symmetry it is possible to assume that the neutral surface lies parallel to the plane of the resultant moment.

This is certainly true for elastic bending, proportional plastic loading and non proportional plastic loading if we assume no unloading of elements. Consider the load case such M_y is constant and M_z varies from zero to some value greater than M_y. The neutral surface will rotate from its initial position (on the M_z axis) to a new position at angle θ from the z axis.

In order to explore the consequences of the rotation of the neutral surface, let us examine the effects on individual elements of the beam. Consider the load case described above. The stress at A, when $M_z = 0$ is given by

$$\sigma_{Ao} = \frac{M_y R \, Sin\theta}{I} \qquad - 4.54$$

If M_z increases, such that $M_z \neq 0$, Fig (4.13), then the stress point A is given by

$$\sigma_{A1} = \frac{(M_z^2 + M_y^2)^{\frac{1}{2}} R(Sin\theta Cos\phi - Cos\theta Sin\phi)}{I} \qquad - 4.55$$

Dividing equation 4.55 by 4.54 gives

$$\frac{\sigma_{A1}}{\sigma_{Ao}} = 1 - \frac{tan\phi}{tan\theta} \qquad - 4.56$$

Remembering that for a particular element in the beam $tan\theta$ is constant, it can be said that as $tan\phi$ changes from zero to $tan\theta$ then the ratio σ_{A1}/σ_{Ao} will correspondingly go from one to zero. Since σ_{Ao} is the initial stress and σ_{A1} is the new stress, then the conclusion must be that stress at a point A is decreasing with increase of M_z.

There are of course other elements in the beam, where it can be shown that stresses are increasing. This creates no particular problems while the beam or elements remain elastic. However the problem of a deformed beam becomes complicated when individual elements become plastic. For example, point A might then follow stress-strain curve 1-2 Fig (4.14) from its initial state, but unload along curve 2-3. Unloading usually occurs very rapidly to zero stress.

However if the strain is totally removed form the element (condition when neutral surface passes through the point) the stress-strain curve will be 3-4. With further increase of Mz the neutral surface will cross point A and the corresponding stress-strain characteristics will be 4-5.

It should be noted that each element on the beam cross-section will unload from different part of the σ-ε curve after as shown in Fig (4.14).

4.6.2 RECTANGULAR BEAM

For a retangular beam Fig (4.6) it can be shown

$$\frac{\sigma_{Al}}{\sigma_{Ao}} = \frac{I_{zz}\ \mathrm{Sin}(\theta - \phi)}{I_{\phi\phi}\ \mathrm{Sin}\theta\ \mathrm{Cos}\alpha} \qquad - 4.57$$

If we let $\alpha \cong \phi$ which is approximatley true for square beam as demonstrated earlier, then

$$\frac{\sigma_{Al}}{\sigma_{Ao}} = \frac{I_{zz}}{I_{\phi\phi}}\left[1 - \frac{\tan\phi}{\tan\theta}\right] \qquad 4.58$$

For a special case of a square sectioned beam it can be shown that $I_{zz} = I_{yy} = I_{\phi\phi}$. The problem reduces to that of symmetrical beam, equation (4.56) and therefore similar arguments on elements unloading must apply.

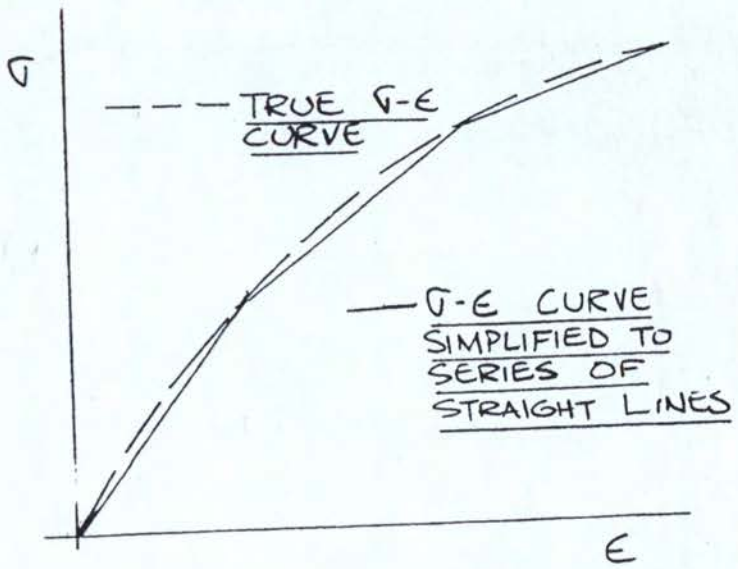

SIMPLIFICATION OF σ-ε CURVE

FIG 4.1

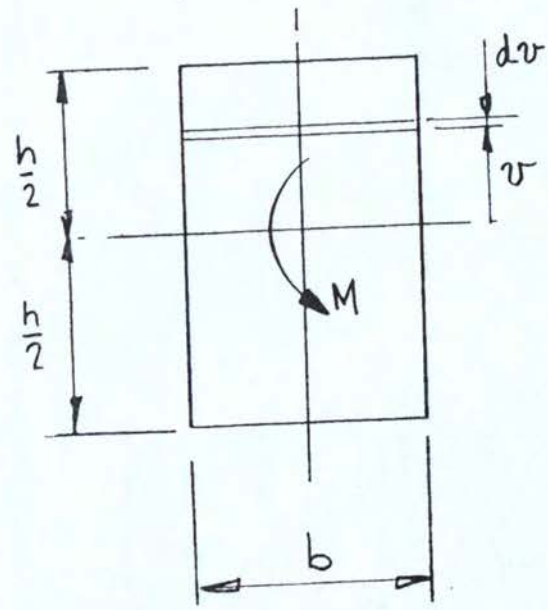

RECTANGULAR BEAM SUBJECTED TO PURE BENDING

FIG 4.2

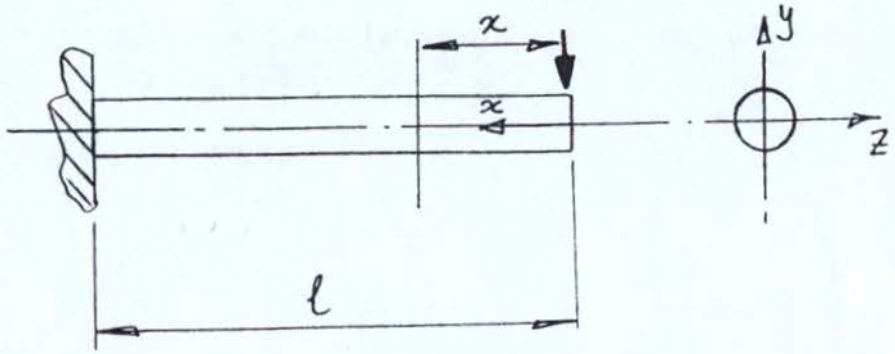

CANTILEVER BEAM

FIG 4.3

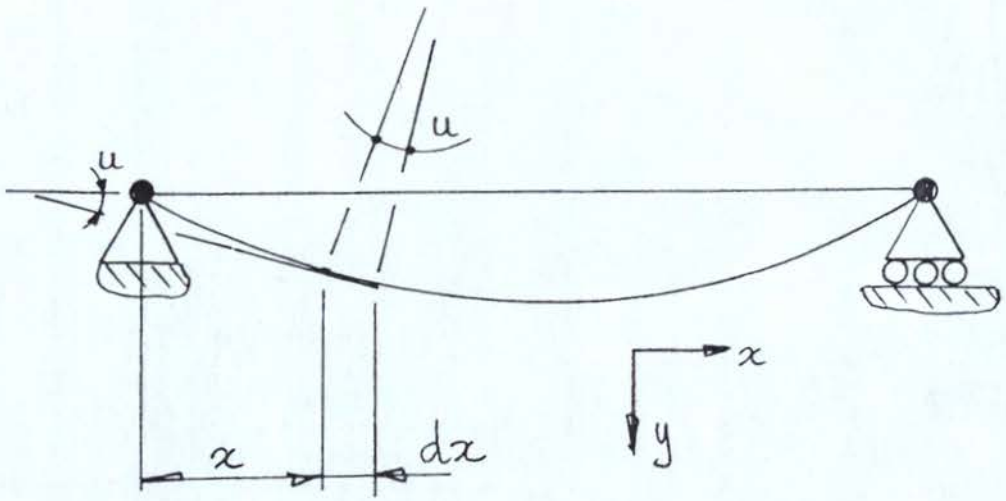

BENDING OF A BEAM

FIG 4.4

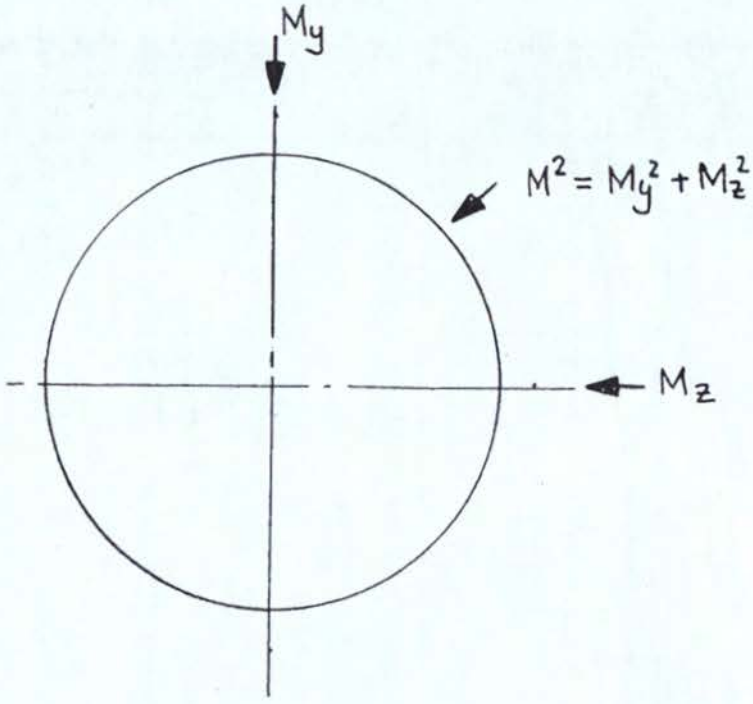

BIAXIAL BENDING
SYMMETRICAL PROBLEM

FIG 4.5

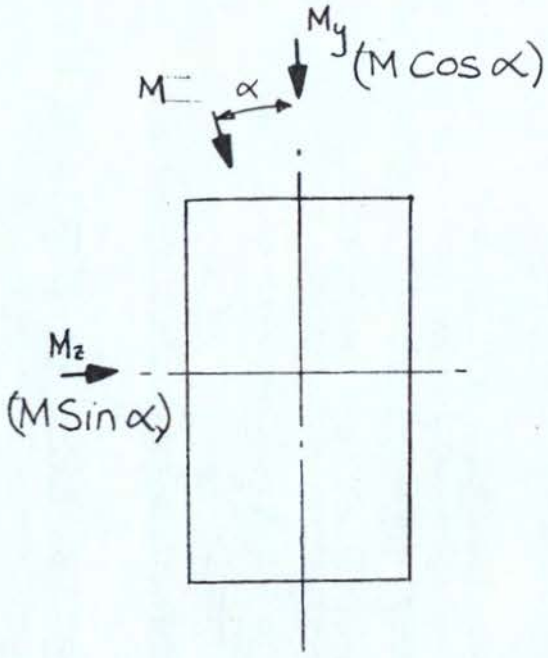

BIAXIAL BENDING
UNSYMMETRICAL PROBLEM

FIG 4.6

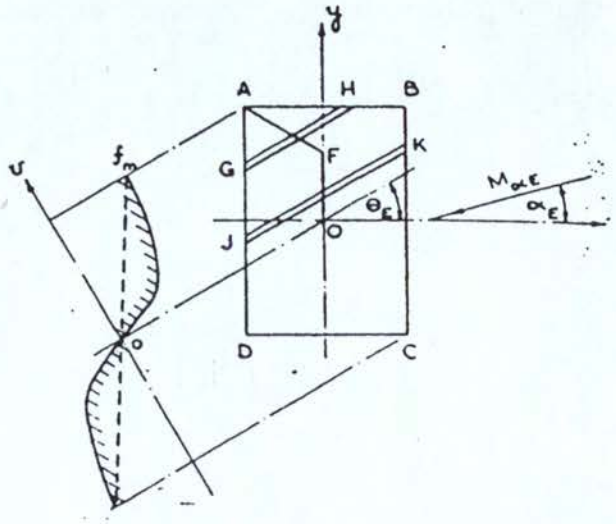

UNSYMMETRIC BENDING
- BARRETT (19)

FIG 4.7

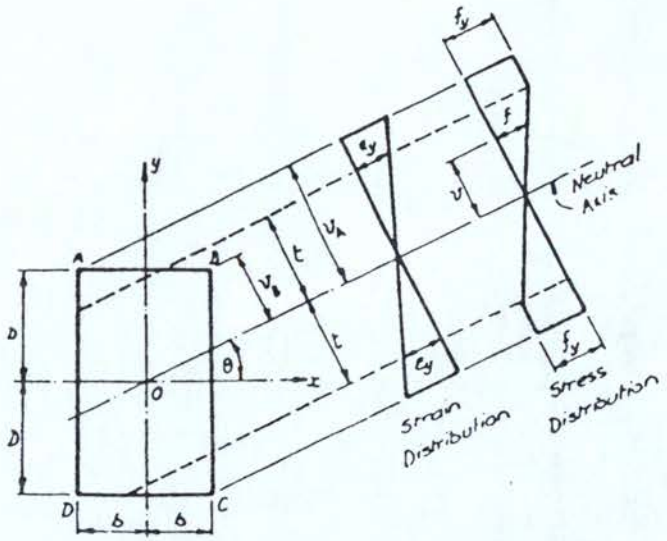

UNSYMMETRIC BENDING
- BROOKS (22)

FIG 4.8

THE FUNCTIONS Φ_0, Φ_1, Φ_2 AND Φ_3

	Φ_0	Φ_1	$\epsilon_4\Phi_2$	Φ_3/ϵ_4
F_5^3	$A^3/3$			
F_5^{n+2}	$AB\dfrac{n+1}{n+2}$			
F_5^{2n+1}	$B^2\dfrac{n}{2n+1}$			
F_M^3		$A^3/3$		
F_M^{n+2}		$AB\dfrac{n+1}{n+2}$		
F_M^{2n+1}		$B^2\dfrac{n}{2n+1}$		
$F_5^2 - F_M^2$				$A/2$
$F_5^4 - F_M^4$			$A^3/4$	
$F_5^{n+1} - F_M^{n+1}$				$B\dfrac{n}{n+1}$
$F_5^{n+3} - F_M^{n+3}$			$A^2B\dfrac{n+2}{n+3}$	
$F_5^{2n+2} - F_M^{2n+2}$			$AB^2\dfrac{2n+1}{2n+2}$	
$F_5^{3n+1} - F_M^{3n+1}$			$B^3\dfrac{n}{3n+1}$	

Note: $F_5 = f_5/f_2$, $F_M = f_M/f_2$, and other symbols have the meanings already assigned.

FUNCTIONS

~AS DEVELOPED BY BARRETT (19)

TABLE 4.1

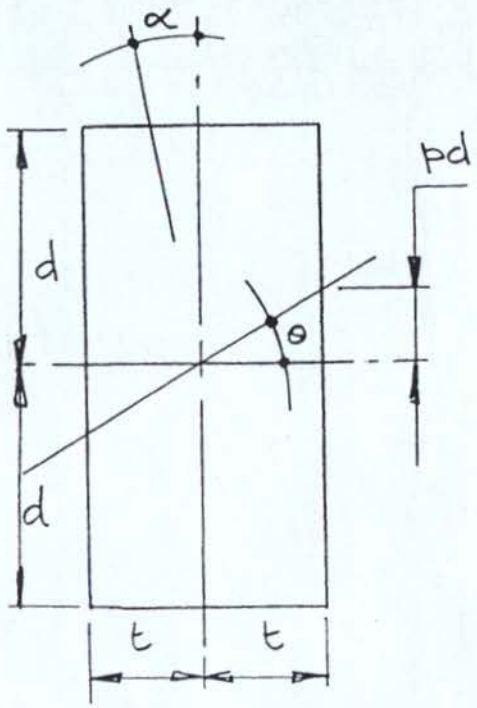

FIG 4.9

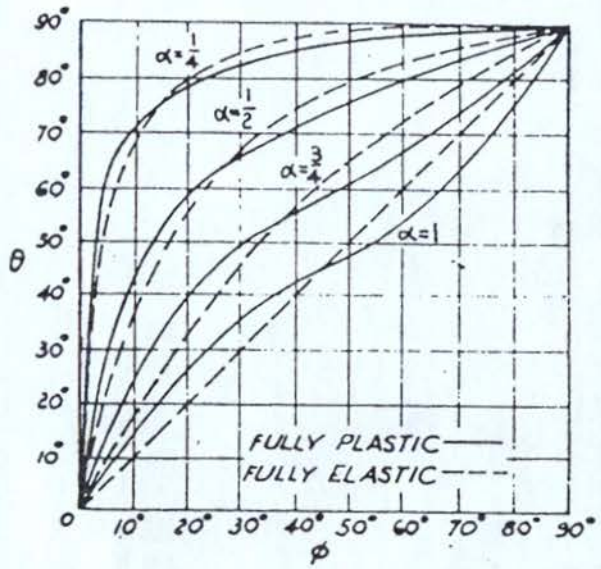

ROTATION OF NEUTRAL SURFACE - AFTER BROOKS (22)

FIG 4.10

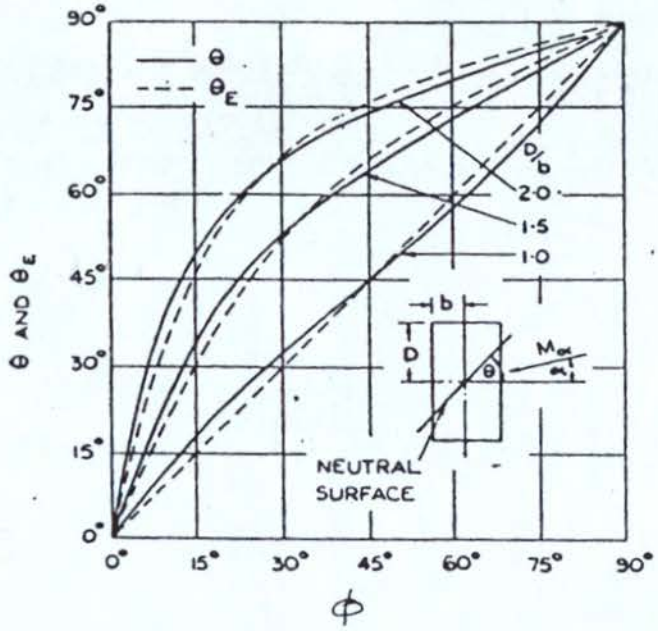

ROTATION OF NEUTRAL SURFACE
- AFTER BARRETT

FIG. 4.11

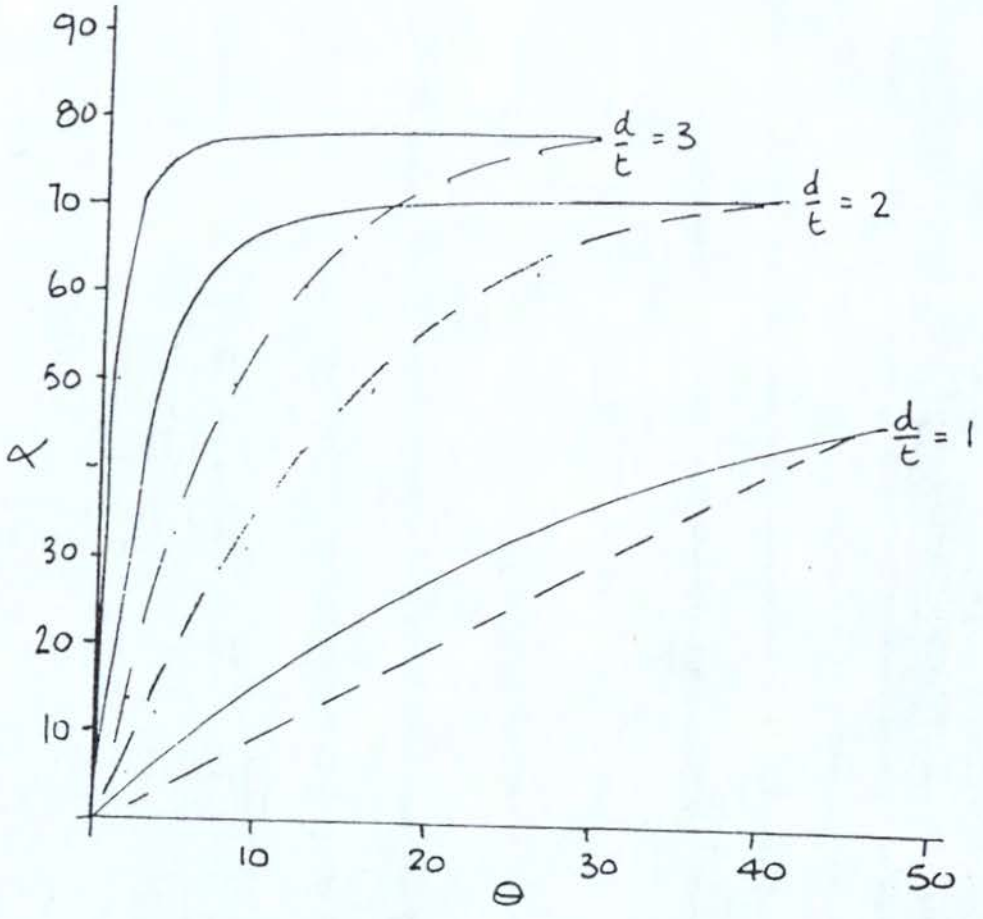

ROTATION OF NEUTRAL SURFACE
- REF. EQUATION 4.53

FIG 4.12

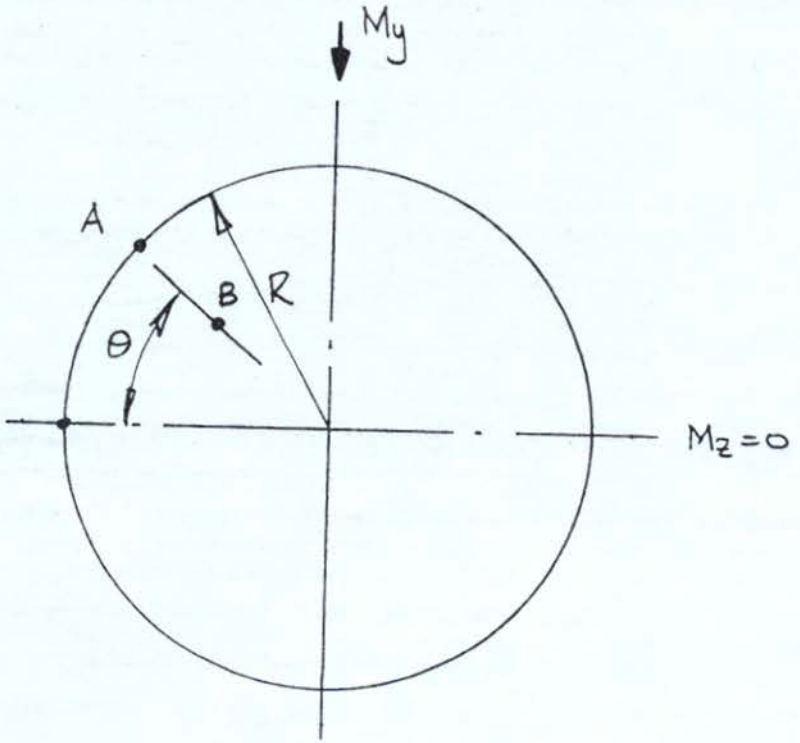

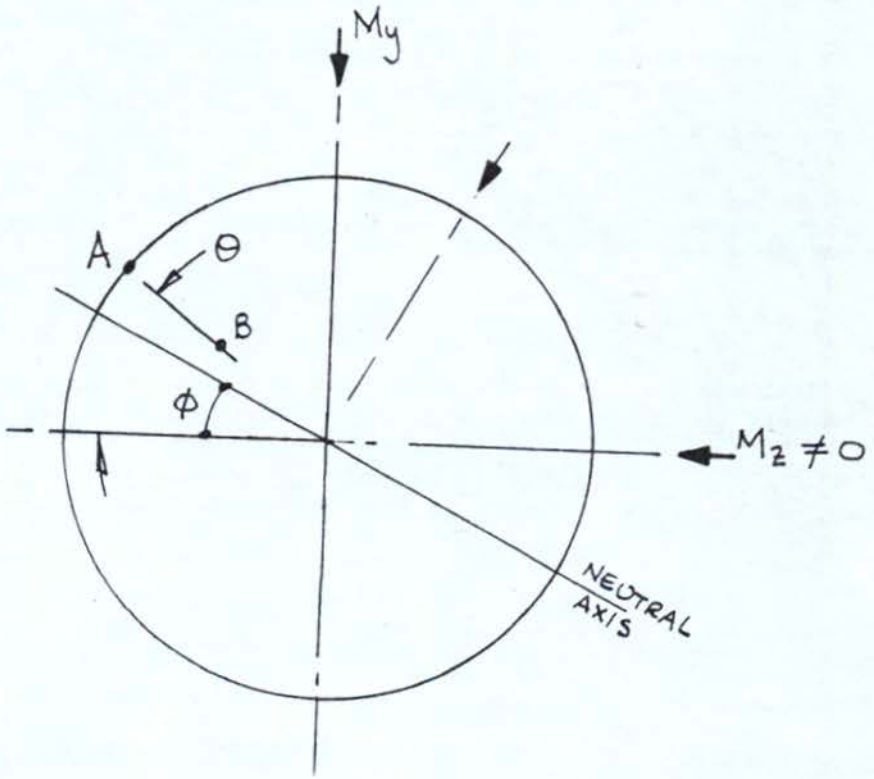

BIAXIAL BENDING NON PROPORTIONAL LOADING

FIG 4.13

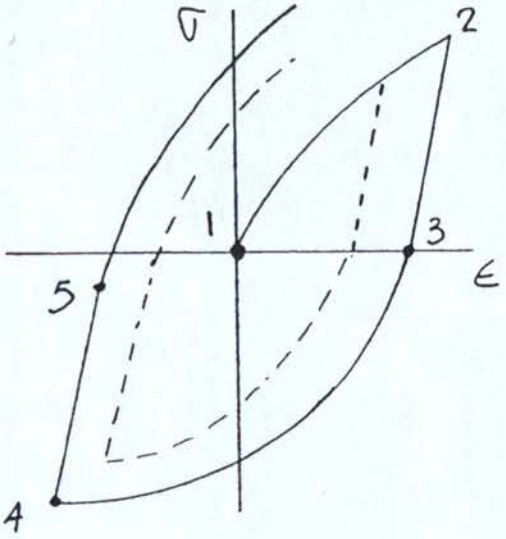

— ELEMENT 'A'

--- ELEMENT B

— REF. FIG 4.13

ELEMENTAL UNLOADING CURVE

FIG 4.14

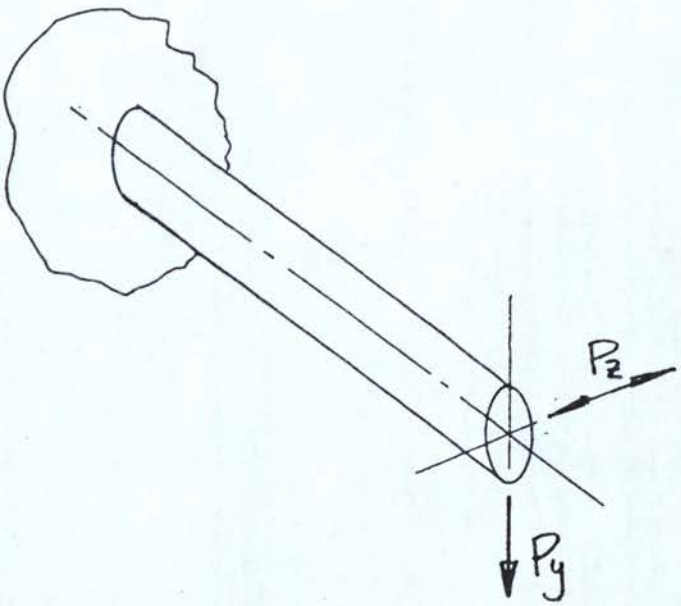

CANTILEVER SUBJECTED TO BIAXIAL CYCLIC BENDING

FIG 4.15

4.7 BIAXIAL CYCLIC - PLASTIC BENDING

4.7.1 THE PROBLEM

The literature has shown very little published material on biaxial plastic bending. The little that has been published (19) (20) (22) (17) (18) has concerned itself almost exclusively with proportional loading and has neglected two major elements.

(i) Rotation of Principal Planes

(ii) Unloading of elements during rotation of the principal planes.

Consider a cantilever with a steady downward load and subjected to increasing horizontal forces Fig (4.15), which induces plastic zones within the beam. As the loading proceeds there is an irriversible downward deflection. If the horizontal forces are cyclic then the downward deflection is cumulative and we have a case of incremental collapse or a ratchet mechanism.

The problem of predicting the downward deflection would be difficult, even for the case, when

a) the applied moments are proportional ie there is no rotation of the principal planes

b) the loading is non-proportional but the rotation of the principal plances is ignored.

However in practical terms we need to assess whether or not these gross simplifications are justified ie we need to consider the principal planes and the effect of unloading.

This poses two main problems:

(i) We need a knowledge of the material properties throughout the loading and unloading process

(ii) We need to follow the deformation of each element in the beam throughout the loading and unloading processes.

If we can include this data in our analysis then the curvature along the beam can be determined and integrating along the length of the beam will give the deflections.

4.7.2 MATERIAL PROPERTIES

One of the basic difficulties in dealing with problems involving plastic deformation, particularly where unloading occurs is to update material data to "current" material data. This is particularly evident in cyclic plasticity work, where the first quarter cycle always produces a notably different type of stress-strain characteristics than the subsequent cycles. Consider, for example, Man-Ten steel (52). Fig (4.16) clearly shows that the monotonic (first quarter cycle) characteristics are notably different from the cyclic characteristics.

In order to make the problem tractable let the non-linear equation, used to represent the monotonic σ-ε curve also represent σ-ε curves then

$$\sigma_{cyclic} = \sigma_{cyclic}\, \varepsilon^{n_{cyclic}} \qquad - 4.59$$

From Fig (4.16) it is evident that all cyclic σ-ε curves have similar shapes. Therefore for a given strain amplitude (Δε) we will have corresponding constants σ_o and n or

$$\sigma_o = f_1(\Delta\varepsilon) \qquad - 4.60$$

$$\text{and} \quad n = f_2(\Delta\varepsilon) \qquad - 4.61$$

If we fit a best curve, using least squares technique, to each of the cyclic curves then we can evaluate σ_o and n for each curve. A plot of σ_o against Δε and n against Δε will give graphical equivalent to equations.

Fig (4.17a) and (4.17b) shows such plots for the Man-Ten steel. It is clear that at high strain amplitudes ie .012 or higher the n and σ_o approach a steady condition where the changes in both of these constants are small.

It is acknowledged that the curves shown in Fig (4.16) are those obtained for steady state, and σ_o and n will also change during the intermediate cycles needed to reach the steady state conditions. In the present investigation these changes will be neglected if the test materials reach a steady state condition after relatively few cycles.

4.7.3 ANALYTICAL SOLUTION

If the cross section of the beam is divided into a number of elemental, Fig (4.18), fibres, then as the moments M_y and M_z are applied, the stress and deformation of each elemental fibre can be identified and its position on the monotonic or cyclic stress-strain curve established.

The effect of unloading "elastic"elements as they are crossed or approached by the neutral surface is obviously zero because no Bauschinger effect is involved. However the unloading and reverse loading of elements which ahve been plastically deformed cannot be ignored. In fact they carry a reduced load which results in an increased load carried by other elements and hence increased stress.

Clearly the problem is of a complex nature, complicated by the fact that elements are unloading from different stess-strain states and therefore it is important that realistic material data is used and a record of individual elements' load history is kept.

If we assume that the material is such that it settles to steady state conditions after the initial plastic deformation then the material behaviour can be modelled using equations 4.60 and 4.61.

Now the resulting moment at any cross-section is given by

$$M = \sum_{\text{element} = 1}^{\text{element} = i} \sigma_{\text{elemental}} \text{ v Area}_{\text{elemental}} \quad - 4.62$$

where i is the total number of elements making up the cross section

and v is the perpendicular distance between the neutral surface and the centroid of the element.

The problem of establishing the position of the neutral surface for a rectangular cross-section is a complex one. Firstly because the rotation is a function of the material property and each element within a cross section is unloading from a different state of stress-strain curve. Therefore it could be regarded that each element has a different material property. Secondly because a cantilever beam could be totally elastic at one end and totally plastic at the other. A typical neutral surface could be positioned within the beam as shown in Fig (4.19).

It will be assumed that over a small elemental length the angle of rotation of the neutral surface is constant as shown in Fig (4.19) from material properties of a fibre which is further from the neutral surface. This will give the other extreme to neglecting the rotation altogether.

4.7.4 COMPUTER PROGRAM

4.7.4.1 GENERAL PROGRAM

The analysis discussed above clearly lends it self to a computer program, due to a vast amount of arithmetic operations and "book-keeping" involved.

A computer program "MOMENT"[NOTE] is developed for a Tektronix 4052A - 64 K desk top computer and Tektronix 4907 (630K) disk drive unit. The listing of the program is shown in appendix 2.

The basic procedure followed in the program as followed.

1 Apply P_y - constant vertical load.

2 Increment P_z from zero to Pmax.

3 Set strain value at the onset of plastic deformation.

4 Calculate geometry of element and hence its area, and co-ordinates with respect to the centroid.

5 Estimate initial strain distribution.

6 Evaluate stress using equation the relationship given in equation (4.6)

7 Calculate the internal bending moment.

8 Check if $M_{calculated} = M_{applied}$.
if this condition is satisfied then move to step 10.

9 Adjust estimated value of maximum strain and return to step 5.

10 Record all data associated with each element on Magnetic disk ie its load history and maximum strains.

NOTE: The listing shows a circular cross-sectioned beam version with various enhancements - discussed later.

Procedures 1 to 10 are repeated for all sections of the beam to evaluate strains. The method developed in the program usually require three to five iterations depending on the initial estimation to establish strains.

When P_z is increased in step 2, the material data is updated according to equation 4.60 amd 4.61 and based on elemental load history. (In practice graphical data of Figs (5.11), (5.12), (5.19) and (5.20) is used and linearly interpolated between data points).

From strains the curvature is evaluated (equation 4.1) and subsequently deflections are calculated.

4.7.4.2 ENHANCEMENTS TO THE COMPUTER PROGRAM

Demonstration of Unloading and Unloading Process.

In order to demonstrate the unloading and the reverse loading process the moment program was enhanced to give graphical output of the current state of each element ie its current position on the stress-strain hysterisis curve. This was however only done for a circular beam, due to its symmetry about all axis passing through the centroids made algorithms more tractable, than a rectangular beam. Fig (4.20) (4.21) shows typcial graphical output. Each element which has undergone a plastic deformation has been coded with a letter A through X. Detailed description of this code is given in section 5.

4.8 THE YIELD SURFACE

The use of the yield surface together with flow rules and the normality rule has received considerable attention in plasticity for plane stress problems. Some yield surfaces have been developed for beams subjected to bending with axial loads (7) but generally the uses of yield surfaces in biaxial bending has not been developed, apart from some work by Heyman (23). He considered the problem of an angle section subjected to pure bending and showed that at full plasticity that strong and weak principal axes of bending resulted. the strong and weak axes are not orthogonal. The yield surface for an angle section is shown Fig (4.22). The general point P represents combinations of bending moments M_y and M_z which will just produce full plasticity of the cross section. In accordance with the normality rule of plasticity the corresponding axis of bending is given by the outward normal to the yield surface as shown. The position of the weak principal axis is also shown. The point A and 'A' are cusps of the yield locus and, similar to the corners in a yield surface, the direction of deformation are indeterminate at these points, being strongly dependent on very slight variations in the ratio of M_z/M_y.

There appears to be no reference to non-proportional loading systems, the effects of work hardening on the shape of the yield surface and the general problem of cyclic bending will result in Bauschinger type effects.

These have been modelled previously in plane stress by a combination of isotropic and kinematic hardening and it is worth exploring the possibility of extending these approaches to the bi-axial bending problem.

It was shown (53) that kinematic models were not generally applicable to incremental collapse in the plane stress problems of tubes subjected to cylic torsion with a sustained end load or tubes subjected to cylic push-pull with models predicted a shakedown condition with a limit on any accumulated ratchetting strains. However it is worth investigating their range of application to the bending problem.

4.8.1 RECTANGULAR BEAM

It has already been shown that for unsymmetrical bending the neutral surface ceases to be perpendicular to the line of applied bending.

Consider the case of rectangular beam under the action of M_y and M_z Fig (4.6).

from equation (4.49) we have

$$P = \frac{3M_z}{4\sigma_0 dt^2} \qquad - \quad 4.63$$

substitute for p into equation (4.50) gives

$$\frac{3}{16}\frac{M_z^2}{\sigma_0^2 d^2 t 4} + \frac{M_y}{2\sigma_0 d^2 t} = 1 \qquad - \quad 4.64$$

A complete plot of this equation, the similar expression for tan θ greater than d/t and of all these expressions with signs reversed (bending in the opposite sense) is shown in Fig (4.23). This is the yield surface for a rectangular cross sectioned beam acted upon by bending moments Mz and My.

If we apply the concept of plastic potential such that

$$dK_y = d\lambda \frac{df}{dM_y} \quad - \quad 4.65$$

and $$dK_z = d\lambda \frac{df}{dM_z} \quad - \quad 4.66$$

then the normality rule applies. Dividing equation (4.65) by equation (4.65) gives

$$\frac{dK_z}{dK_y} = \frac{dM_y}{dM_z} \quad - \quad 4.67$$

Differentiating equation (4.64) gives

$$\frac{dM_y}{dM_z} = \frac{-3M_z}{4t^3\sigma_0} \quad - \quad 4.68$$

Substituting for Mz (from equation (4.63)) we have

$$\frac{dM_y}{dM_z} = -\frac{pd}{t}$$

$$= - \tan \theta \quad - \quad 4.69$$

$$\frac{dM_y}{dM_z} = \frac{dK_z}{dK_y} = - \tan \theta \quad - \quad 4.70$$

this is the same θ as that of equation (4.53).

Superimposing this on the yield suraface will indicate the relative proportion and the directions of the deformations.

From equation (4.67) the value of M is maximum or minimum when

$$M_x \, dM_x + M_y \, dM_y = 0 \qquad - \quad 4.71$$

or $$\tan \theta = \tan \alpha \qquad - \quad 4.72$$

thus the neutral axis and the axis of applied bending will coincide when M is maximum or minimum. It is these positions which Heyman (23) called strong and weak axis.

4.8.2 CIRCULAR BEAM

This is probably the simplest case to consider. There are no strong and weak axes to consider and the yield surface will be given by

$$M_z^2 + M_y^2 = \left[\frac{2}{3} \sigma_0 R^3\right]^2 \qquad - \quad 4.73$$

Applying the concept of the plastic potential give

$$\frac{dK_z}{dK_y} = \tan \alpha$$

Now for purely radial loading ie no rotation of the neutral surface it would be possible to model cyclic bending with kinematic type hardening and the yield surface would translate normal to the radial load. This would give a reduced moment on reversal of the moment and therefore model the Bauschinger effect. Other models could be used, such as given by Mroz (41) which consists of a series of concentric circles, each representing different work hardening moduli.

It should be possible therefore to model the cyclic moment curvature relationship for radial loading conditions. However we must conclude that radial loading conditions are unlikely to occur in practice and we are faced with the condition of sustained steady loads together with cyclic loads. In this case the neutral surface will rotate and elemental fibres will unload. If we neglected this factor and assumed no unloading we can see the kinematic model would predict a shakedown and a limit to the downward deflection. This is because the yield surface would eventually only move vertically up and down and there would not be any component of curvature in the direction of the follow up load.

If we now consider the effect of unloading due to rotation of the neutral surface we can conclude that elemental fibres are carrying reduced or no stress at all. If for the sake of argument the elements shaded Fig (4.24) are unloading and are carrying no stress, then the strength contributing elements of the beam make up a different shape (unshaded part of Fig (4.24)). It is clear that due to elements not contributing to the beam strength, it is considerably weaker about the M_y axis and its effect about the M_z axis is small. The correnspondingyield surface may also be modified as shown Fig (4.25).

It is clear that the yield surface is changing in a very complex manner in bi-axial cyclic bending and it was felt that there would be little to be gained in attempting to model the yield surface as a means of predicting the ratchetting deflections.

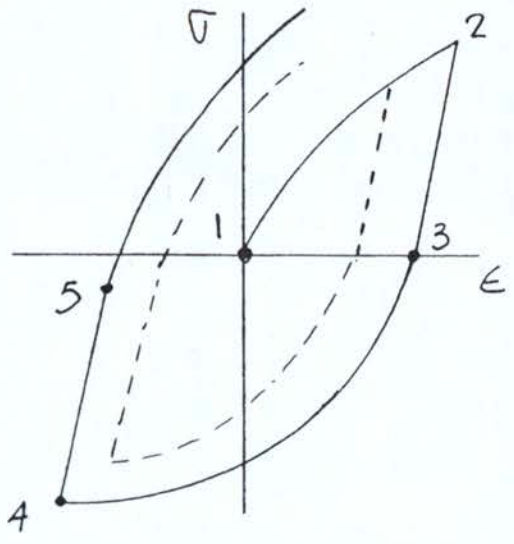

ELEMENTAL UNLOADING CURVE

FIG 4.14

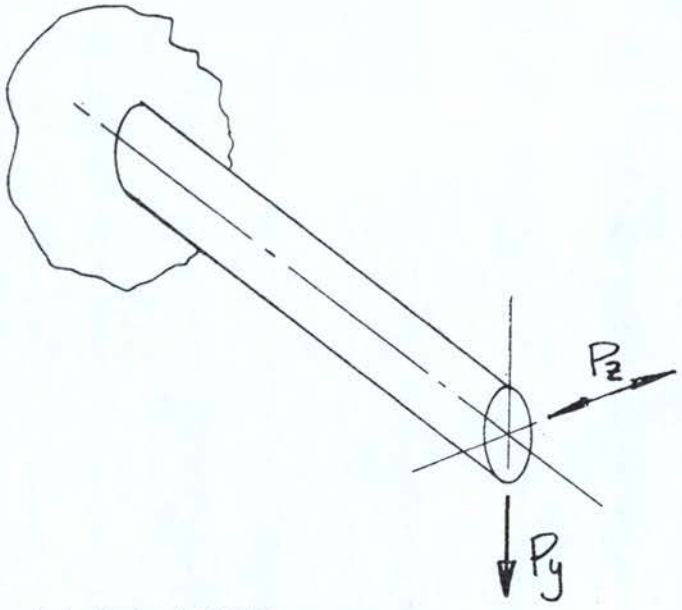

CANTILEVER SUBJECTED TO BIAXIAL CYCLIC BENDING

FIG 4.15

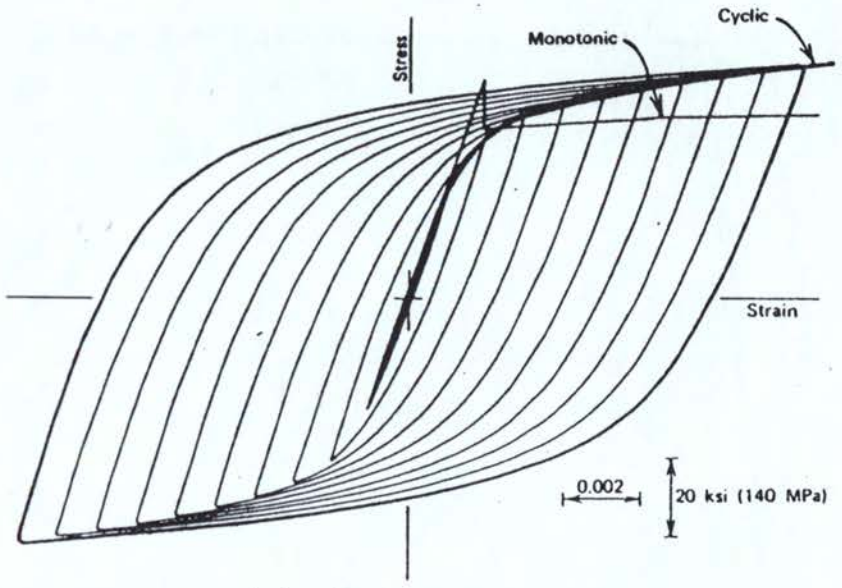

CYCLIC STRESS - STRAIN CURVES - COMPARED WITH MONOTONIC STRESS - STRAIN CURVE – REF (52)

FIG 4.16

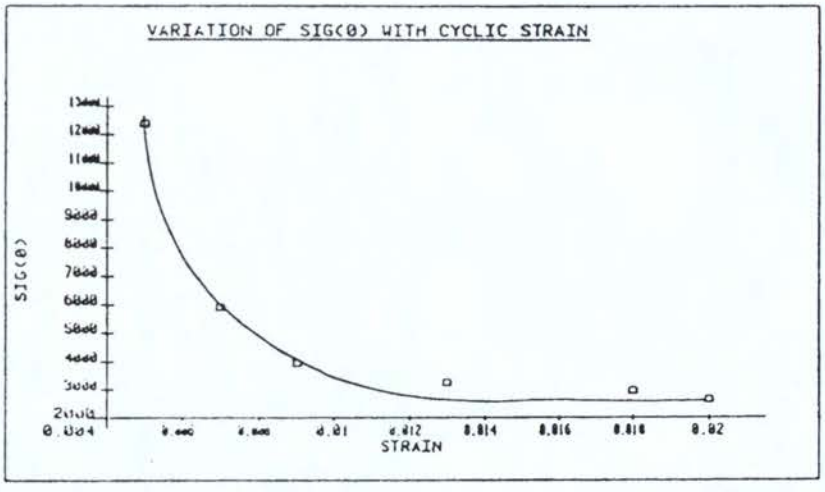

FIG 4.17 (a)

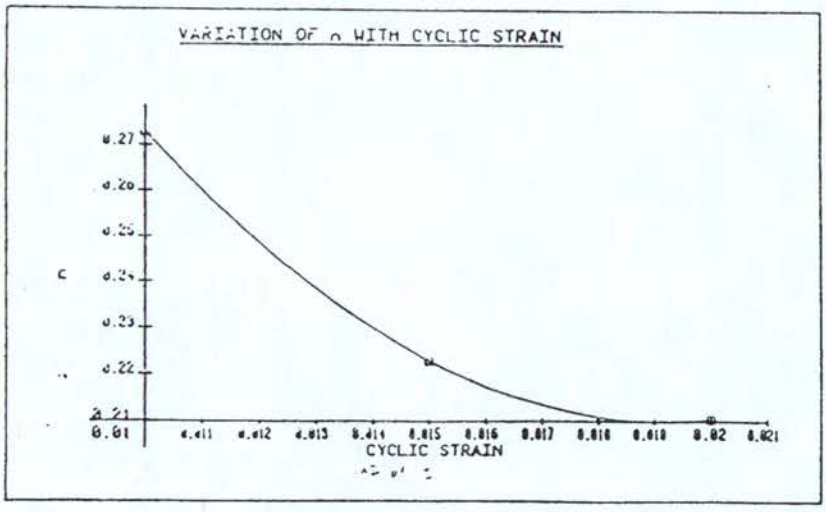

FIG 4.17 (b)

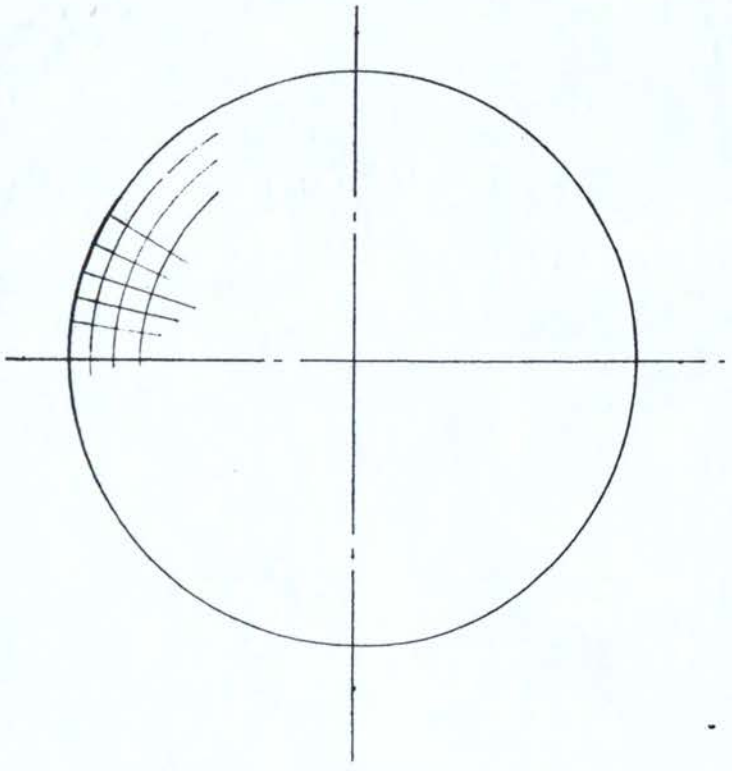

BEAM - DIVIDED INTO ELEMENTAL FIBRES

FIG 4.18

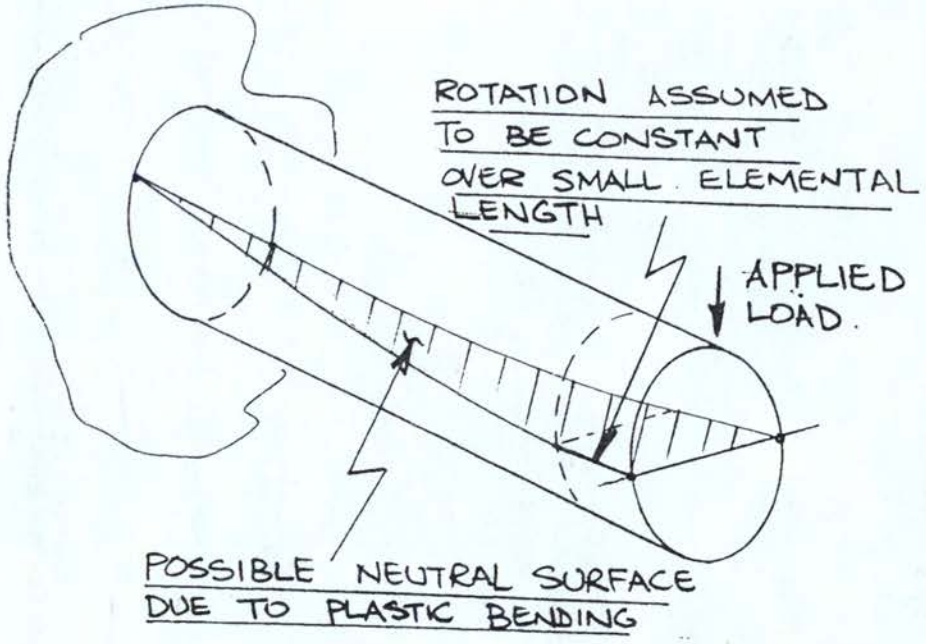

FIG 4.19

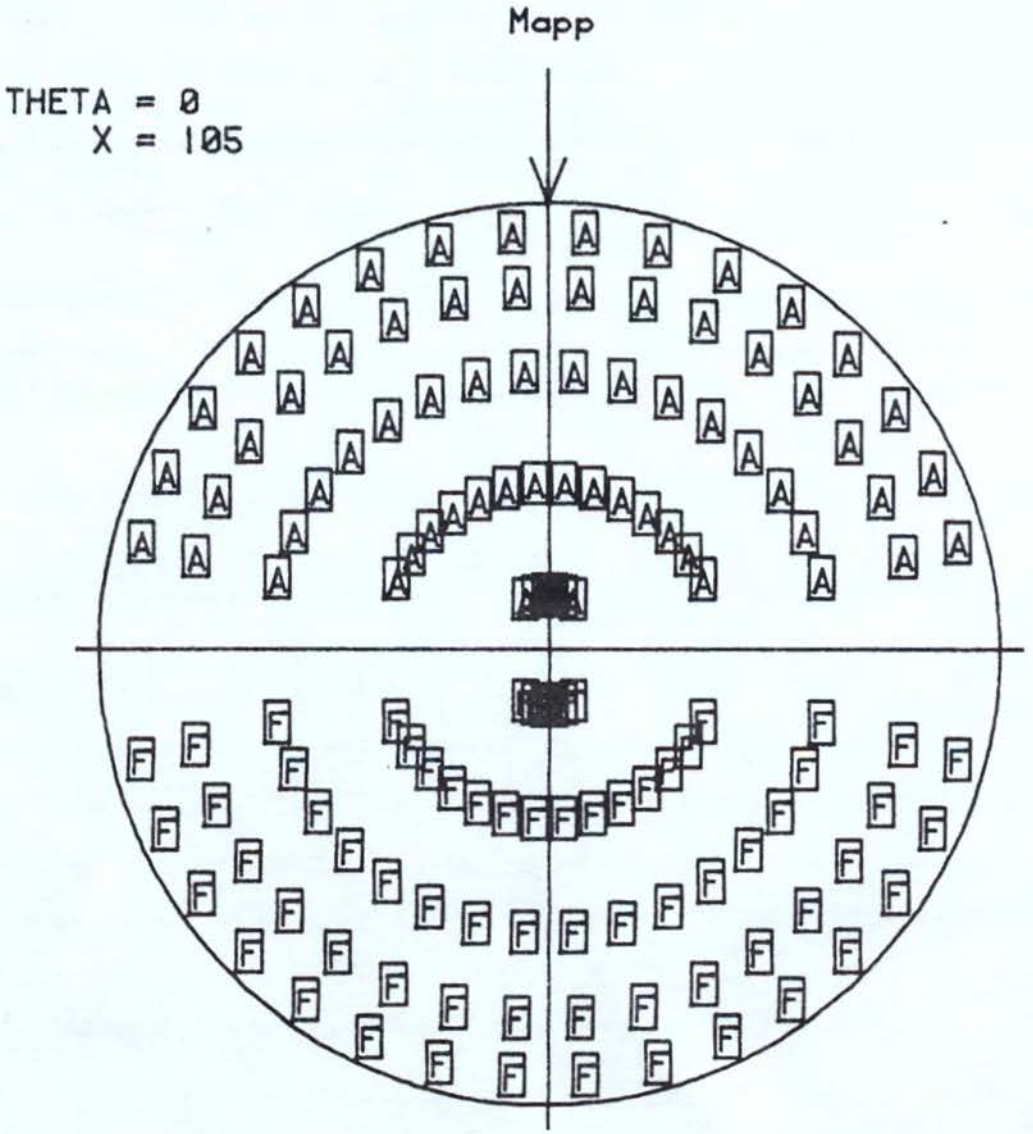

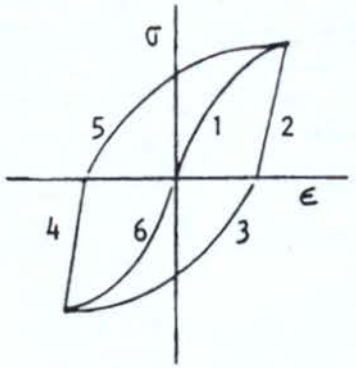

A	1
B	2
C	3
D	4
E	5
F	6
H	1 - 6
I	6 - 1
J	1 - 2
K	1 - 2 - 3
L	6 - 4
M	6 - 4 - 5
N	3 - 4
P	3 - 4 - 5
R	5 - 2
S	5 - 2 - 3
W	2 - 3
X	4 - 5

FIG 4.20

THETA = 45
X = 105

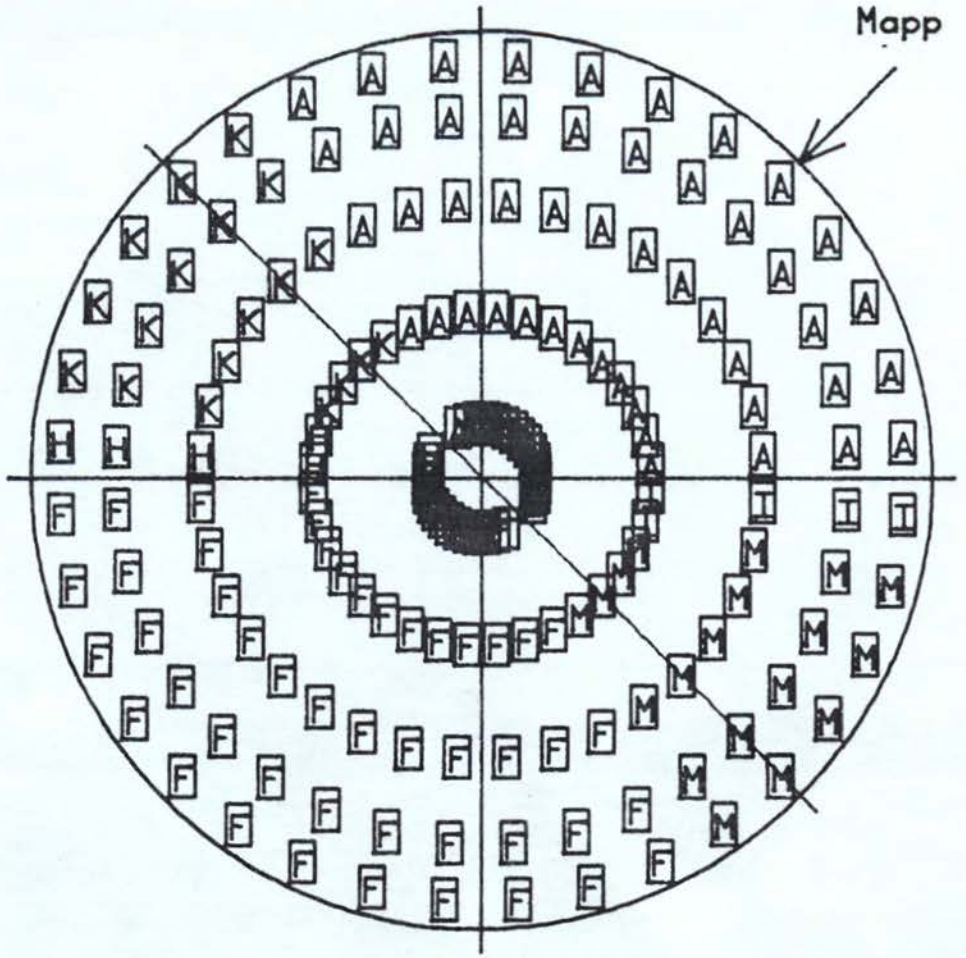

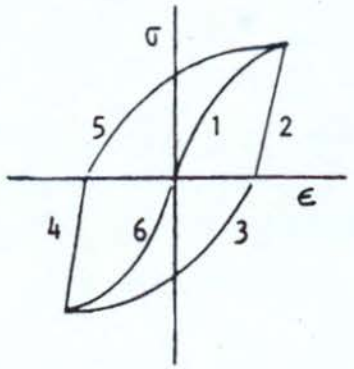

A	1
B	2
C	3
D	4
E	5
F	6
H	1 - 6
I	6 - 1
J	1 - 2
K	1 - 2 - 3
L	6 - 4
M	6 - 4 - 5
N	3 - 4
P	3 - 4 - 5
R	5 - 2
S	5 - 2 - 3
W	2 - 3
X	4 - 5

FIG. 4.21

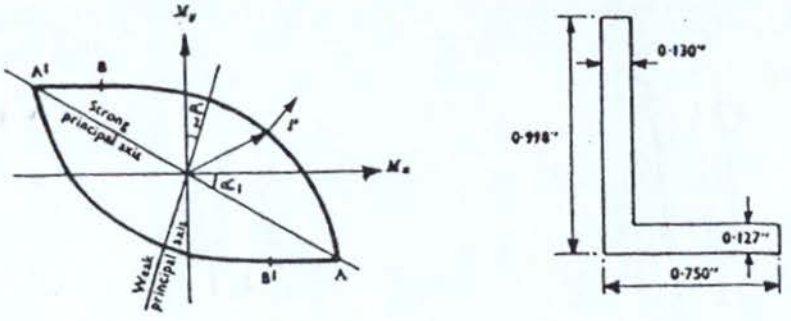

YIELD SURFACE FOR ANGLE SECTION
-AFTER HEYMAN (23)

FIG 4.22

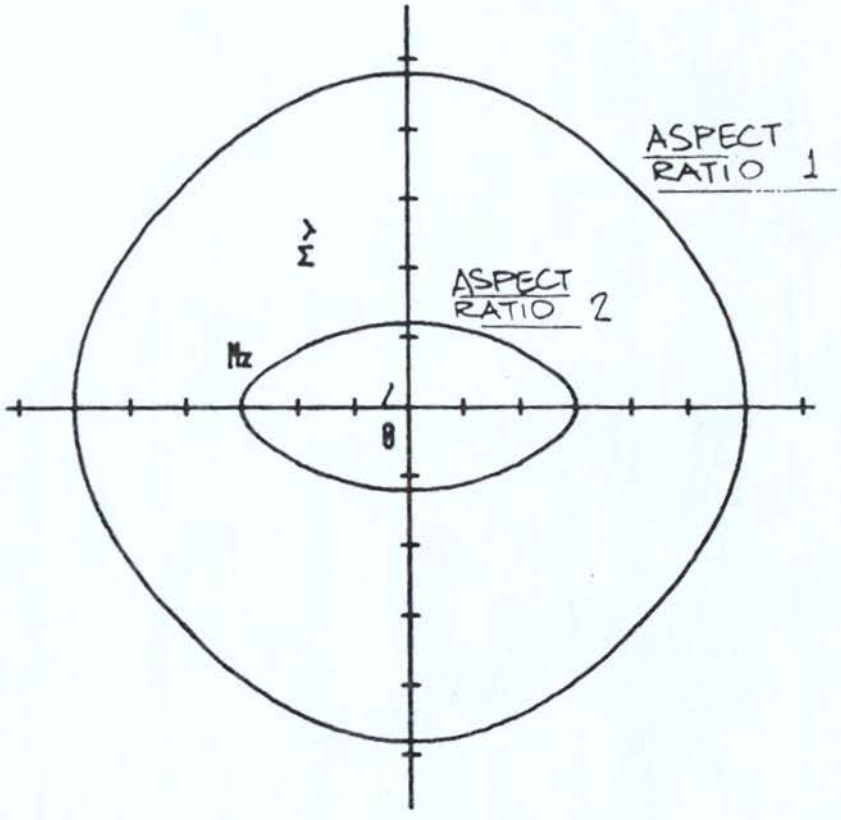

YIELD SURFACE FOR RECTANGULAR SECTION

FIG 4.23

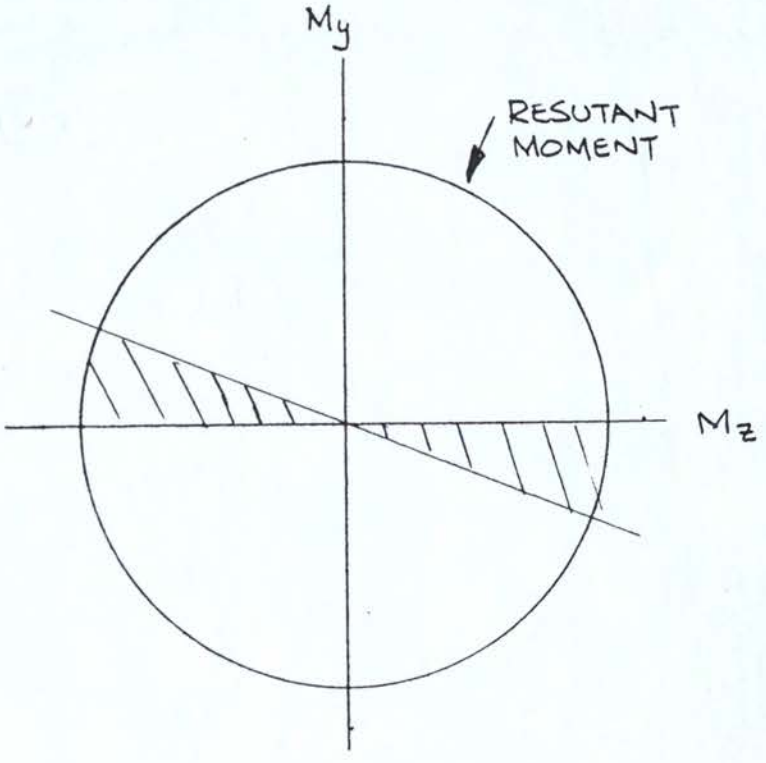

EFFECT OF UNLOADING

FIG 4.24

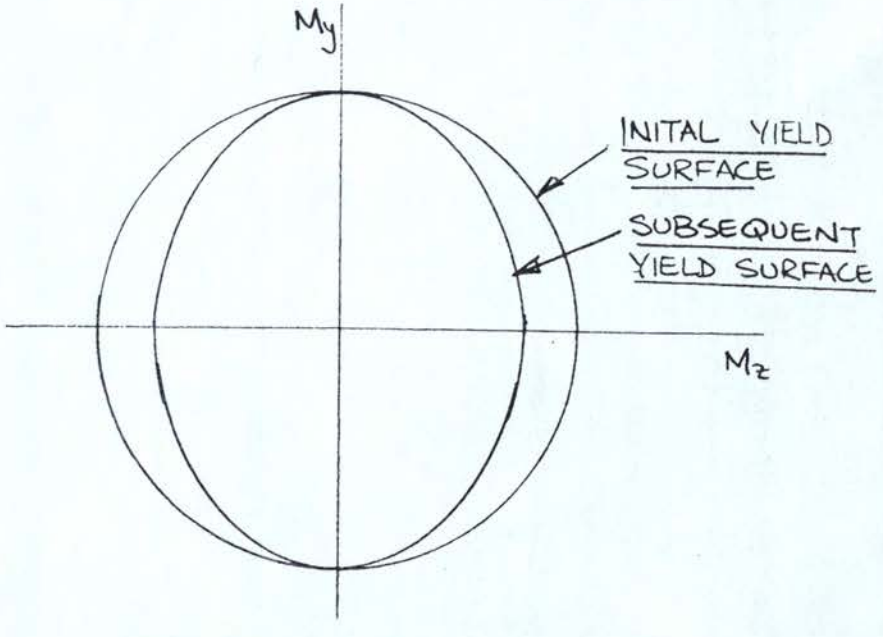

MODIFICATION OF THE YIELD
SURFACE DUE TO UNLOADING

FIG. 4.25

CHAPTER 5

RESULTS AND DISCUSSION

CHAPTER FIVE

5.0 RESULTS AND DISCUSSION

5.1 MATERIAL DATA

5.1.1 MONOTONIC TENSILE PROPERTIES

The uniaxial tensile stress-strain characteristics for the stainless steel (AISI 321) and the mild steel (EN32B) are shown in Figs (5.1) and (5.2). The stainless steel shows the typical strain hardening characteristics associated with this austensite - martensite transforming steel, with hardening continuing up to 60% direct strain, reaching an ultimate tensile strength of 650 N/mm^2 after yielding at approximately 230 N/mm^2. The mild steel shows upper and lower yield point characteristics, a period of non-homogeneous deformations, an initial yield pint of 300 N/mm^2 and a UTS of 450 N/mm^2. The figures also show the best curve fit using the power law

$$\sigma = \sigma_0 \, \varepsilon^n \qquad - \quad 4.6$$

It is clear that the discontinuity in the mild steel characteristics make modelling of this material very difficult and there are obviously gross errors in the region of initial yield. However the power law models material behaviour very well at the higher strains. The power law models the stainless steel characteristic quite well, although errors can be detected at low strain levels.

Using the theoretical stress strain curves, the moment-curvature relationships for square and circular beams have been derived for both materials and are shown in Figs (5.3) and (5.4).

5.1.2 CYCLIC MATERIAL PROPERTIES

Both materials settled down to a steady state condition very rapidly, with little difference being observed after 2 cycles. The steady state cyclic stress strain curves for mild steel at strains of ±0.5%, 1%, 1.25%, 1.5%, 1.75% and 2% are shown in Figs (5.5), (5.6), (5.7), (5.8), (5.9), (5.10), together with the best curve fits from the power law. It can be seen that the simple power law has its limitations in modelling cyclic material behaviour at these relatively small plastic strain levels although a reasonable fit is obtained at all the strain levels. The variation of the material constant n, with the cyclic strain range is shown in Fig (5.11) and the indications are that it quickly falls to a fairly constant value between 0.25 - 0.3 for cyclic strains above ±1.75%. Similarly the material constant σ_0 is seen to settle at a value of 1250 in Fig (5.12).

The steady state cyclic stress-strain curves for the stainless steel are shown in Figs (5.13), (5.14), (5.15), (5.16), (5.17), (5.18) together with the best curve fit. The power law models this material better than the mild steel but there are still significant errors at some parts of the curves. The variation of the material constant σ- and n are shown in Fig (5.19) and (5.20) and it can be seen that they also tend towards stable but higher values than the mild steel.

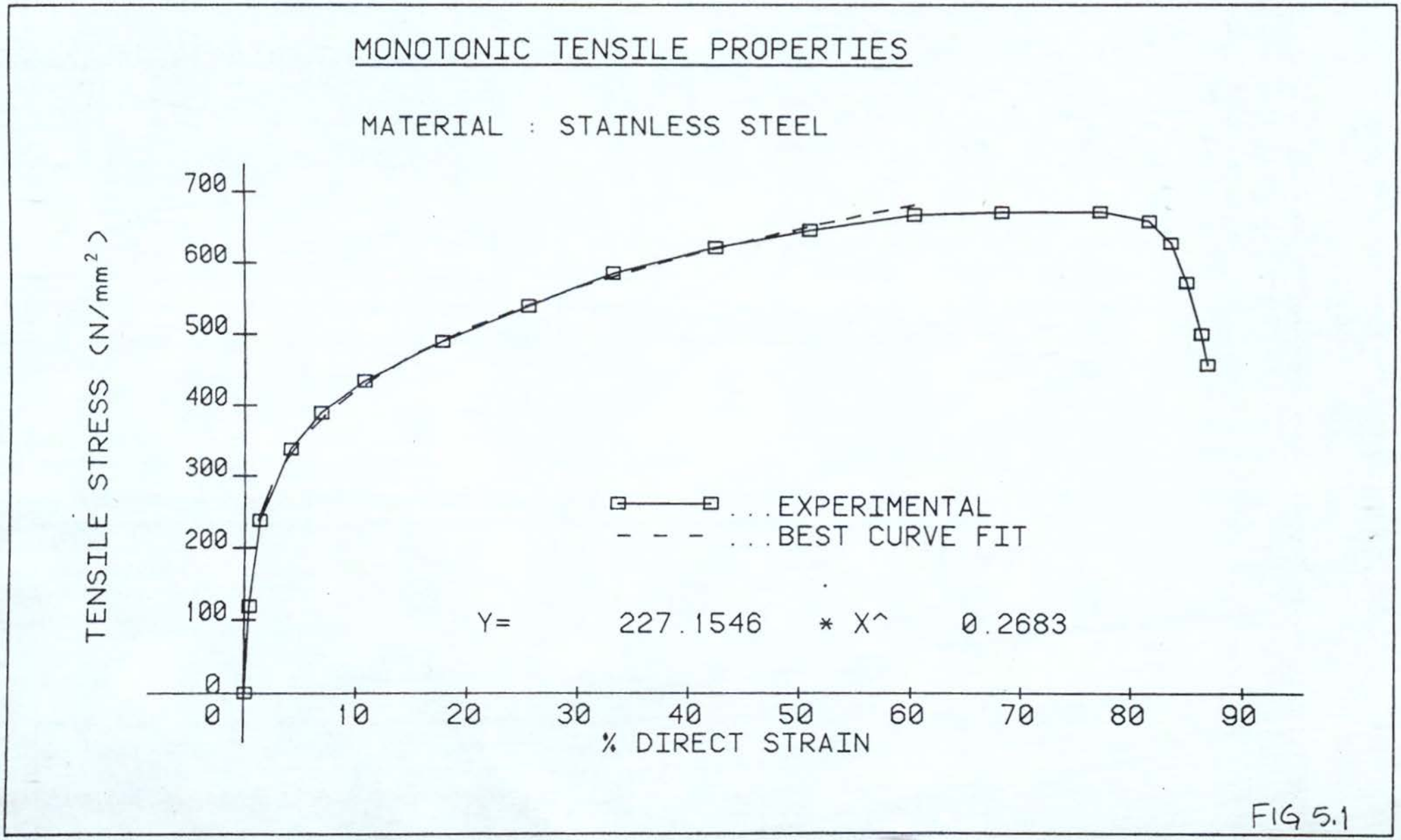
MONOTONIC TENSILE PROPERTIES
MATERIAL : STAINLESS STEEL
TENSILE STRESS (N/mm²)
700
600
500
400
300
200
100
0
0
10
20
30
40
50
60
70
80
90
% DIRECT STRAIN
...EXPERIMENTAL
...BEST CURVE FIT
Y= 227.1546 * X^ 0.2683

FIG 5.1

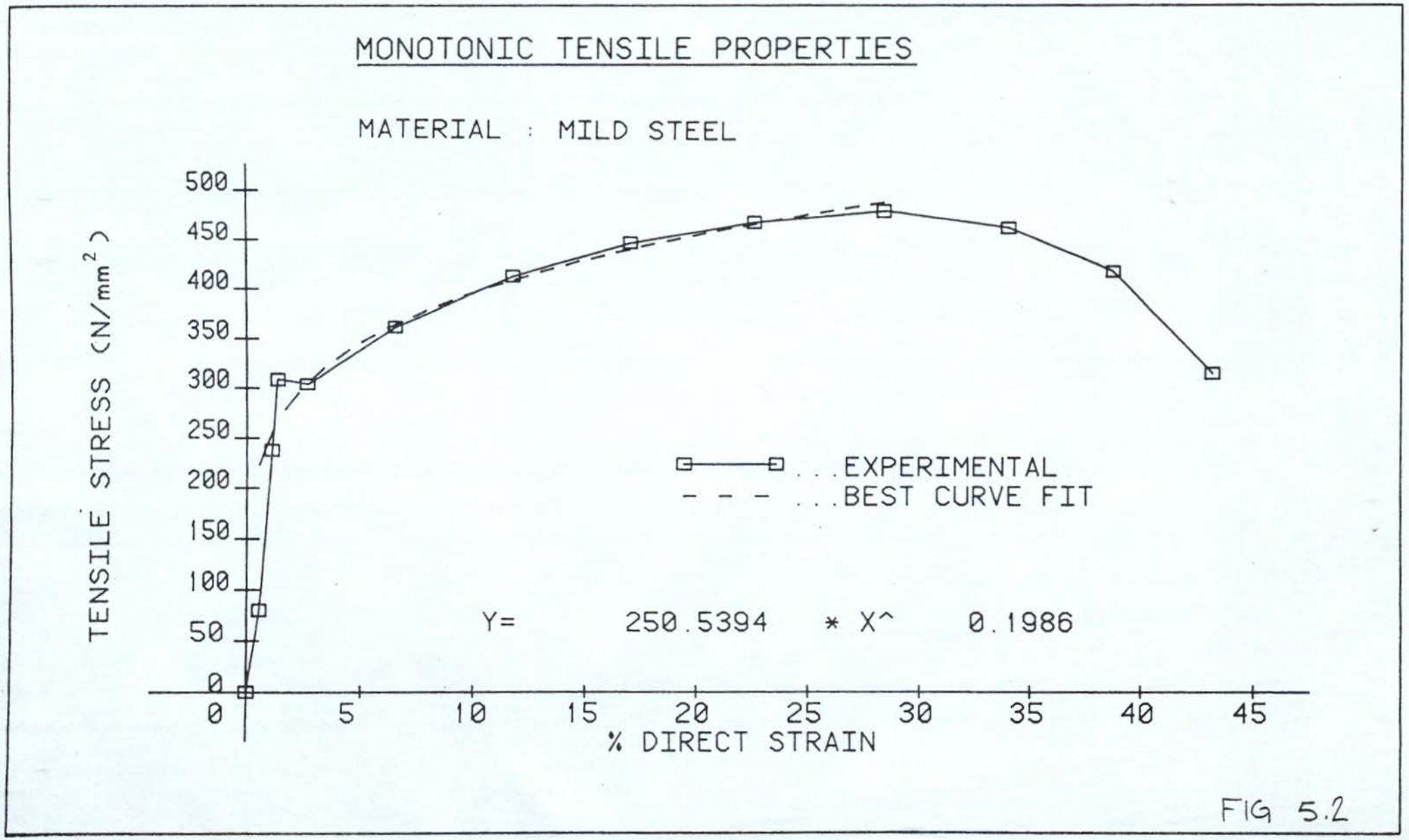
MONOTONIC TENSILE PROPERTIES
MATERIAL : MILD STEEL
TENSILE STRESS (N/mm²)
500
450
400
350
300
250
200
150
100
50
0
0
5
10
15
20
25
30
35
40
45
% DIRECT STRAIN
...EXPERIMENTAL
- - - ...BEST CURVE FIT
Y= 250.5394 * X^ 0.1986

FIG 5.2

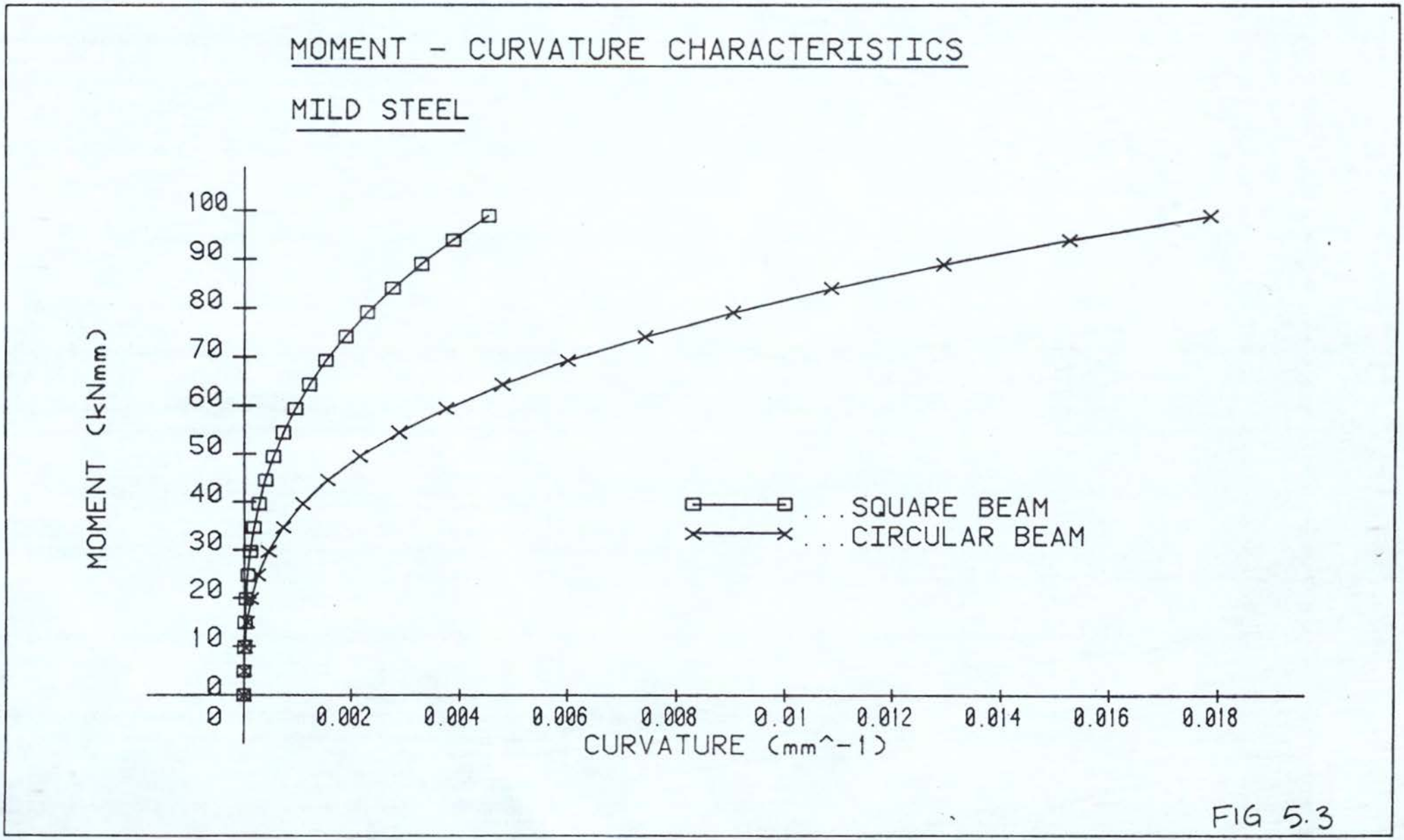
MOMENT - CURVATURE CHARACTERISTICS
MILD STEEL
MOMENT (kNmm)
100
90
80
70
60
50
40
30
20
10
0
0
0.002
0.004
0.006
0.008
0.01
0.012
0.014
0.016
0.018
CURVATURE (mm^-1)
...SQUARE BEAM
...CIRCULAR BEAM

FIG 5.3

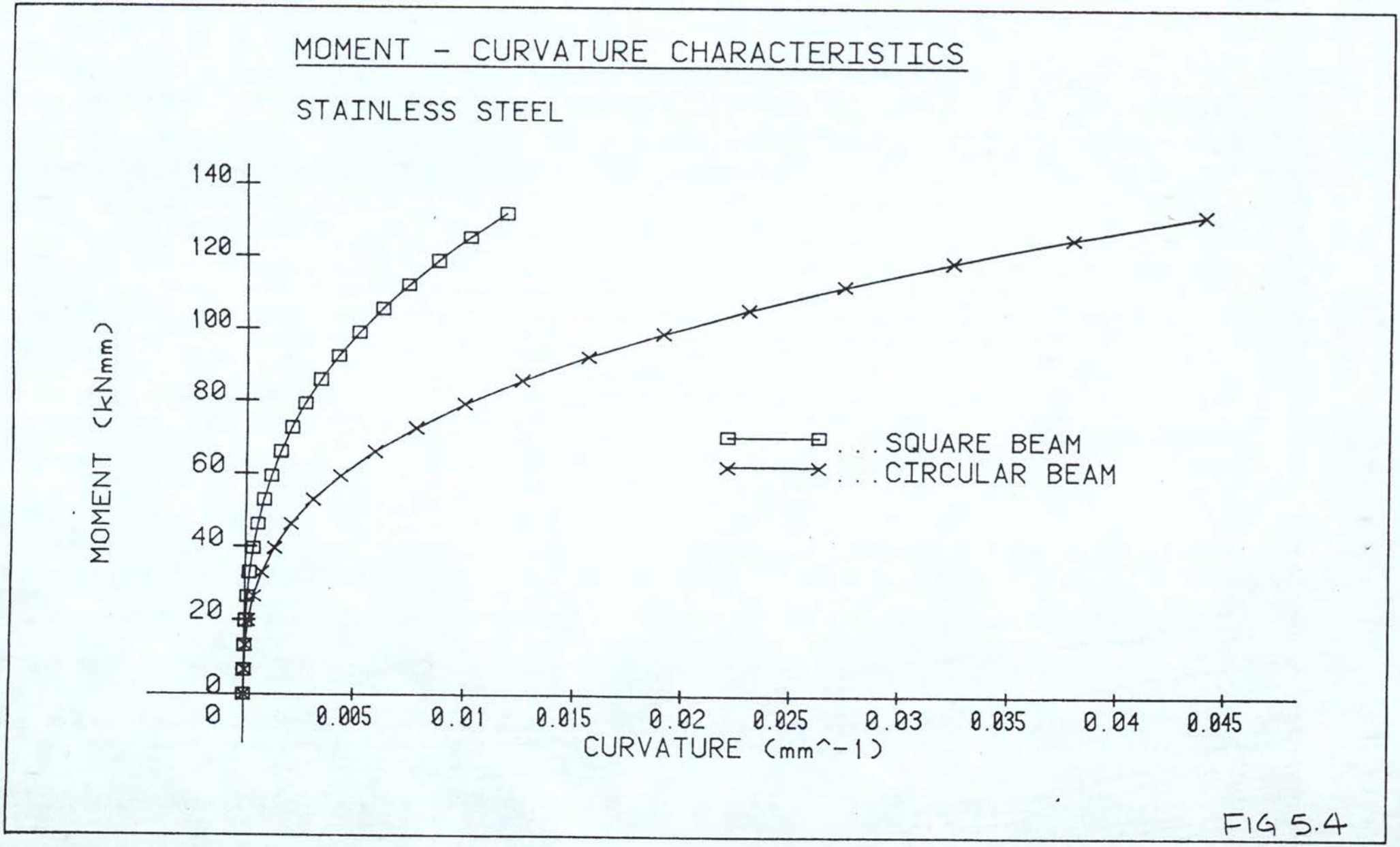
MOMENT - CURVATURE CHARACTERISTICS
STAINLESS STEEL
MOMENT (kNmm)
140
120
100
80
60
40
20
0
0
0.005
0.01
0.015
0.02
0.025
0.03
0.035
0.04
0.045
CURVATURE (mm^-1)
...SQUARE BEAM
...CIRCULAR BEAM

FIG 5.4

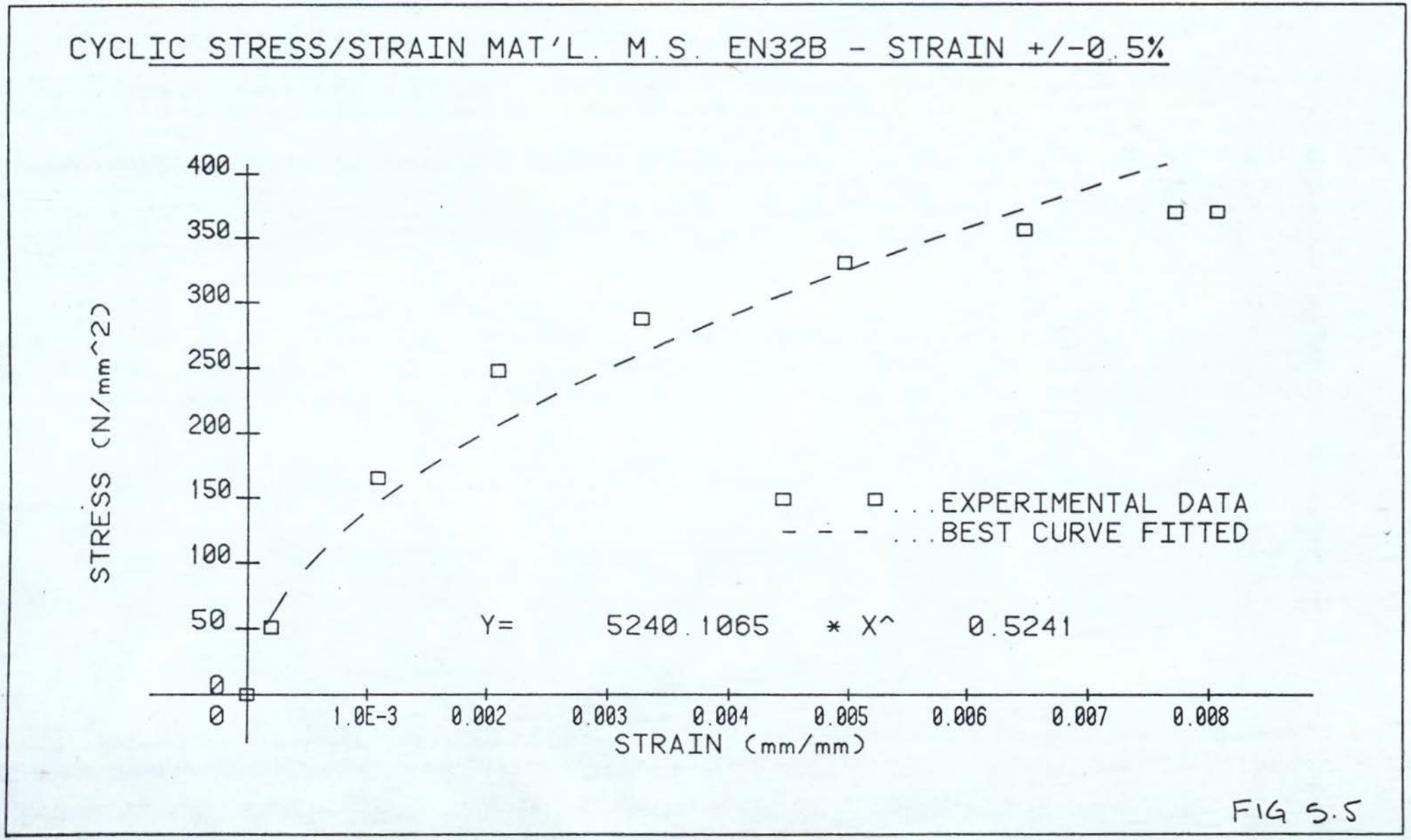
CYCLIC STRESS/STRAIN MAT'L. M.S. EN32B - STRAIN +/-0.5%
STRESS (N/mm^2)
400
350
300
250
200
150
100
50
0
0
1.0E-3
0.002
0.003
0.004
0.005
0.006
0.007
0.008
STRAIN (mm/mm)
□ □ . . . EXPERIMENTAL DATA
- - - . . . BEST CURVE FITTED
Y= 5240.1065 * X^ 0.5241

FIG 5.5

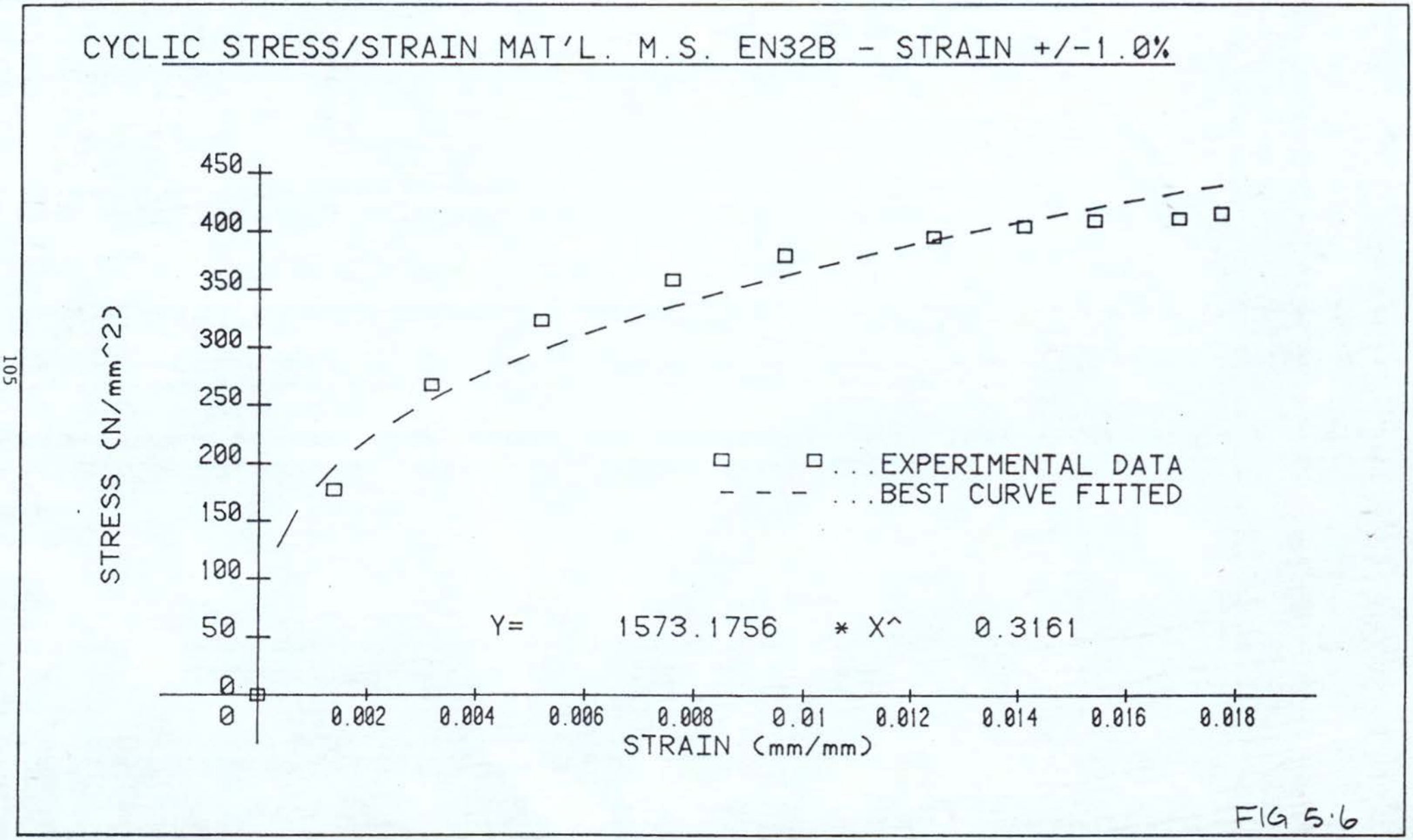
CYCLIC STRESS/STRAIN MAT'L. M.S. EN32B - STRAIN +/-1.0%
STRESS (N/mm^2)
450
400
350
300
250
200
150
100
50
0
0
0.002
0.004
0.006
0.008
0.01
0.012
0.014
0.016
0.018
STRAIN (mm/mm)
...EXPERIMENTAL DATA
...BEST CURVE FITTED
Y= 1573.1756 * X^ 0.3161

FIG 5.6

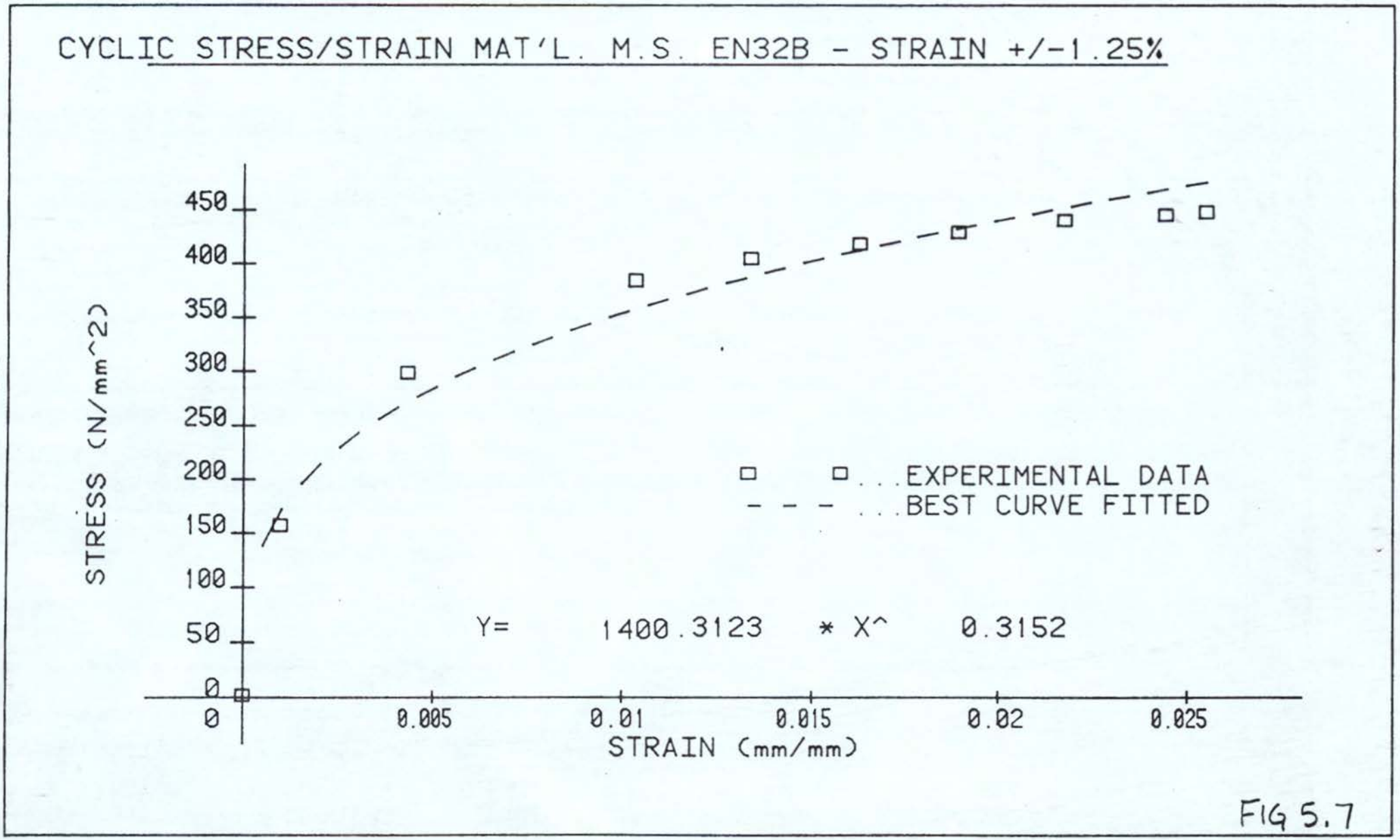
CYCLIC STRESS/STRAIN MAT'L. M.S. EN32B - STRAIN +/-1.25%
STRESS (N/mm^2)
450
400
350
300
250
200
150
100
50
0
0
0.005
0.01
0.015
0.02
0.025
STRAIN (mm/mm)
...EXPERIMENTAL DATA
...BEST CURVE FITTED
Y= 1400.3123 * X^ 0.3152

FIG 5.7

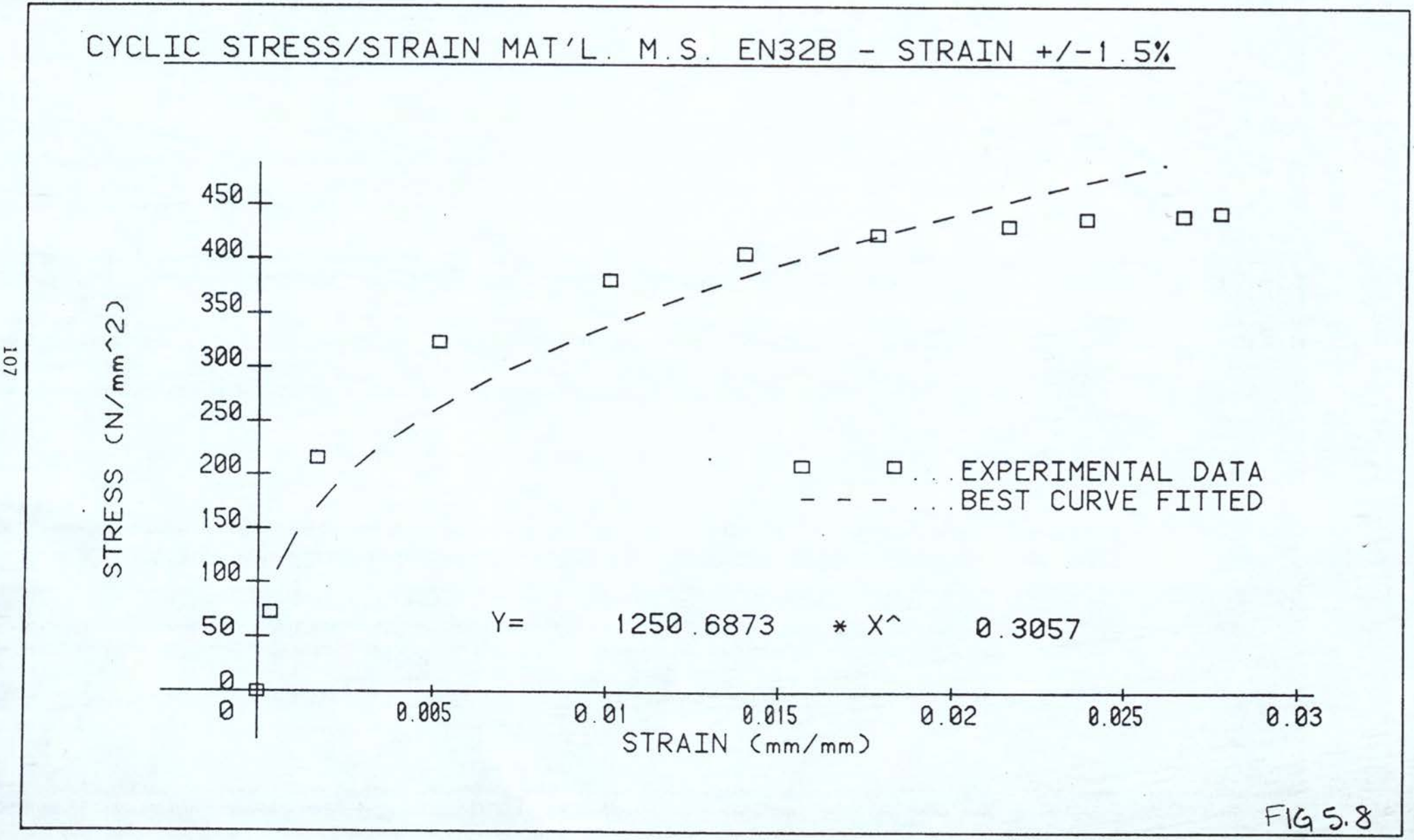
CYCLIC STRESS/STRAIN MAT'L. M.S. EN32B - STRAIN +/-1.5%
STRESS (N/mm^2)
450
400
350
300
250
200
150
100
50
0
0
0.005
0.01
0.015
0.02
0.025
0.03
STRAIN (mm/mm)
. . .EXPERIMENTAL DATA
- - - . . .BEST CURVE FITTED
Y= 1250.6873 * X^ 0.3057

FIG 5.8

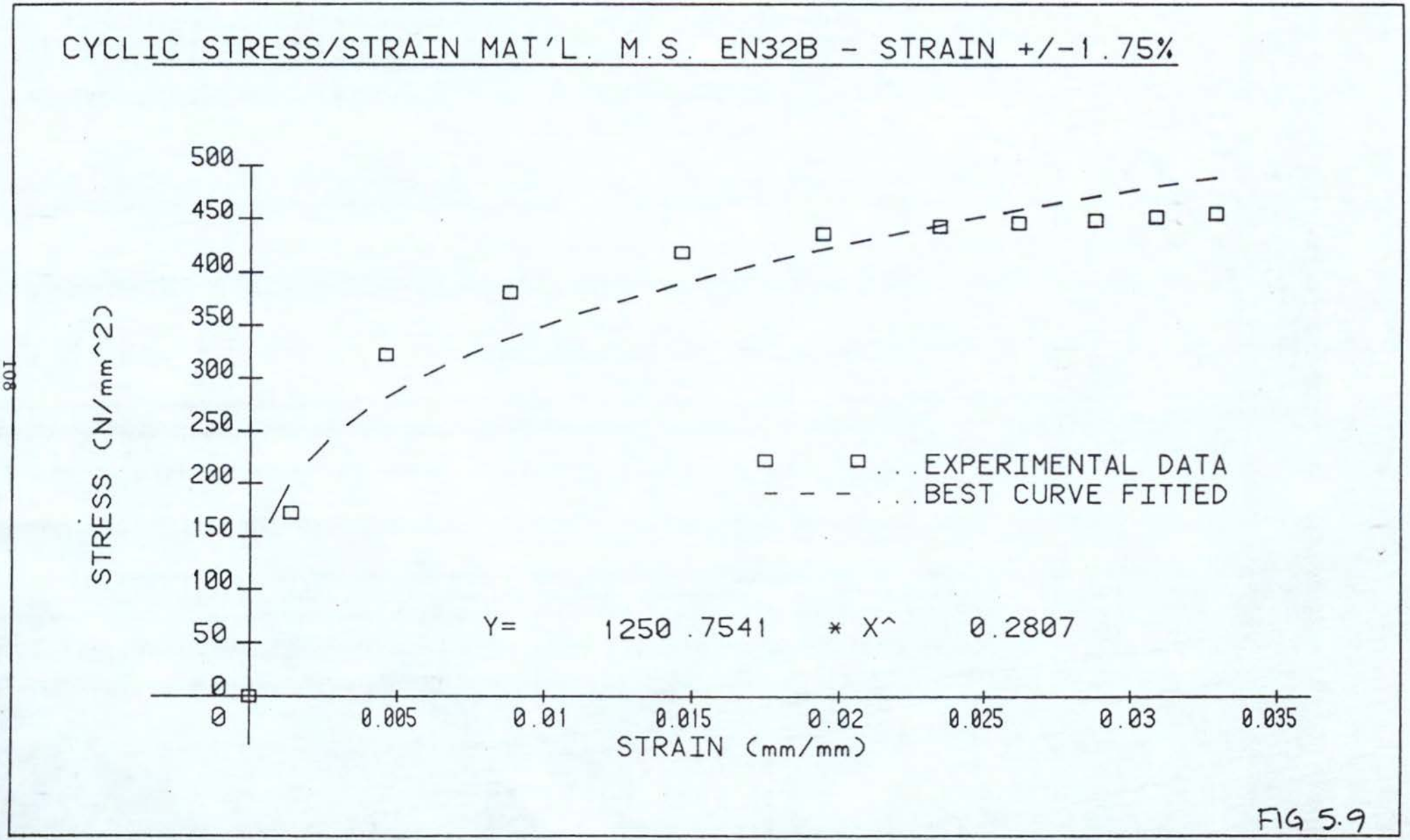
CYCLIC STRESS/STRAIN MAT'L. M.S. EN32B - STRAIN +/-1.75%
STRESS (N/mm^2)
500
450
400
350
300
250
200
150
100
50
0
0
0.005
0.01
0.015
0.02
0.025
0.03
0.035
STRAIN (mm/mm)
□ □ . . . EXPERIMENTAL DATA
- - - . . . BEST CURVE FITTED
Y= 1250.7541 * X^ 0.2807

FIG 5.9

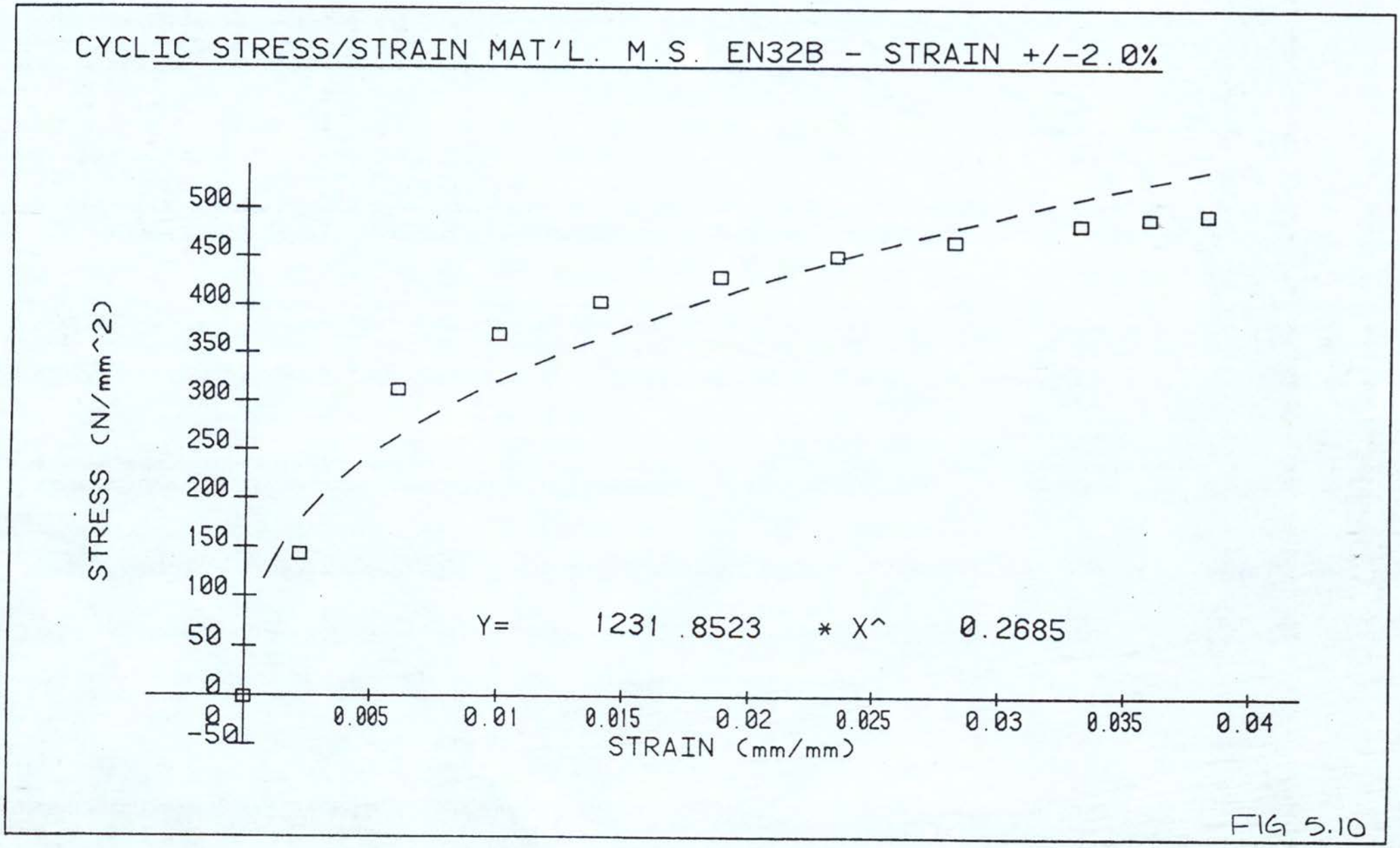
CYCLIC STRESS/STRAIN MAT'L. M.S. EN32B - STRAIN +/-2.0%
STRESS (N/mm^2)
500
450
400
350
300
250
200
150
100
50
0
0
-50
0.005
0.01
0.015
0.02
0.025
0.03
0.035
0.04
STRAIN (mm/mm)
Y= 1231.8523 * X^ 0.2685

FIG 5.10

VARIATION OF MATERIAL CONSTANT n WITH STRAIN

MATERIAL : MILD STEEL

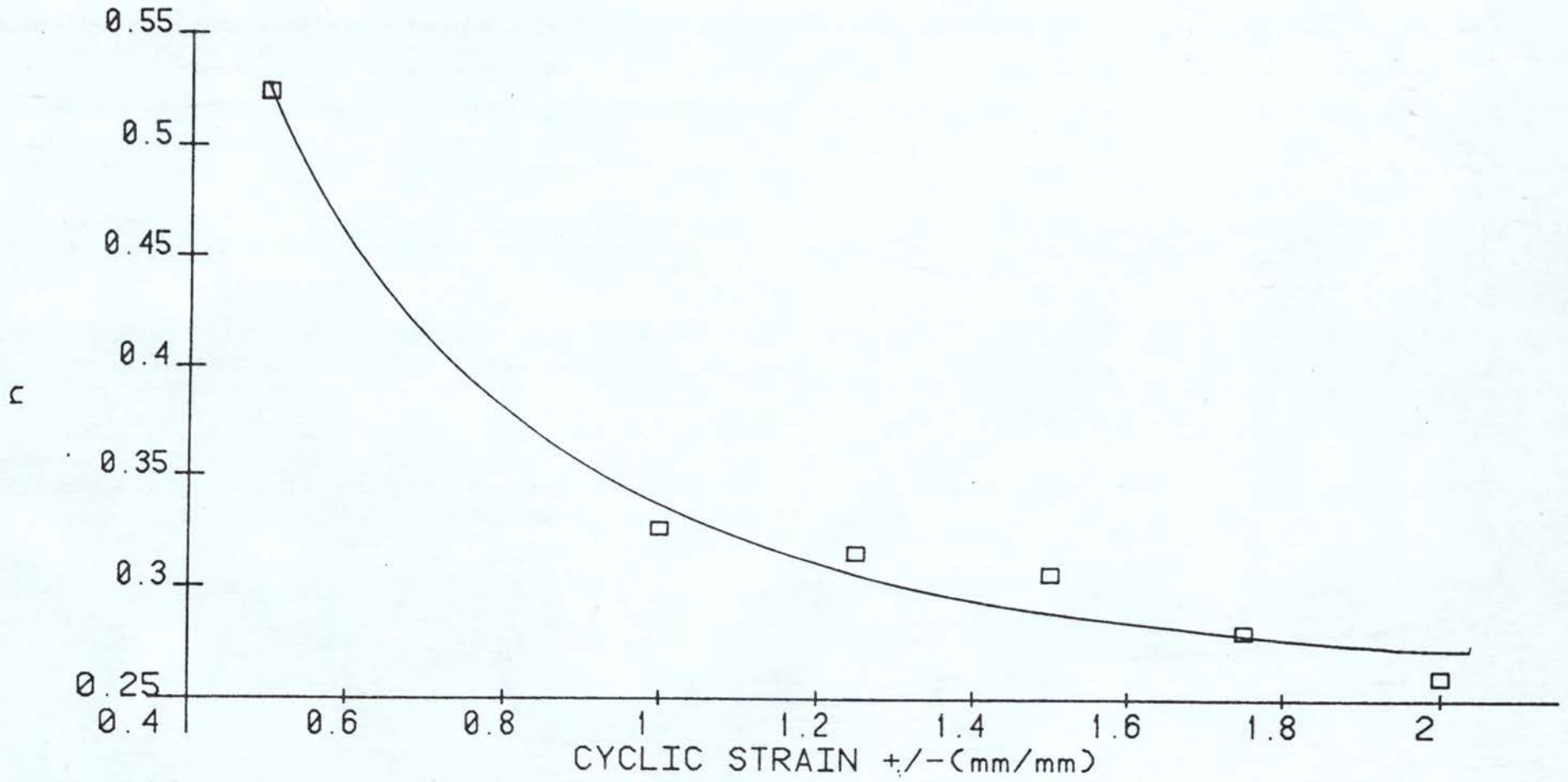

FIG 5.11

VARIATION OF MATERIAL CONSTANT G_0 WITH STRAIN

MATERIAL : MILD STEEL

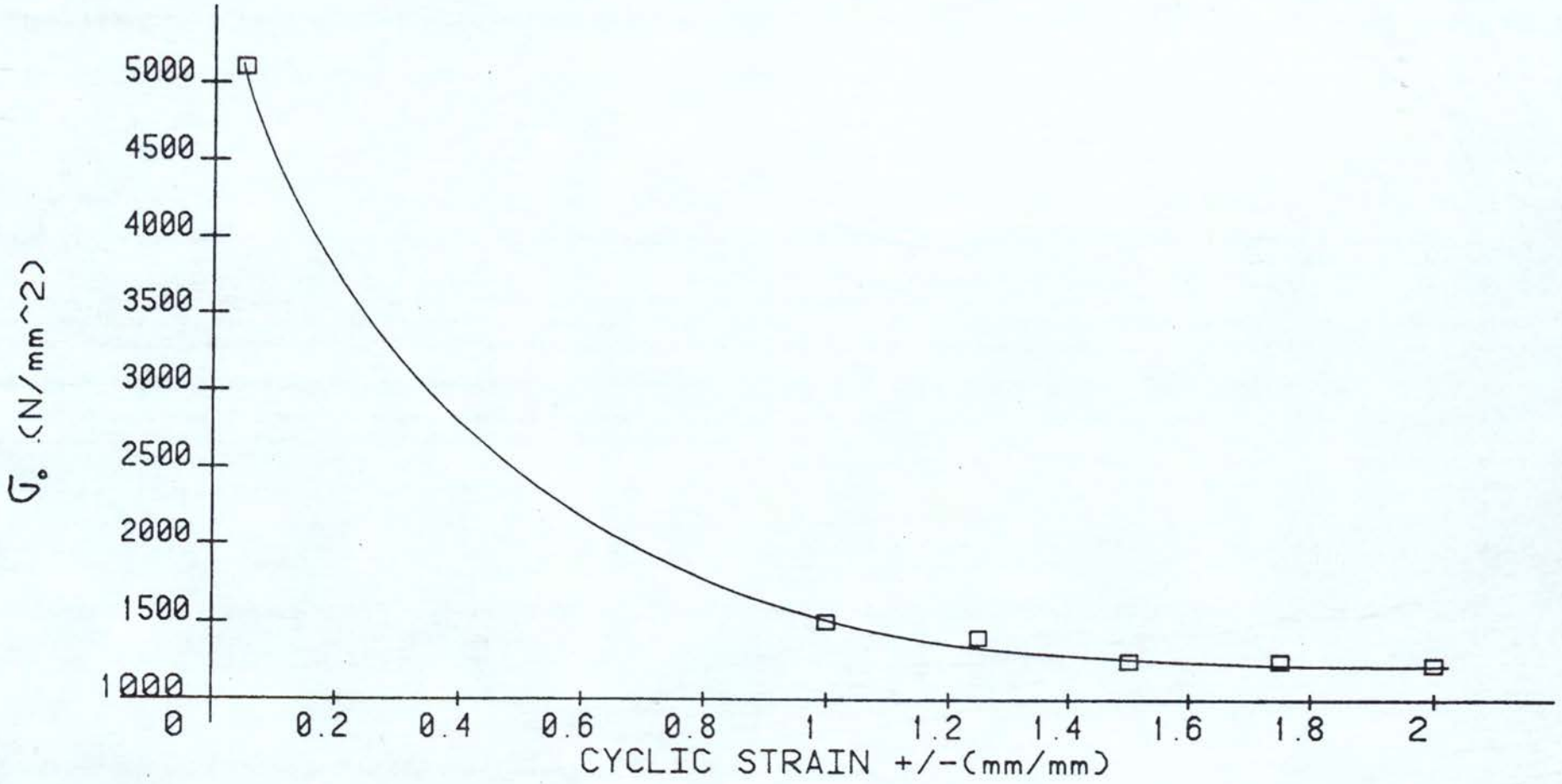

FIG 5.12

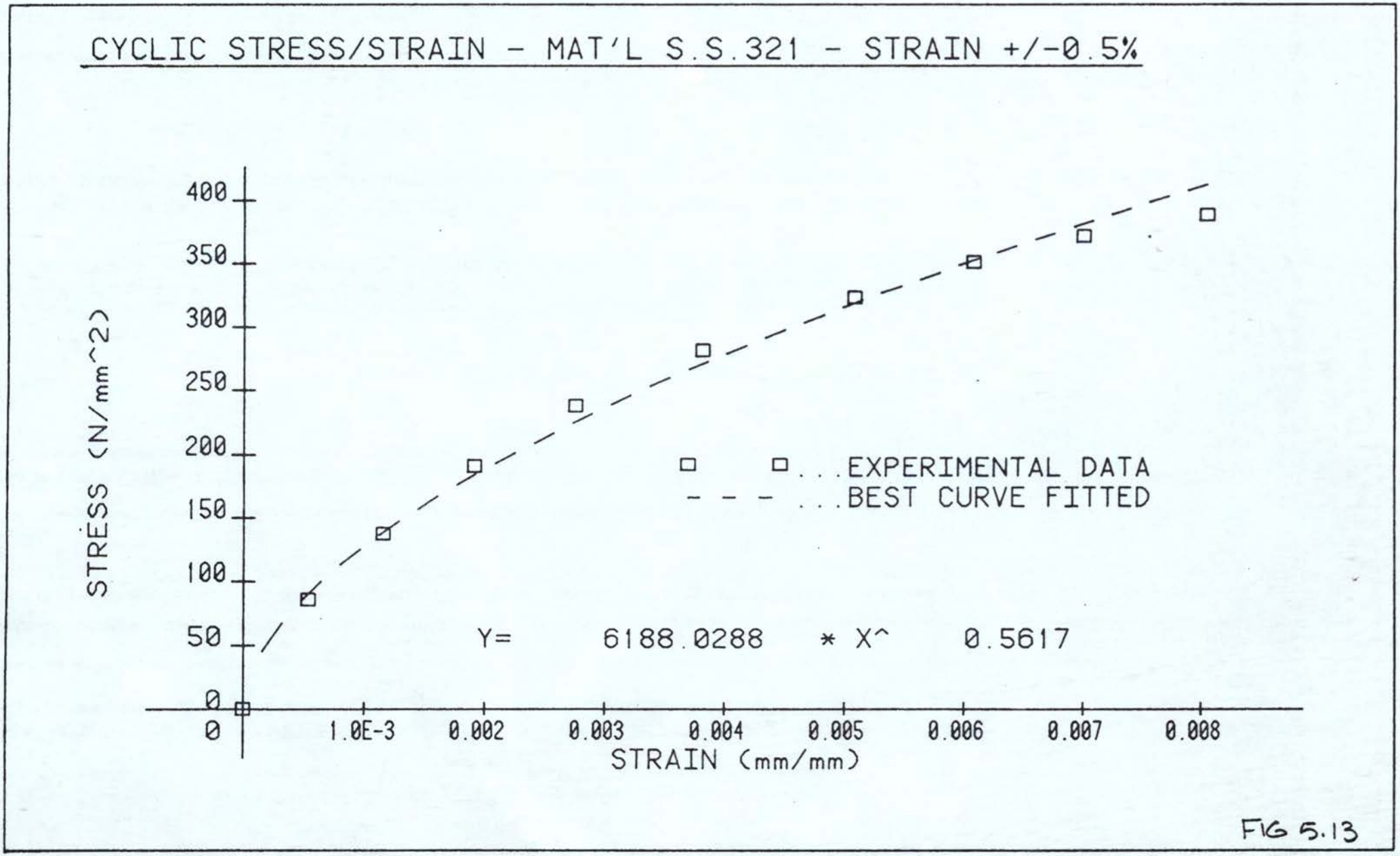
CYCLIC STRESS/STRAIN - MAT'L S.S.321 - STRAIN +/-0.5%
STRESS (N/mm^2)
400
350
300
250
200
150
100
50
0
0
1.0E-3
0.002
0.003
0.004
0.005
0.006
0.007
0.008
STRAIN (mm/mm)
...EXPERIMENTAL DATA
...BEST CURVE FITTED
Y= 6188.0288 * X^ 0.5617

FIG 5.13

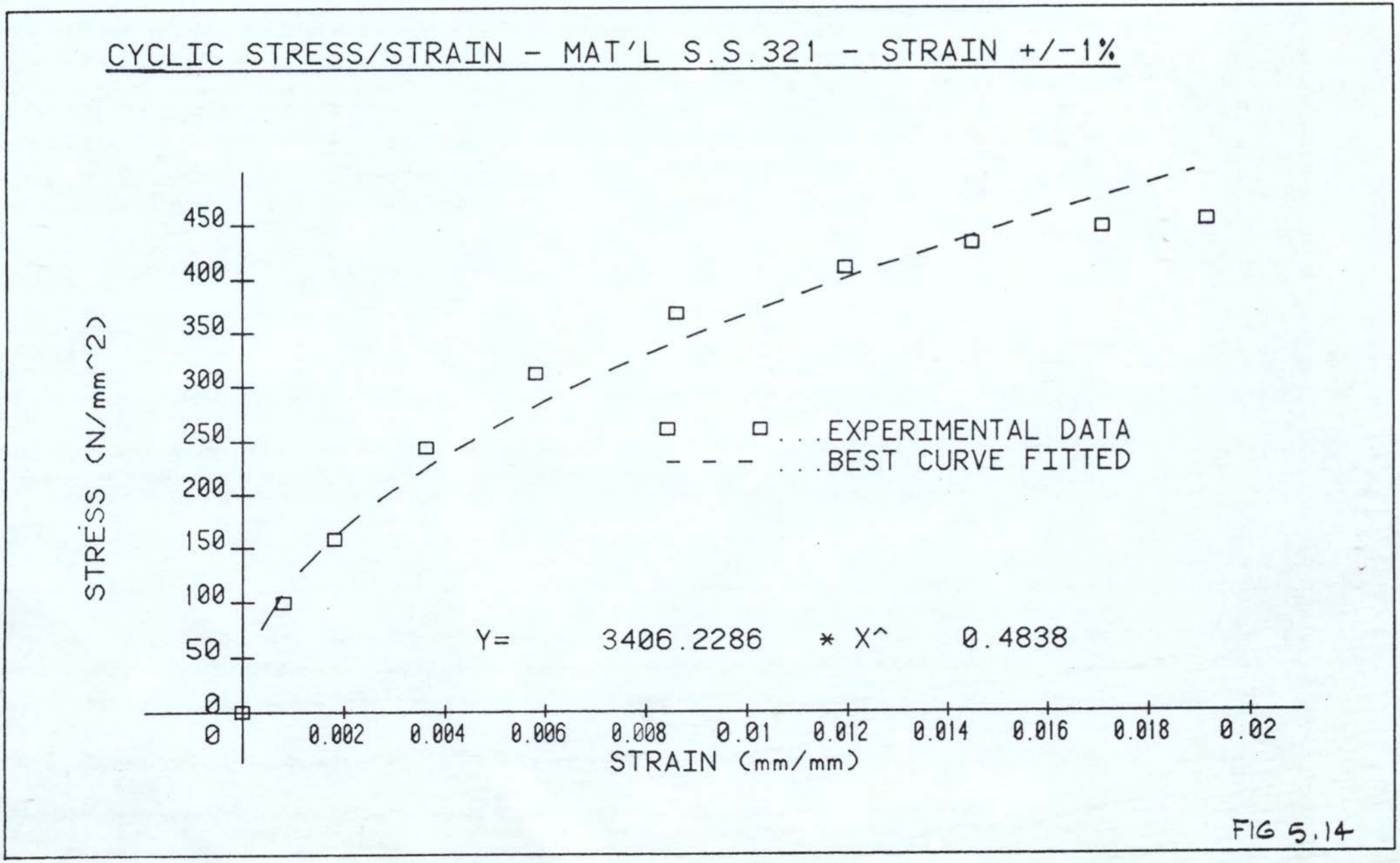
CYCLIC STRESS/STRAIN - MAT'L S.S.321 - STRAIN +/-1%
STRESS (N/mm^2)
450
400
350
300
250
200
150
100
50
0
0
0.002
0.004
0.006
0.008
0.01
0.012
0.014
0.016
0.018
0.02
STRAIN (mm/mm)
. . .EXPERIMENTAL DATA
- - - . . .BEST CURVE FITTED
Y= 3406.2286 * X^ 0.4838

FIG 5.14

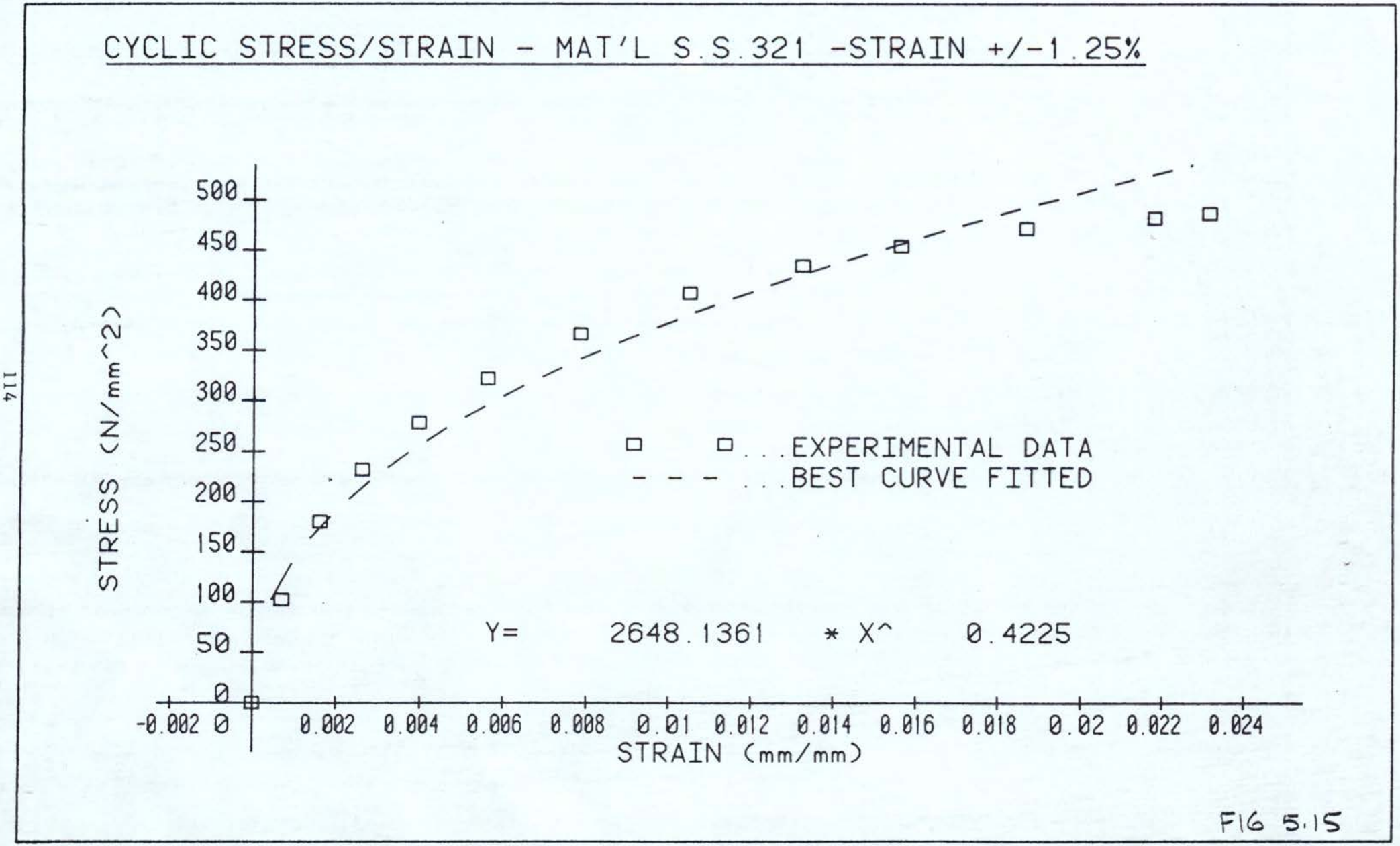
CYCLIC STRESS/STRAIN - MAT'L S.S.321 -STRAIN +/-1.25%
STRESS (N/mm^2)
500
450
400
350
300
250
200
150
100
50
0
-0.002 0
0.002
0.004
0.006
0.008
0.01
0.012
0.014
0.016
0.018
0.02
0.022
0.024
STRAIN (mm/mm)
. . .EXPERIMENTAL DATA
- - - . . .BEST CURVE FITTED
Y= 2648.1361 * X^ 0.4225

FIG 5.15

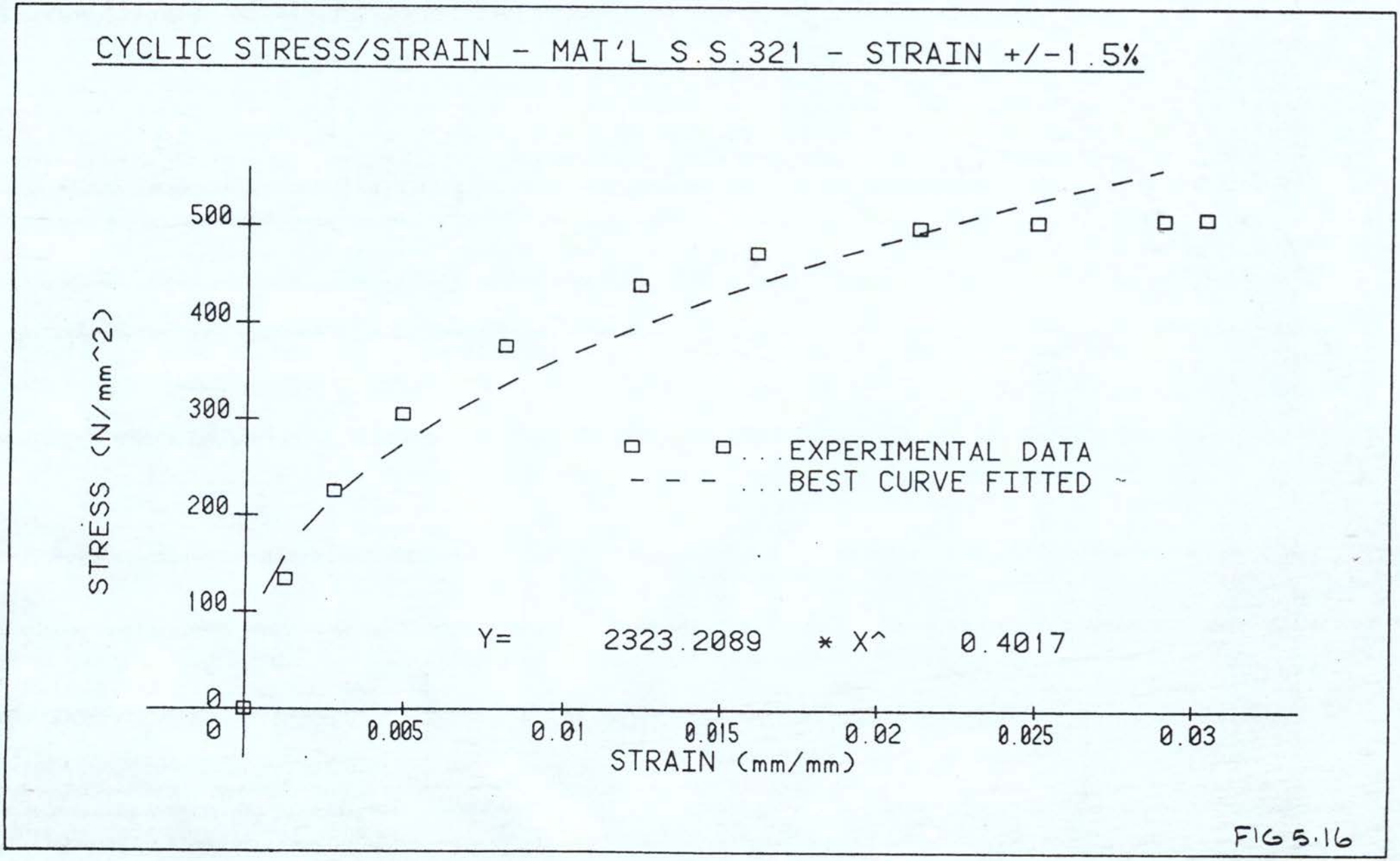
CYCLIC STRESS/STRAIN - MAT'L S.S.321 - STRAIN +/-1.5%
STRESS (N/mm^2)
500
400
300
200
100
0
0
0.005
0.01
0.015
0.02
0.025
0.03
STRAIN (mm/mm)
□ □ . . . EXPERIMENTAL DATA
- - - . . . BEST CURVE FITTED
Y= 2323.2089 * X^ 0.4017

FIG 5.16

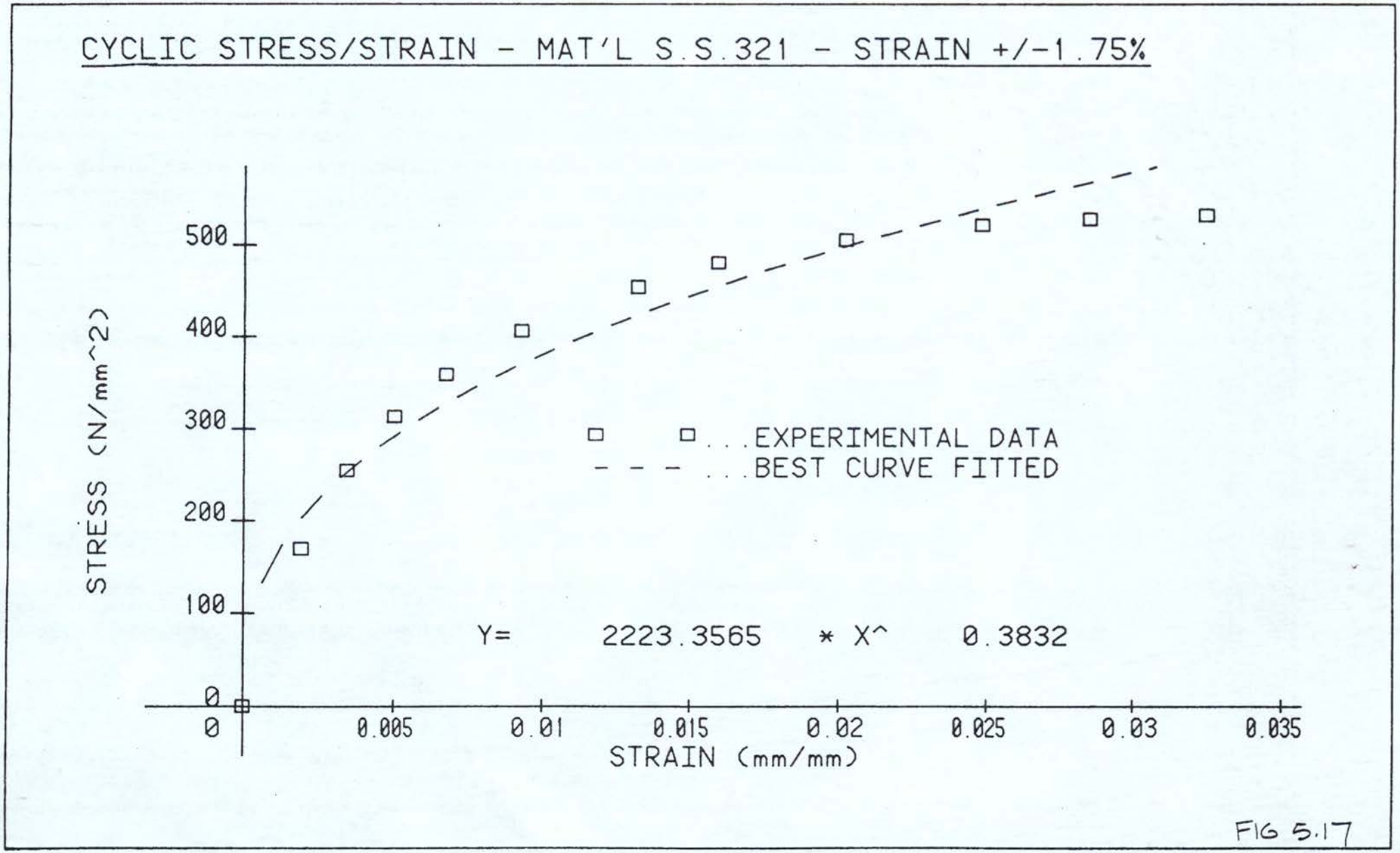
CYCLIC STRESS/STRAIN - MAT'L S.S.321 - STRAIN +/-1.75%
STRESS (N/mm^2)
500
400
300
200
100
0
0
0.005
0.01
0.015
0.02
0.025
0.03
0.035
STRAIN (mm/mm)
...EXPERIMENTAL DATA
- - - ...BEST CURVE FITTED
Y= 2223.3565 * X^ 0.3832

FIG 5.17

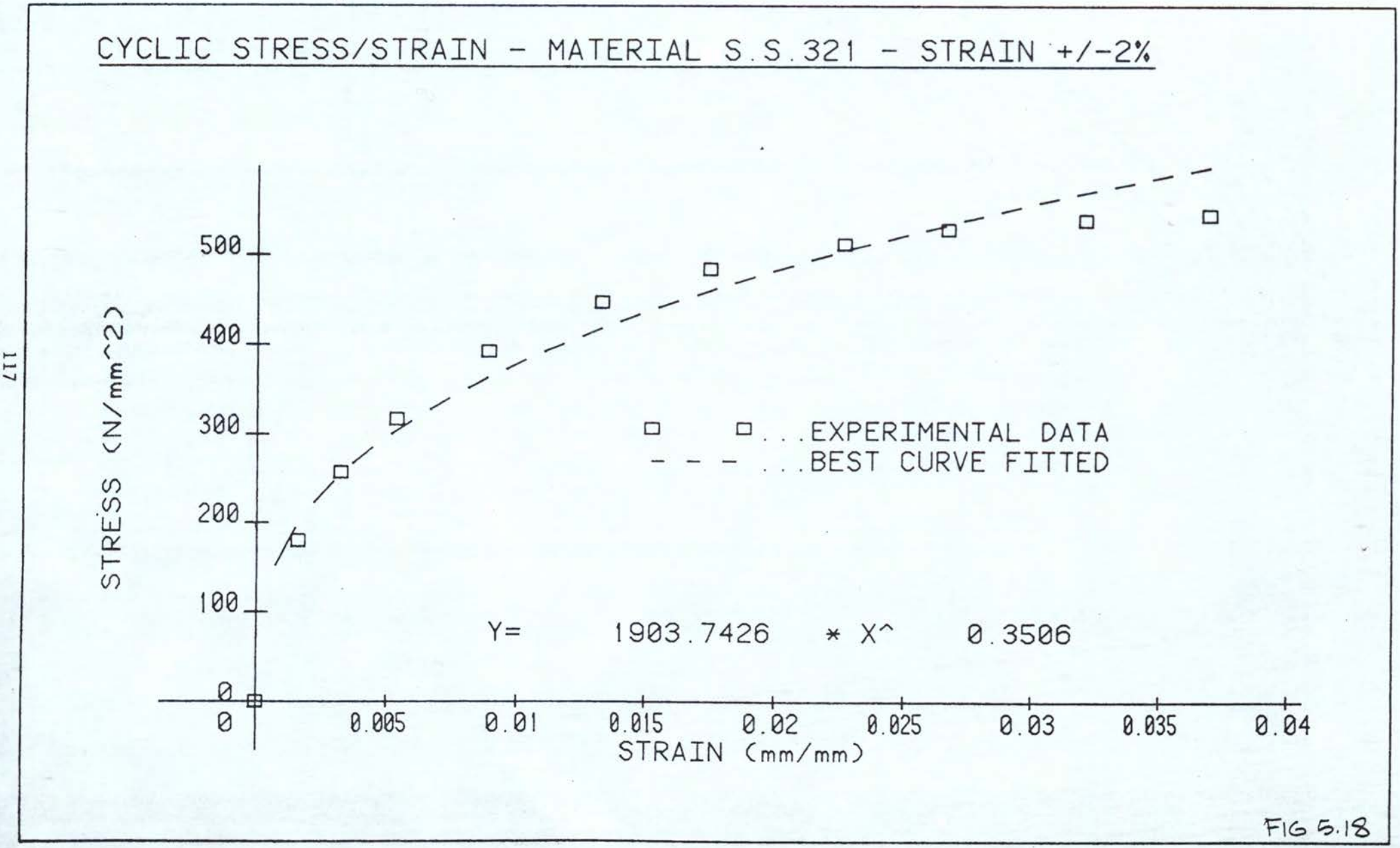
CYCLIC STRESS/STRAIN - MATERIAL S.S.321 - STRAIN +/-2%
STRESS (N/mm^2)
500
400
300
200
100
0
0
0.005
0.01
0.015
0.02
0.025
0.03
0.035
0.04
STRAIN (mm/mm)
□ □ . . .EXPERIMENTAL DATA
- - - . . .BEST CURVE FITTED
Y= 1903.7426 * X^ 0.3506

FIG 5.18

VARIATION OF MATERIAL CONSTANT σ_o WITH STRAIN

MATERIAL : STAINLESS STEEL

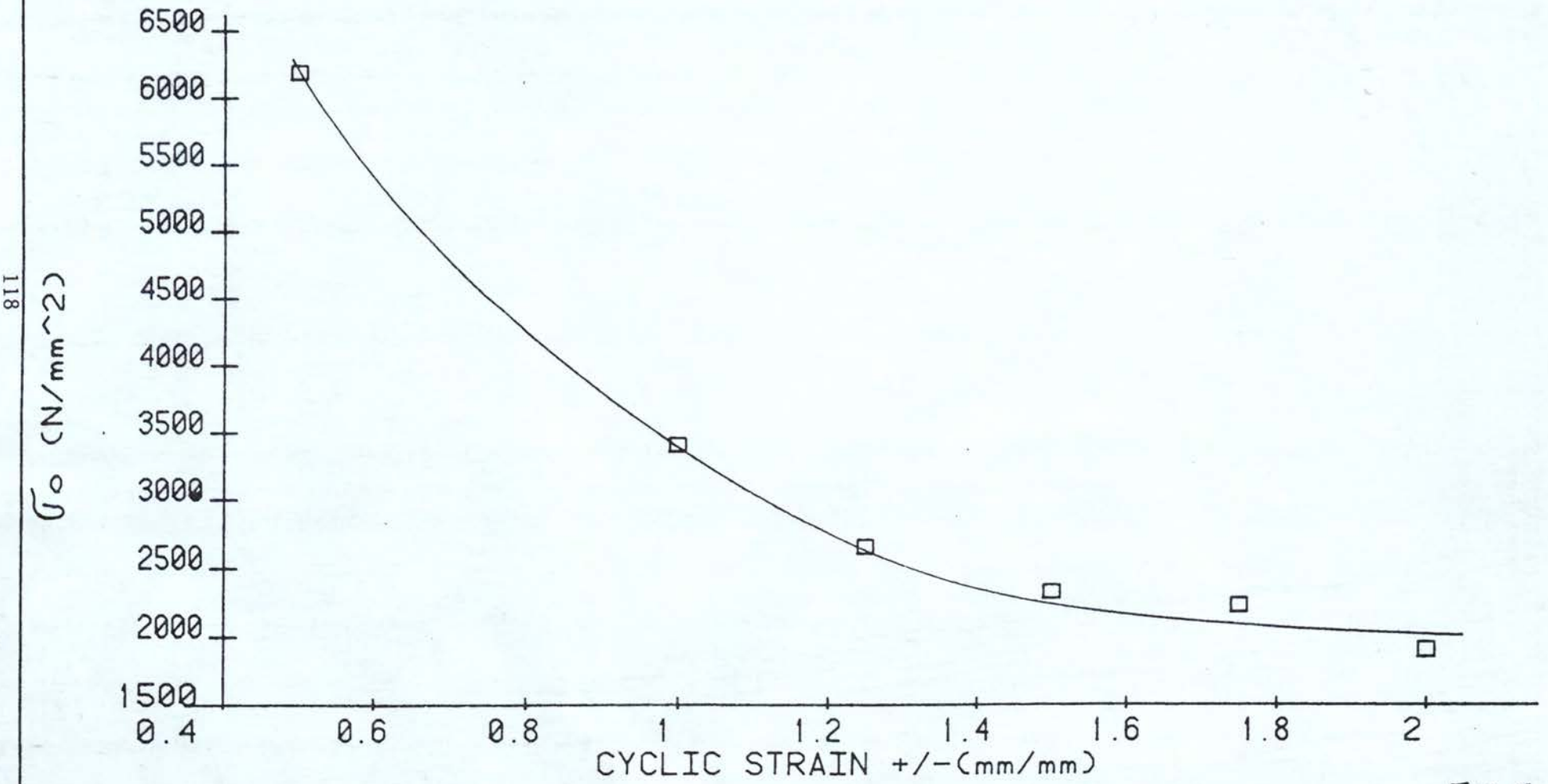

FIG 5.19

VARIATION OF MATERIAL CONSTANT n WITH STRAIN

MATERIAL : STAINLESS STEEL

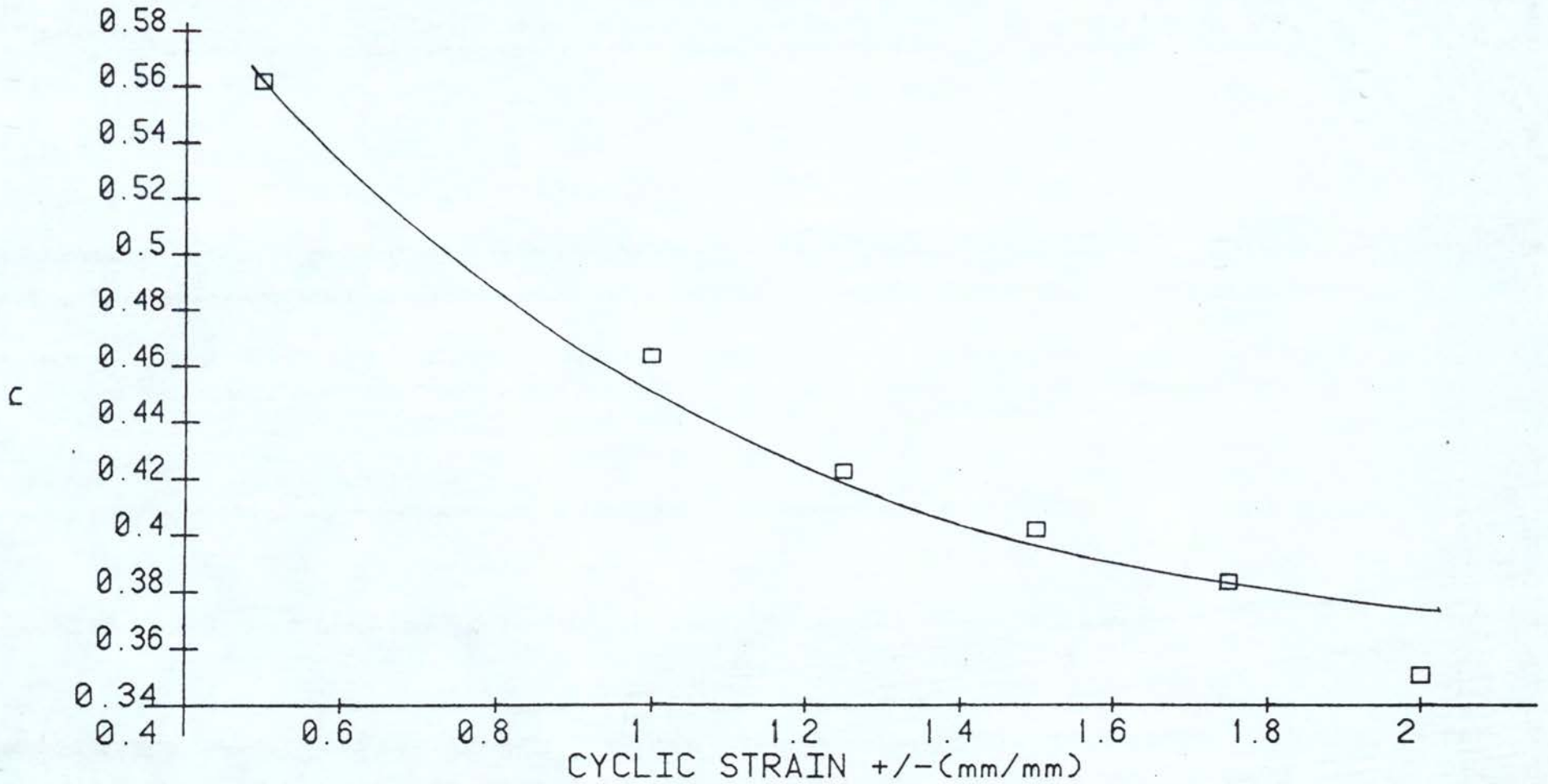

FIG 5.20

5.1.3 MONOTONIC LOAD DEFLECTION CHARACTERISTICS

This is the simplest bending condition to consider, with elemental fibres subjected to simple tension and compression during the first quarter cycle. There is no rotation of the neutral surface and therefore no unloading. The theoretical predictions were made using

a) The simplified curvature equation.

b) The full curvature equation.

However, the difference between the two methods were so small for the range of deflections considered that the results using the simplified curvature equation were used in most cases. The load-deflection results for square and round mild steel beams are shown in Fig (5.21) and Fig (5.22). The lack of correlation between experimental and predicted results could have been expected, given the errors in modelling this material behaviour, but consistent results are obtained and the predictions improve as the strains increase. The large errors occur at the lower deflection, ie when the plastic strains are small and of elastic order. The results are consistent in that the theoretical material is "stronger" for most of the elastic region, then becomes "weaker" for a short period and then becomes very slightly stronger again. It is in the last region that the predictions improve.

The load-deflection curves for the stainless steel are shown in Figs (5.23) and (5.24) and again the results were predictable. The theoretical material is "stronger" in part of the plastic region and the errors are only beginning to be reduced at the higher levels of strain. The variation in outer fibre strain along the beams are shown in Figs

5.1.4 CYCLIC CONDITION - LOAD-DEFLECTION RESULTS

Experimental and predicted load-deflection curves for monotonic bending in the cyclic steady state condition are shown in Figs (5.25), (5.26), (5.27) and (5.28) for square and round beams of both materials. The predicted results for the stainless steels are particularly good and a little better than the mild steel predictions. This is obviously due to our ability to model material behaviour much better in the cyclic condition with a power law. One of the reasons for this is the very much reduced elastic region in the cyclic stress strain hysteresis curves. For some strains, the elastic portion is often negligibly small and yielding can occur on unloading and in these cases a simple power law would appear to be adequate to model cyclic material behaviour.

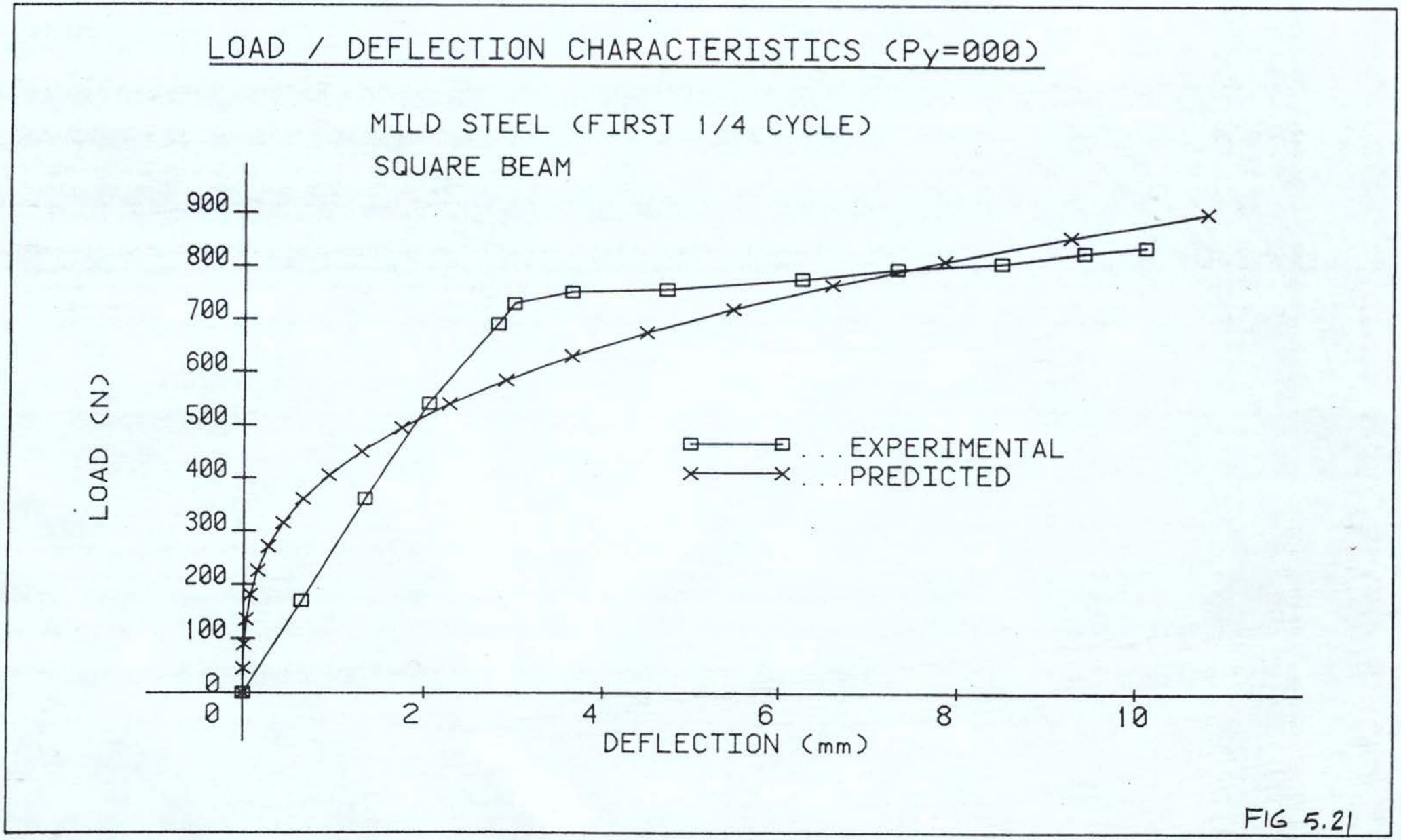
LOAD / DEFLECTION CHARACTERISTICS (Py=000)
MILD STEEL (FIRST 1/4 CYCLE)
SQUARE BEAM
LOAD (N)
900
800
700
600
500
400
300
200
100
0
0
2
4
6
8
10
DEFLECTION (mm)
. . . EXPERIMENTAL
. . . PREDICTED

FIG 5.21

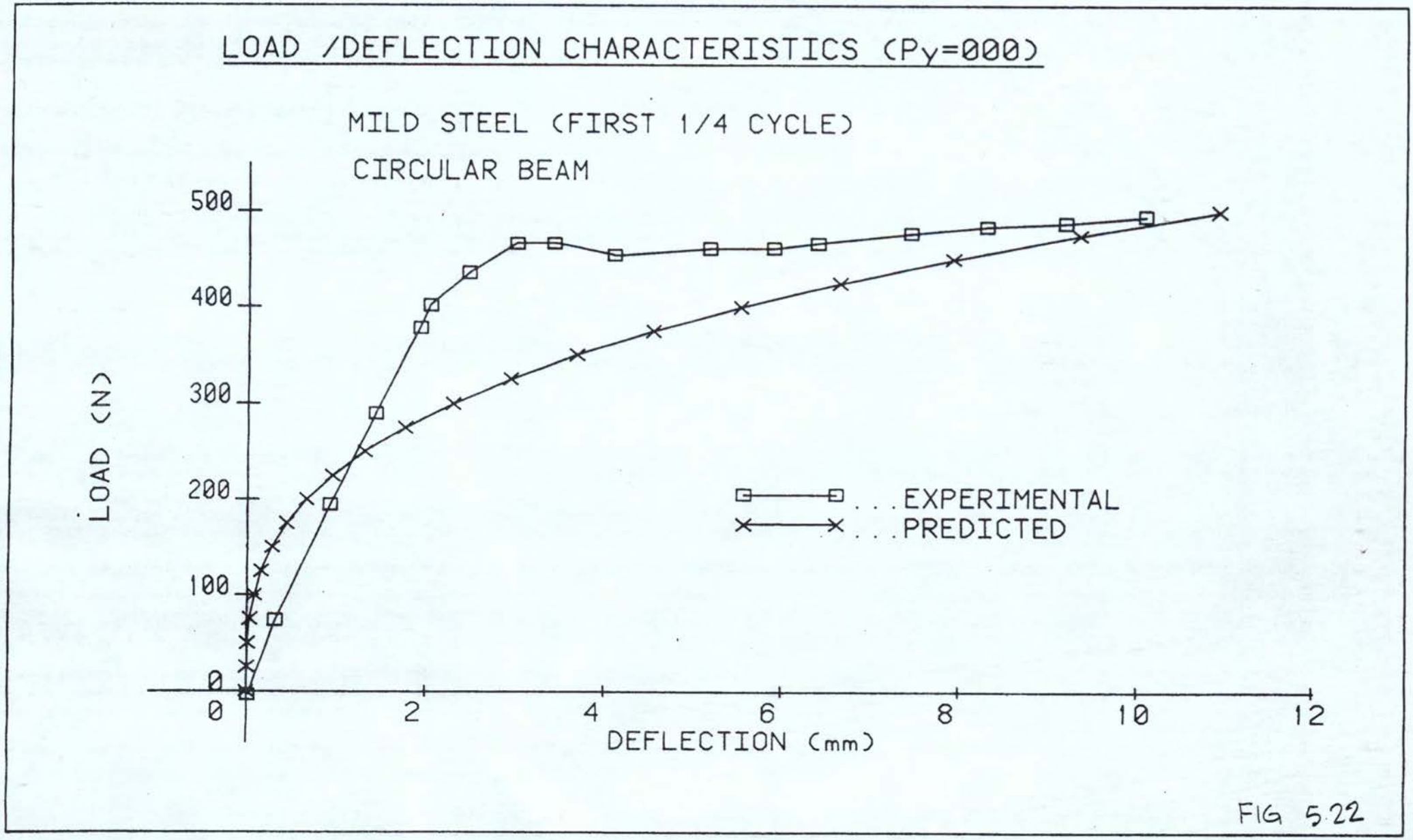
LOAD /DEFLECTION CHARACTERISTICS (Py=000)
MILD STEEL (FIRST 1/4 CYCLE)
CIRCULAR BEAM
LOAD (N)
500
400
300
200
100
0
0
2
4
6
8
10
12
DEFLECTION (mm)
. . .EXPERIMENTAL
. . .PREDICTED

FIG 5.22

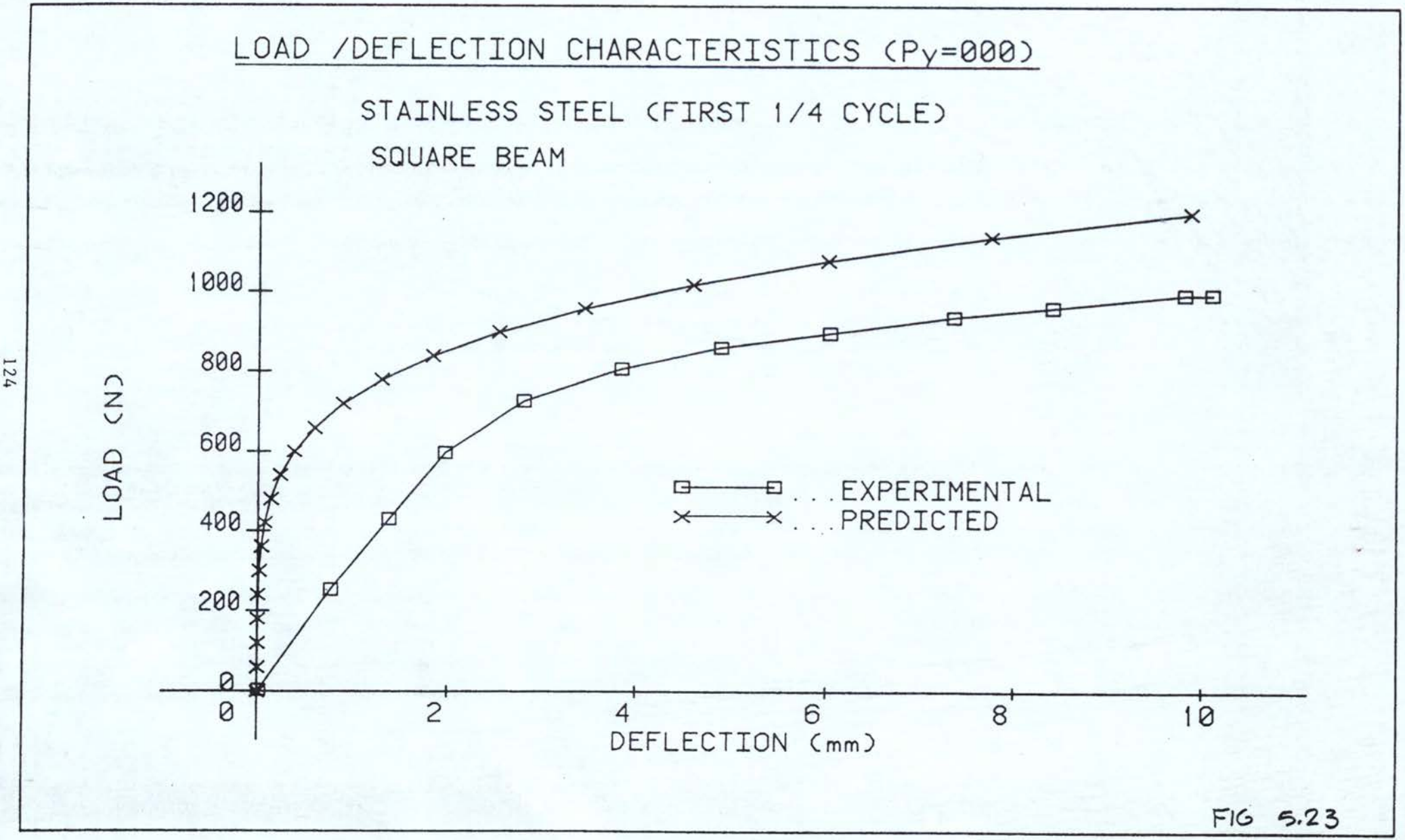
LOAD /DEFLECTION CHARACTERISTICS (Py=000)
STAINLESS STEEL (FIRST 1/4 CYCLE)
SQUARE BEAM
LOAD (N)
1200
1000
800
600
400
200
0
0
2
4
6
8
10
DEFLECTION (mm)
...EXPERIMENTAL
...PREDICTED

FIG 5.23

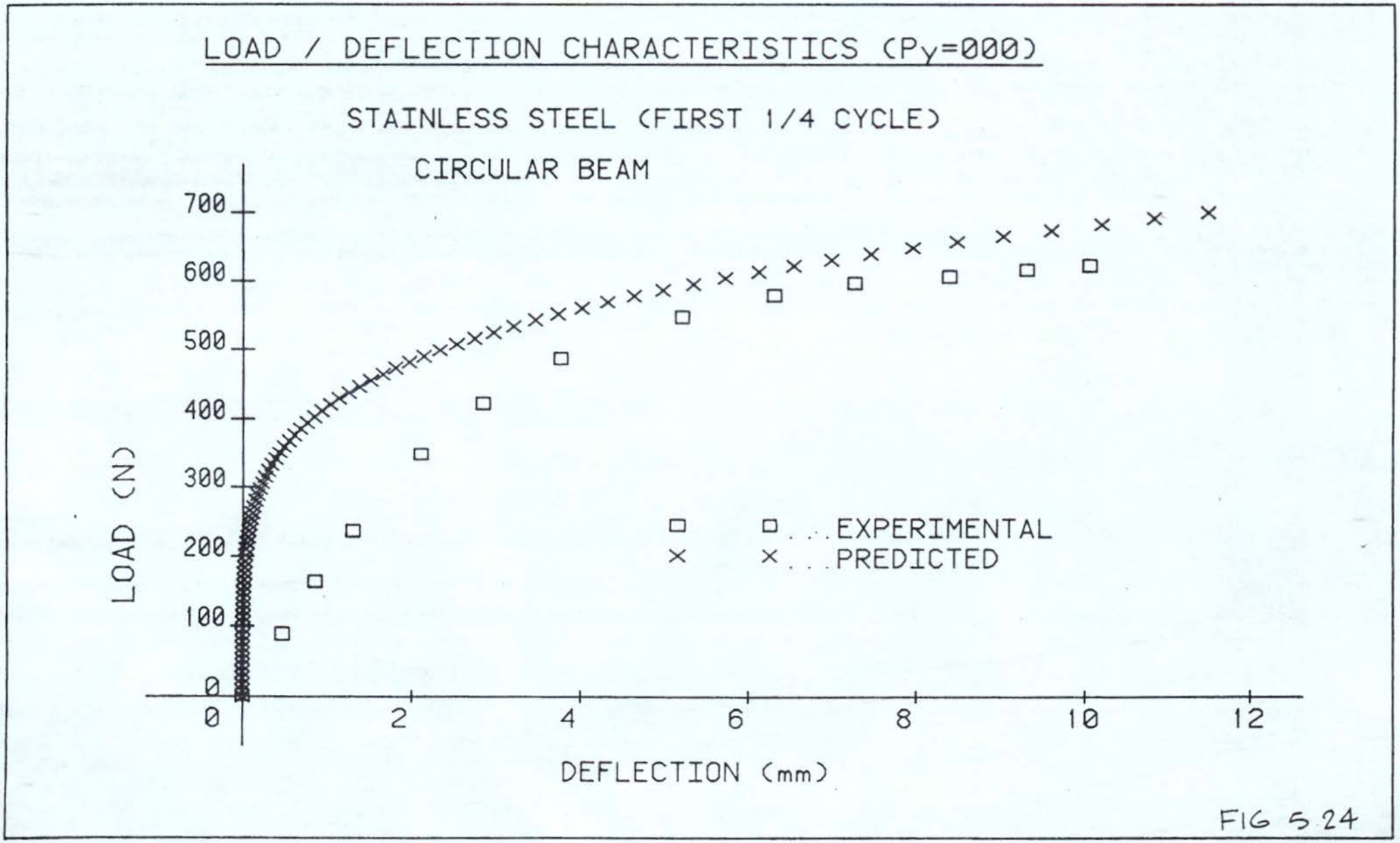
LOAD / DEFLECTION CHARACTERISTICS (Py=000)
STAINLESS STEEL (FIRST 1/4 CYCLE)
CIRCULAR BEAM
LOAD (N)
700
600
500
400
300
200
100
0
0
2
4
6
8
10
12
DEFLECTION (mm)
□ . . . EXPERIMENTAL
× . . . PREDICTED

FIG 5.24

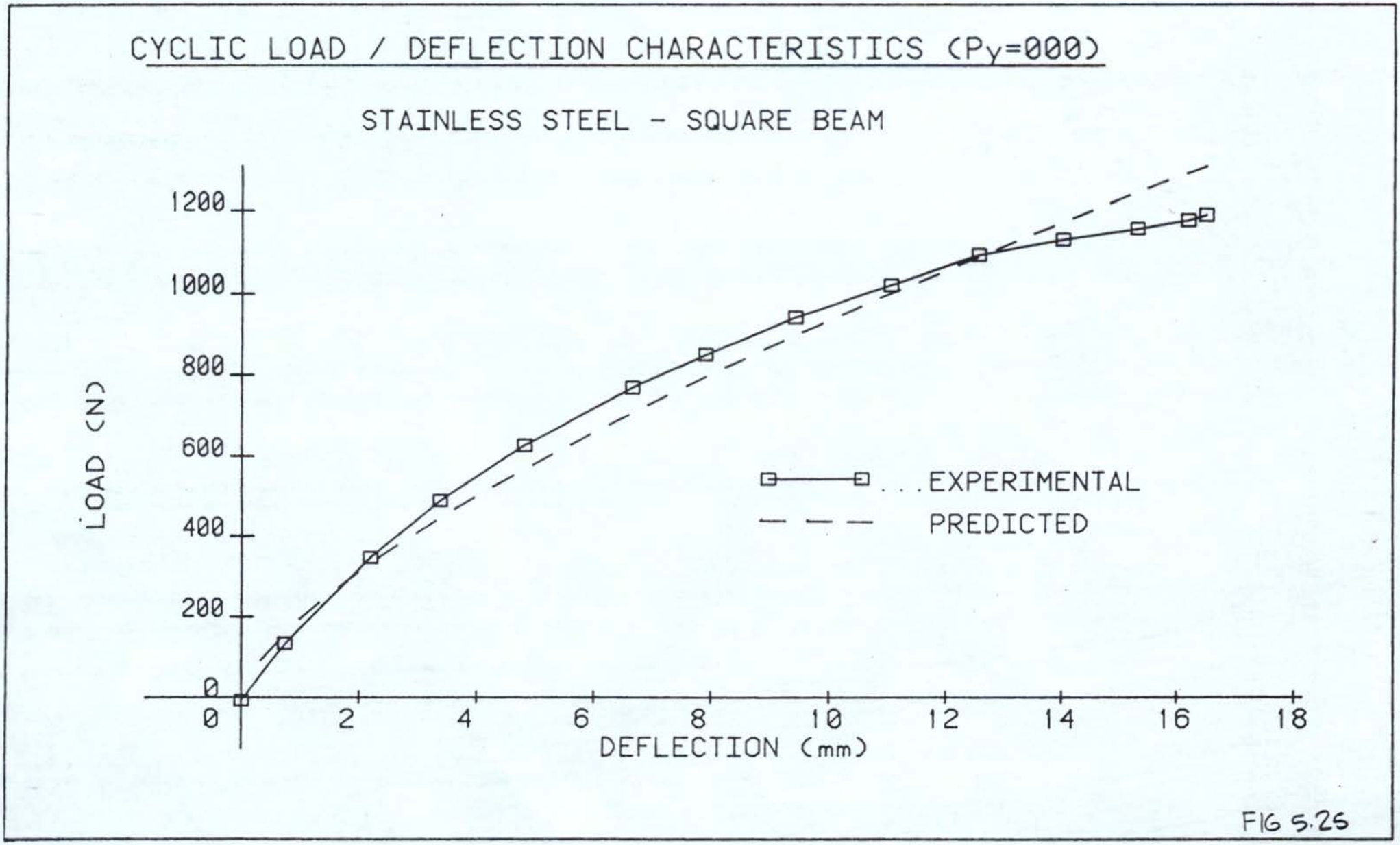
CYCLIC LOAD / DEFLECTION CHARACTERISTICS (Py=000)
STAINLESS STEEL - SQUARE BEAM
LOAD (N)
1200
1000
800
600
400
200
0
0
2
4
6
8
10
12
14
16
18
DEFLECTION (mm)
EXPERIMENTAL
PREDICTED

FIG 5.25

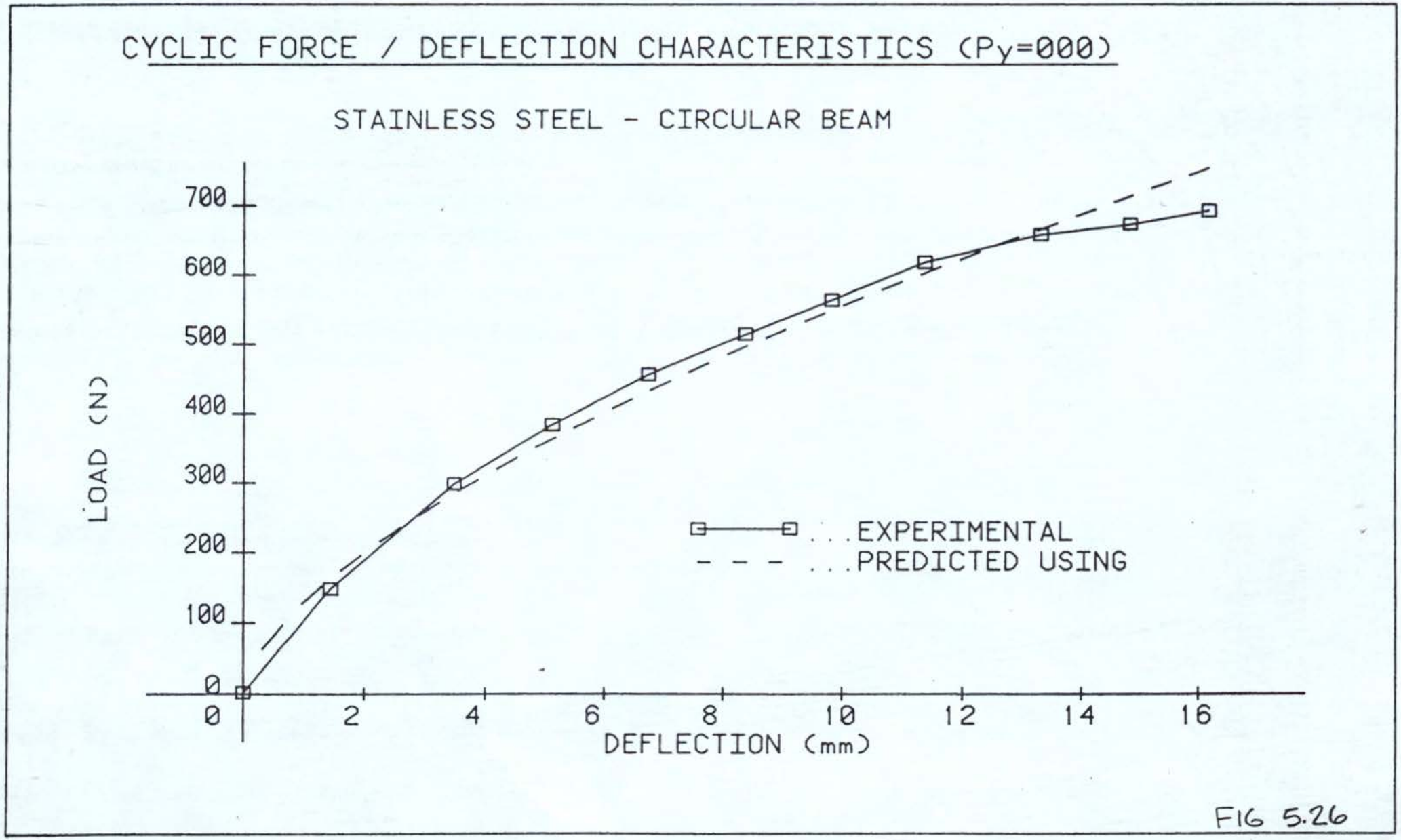
CYCLIC FORCE / DEFLECTION CHARACTERISTICS (Py=000)
STAINLESS STEEL - CIRCULAR BEAM
LOAD (N)
700
600
500
400
300
200
100
0
0
2
4
6
8
10
12
14
16
DEFLECTION (mm)
...EXPERIMENTAL
- - - ...PREDICTED USING

FIG 5.26

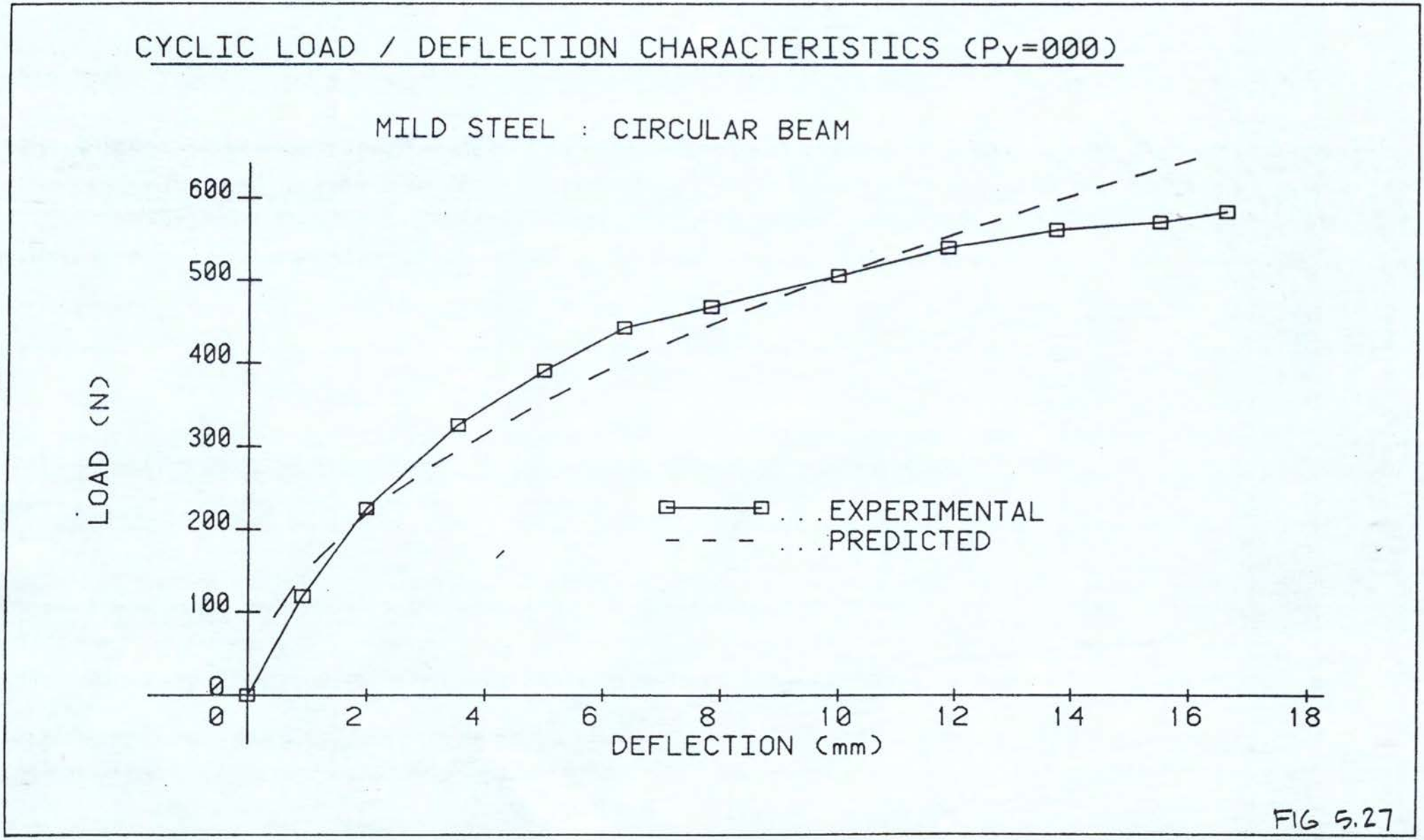
CYCLIC LOAD / DEFLECTION CHARACTERISTICS (Py=000)
MILD STEEL : CIRCULAR BEAM
LOAD (N)
600
500
400
300
200
100
0
0
2
4
6
8
10
12
14
16
18
DEFLECTION (mm)
...EXPERIMENTAL
...PREDICTED

FIG 5.27

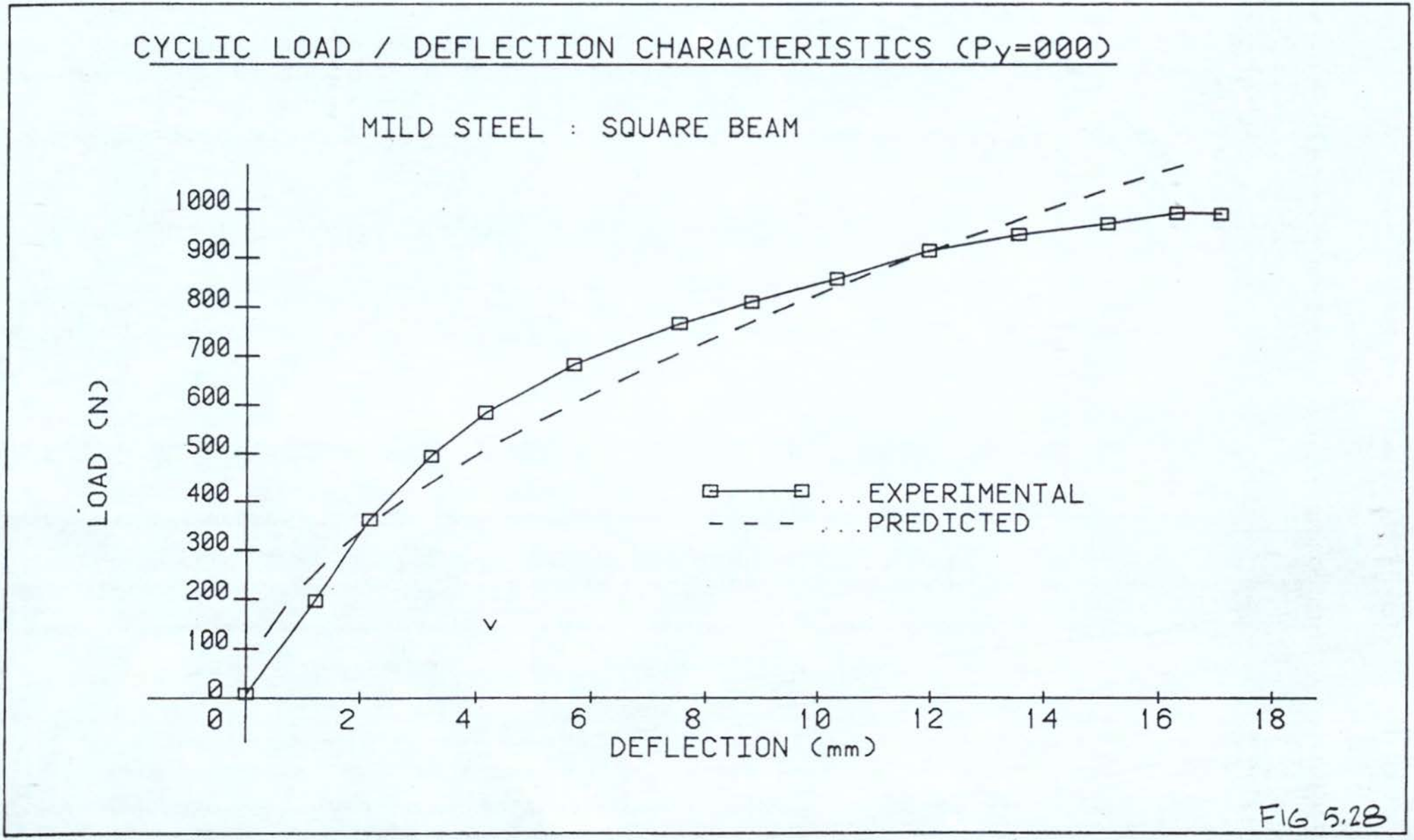
CYCLIC LOAD / DEFLECTION CHARACTERISTICS (Py=000)
MILD STEEL : SQUARE BEAM
LOAD (N)
1000
900
800
700
600
500
400
300
200
100
0
0
2
4
6
8
10
12
14
16
18
DEFLECTION (mm)
...EXPERIMENTAL
...PREDICTED

FIG 5.28

5.1.5 BI-AXIAL BENDING - LOAD DEFLECTION CURVES

5.1.5.1 FIRST QUARTER CYCLE

Some experimental and predicted relationships for stainless square and round beams are shown in Figs (5.29) - (5.34). Generally the predictions are quite good for this material. The sustained vertical loads varied between 240 and 360 N and the theoretical predictions were based on two methods.

a) Converting the actual loads into an equivalent radial load and ignoring any effects due to the rotation of the neutral surface.

b) Following the history of each elemental fibre and allowing for unloading due to rotation of the neutral surface.

The predictions are again quite good for both methods at the higher levels of strain. Many of the errors are still due to our inability to model material behaviour in the first quarter cycle because of the significant elastic region. Of the two theoretical approaches, the computer based approach (b) which follows the history of loading gives more realistic results, particularly in the early stages of deformation. This is more obvious for the square beam where methods (a) grossly over-predicts the bending load at lower deflections.

For the mild steel, methods (a) and (b) give similar predications, Figs (5.36) to (5.39) but our inability to model material behaviour during the first quarter cycle makes comparison with the experimental results difficult. From these results, and the earlier ones without the sustained vertical load it would appear that most of the deformation is occurring within the lower yield point region of non-homogeneous deformation and we are observing a plastic hinge developing without any work hardening.

5.1.5.2 CYCLIC STEADY STATE CONDITION

The load-deflection characteristics in the cyclic steady state condition for mild steel circular and square beams are shown in Figs (5.40) to (5.43) and (5.46) to (5.48). It is difficult to assess the theoretical approaches (a) and (b) because different load deflection characteristics were developed during bending in the forward and reverse directions. This may be due to non-homogeneous deformation occurring during the first quarter cycle which is not corrected in subsequent cycles. This effect is considerably greater for the round beam compared to the square beam. The theoretical prediction for the square beam are felt to be quite good using either method but following the history of loading gives much better predictions in the early stages of deformation.

The results for the stainless material are shown in Figs (5.43), (5.45), and (5.49) to (5.50).

The theoretical predictions following the history of loading are felt to be very good and much superior to method (a) which over estimates the bending loads considerably.

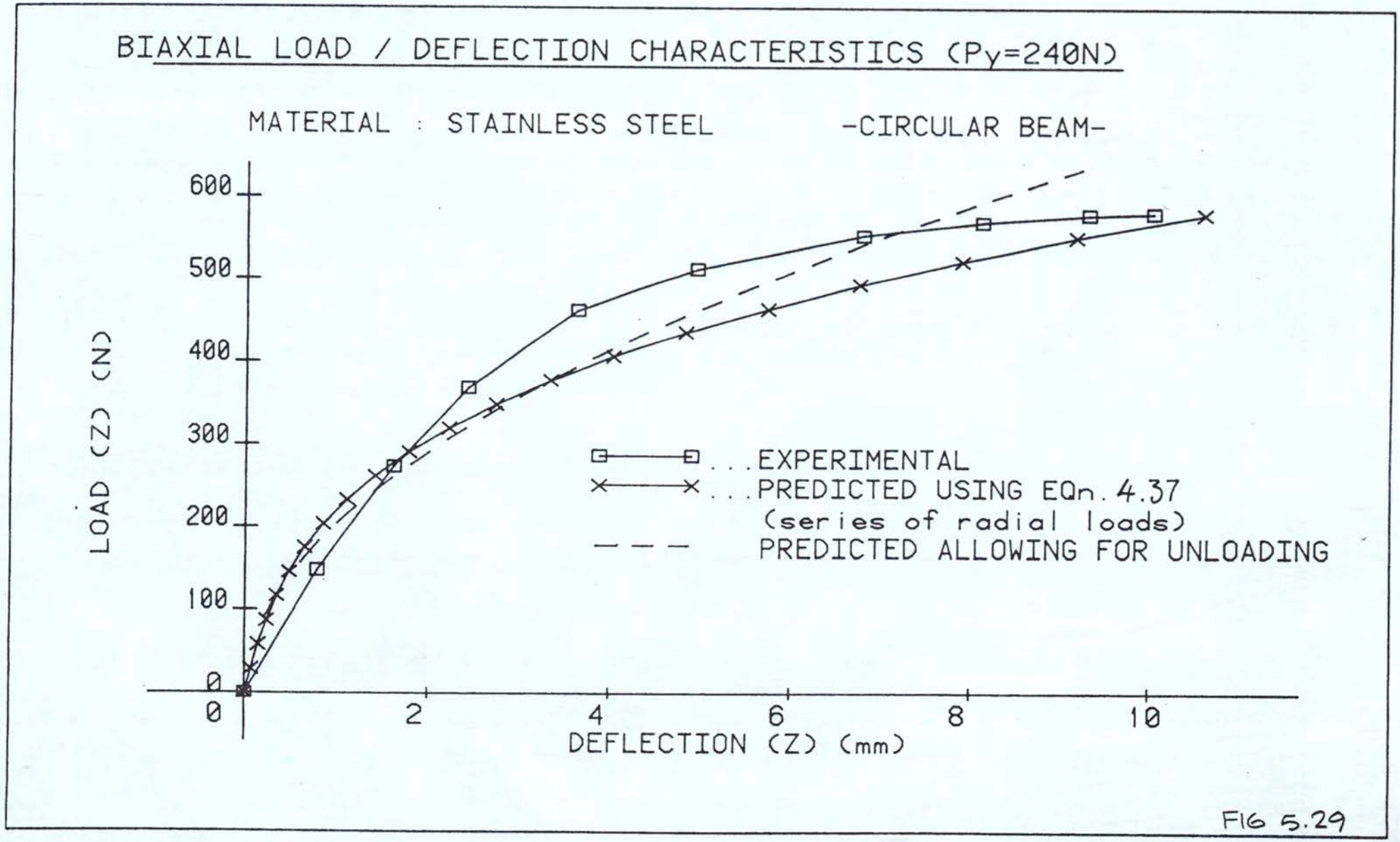
BIAXIAL LOAD / DEFLECTION CHARACTERISTICS (Py=240N)
MATERIAL : STAINLESS STEEL
-CIRCULAR BEAM-
LOAD (Z) (N)
600
500
400
300
200
100
0
0
2
4
6
8
10
DEFLECTION (Z) (mm)
...EXPERIMENTAL
...PREDICTED USING EQn. 4.37
(series of radial loads)
PREDICTED ALLOWING FOR UNLOADING

FIG 5.29

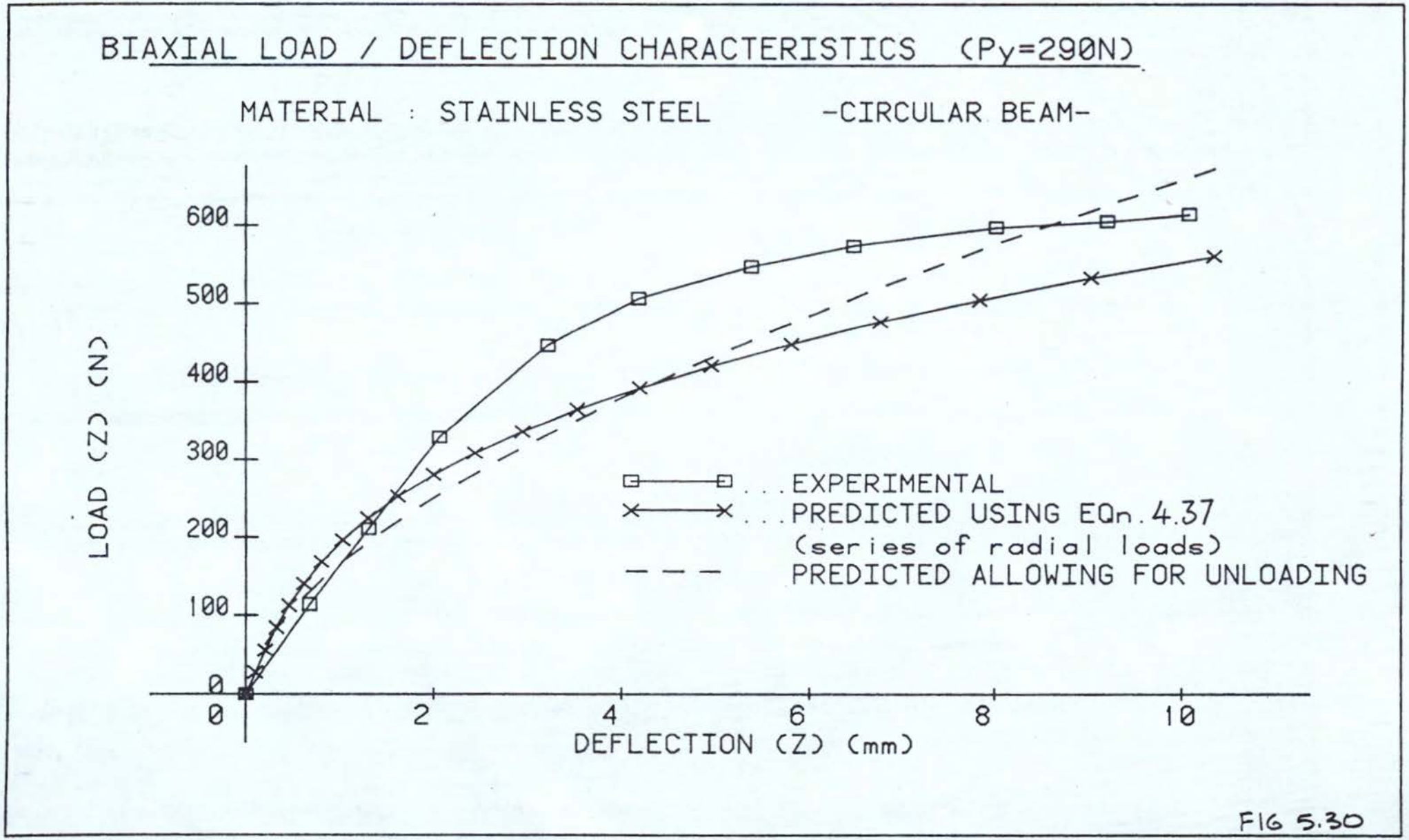
BIAXIAL LOAD / DEFLECTION CHARACTERISTICS (Py=290N)
MATERIAL : STAINLESS STEEL -CIRCULAR BEAM-
LOAD (Z) (N)
600
500
400
300
200
100
0
0
2
4
6
8
10
DEFLECTION (Z) (mm)
...EXPERIMENTAL
...PREDICTED USING EQn.4.37
(series of radial loads)
PREDICTED ALLOWING FOR UNLOADING

FIG 5.30

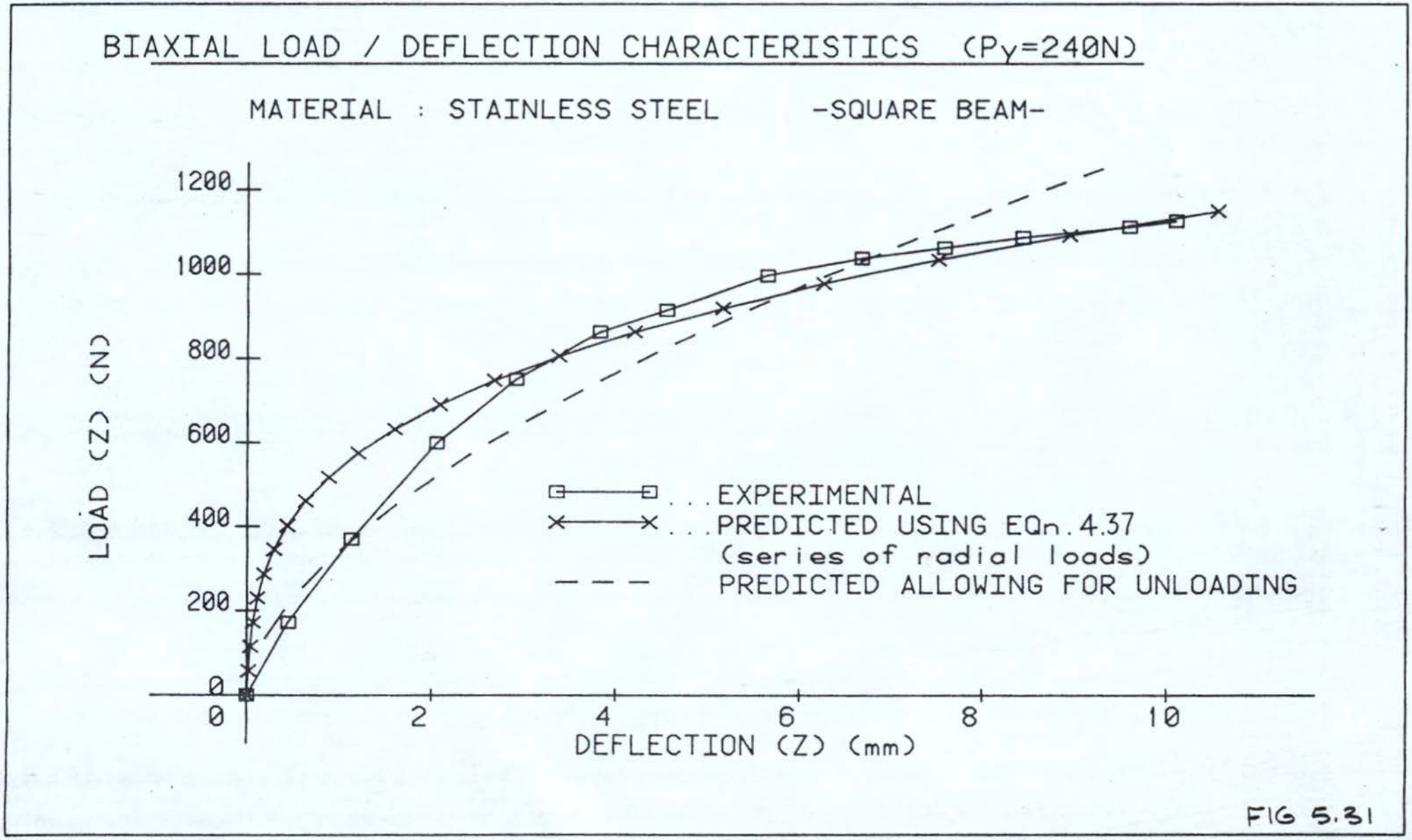
BIAXIAL LOAD / DEFLECTION CHARACTERISTICS (Py=240N)
MATERIAL : STAINLESS STEEL -SQUARE BEAM-
LOAD (Z) (N)
1200
1000
800
600
400
200
0
0
2
4
6
8
10
DEFLECTION (Z) (mm)
...EXPERIMENTAL
...PREDICTED USING EQn.4.37
(series of radial loads)
PREDICTED ALLOWING FOR UNLOADING

FIG 5.31

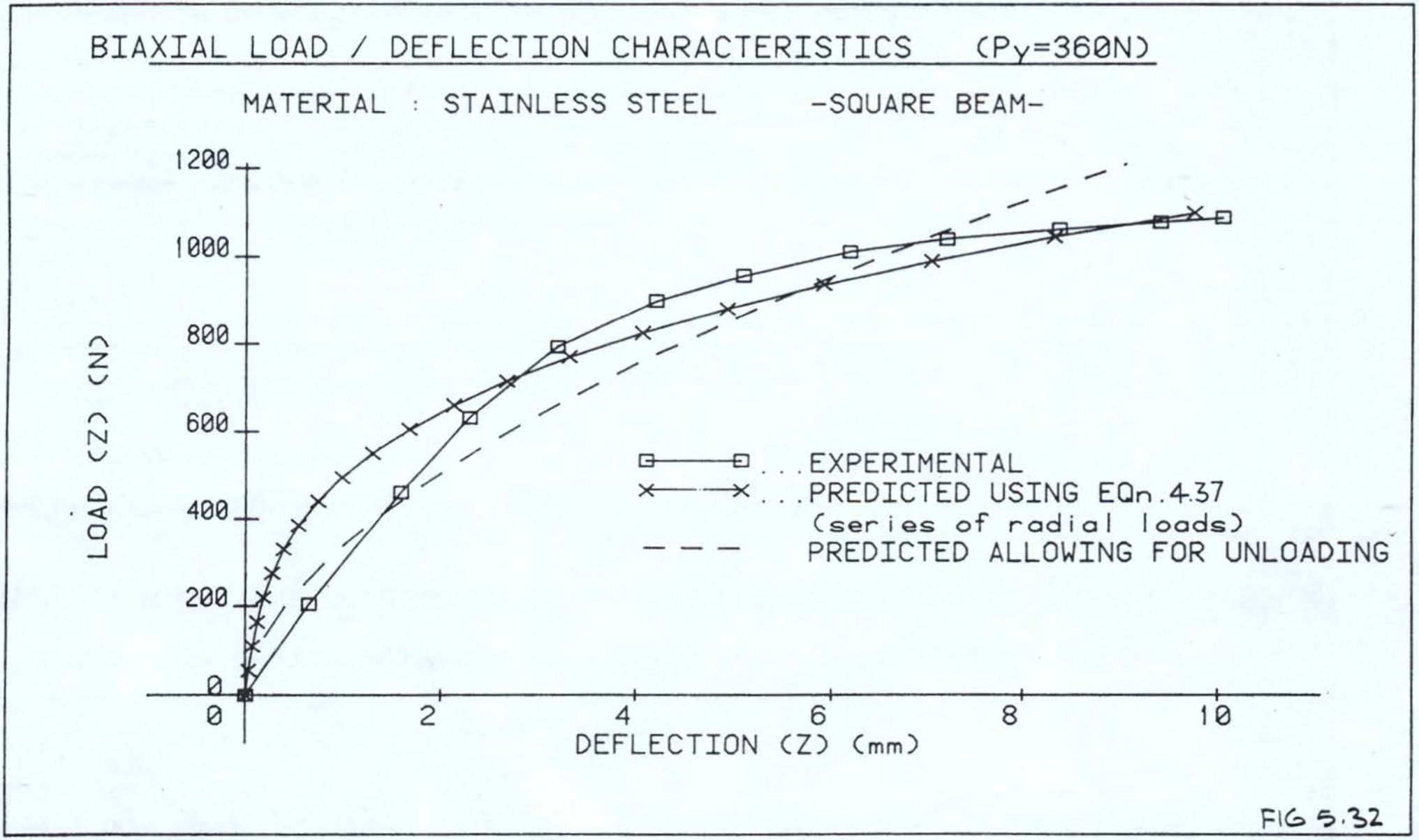
BIAXIAL LOAD / DEFLECTION CHARACTERISTICS (Py=360N)
MATERIAL : STAINLESS STEEL -SQUARE BEAM-
LOAD (Z) (N)
1200
1000
800
600
400
200
0
0
2
4
6
8
10
DEFLECTION (Z) (mm)
...EXPERIMENTAL
...PREDICTED USING EQn.4.37
(series of radial loads)
PREDICTED ALLOWING FOR UNLOADING

FIG 5.32

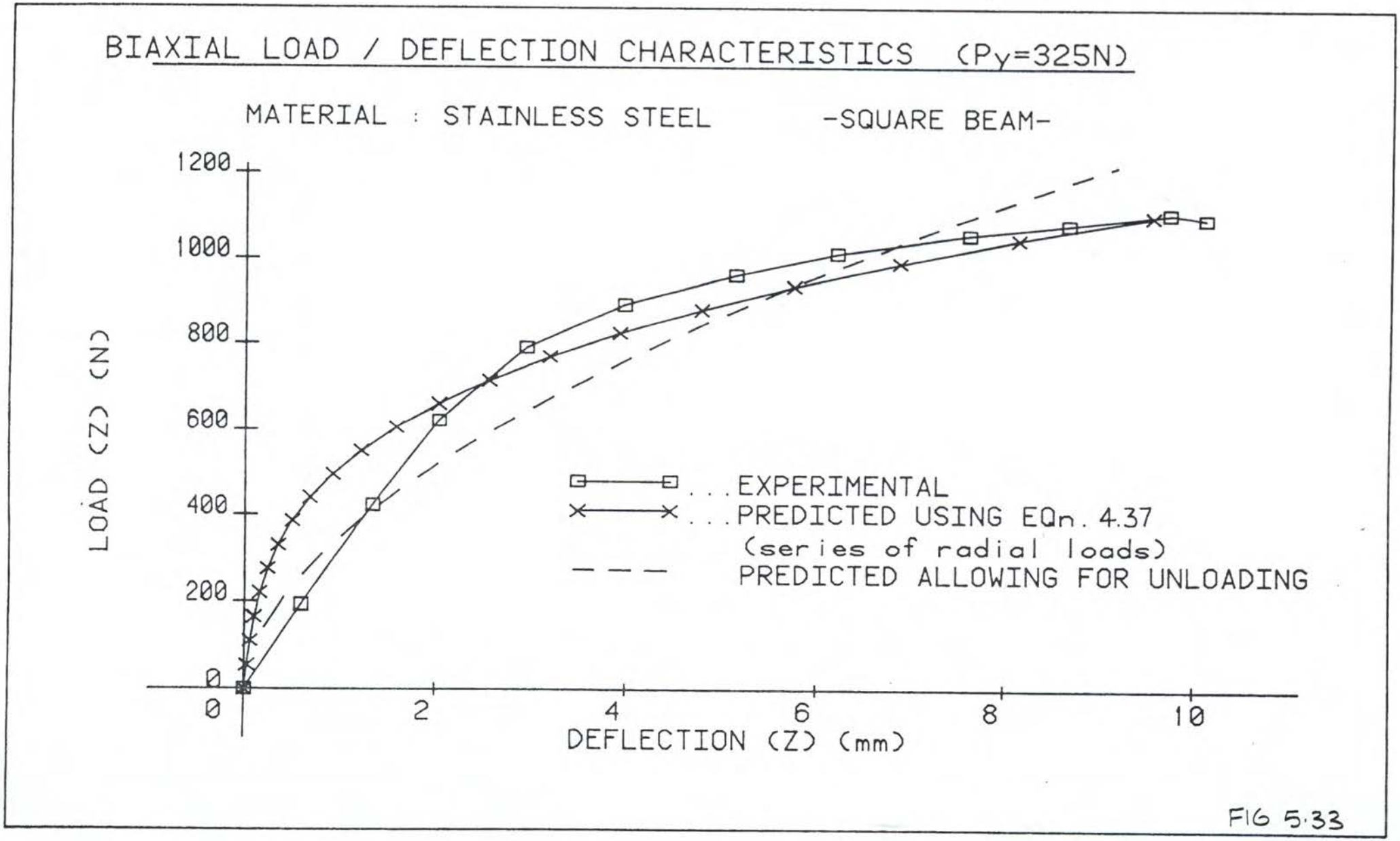
BIAXIAL LOAD / DEFLECTION CHARACTERISTICS (Py=325N)
MATERIAL : STAINLESS STEEL -SQUARE BEAM-
LOAD (Z) (N)
1200
1000
800
600
400
200
0
0
2
4
6
8
10
DEFLECTION (Z) (mm)
...EXPERIMENTAL
...PREDICTED USING EQn. 4.37
(series of radial loads)
PREDICTED ALLOWING FOR UNLOADING

FIG 5.33

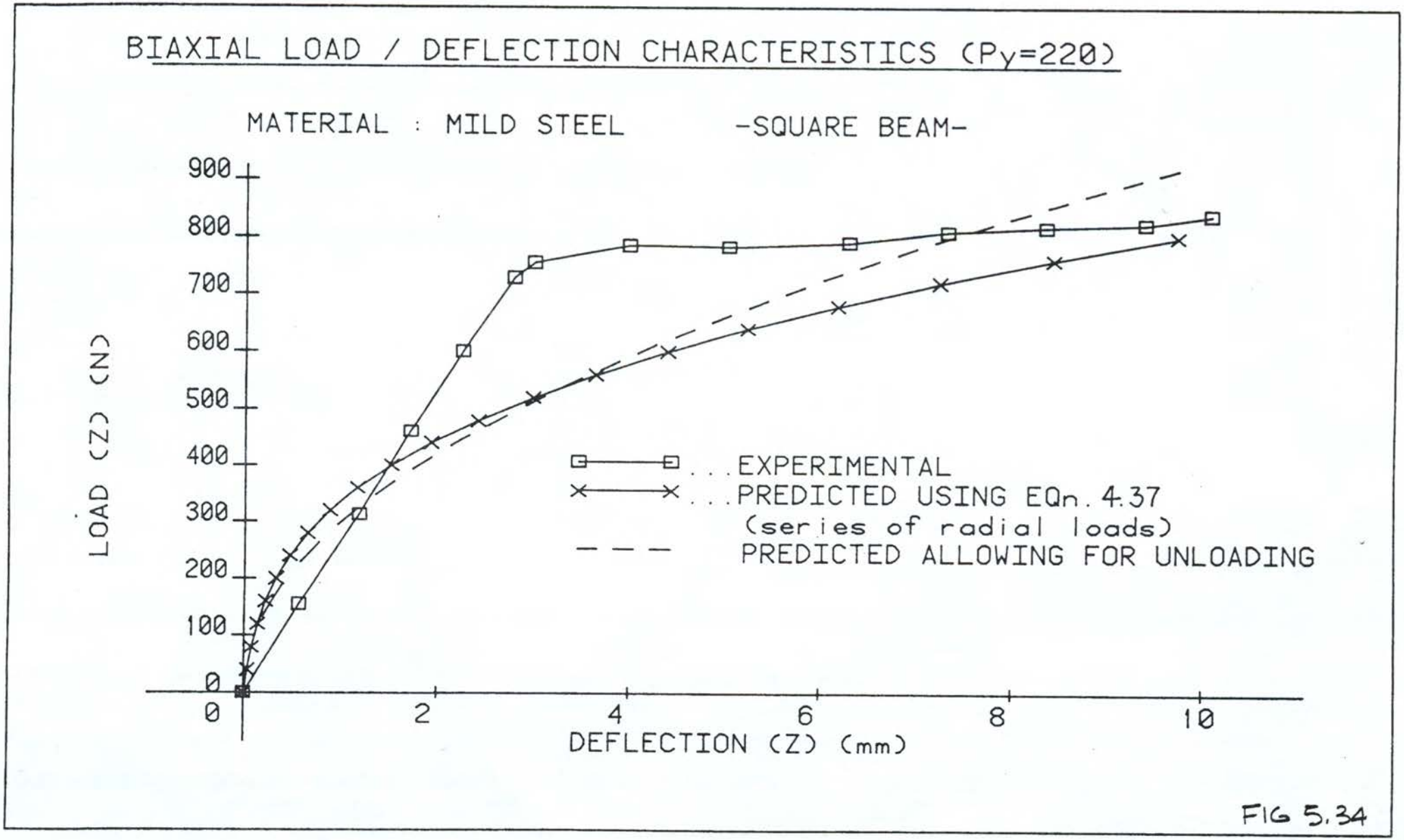
BIAXIAL LOAD / DEFLECTION CHARACTERISTICS (Py=220)
MATERIAL : MILD STEEL -SQUARE BEAM-
LOAD (Z) (N)
900
800
700
600
500
400
300
200
100
0
0
2
4
6
8
10
DEFLECTION (Z) (mm)
...EXPERIMENTAL
...PREDICTED USING EQn. 4.37
(series of radial loads)
PREDICTED ALLOWING FOR UNLOADING

FIG 5.34

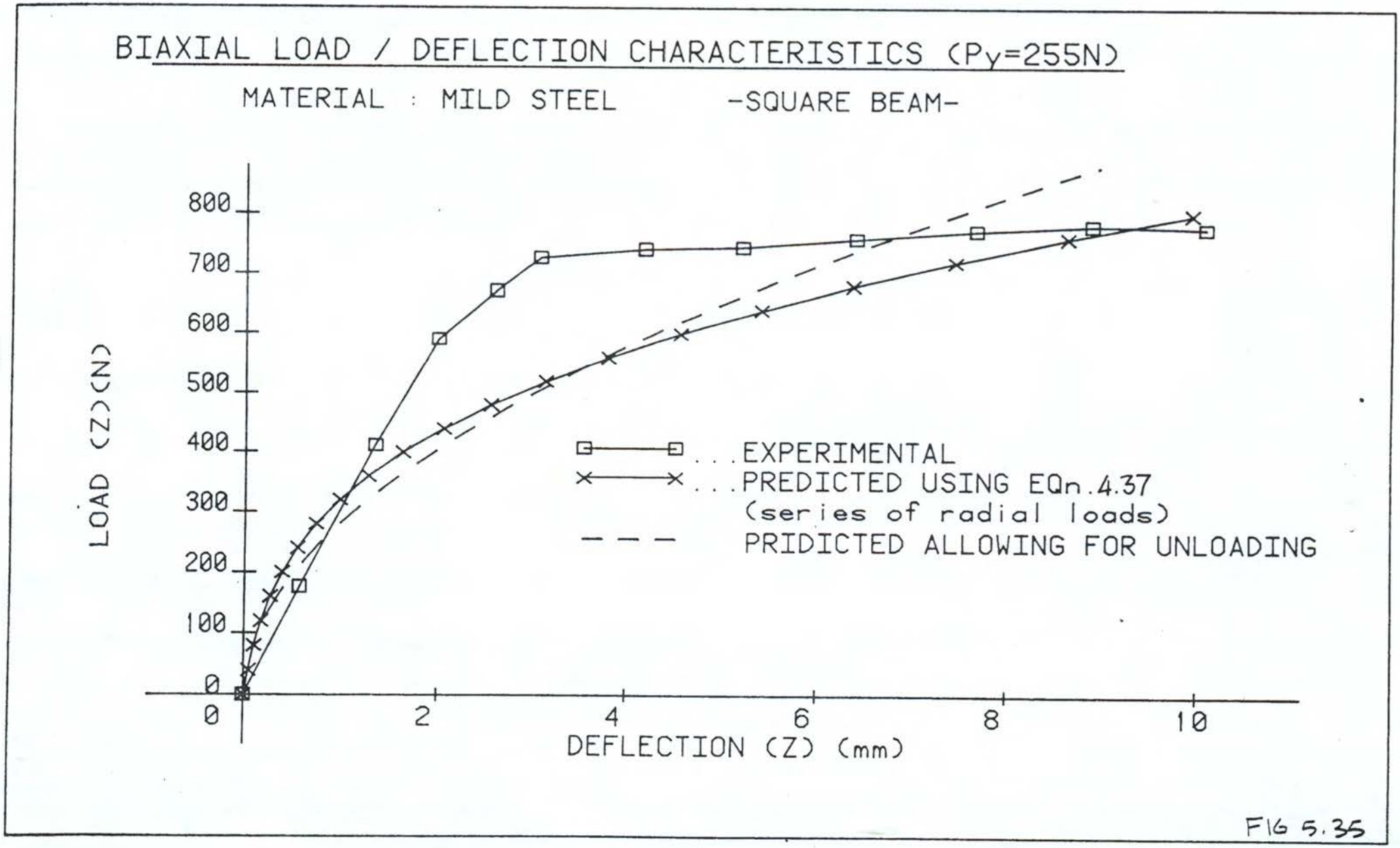
BIAXIAL LOAD / DEFLECTION CHARACTERISTICS (Py=255N)
MATERIAL : MILD STEEL -SQUARE BEAM-
LOAD (Z)(N)
800
700
600
500
400
300
200
100
0
0
2
4
6
8
10
DEFLECTION (Z) (mm)
...EXPERIMENTAL
...PREDICTED USING EQn.4.37
(series of radial loads)
PRIDICTED ALLOWING FOR UNLOADING

FIG 5.35

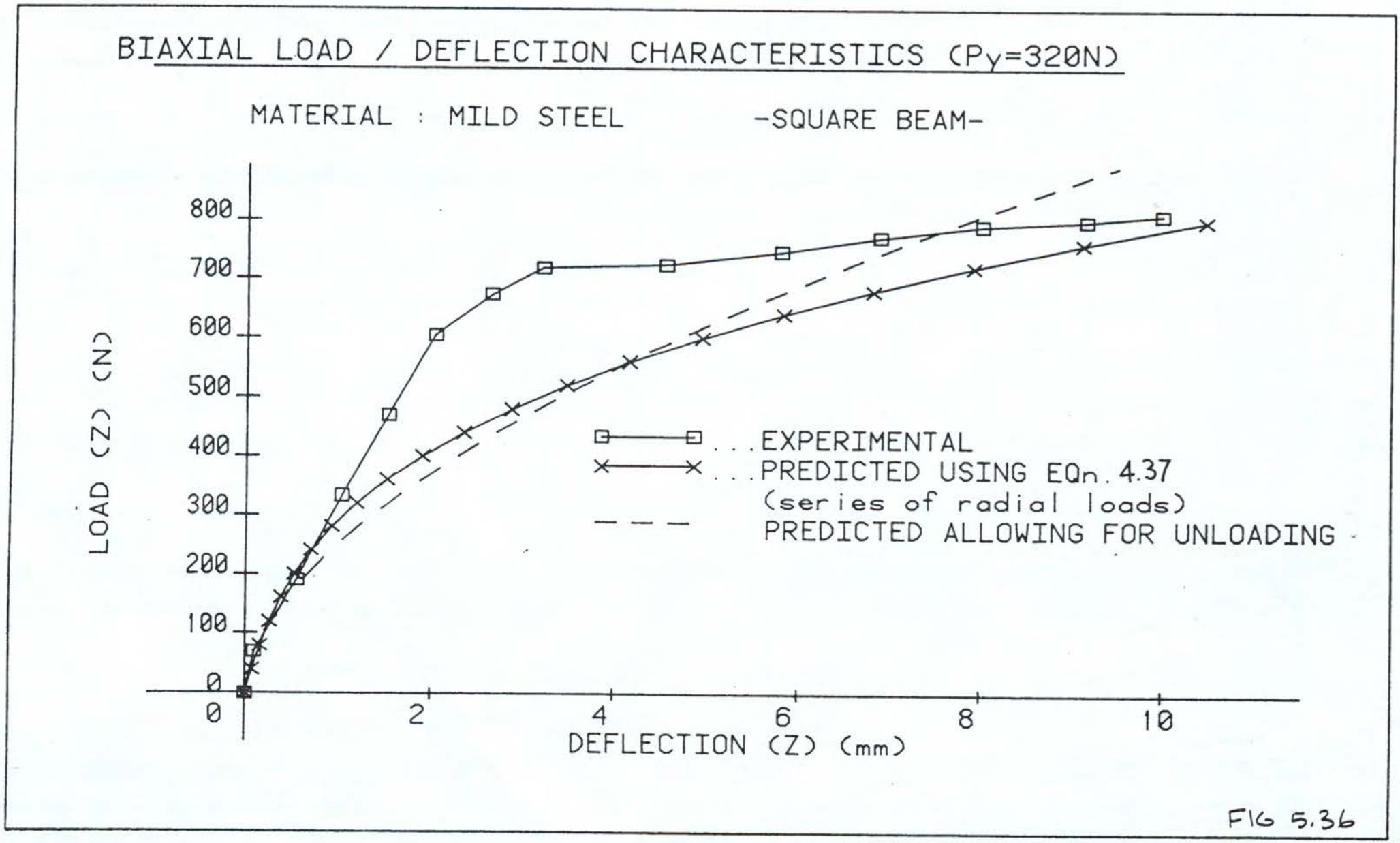
BIAXIAL LOAD / DEFLECTION CHARACTERISTICS (Py=320N)
MATERIAL : MILD STEEL
-SQUARE BEAM-
LOAD (Z) (N)
800
700
600
500
400
300
200
100
0
0
2
4
6
8
10
DEFLECTION (Z) (mm)
...EXPERIMENTAL
...PREDICTED USING EQn. 4.37
(series of radial loads)
PREDICTED ALLOWING FOR UNLOADING

FIG 5.36

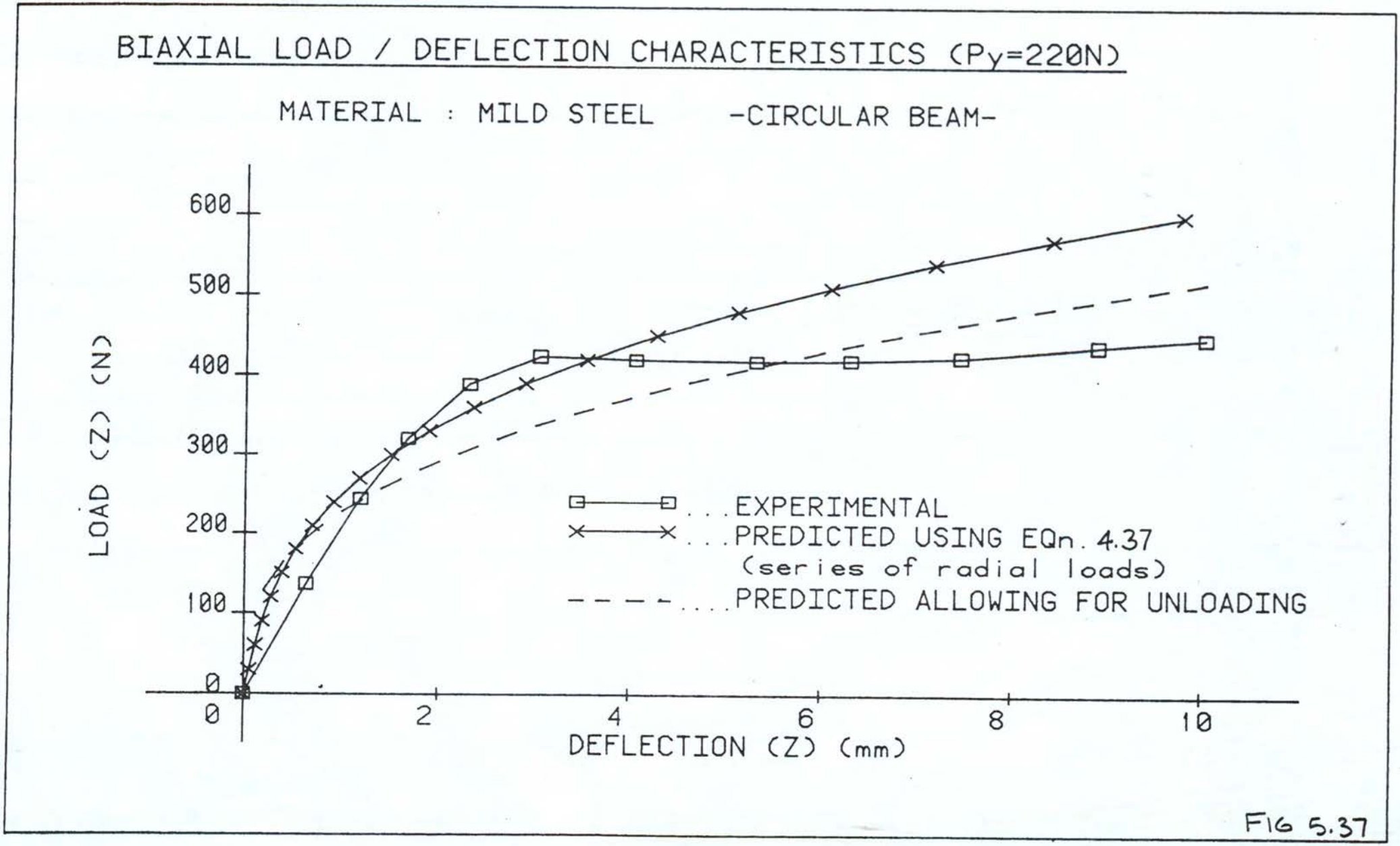
BIAXIAL LOAD / DEFLECTION CHARACTERISTICS (Py=220N)
MATERIAL : MILD STEEL -CIRCULAR BEAM-
LOAD (Z) (N)
600
500
400
300
200
100
0
0
2
4
6
8
10
DEFLECTION (Z) (mm)
...EXPERIMENTAL
...PREDICTED USING EQn. 4.37
(series of radial loads)
....PREDICTED ALLOWING FOR UNLOADING

FIG 5.37

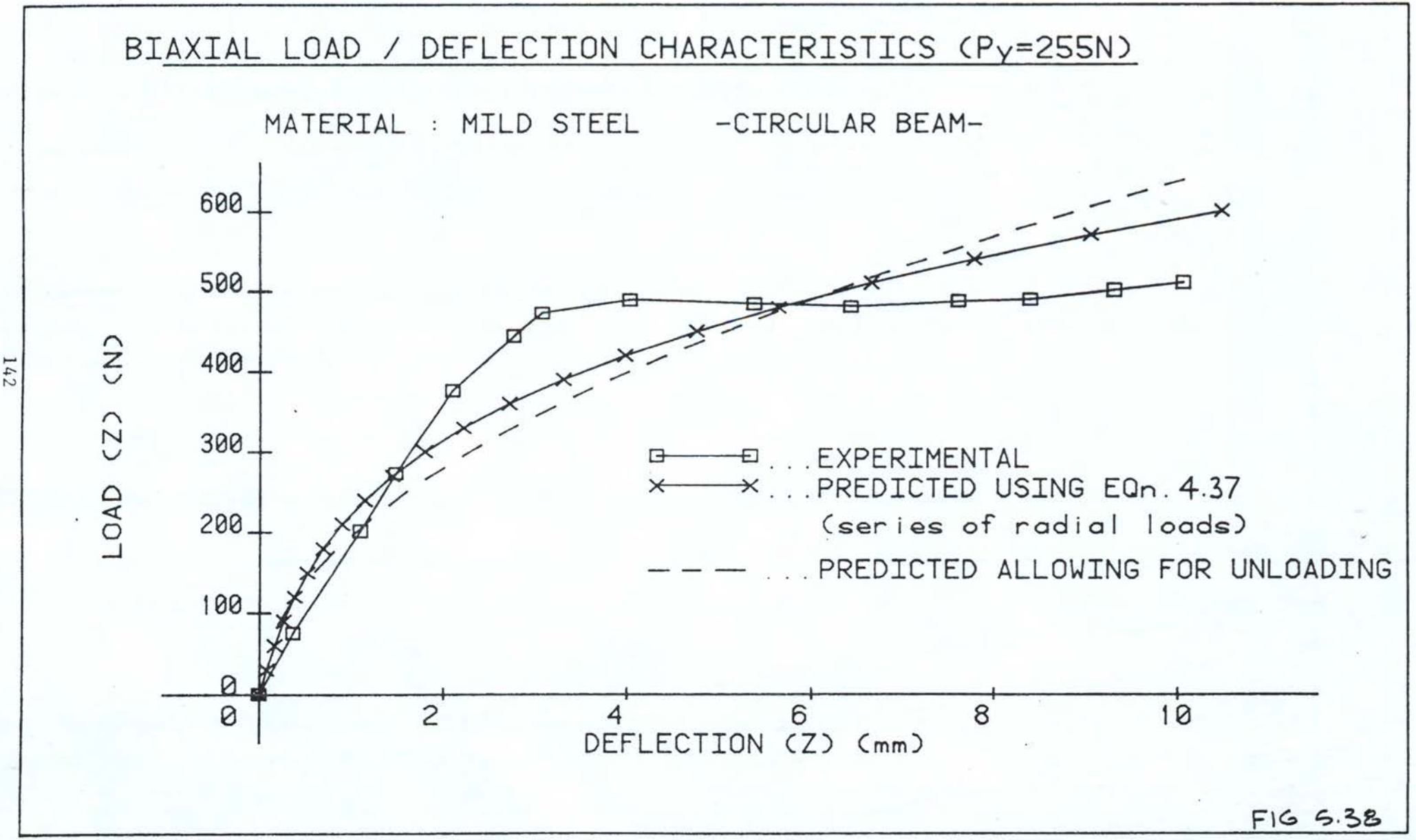
BIAXIAL LOAD / DEFLECTION CHARACTERISTICS (Py=255N)
MATERIAL : MILD STEEL -CIRCULAR BEAM-
LOAD (Z) (N)
600
500
400
300
200
100
0
0
2
4
6
8
10
DEFLECTION (Z) (mm)
...EXPERIMENTAL
...PREDICTED USING EQn. 4.37
(series of radial loads)
...PREDICTED ALLOWING FOR UNLOADING

FIG 5.38

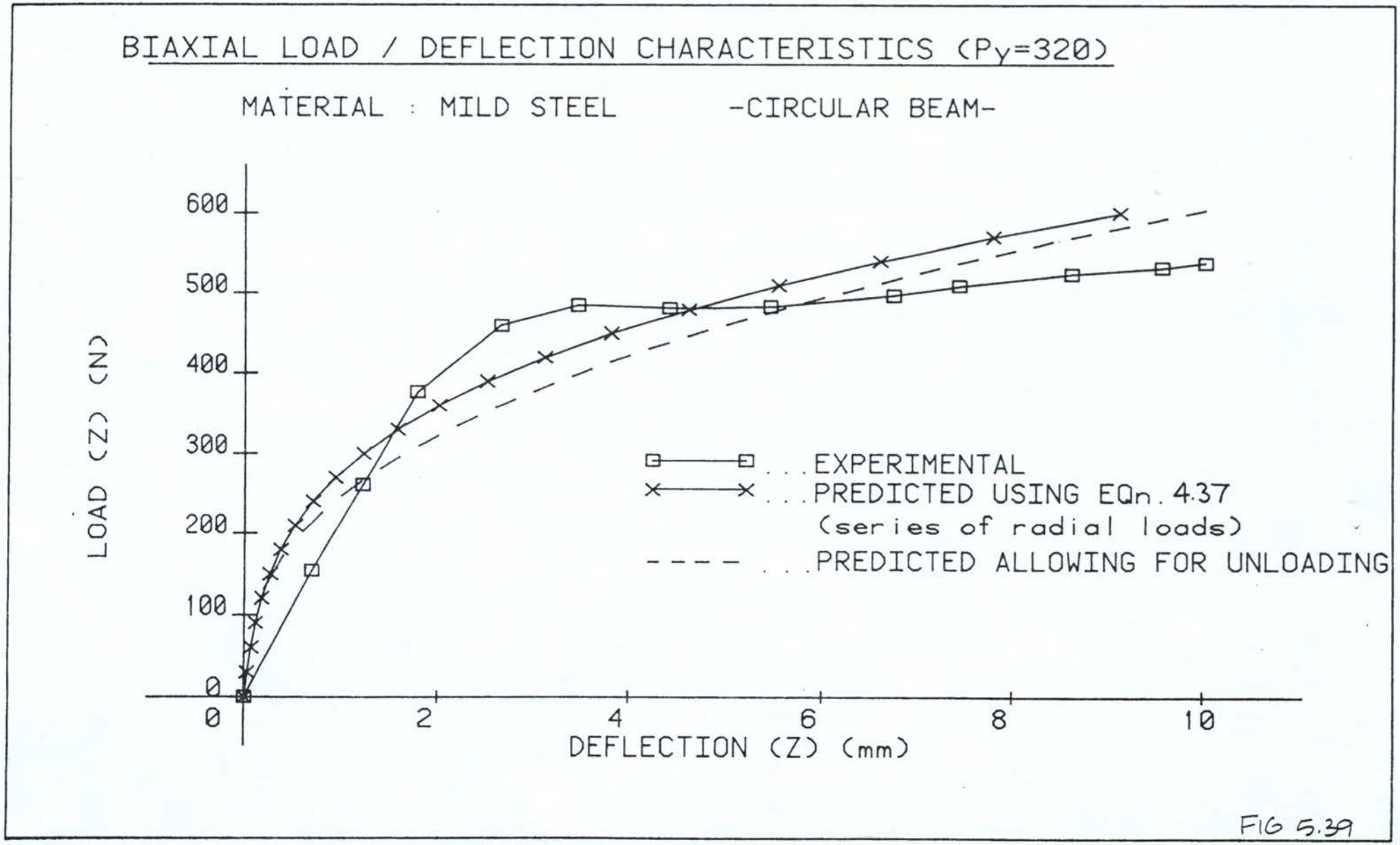
BIAXIAL LOAD / DEFLECTION CHARACTERISTICS (Py=320)
MATERIAL : MILD STEEL -CIRCULAR BEAM-
LOAD (Z) (N)
600
500
400
300
200
100
0
0
2
4
6
8
10
DEFLECTION (Z) (mm)
. . . EXPERIMENTAL
. . . PREDICTED USING EQn. 4.37
(series of radial loads)
. . . . PREDICTED ALLOWING FOR UNLOADING

FIG 5.39

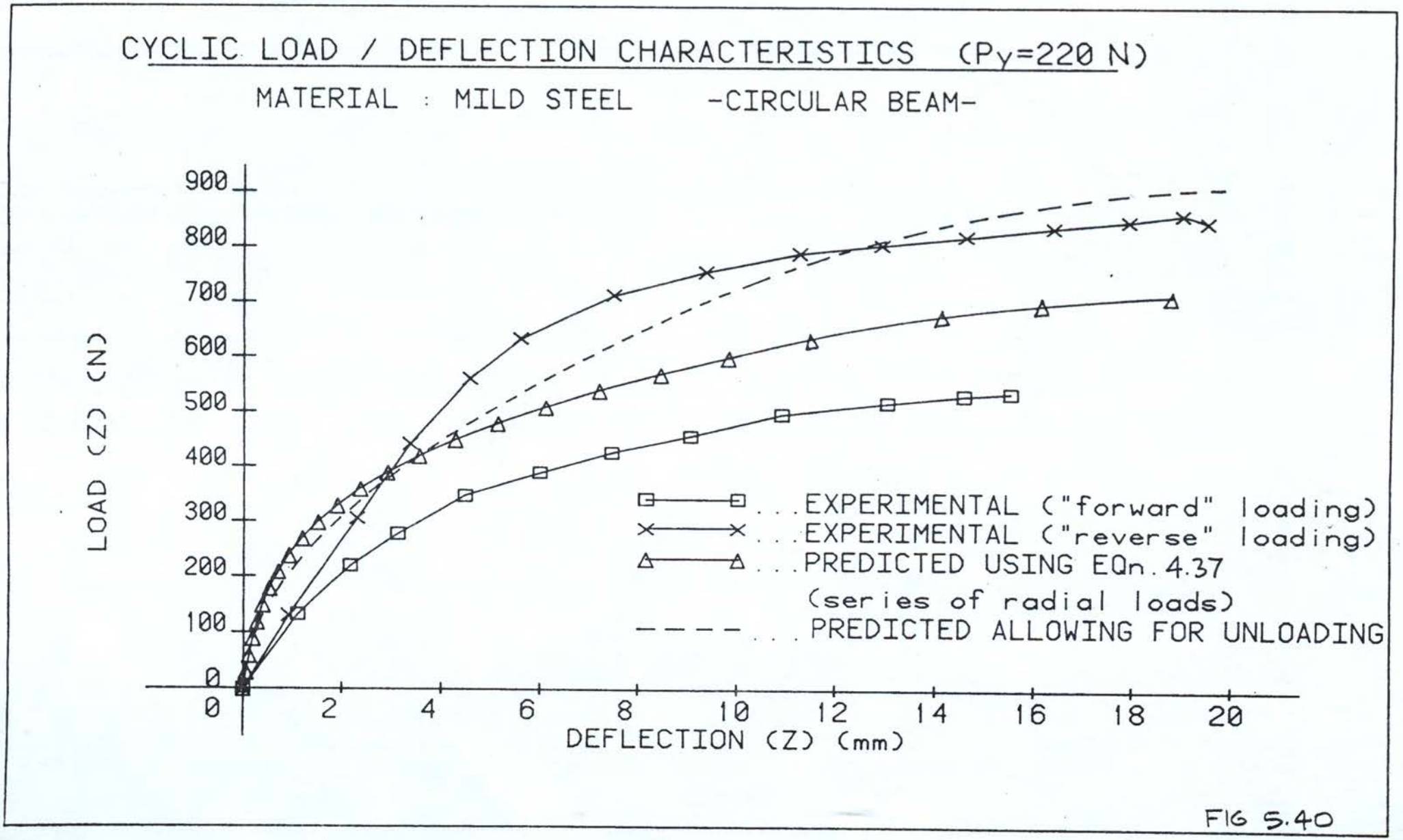
CYCLIC LOAD / DEFLECTION CHARACTERISTICS (Py=220 N)
MATERIAL : MILD STEEL -CIRCULAR BEAM-
LOAD (Z) (N)
900
800
700
600
500
400
300
200
100
0
0
2
4
6
8
10
12
14
16
18
20
DEFLECTION (Z) (mm)
...EXPERIMENTAL ("forward" loading)
...EXPERIMENTAL ("reverse" loading)
...PREDICTED USING EQn. 4.37
(series of radial loads)
...PREDICTED ALLOWING FOR UNLOADING

FIG 5.40

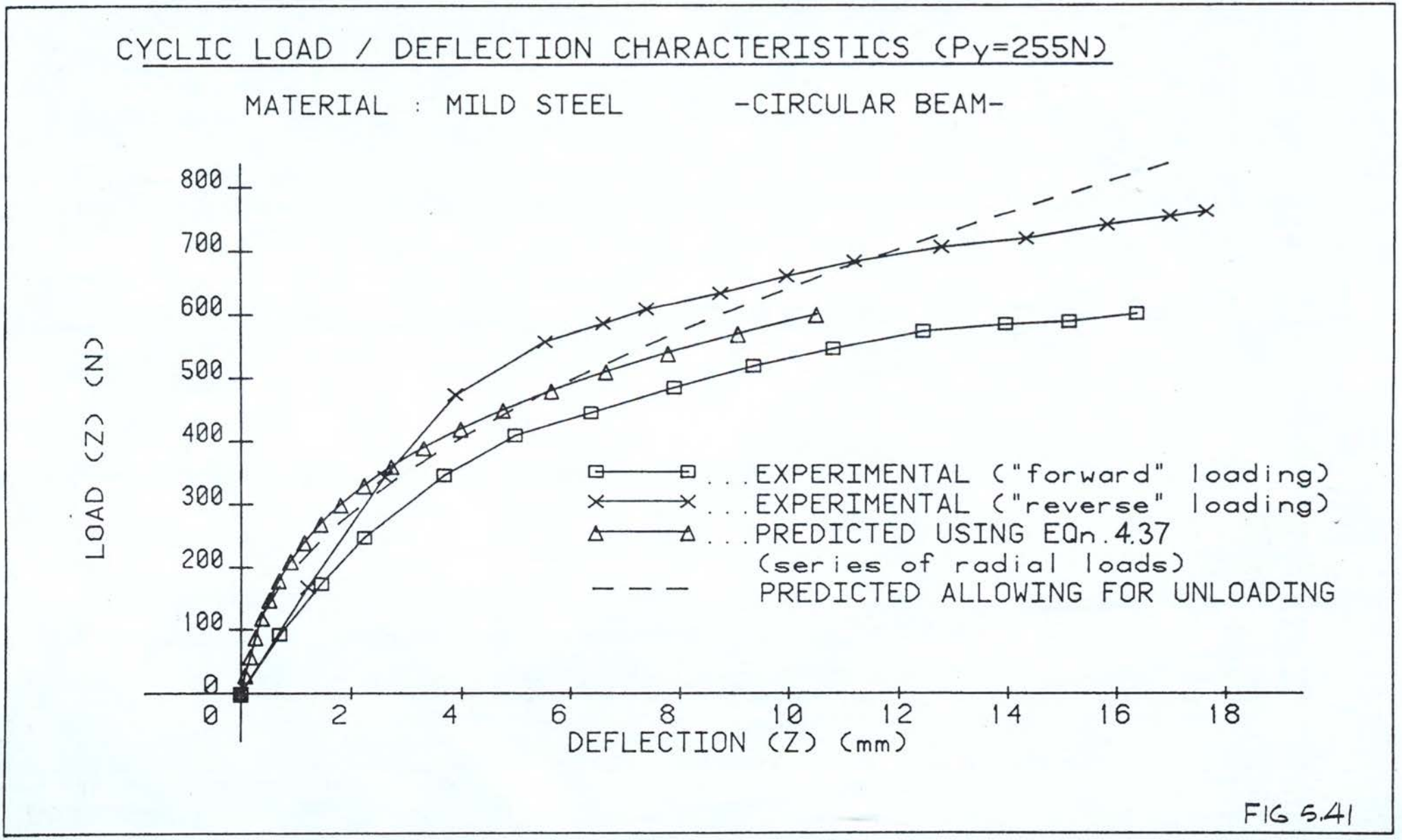
CYCLIC LOAD / DEFLECTION CHARACTERISTICS (Py=255N)
MATERIAL : MILD STEEL -CIRCULAR BEAM-
LOAD (Z) (N)
800
700
600
500
400
300
200
100
0
0
2
4
6
8
10
12
14
16
18
DEFLECTION (Z) (mm)
...EXPERIMENTAL ("forward" loading)
...EXPERIMENTAL ("reverse" loading)
...PREDICTED USING EQn.4.37
(series of radial loads)
PREDICTED ALLOWING FOR UNLOADING

FIG 5.41

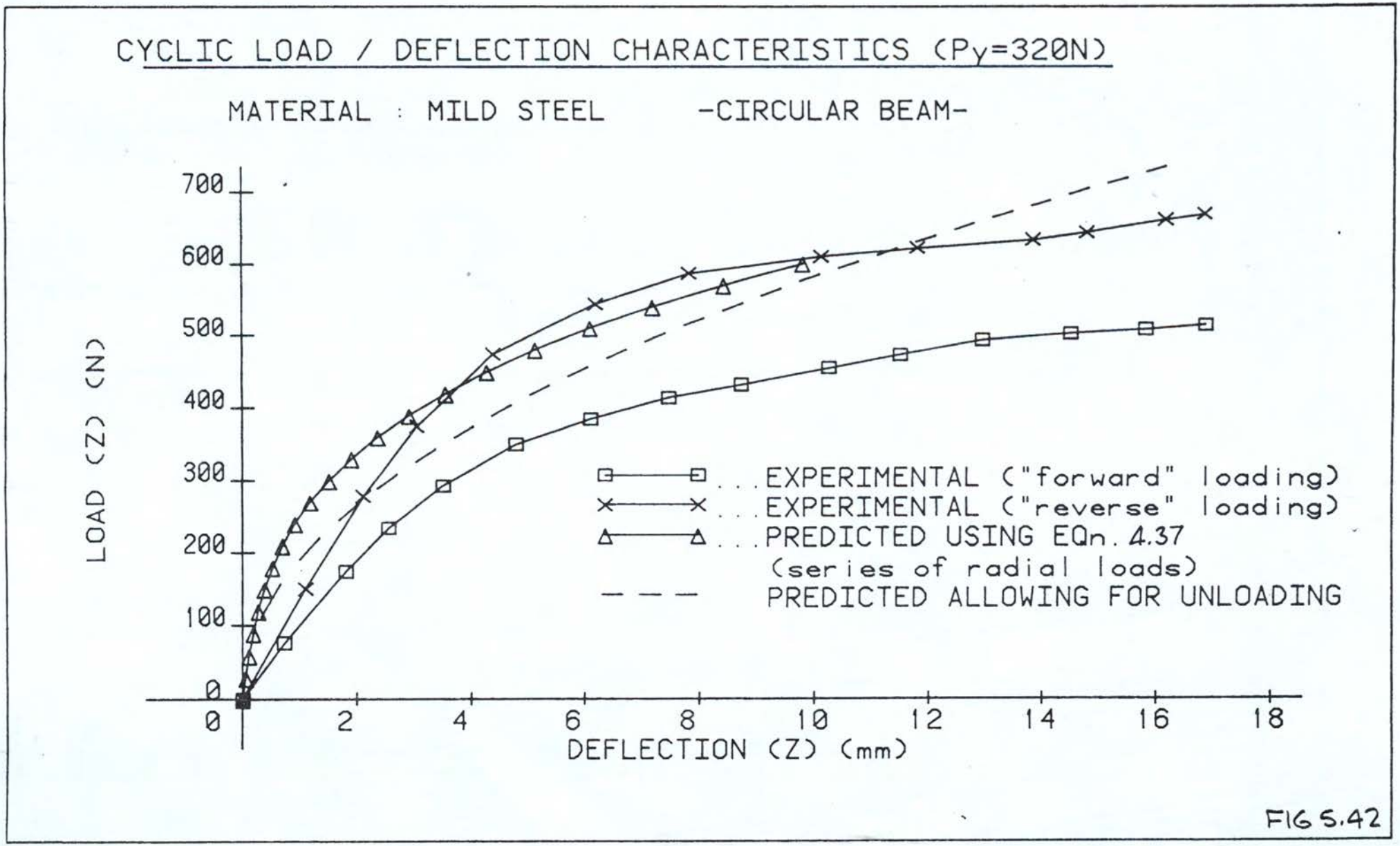
CYCLIC LOAD / DEFLECTION CHARACTERISTICS (Py=320N)
MATERIAL : MILD STEEL -CIRCULAR BEAM-
LOAD (Z) (N)
700
600
500
400
300
200
100
0
0
2
4
6
8
10
12
14
16
18
DEFLECTION (Z) (mm)
...EXPERIMENTAL ("forward" loading)
...EXPERIMENTAL ("reverse" loading)
...PREDICTED USING EQn. 4.37
(series of radial loads)
PREDICTED ALLOWING FOR UNLOADING

FIG 5.42

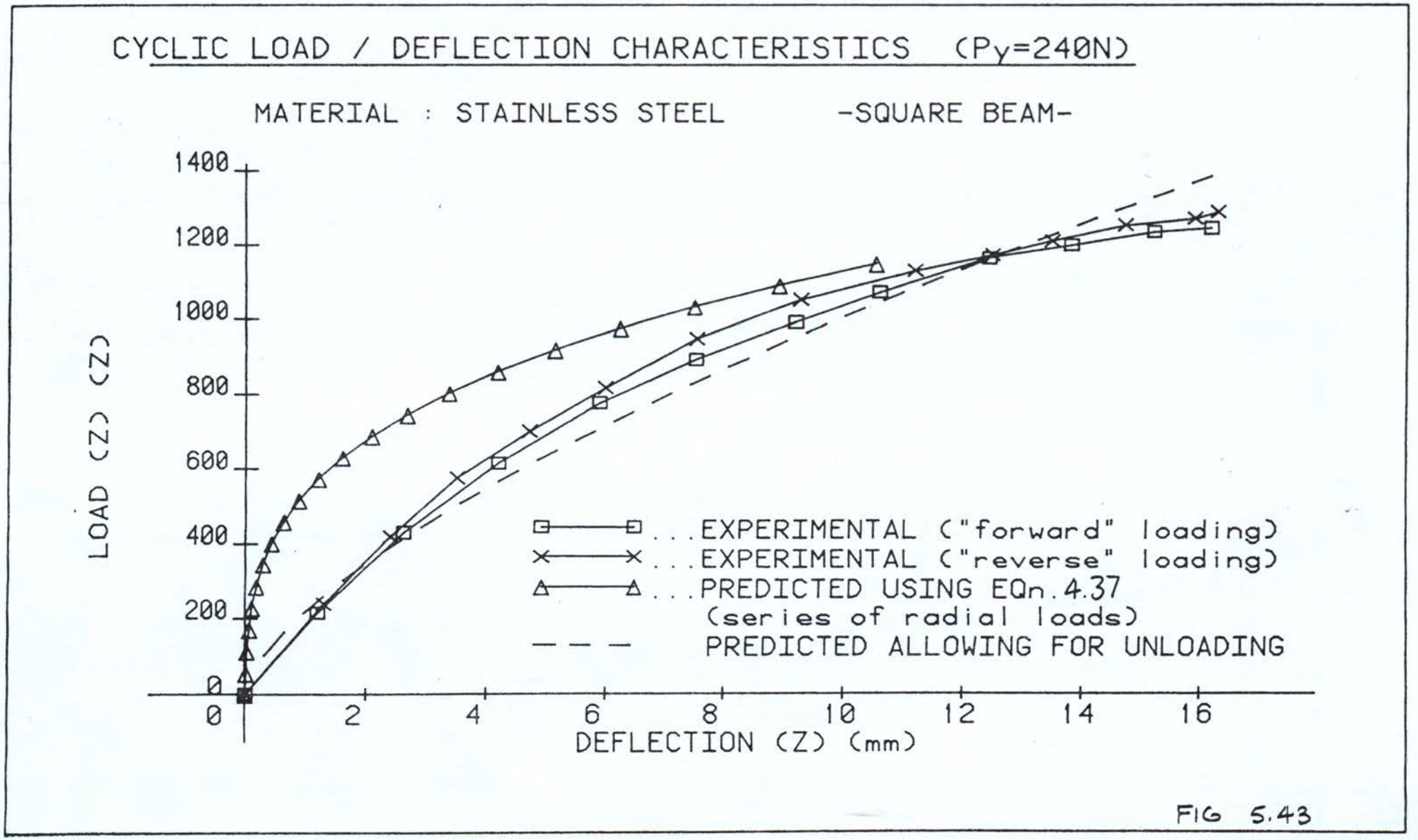
CYCLIC LOAD / DEFLECTION CHARACTERISTICS (Py=240N)
MATERIAL : STAINLESS STEEL -SQUARE BEAM-
LOAD (Z) (Z)
1400
1200
1000
800
600
400
200
0
0
2
4
6
8
10
12
14
16
DEFLECTION (Z) (mm)
...EXPERIMENTAL ("forward" loading)
...EXPERIMENTAL ("reverse" loading)
...PREDICTED USING EQn.4.37
(series of radial loads)
PREDICTED ALLOWING FOR UNLOADING

FIG 5.43

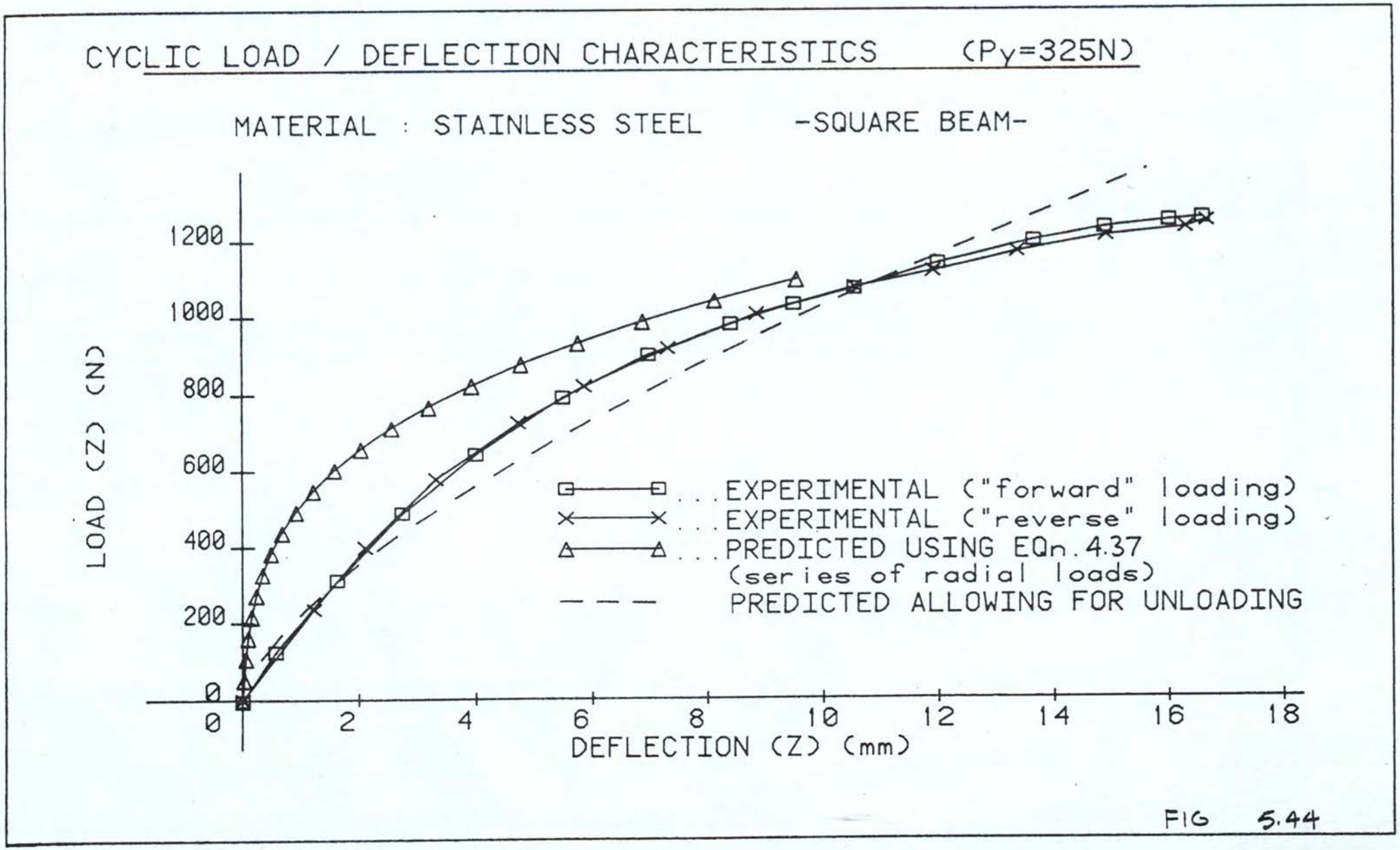
CYCLIC LOAD / DEFLECTION CHARACTERISTICS (Py=325N)
MATERIAL : STAINLESS STEEL -SQUARE BEAM-
LOAD (Z) (N)
1200
1000
800
600
400
200
0
0
2
4
6
8
10
12
14
16
18
DEFLECTION (Z) (mm)
...EXPERIMENTAL ("forward" loading)
...EXPERIMENTAL ("reverse" loading)
...PREDICTED USING EQn.4.37
(series of radial loads)
PREDICTED ALLOWING FOR UNLOADING

FIG 5.44

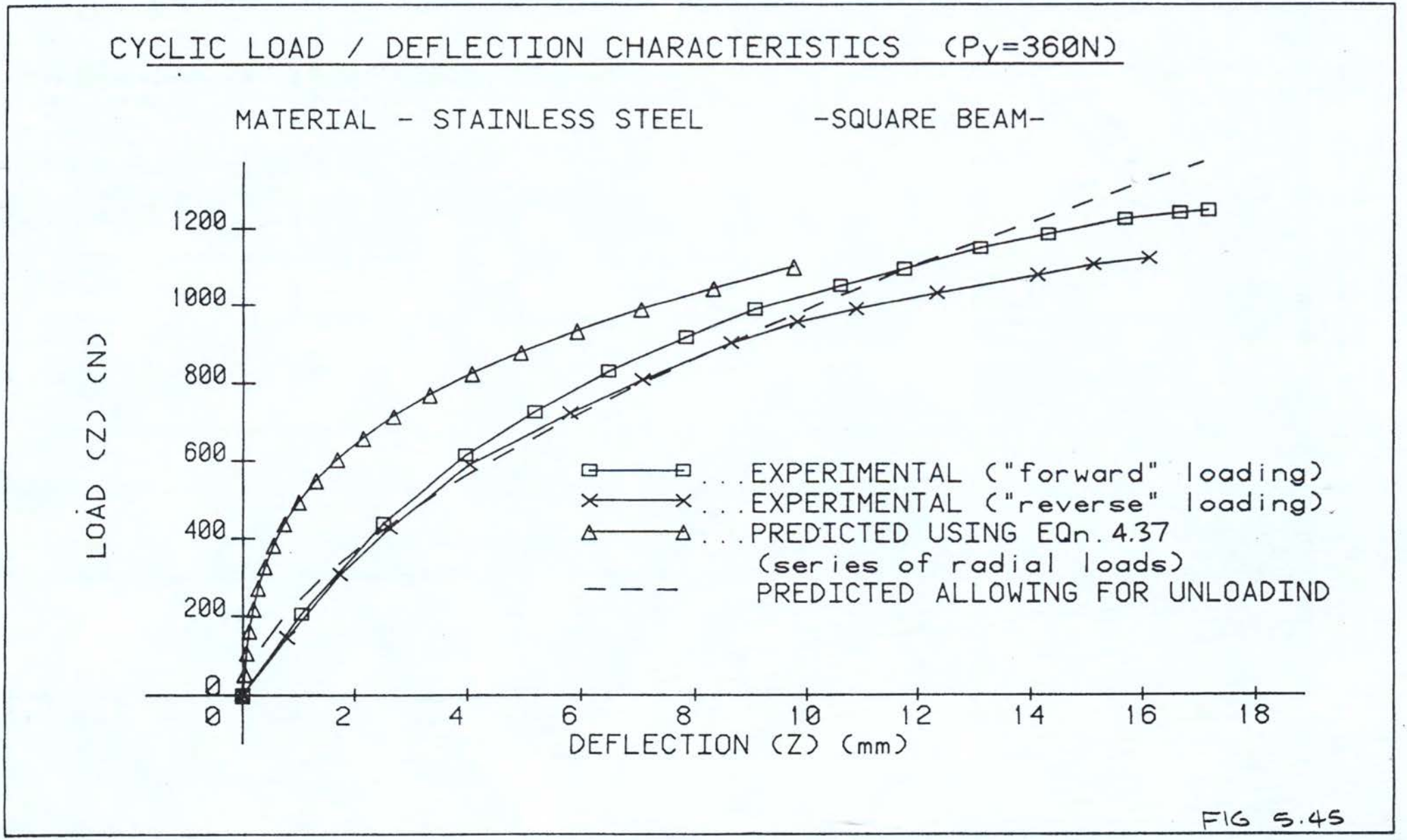
CYCLIC LOAD / DEFLECTION CHARACTERISTICS (Py=360N)
MATERIAL - STAINLESS STEEL -SQUARE BEAM-
LOAD (Z) (N)
1200
1000
800
600
400
200
0
0
2
4
6
8
10
12
14
16
18
DEFLECTION (Z) (mm)
...EXPERIMENTAL ("forward" loading)
...EXPERIMENTAL ("reverse" loading)
...PREDICTED USING EQn. 4.37
(series of radial loads)
PREDICTED ALLOWING FOR UNLOADIND

FIG 5.45

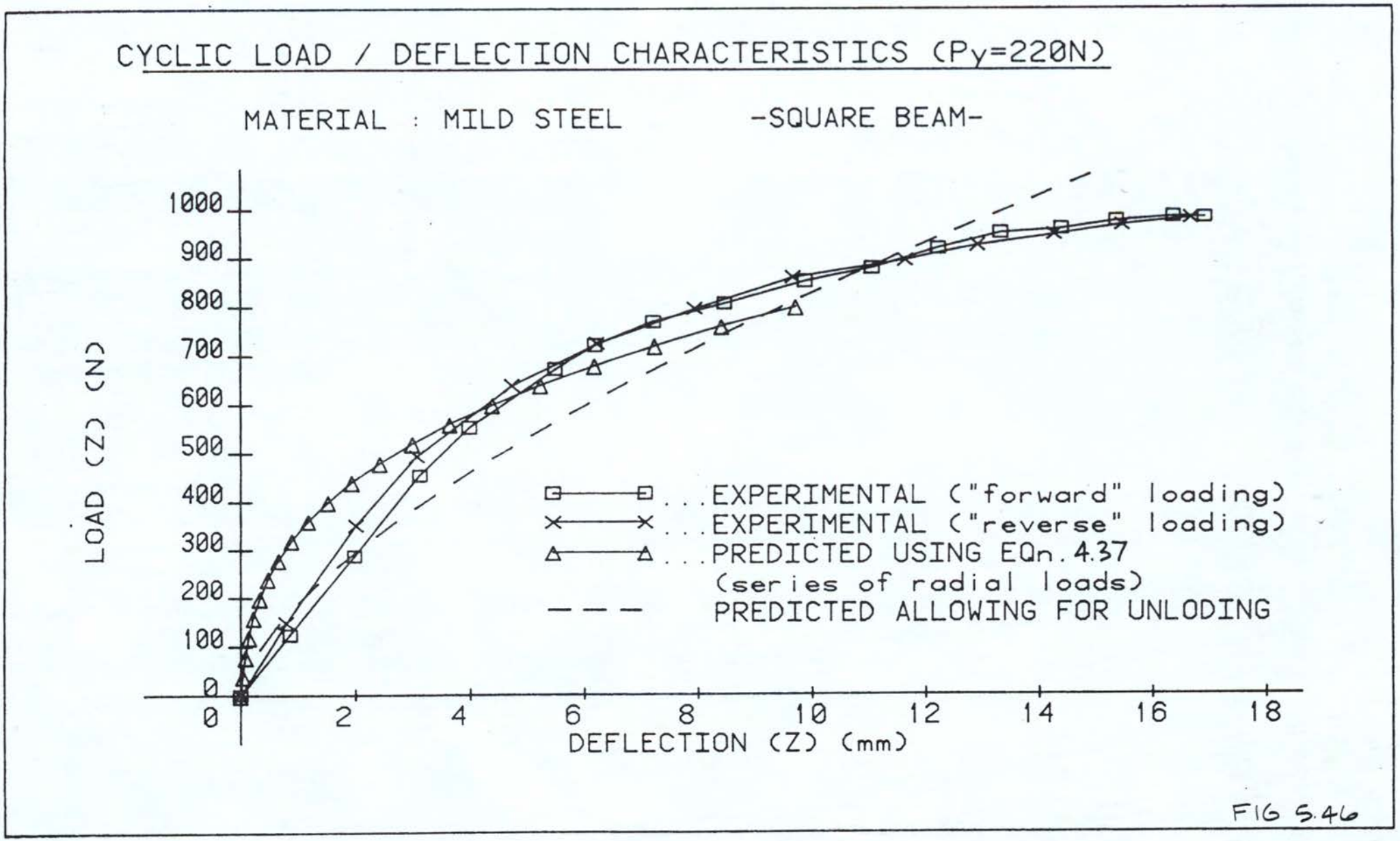
CYCLIC LOAD / DEFLECTION CHARACTERISTICS (Py=220N)
MATERIAL : MILD STEEL -SQUARE BEAM-
LOAD (Z) (N)
1000
900
800
700
600
500
400
300
200
100
0
0
2
4
6
8
10
12
14
16
18
DEFLECTION (Z) (mm)
...EXPERIMENTAL ("forward" loading)
...EXPERIMENTAL ("reverse" loading)
...PREDICTED USING EQn. 4.37
(series of radial loads)
PREDICTED ALLOWING FOR UNLODING

FIG 5.46

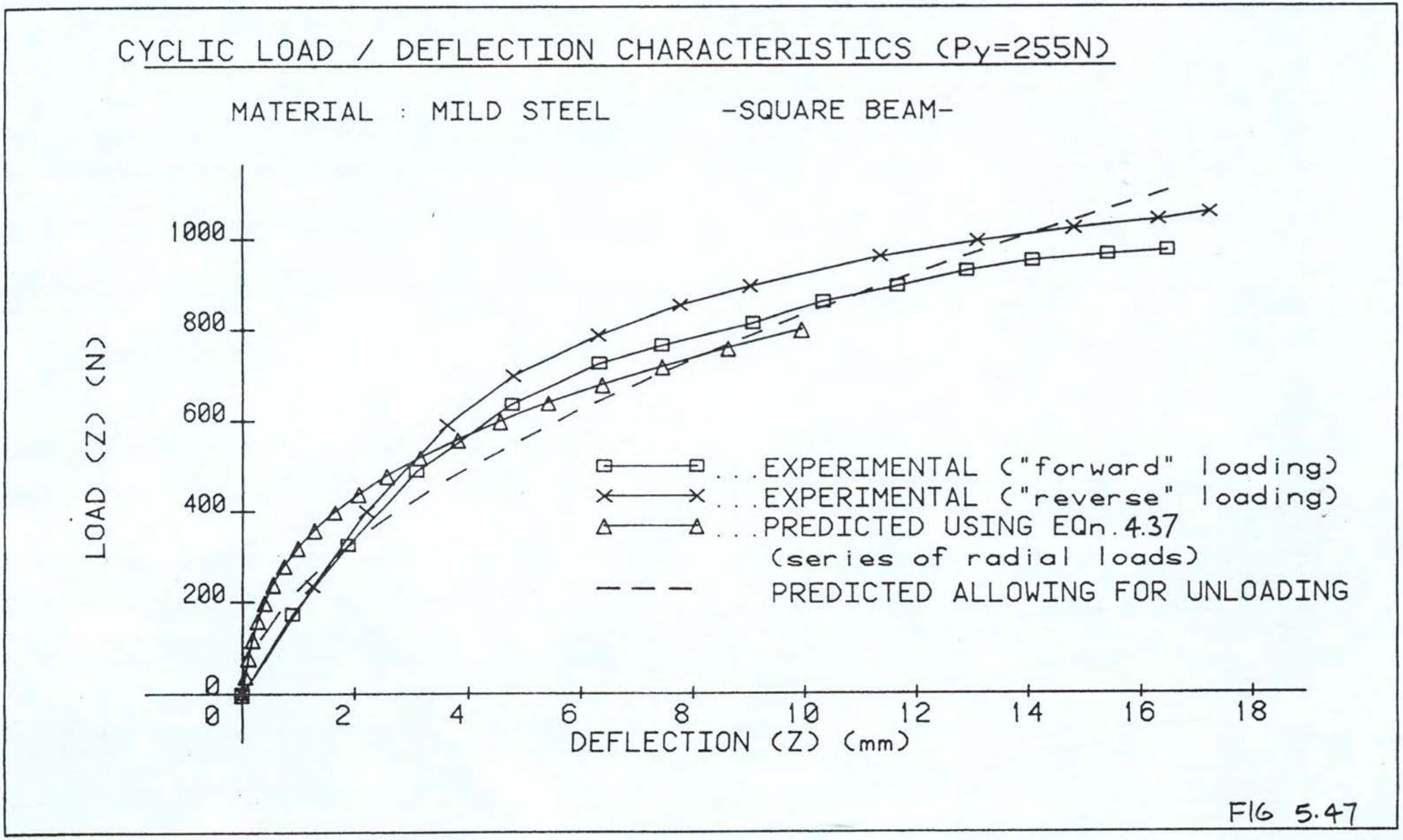
CYCLIC LOAD / DEFLECTION CHARACTERISTICS (Py=255N)
MATERIAL : MILD STEEL -SQUARE BEAM-
LOAD (Z) (N)
1000
800
600
400
200
0
0
2
4
6
8
10
12
14
16
18
DEFLECTION (Z) (mm)
...EXPERIMENTAL ("forward" loading)
...EXPERIMENTAL ("reverse" loading)
...PREDICTED USING EQn.4.37
(series of radial loads)
PREDICTED ALLOWING FOR UNLOADING

FIG 5.47

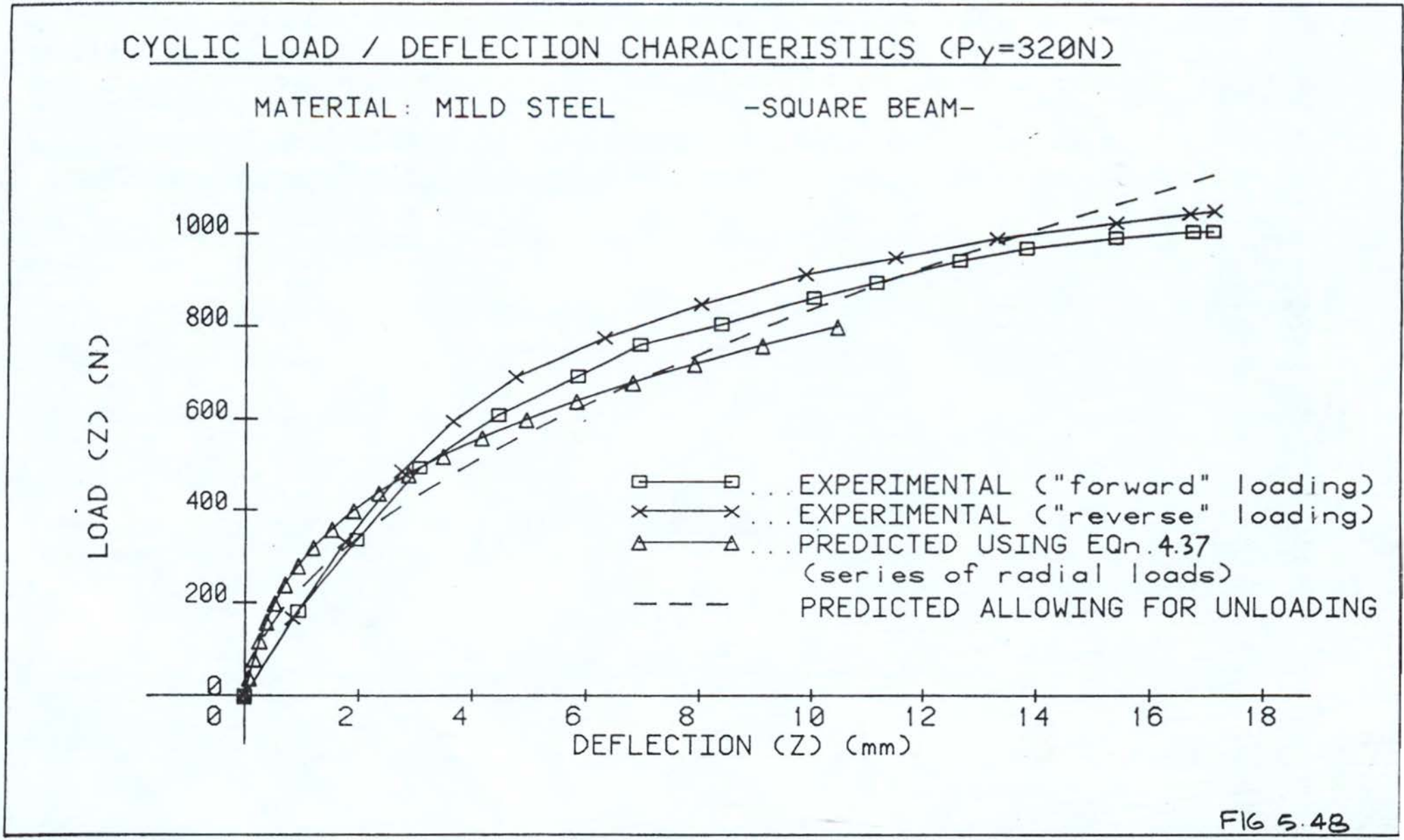
CYCLIC LOAD / DEFLECTION CHARACTERISTICS (Py=320N)
MATERIAL: MILD STEEL -SQUARE BEAM-
LOAD (Z) (N)
1000
800
600
400
200
0
0
2
4
6
8
10
12
14
16
18
DEFLECTION (Z) (mm)
...EXPERIMENTAL ("forward" loading)
...EXPERIMENTAL ("reverse" loading)
...PREDICTED USING EQn.4.37
(series of radial loads)
PREDICTED ALLOWING FOR UNLOADING

FIG 5.48

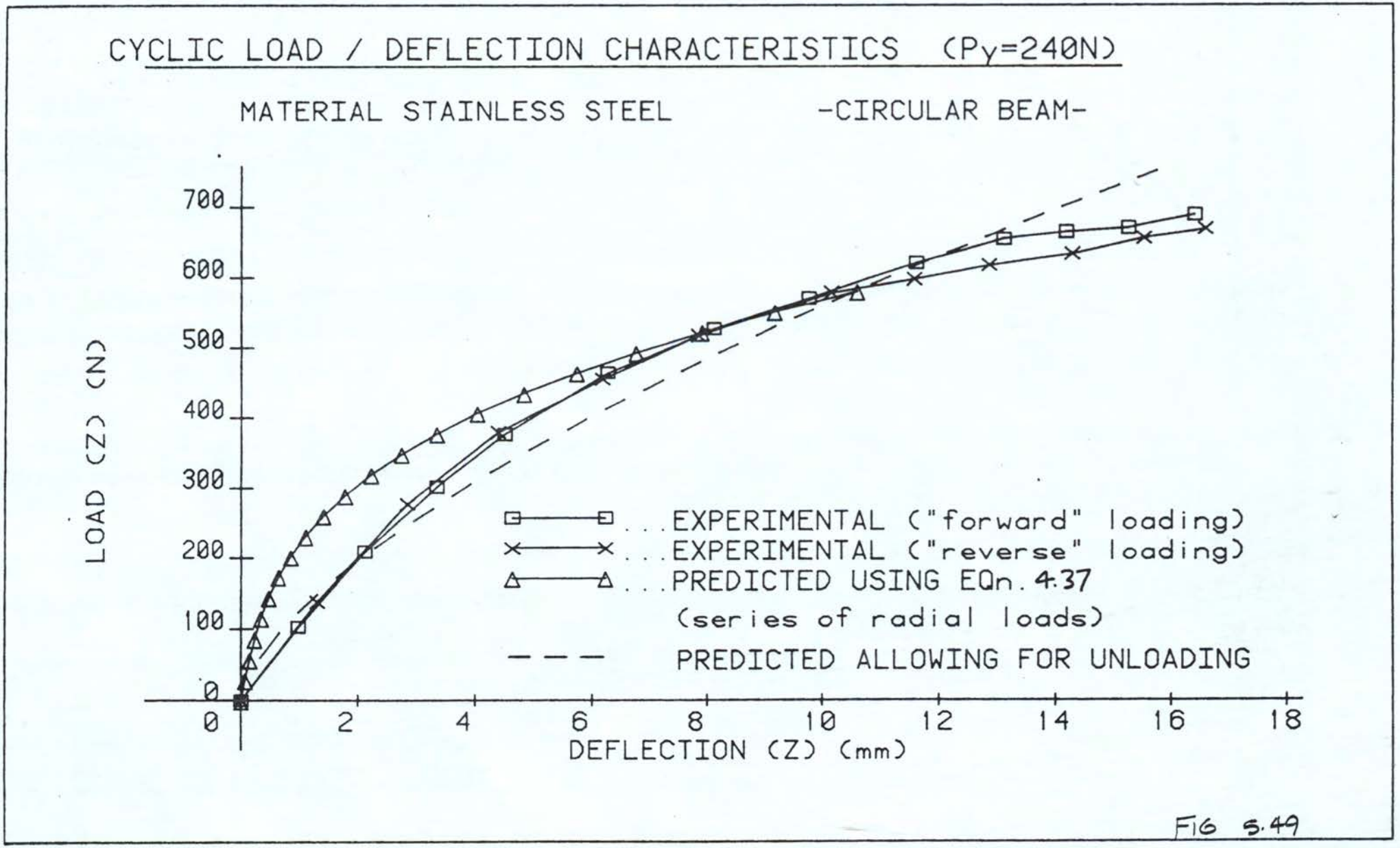
CYCLIC LOAD / DEFLECTION CHARACTERISTICS (Py=240N)
MATERIAL STAINLESS STEEL -CIRCULAR BEAM-
LOAD (Z) (N)
700
600
500
400
300
200
100
0
0
2
4
6
8
10
12
14
16
18
DEFLECTION (Z) (mm)
...EXPERIMENTAL ("forward" loading)
...EXPERIMENTAL ("reverse" loading)
...PREDICTED USING EQn. 4.37
(series of radial loads)
PREDICTED ALLOWING FOR UNLOADING

FIG 5.49

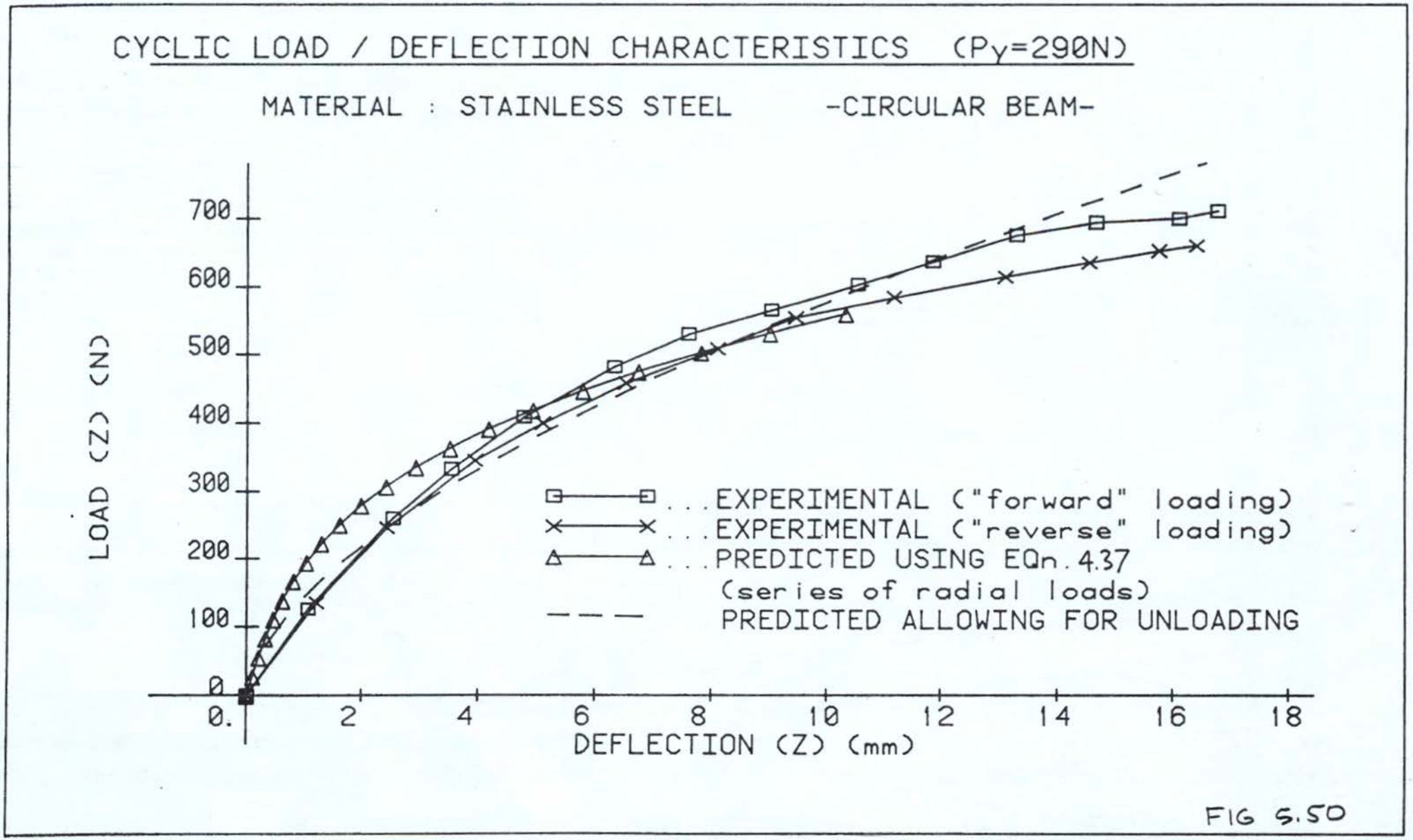
CYCLIC LOAD / DEFLECTION CHARACTERISTICS (Py=290N)
MATERIAL : STAINLESS STEEL -CIRCULAR BEAM-
LOAD (Z) (N)
700
600
500
400
300
200
100
0
0.
2
4
6
8
10
12
14
16
18
DEFLECTION (Z) (mm)
...EXPERIMENTAL ("forward" loading)
...EXPERIMENTAL ("reverse" loading)
...PREDICTED USING EQn. 4.37
(series of radial loads)
PREDICTED ALLOWING FOR UNLOADING

FIG 5.50

5.1.6.1 VERTICAL DEFLECTIONS - 1ST QUARTER CYCLE

The magnitude and mode of deformation for stainless circular and square beams are shown in Figs (5.51) to (5.55). The theoretical predictions are not particularly good. The predictions assuming equivalent radial loads over estimates the downward deflection in all cases and would provide a conservative design solution. Although the method over predicts the deflection, the major error occurs in the initial stages and the latter part of the deflection is predicted quite well. The predictions following the history of loading over estimates the deflections in the early stages of bending and under-estimate in the latter stages. However the mode of deformation observed was not as might be expected, since an isotropic or kinematic hardening model or a combination of them would have predicted a reduced rate of deflection as the horizontal moment was increased.

Similar results were obtained for the mild steel material, Figs (5.56) to (5.61) and although overall deflections predicted using the loading history approach were quite good the mode of deformation during the first quarter cycle was unexpected.

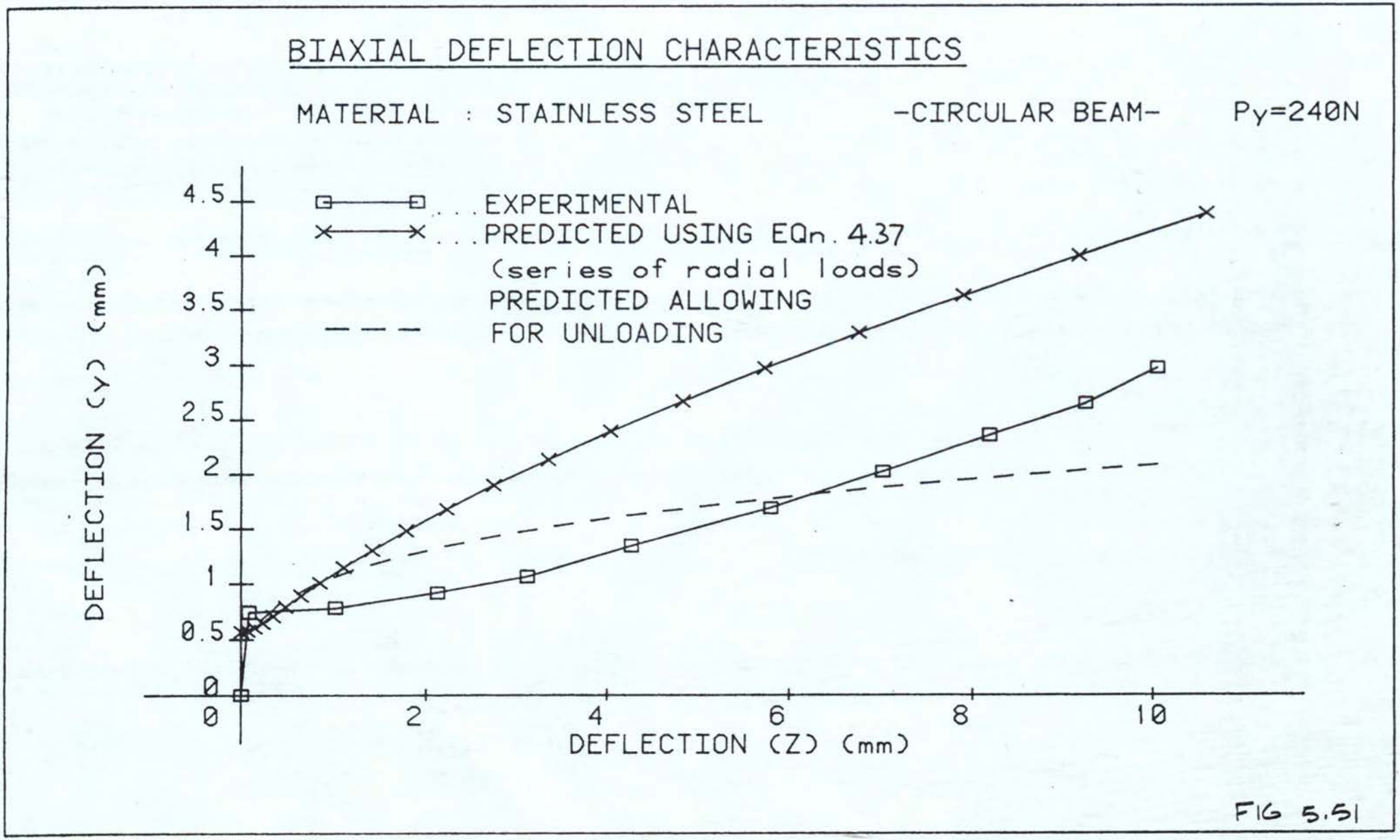
BIAXIAL DEFLECTION CHARACTERISTICS
MATERIAL : STAINLESS STEEL
-CIRCULAR BEAM-
Py=240N
EXPERIMENTAL
PREDICTED USING EQn. 4.37
(series of radial loads)
PREDICTED ALLOWING
FOR UNLOADING
DEFLECTION (y) (mm)
DEFLECTION (Z) (mm)
0
0.5
1
1.5
2
2.5
3
3.5
4
4.5
0
2
4
6
8
10

FIG 5.51

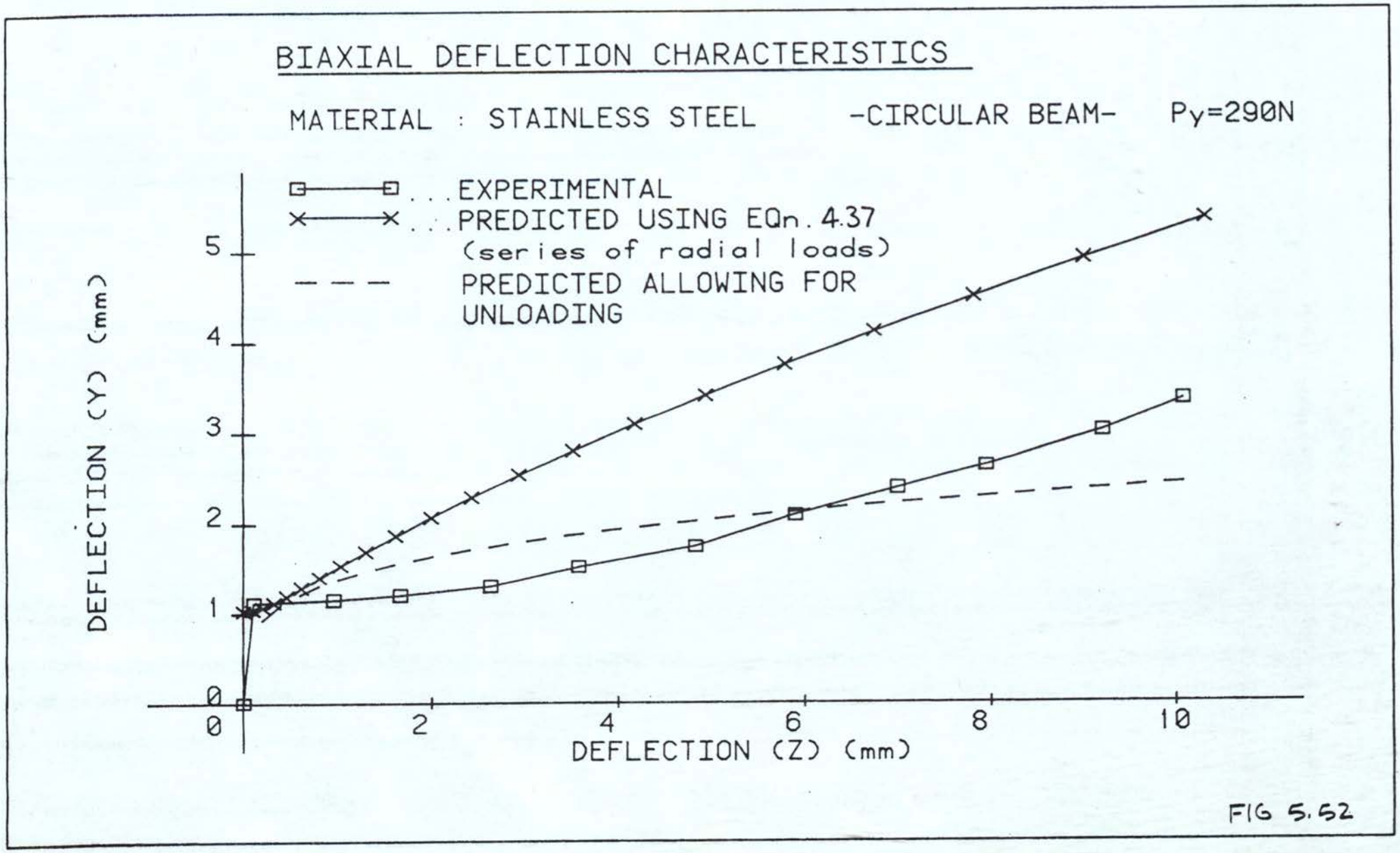
BIAXIAL DEFLECTION CHARACTERISTICS
MATERIAL : STAINLESS STEEL -CIRCULAR BEAM- Py=290N
. . . EXPERIMENTAL
. . . PREDICTED USING EQn. 4.37 (series of radial loads)
PREDICTED ALLOWING FOR UNLOADING
DEFLECTION (Y) (mm)
DEFLECTION (Z) (mm)
0
1
2
3
4
5
0
2
4
6
8
10

FIG 5.52

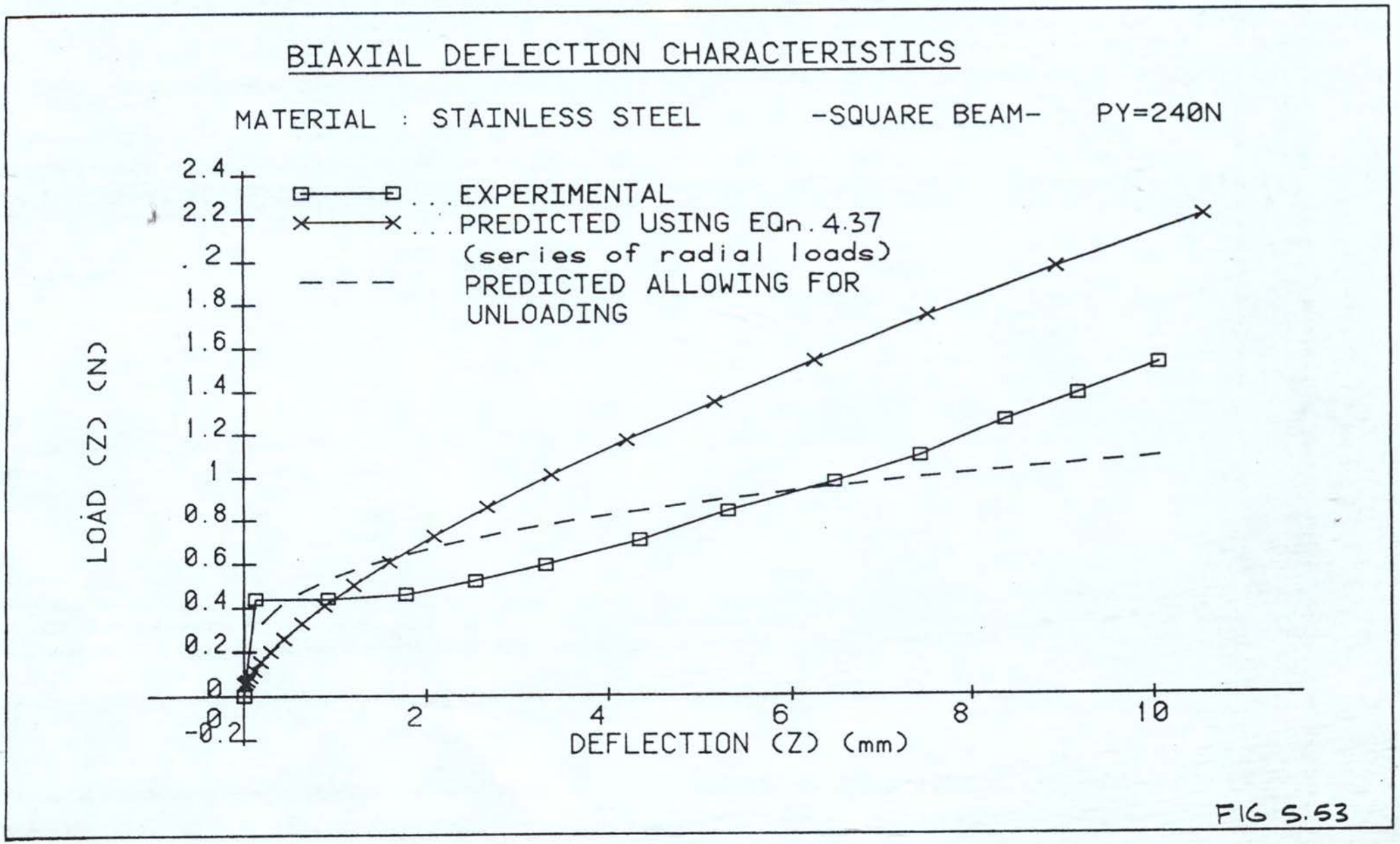
BIAXIAL DEFLECTION CHARACTERISTICS
MATERIAL : STAINLESS STEEL
-SQUARE BEAM-
PY=240N
EXPERIMENTAL
PREDICTED USING EQn.4.37
(series of radial loads)
PREDICTED ALLOWING FOR
UNLOADING
LOAD (Z) (N)
2.4
2.2
2
1.8
1.6
1.4
1.2
1
0.8
0.6
0.4
0.2
0
-0.2
0
2
4
6
8
10
DEFLECTION (Z) (mm)

FIG 5.53

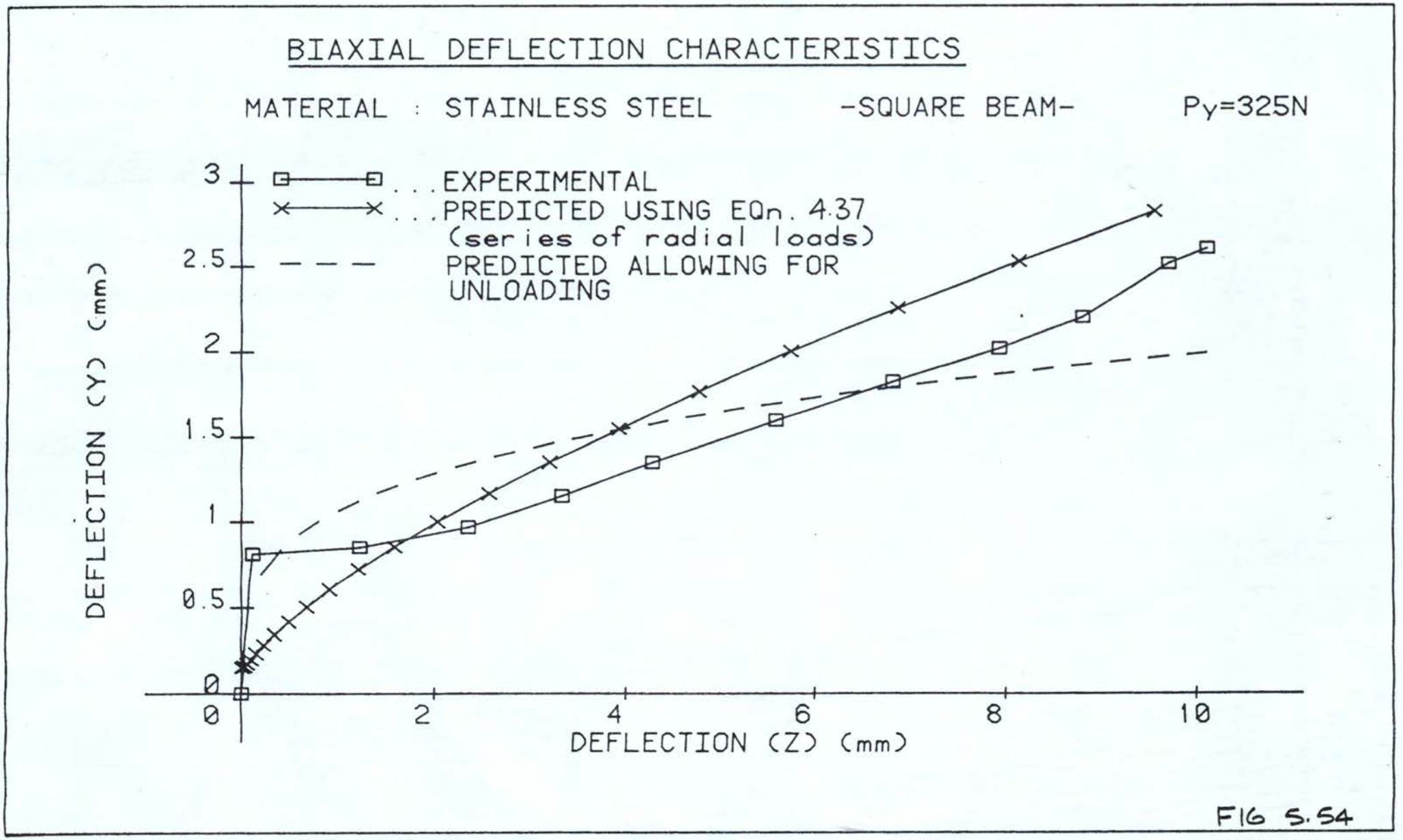
BIAXIAL DEFLECTION CHARACTERISTICS
MATERIAL : STAINLESS STEEL
-SQUARE BEAM-
Py=325N
...EXPERIMENTAL
...PREDICTED USING EQn. 4.37
(series of radial loads)
PREDICTED ALLOWING FOR
UNLOADING
DEFLECTION (Y) (mm)
DEFLECTION (Z) (mm)
0
0.5
1
1.5
2
2.5
3
0
2
4
6
8
10

FIG 5.54

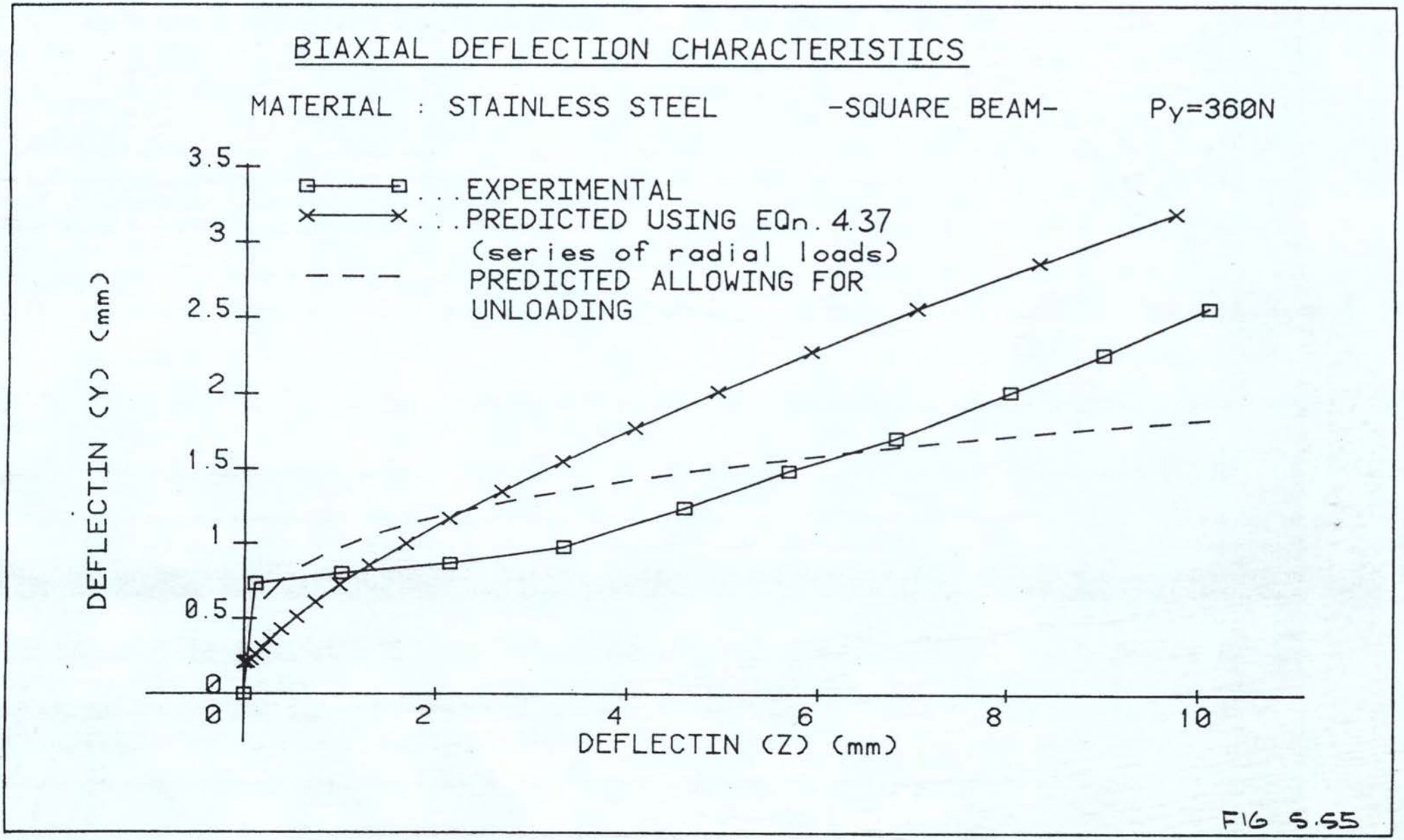
BIAXIAL DEFLECTION CHARACTERISTICS
MATERIAL : STAINLESS STEEL
-SQUARE BEAM-
Py=360N
...EXPERIMENTAL
...PREDICTED USING EQn. 4.37
(series of radial loads)
PREDICTED ALLOWING FOR
UNLOADING
DEFLECTIN (Y) (mm)
DEFLECTIN (Z) (mm)
0
0.5
1
1.5
2
2.5
3
3.5
0
2
4
6
8
10

FIG 5.55

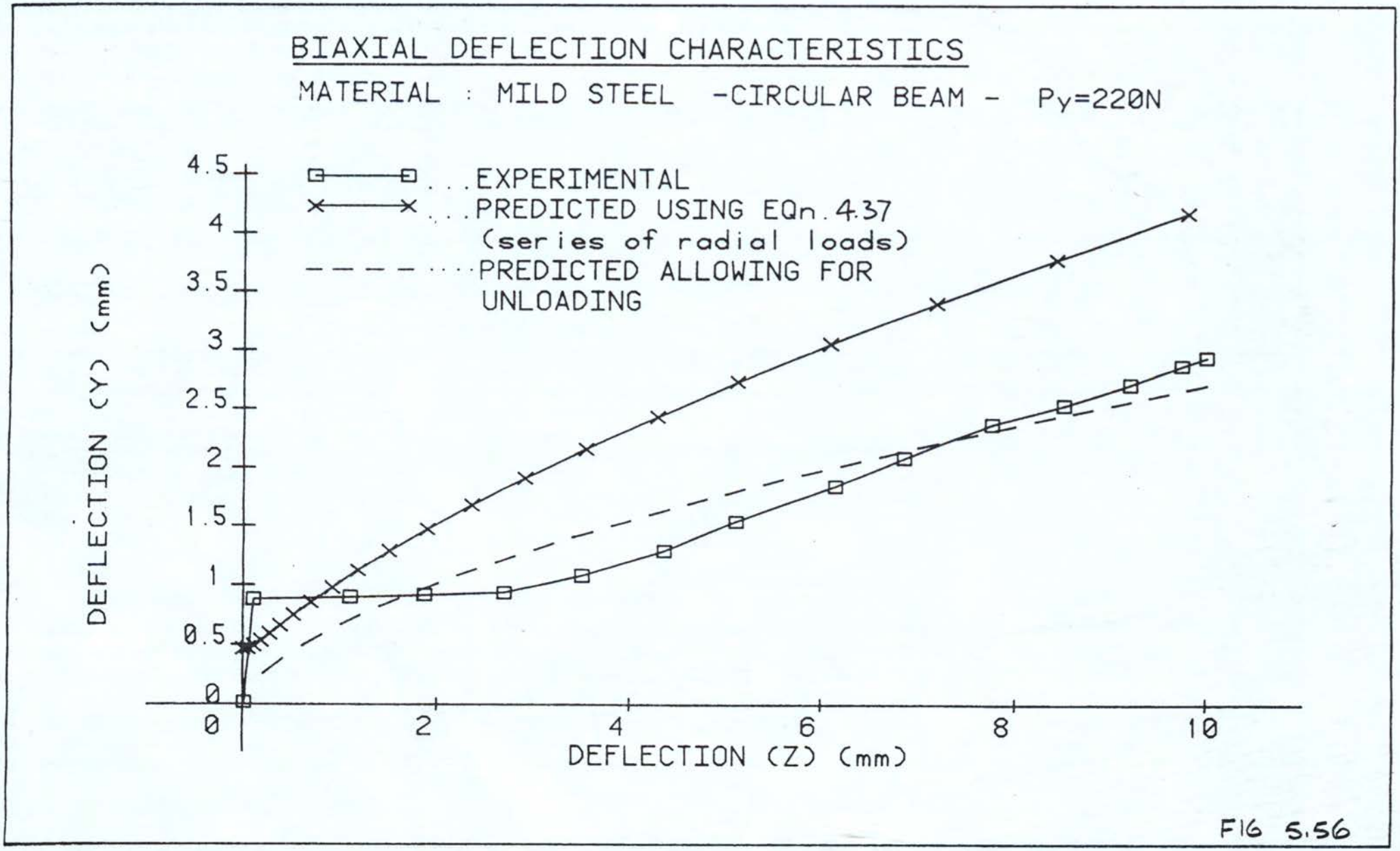
BIAXIAL DEFLECTION CHARACTERISTICS
MATERIAL : MILD STEEL -CIRCULAR BEAM - Py=220N
...EXPERIMENTAL
...PREDICTED USING EQn.4.37
(series of radial loads)
....PREDICTED ALLOWING FOR
UNLOADING
DEFLECTION (Y) (mm)
DEFLECTION (Z) (mm)
0
0.5
1
1.5
2
2.5
3
3.5
4
4.5
0
2
4
6
8
10

FIG 5.56

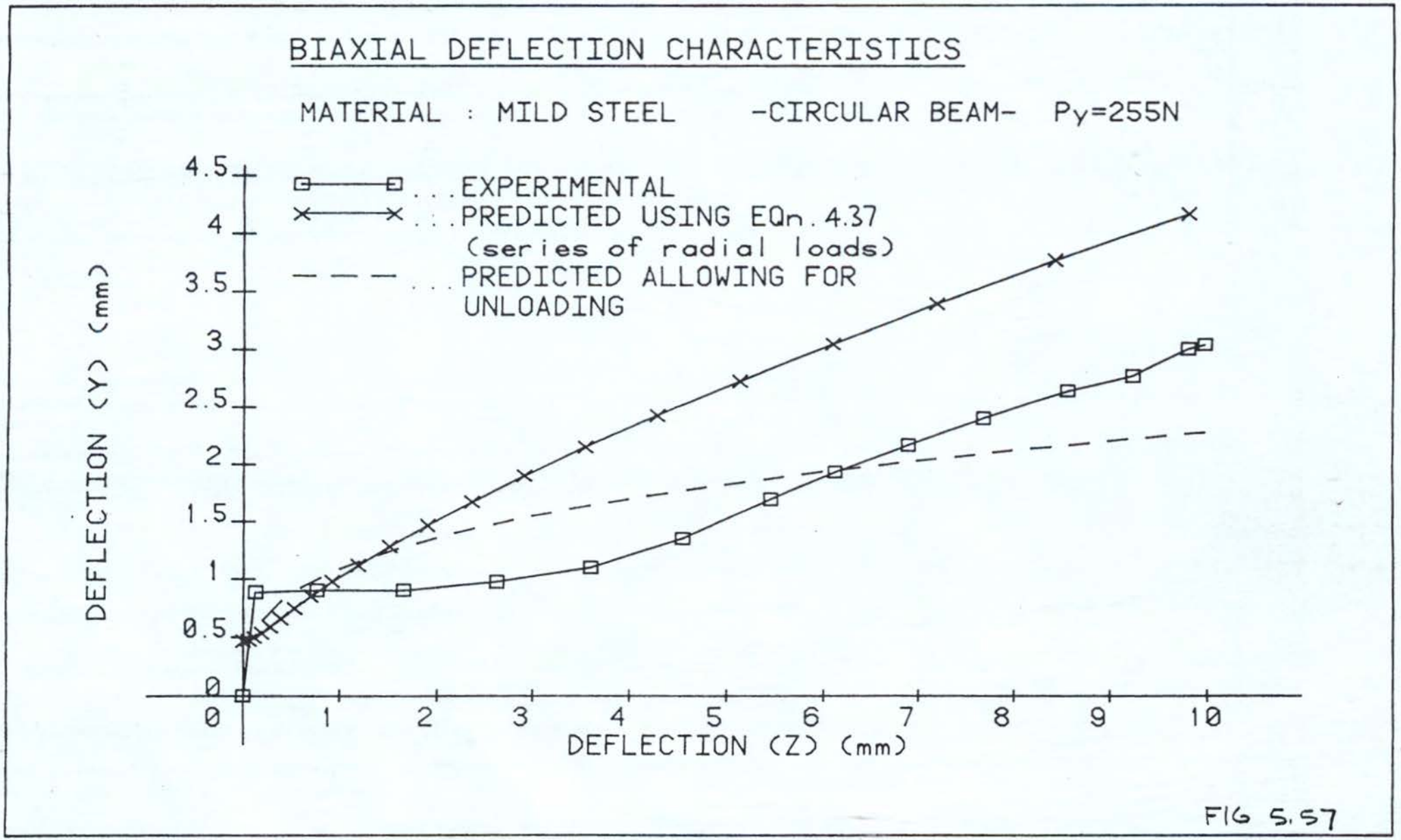
BIAXIAL DEFLECTION CHARACTERISTICS
MATERIAL : MILD STEEL -CIRCULAR BEAM- Py=255N
...EXPERIMENTAL
...PREDICTED USING EQn.4.37
(series of radial loads)
...PREDICTED ALLOWING FOR
UNLOADING
DEFLECTION (Y) (mm)
DEFLECTION (Z) (mm)
0
0.5
1
1.5
2
2.5
3
3.5
4
4.5
0
1
2
3
4
5
6
7
8
9
10

FIG 5.57

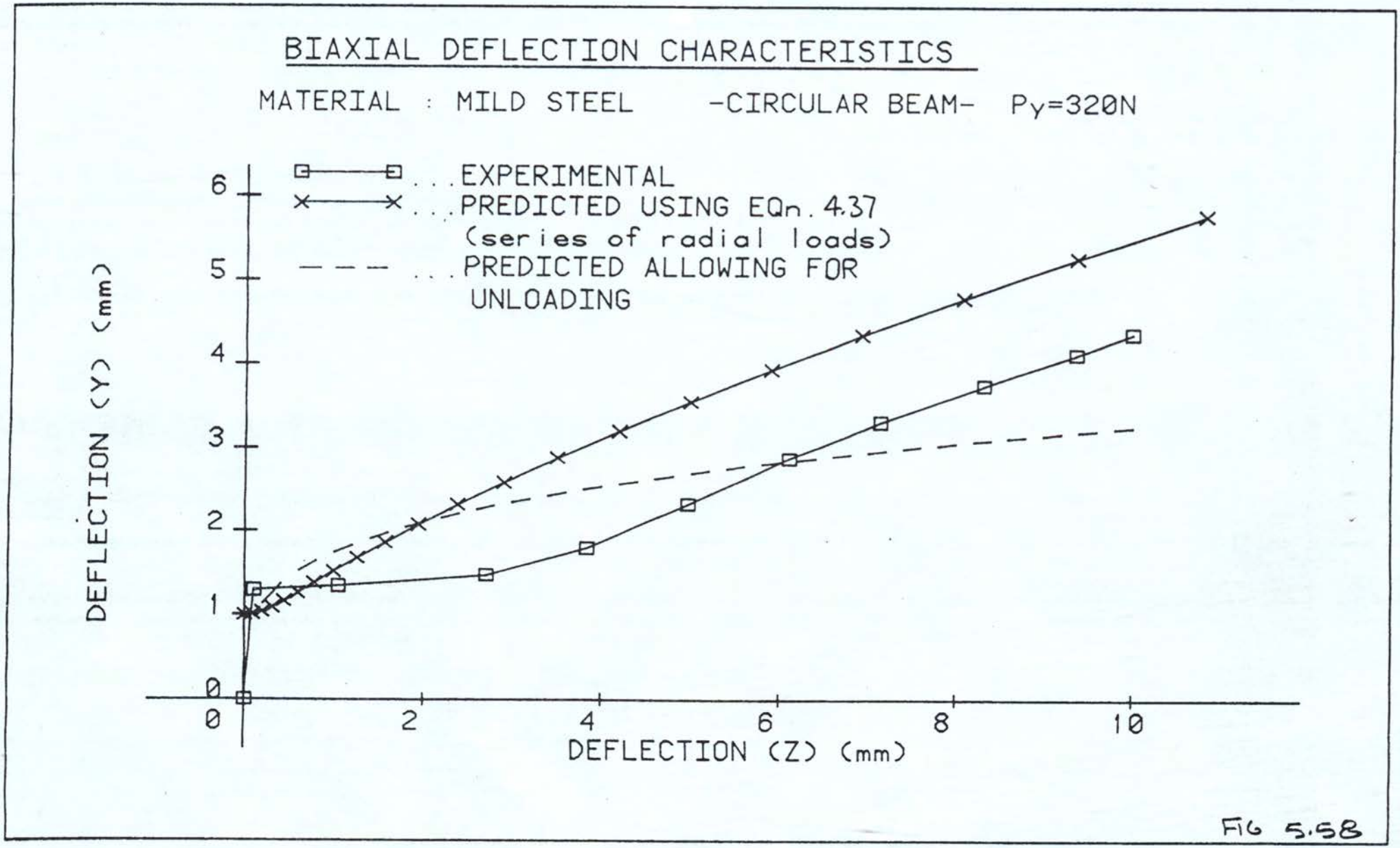
BIAXIAL DEFLECTION CHARACTERISTICS
MATERIAL : MILD STEEL -CIRCULAR BEAM- Py=320N
...EXPERIMENTAL
...PREDICTED USING EQn. 4.37
(series of radial loads)
...PREDICTED ALLOWING FOR
UNLOADING
DEFLECTION (Y) (mm)
DEFLECTION (Z) (mm)
0
1
2
3
4
5
6
0
2
4
6
8
10

FIG 5.58

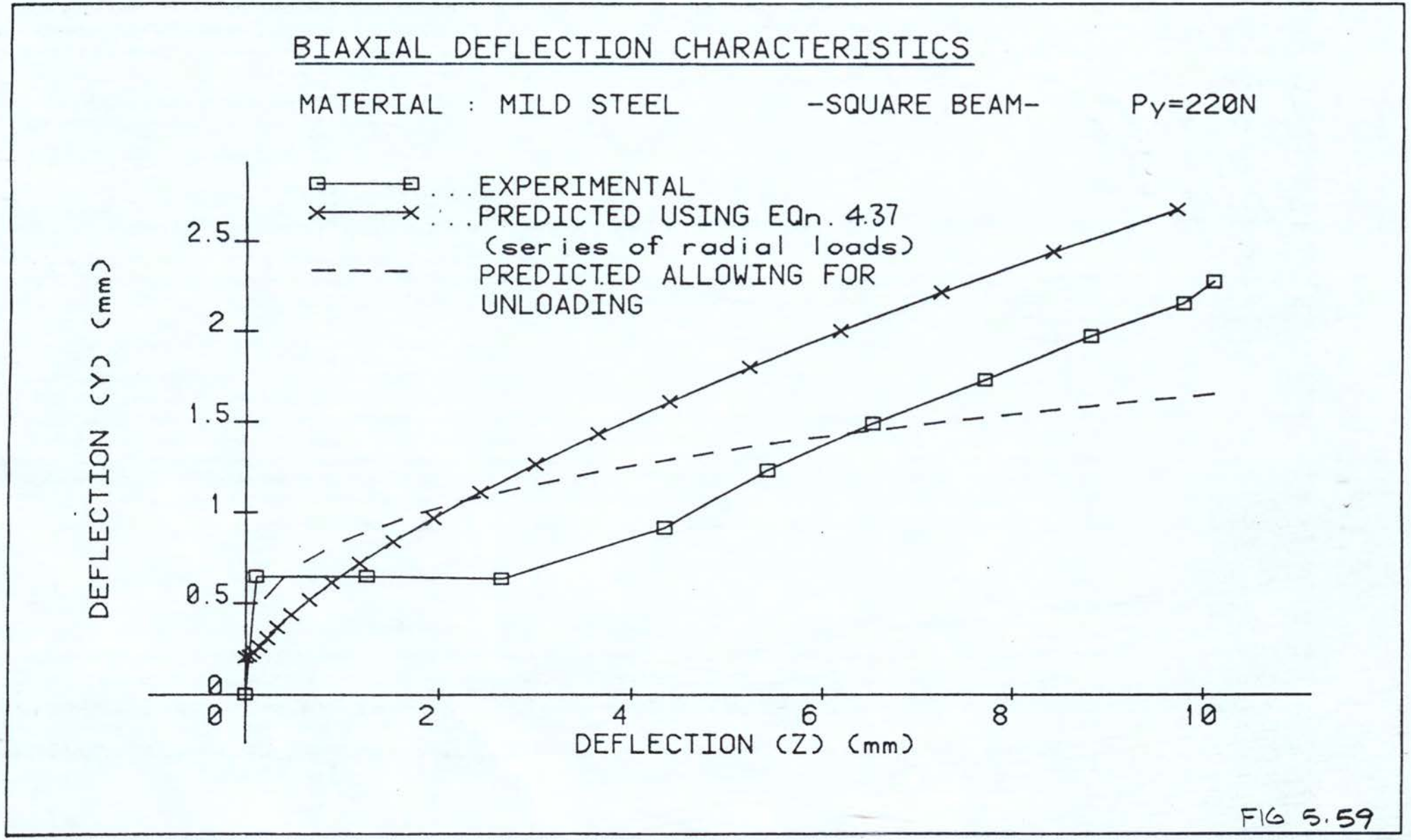
BIAXIAL DEFLECTION CHARACTERISTICS
MATERIAL : MILD STEEL
-SQUARE BEAM-
Py=220N
...EXPERIMENTAL
...PREDICTED USING EQn. 4.37
(series of radial loads)
PREDICTED ALLOWING FOR
UNLOADING
DEFLECTION (Y) (mm)
DEFLECTION (Z) (mm)
0
0.5
1
1.5
2
2.5
0
2
4
6
8
10

FIG 5.59

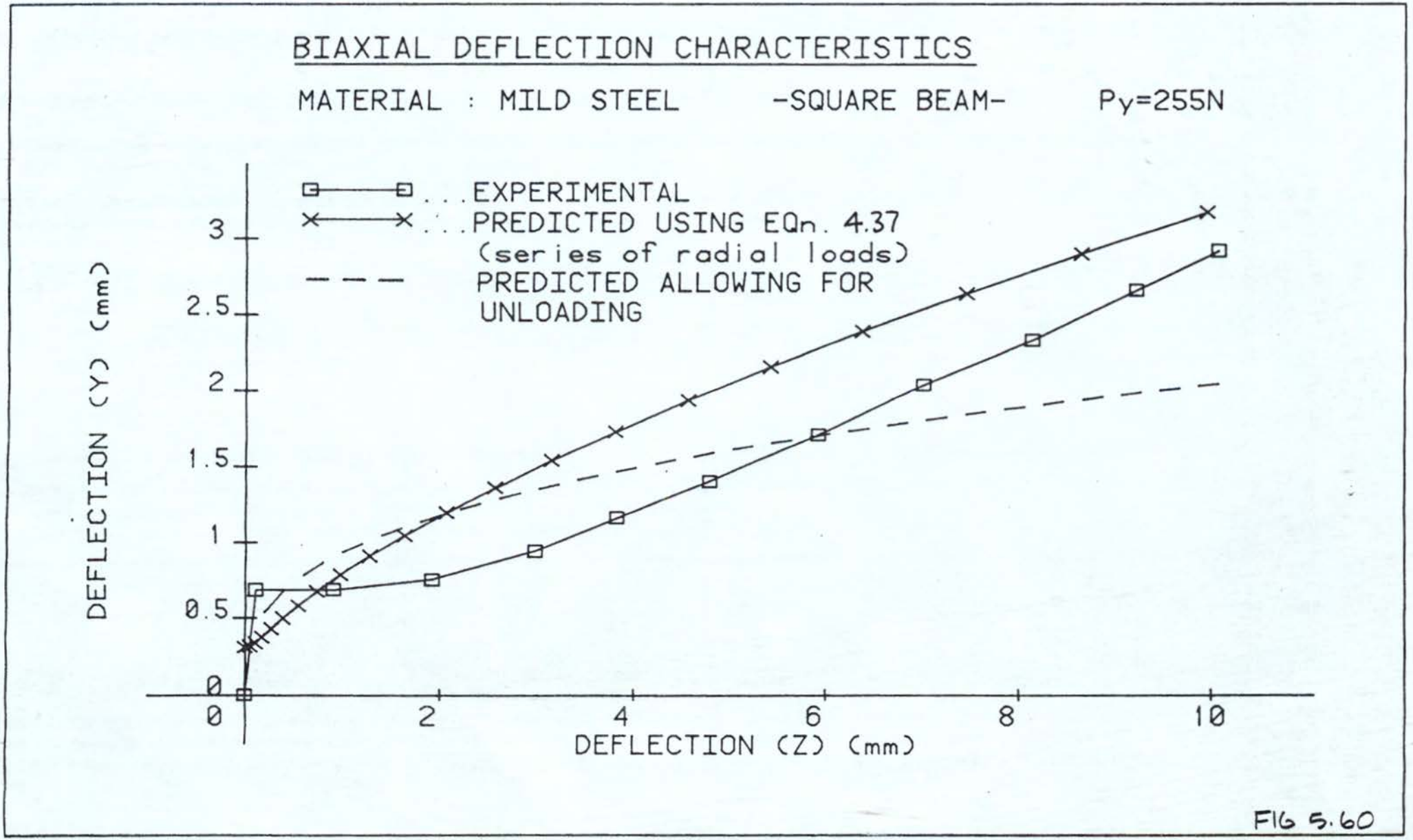
BIAXIAL DEFLECTION CHARACTERISTICS
MATERIAL : MILD STEEL
-SQUARE BEAM-
Py=255N
...EXPERIMENTAL
...PREDICTED USING EQn. 4.37
(series of radial loads)
PREDICTED ALLOWING FOR
UNLOADING
DEFLECTION (Y) (mm)
DEFLECTION (Z) (mm)
0
0.5
1
1.5
2
2.5
3
0
2
4
6
8
10

FIG 5.60

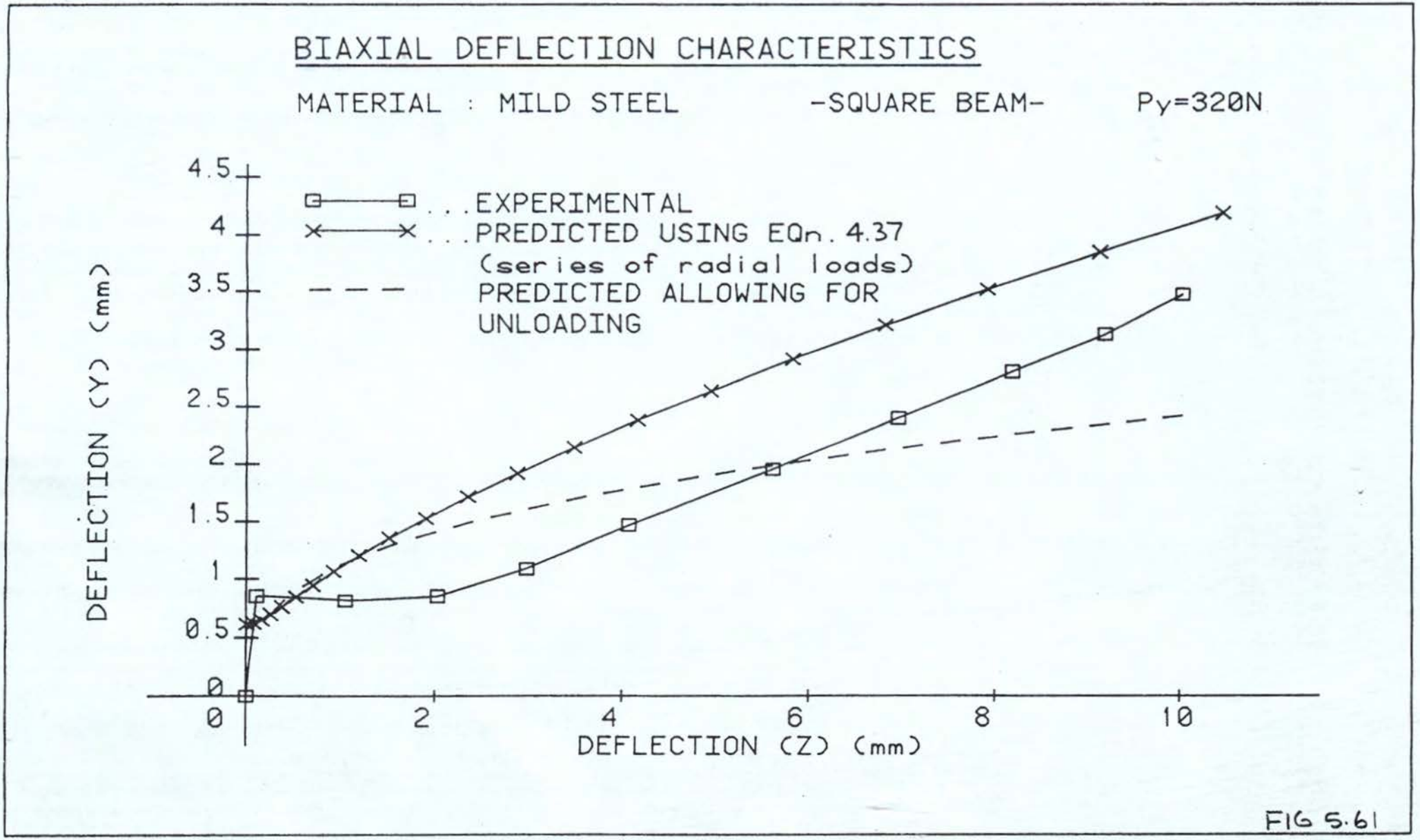
BIAXIAL DEFLECTION CHARACTERISTICS
MATERIAL : MILD STEEL
-SQUARE BEAM-
Py=320N
...EXPERIMENTAL
...PREDICTED USING EQn. 4.37
(series of radial loads)
PREDICTED ALLOWING FOR
UNLOADING
DEFLECTION (Y) (mm)
DEFLECTION (Z) (mm)
4.5
4
3.5
3
2.5
2
1.5
1
0.5
0
0
2
4
6
8
10

FIG 5.61

5.1.6.2 CYCLIC CUMULATIVE DEFLECTIONS

The growth of vertical deflections with cycles are shown for both materials and section shapes in Figs (5.62) to (5.72).

The predicted deflections following the loading history are also shown and it can be concluded that the predictions are good both with regard to magnitude and mode of deformation. Allowing for some initial errors the predictions in the later cycles are quite good.

The initial errors may be due to modelling problems, as previously discussed, but in addition the effect of any anisotropy in material properties may take several cycles to diminish. The general mode of deformation appears to be predicted quite reasonably in the latter cycles. The unusual mode of deformation in the first quarter cycle, increasing deflections with increase in horizontal moment is seen to persist into the next ¼ cycle.

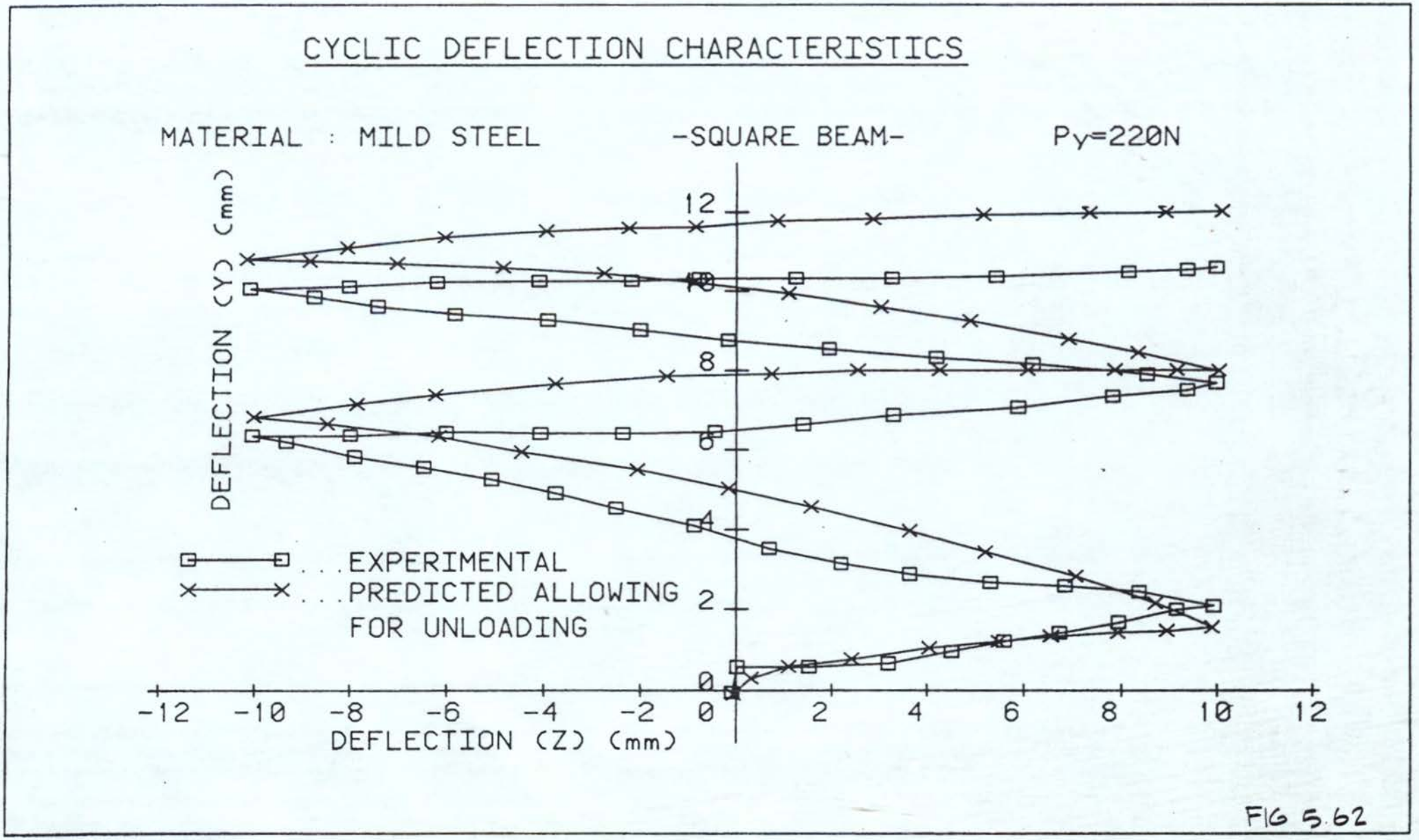
CYCLIC DEFLECTION CHARACTERISTICS
MATERIAL : MILD STEEL
-SQUARE BEAM-
Py=220N
DEFLECTION (Y) (mm)
12
8
6
4
2
0
. . . EXPERIMENTAL
. . . PREDICTED ALLOWING FOR UNLOADING
-12 -10 -8 -6 -4 -2 0 2 4 6 8 10 12
DEFLECTION (Z) (mm)

FIG 5.62

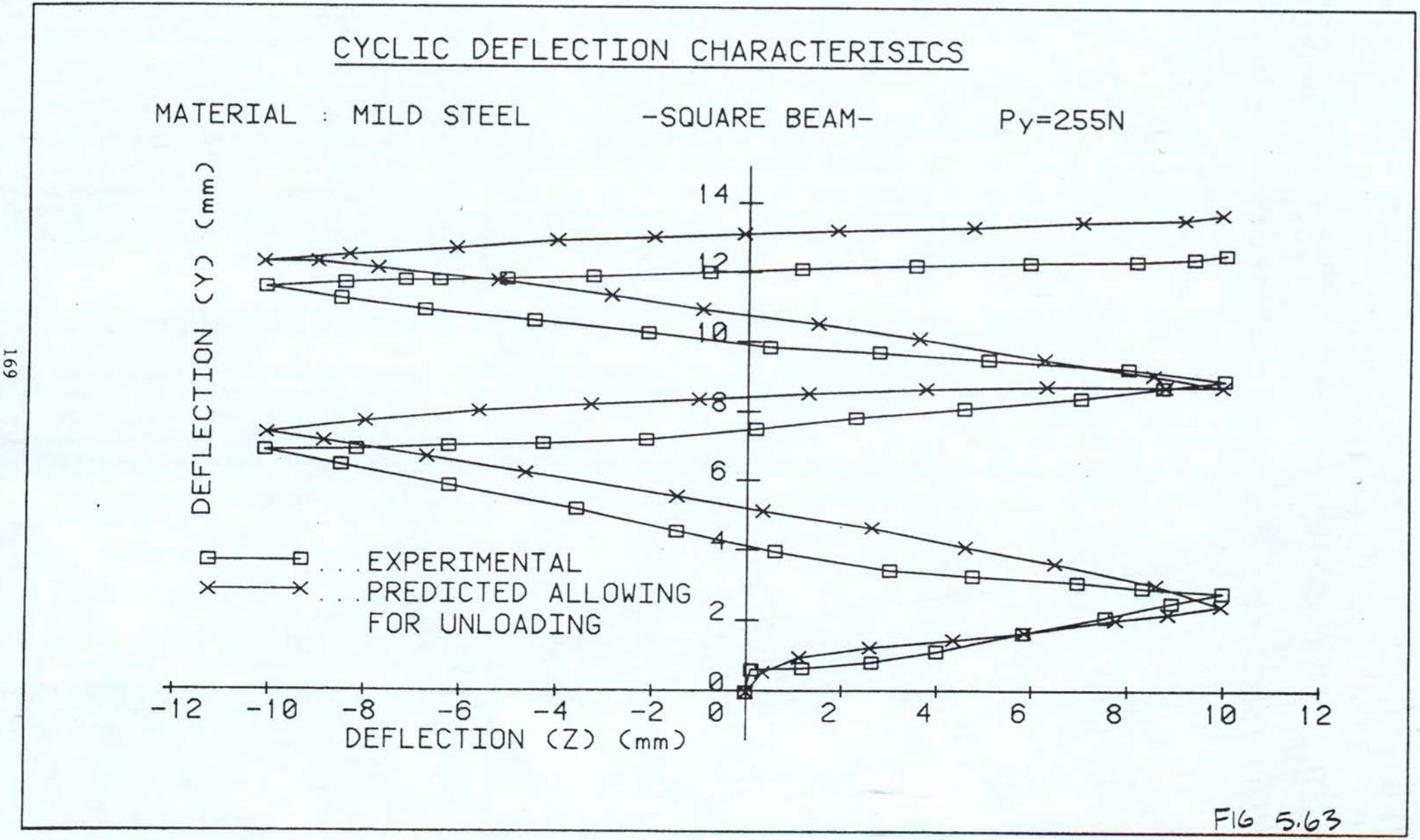
CYCLIC DEFLECTION CHARACTERISICS
MATERIAL : MILD STEEL
-SQUARE BEAM-
Py=255N
DEFLECTION (Y) (mm)
14
12
10
8
6
4
2
0
-12
-10
-8
-6
-4
-2
0
2
4
6
8
10
12
DEFLECTION (Z) (mm)
. . . EXPERIMENTAL
. . . PREDICTED ALLOWING FOR UNLOADING

FIG 5.63

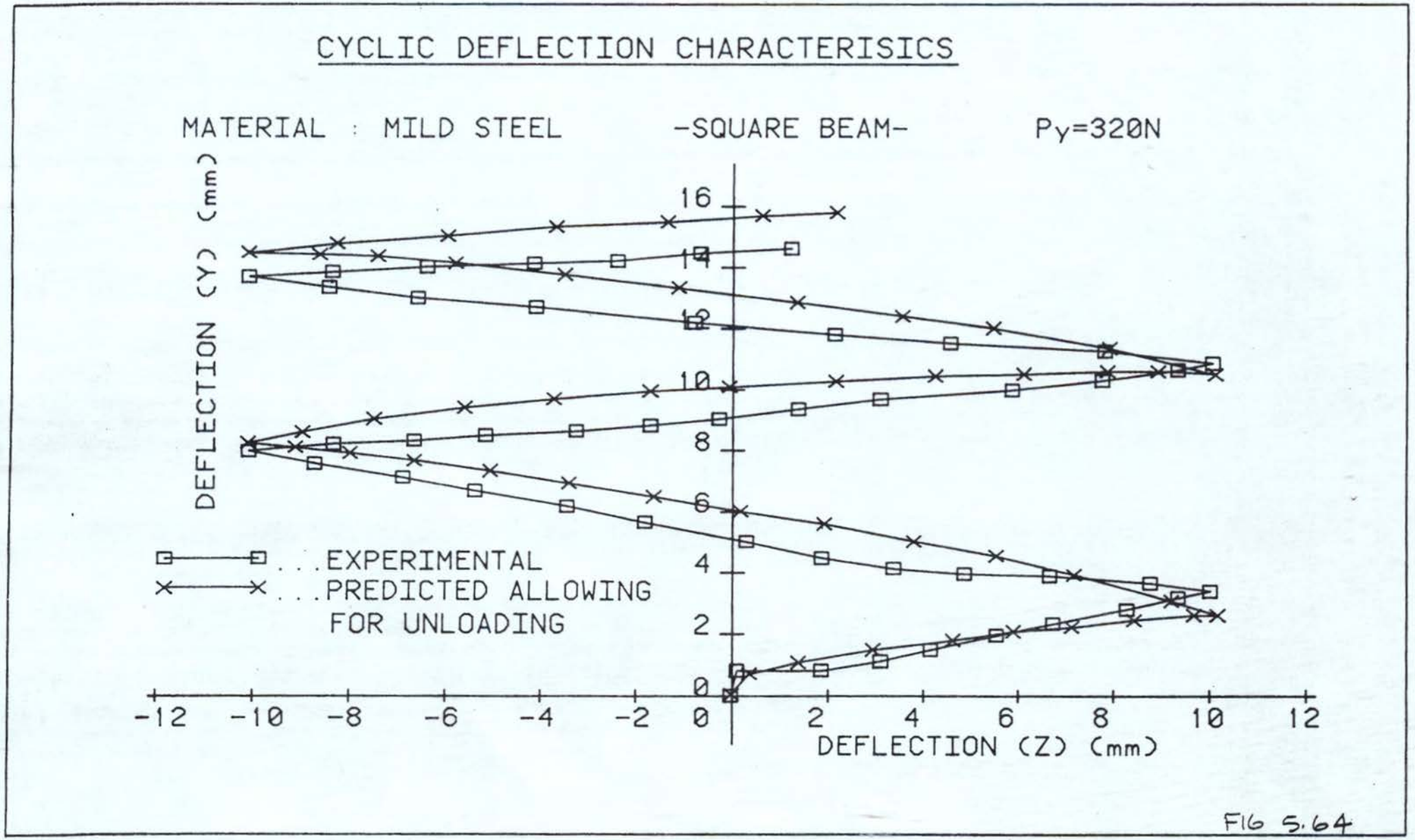
CYCLIC DEFLECTION CHARACTERISICS
MATERIAL : MILD STEEL
-SQUARE BEAM-
Py=320N
DEFLECTION (Y) (mm)
16
14
12
10
8
6
4
2
0
-12
-10
-8
-6
-4
-2
0
2
4
6
8
10
12
DEFLECTION (Z) (mm)
...EXPERIMENTAL
...PREDICTED ALLOWING FOR UNLOADING

FIG 5.64

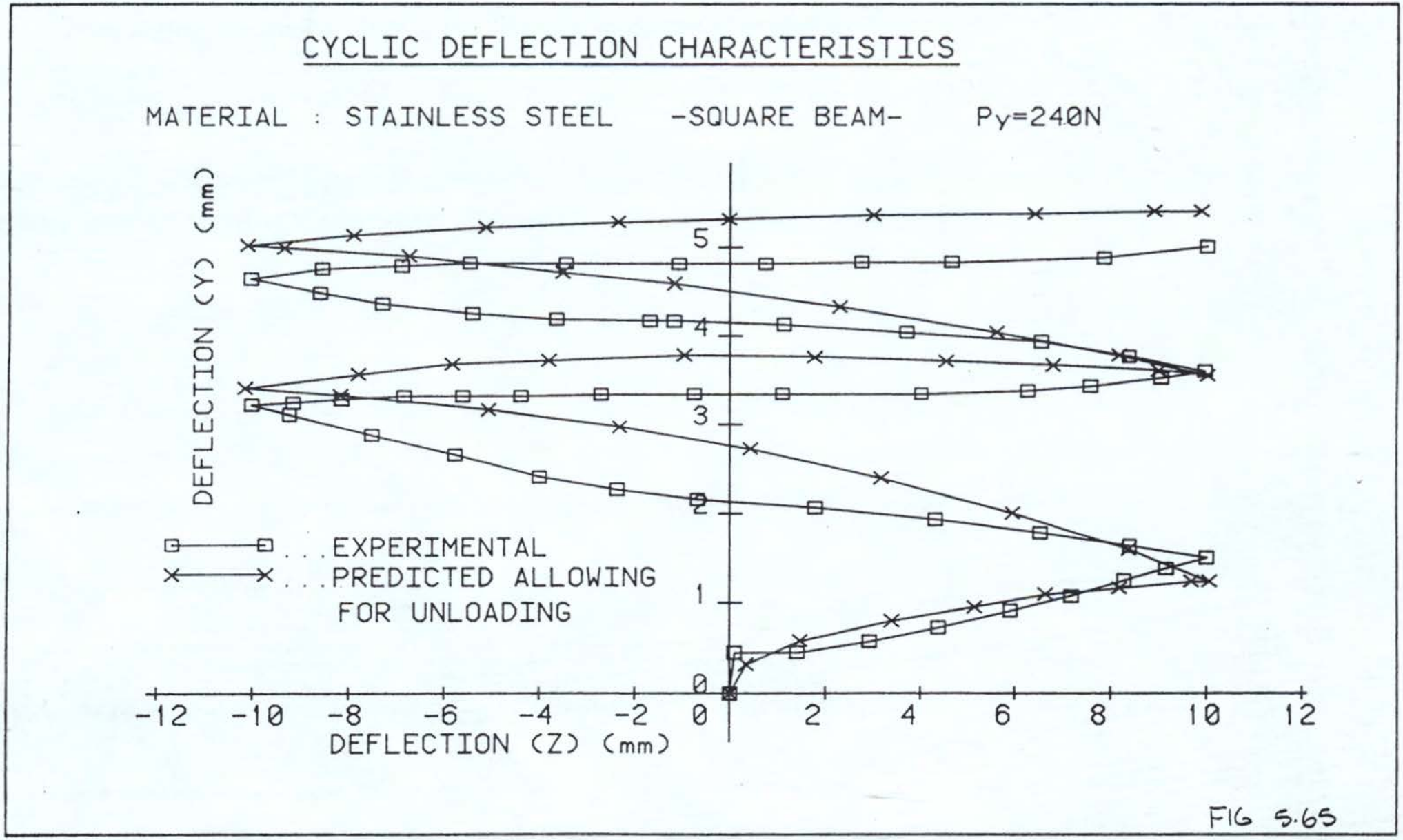
CYCLIC DEFLECTION CHARACTERISTICS
MATERIAL : STAINLESS STEEL -SQUARE BEAM- Py=240N
DEFLECTION (Y) (mm)
5
4
3
2
1
0
. . .EXPERIMENTAL
. . .PREDICTED ALLOWING FOR UNLOADING
-12 -10 -8 -6 -4 -2 0 2 4 6 8 10 12
DEFLECTION (Z) (mm)

FIG 5.65

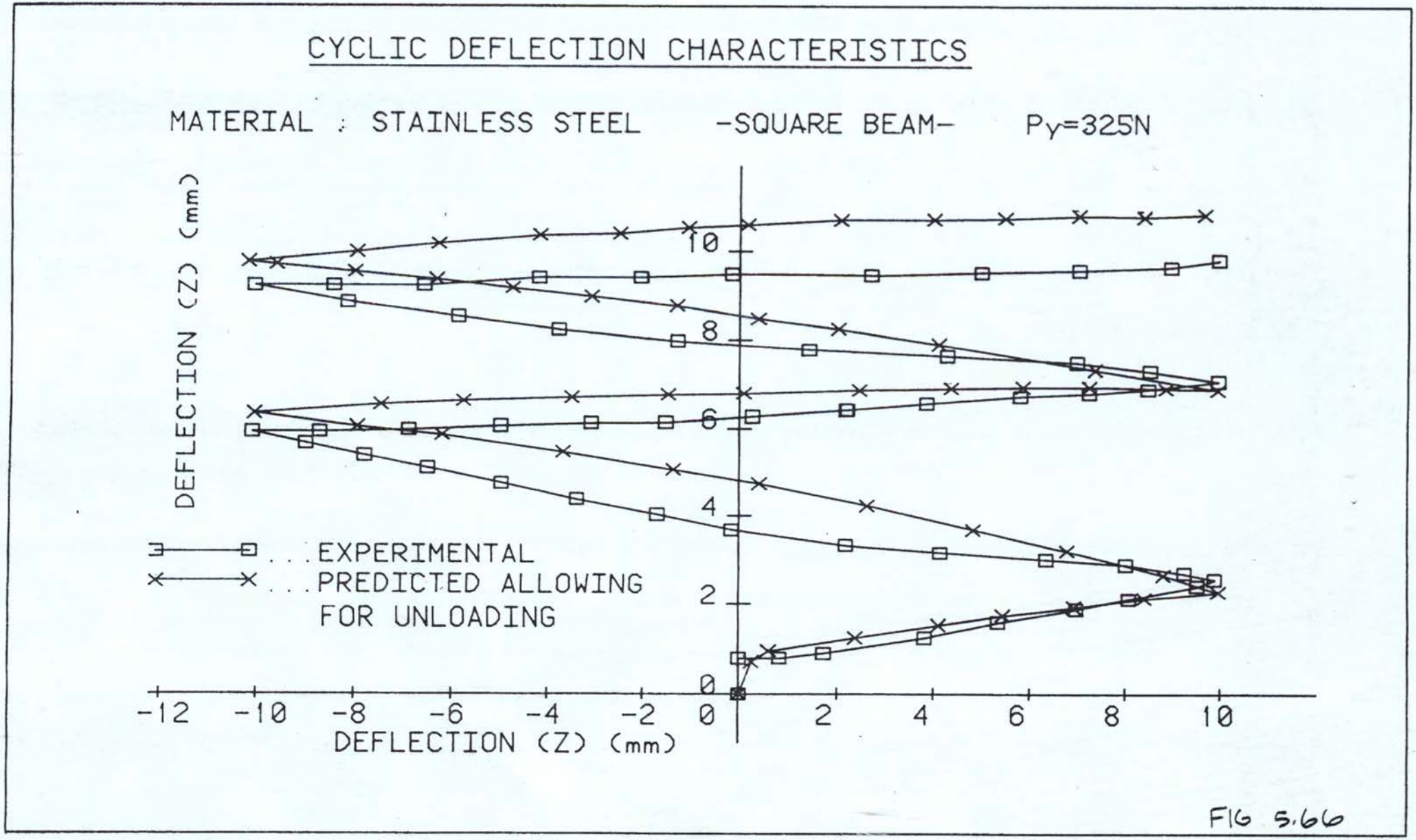
CYCLIC DEFLECTION CHARACTERISTICS
MATERIAL : STAINLESS STEEL -SQUARE BEAM- Py=325N
DEFLECTION (Z) (mm)
10
8
6
4
2
0
. . . EXPERIMENTAL
. . . PREDICTED ALLOWING FOR UNLOADING
-12 -10 -8 -6 -4 -2 0 2 4 6 8 10
DEFLECTION (Z) (mm)

FIG 5.66

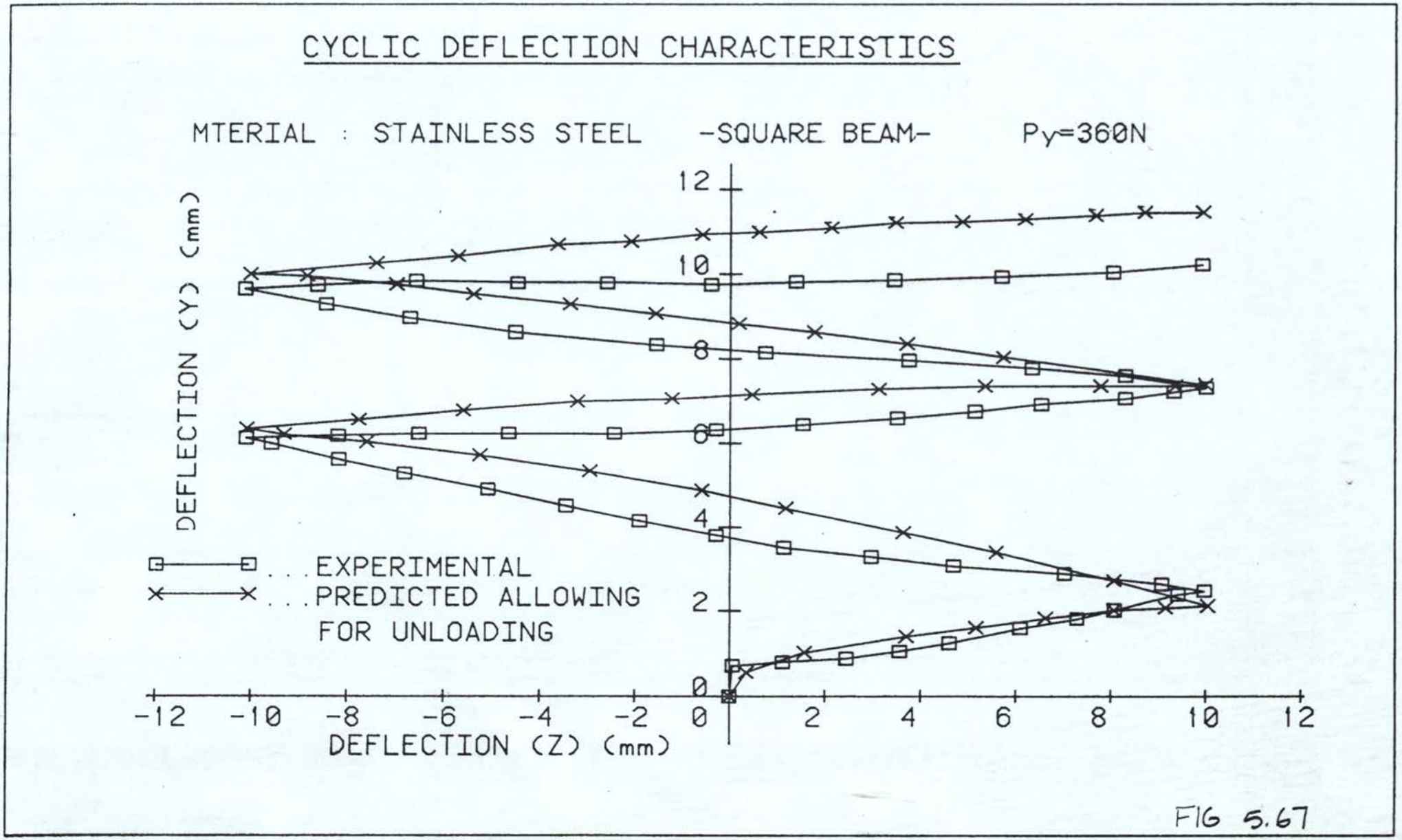
CYCLIC DEFLECTION CHARACTERISTICS
MTERIAL : STAINLESS STEEL -SQUARE BEAM- Py=360N
DEFLECTION (Y) (mm)
12
10
8
6
4
2
0
. . .EXPERIMENTAL
. . .PREDICTED ALLOWING FOR UNLOADING
-12 -10 -8 -6 -4 -2 0 2 4 6 8 10 12
DEFLECTION (Z) (mm)

FIG 5.67

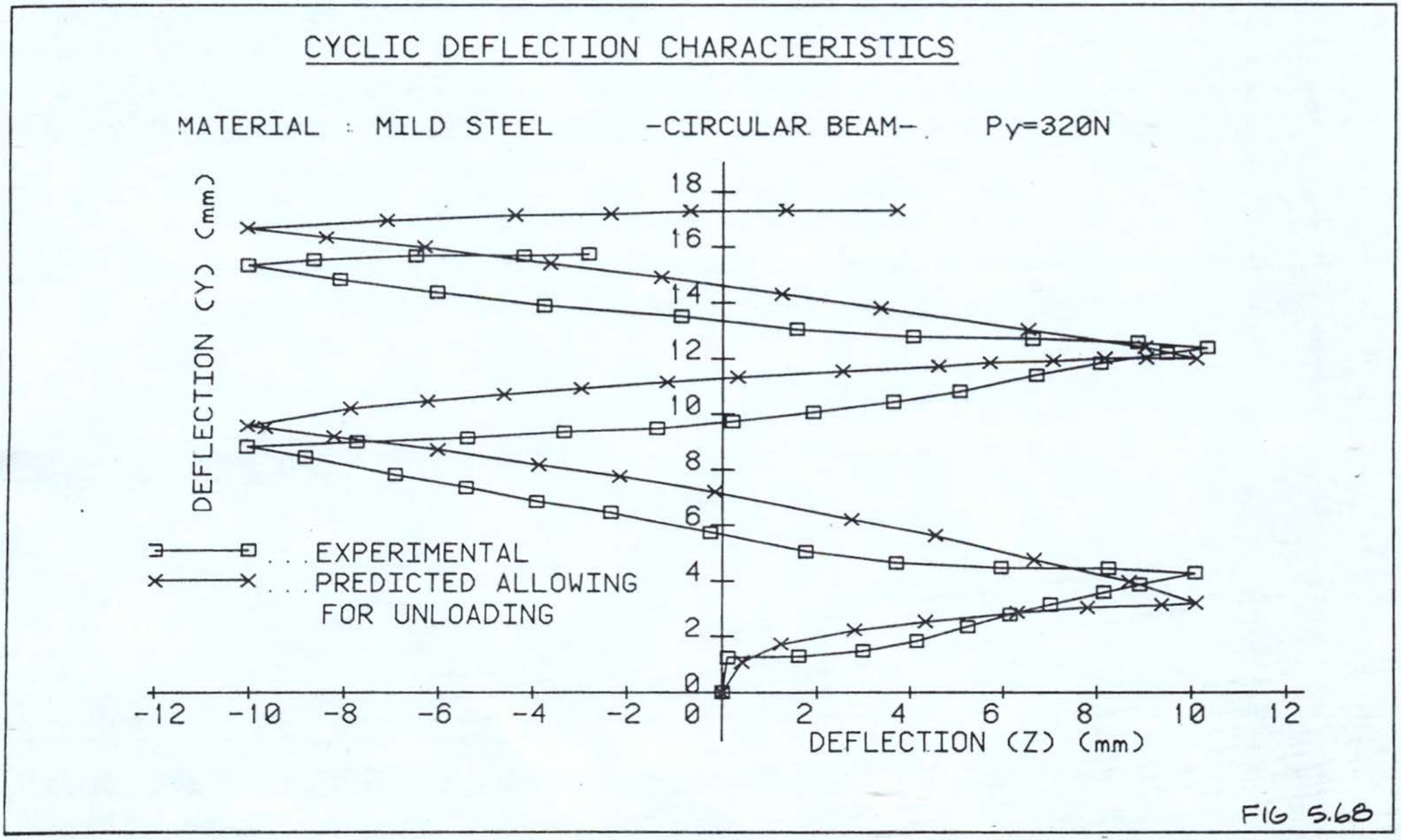
CYCLIC DEFLECTION CHARACTERISTICS
MATERIAL : MILD STEEL
-CIRCULAR BEAM-
Py=320N
DEFLECTION (Y) (mm)
18
16
14
12
10
8
6
4
2
0
-12
-10
-8
-6
-4
-2
0
2
4
6
8
10
12
DEFLECTION (Z) (mm)
. . . EXPERIMENTAL
. . . PREDICTED ALLOWING FOR UNLOADING

FIG 5.68

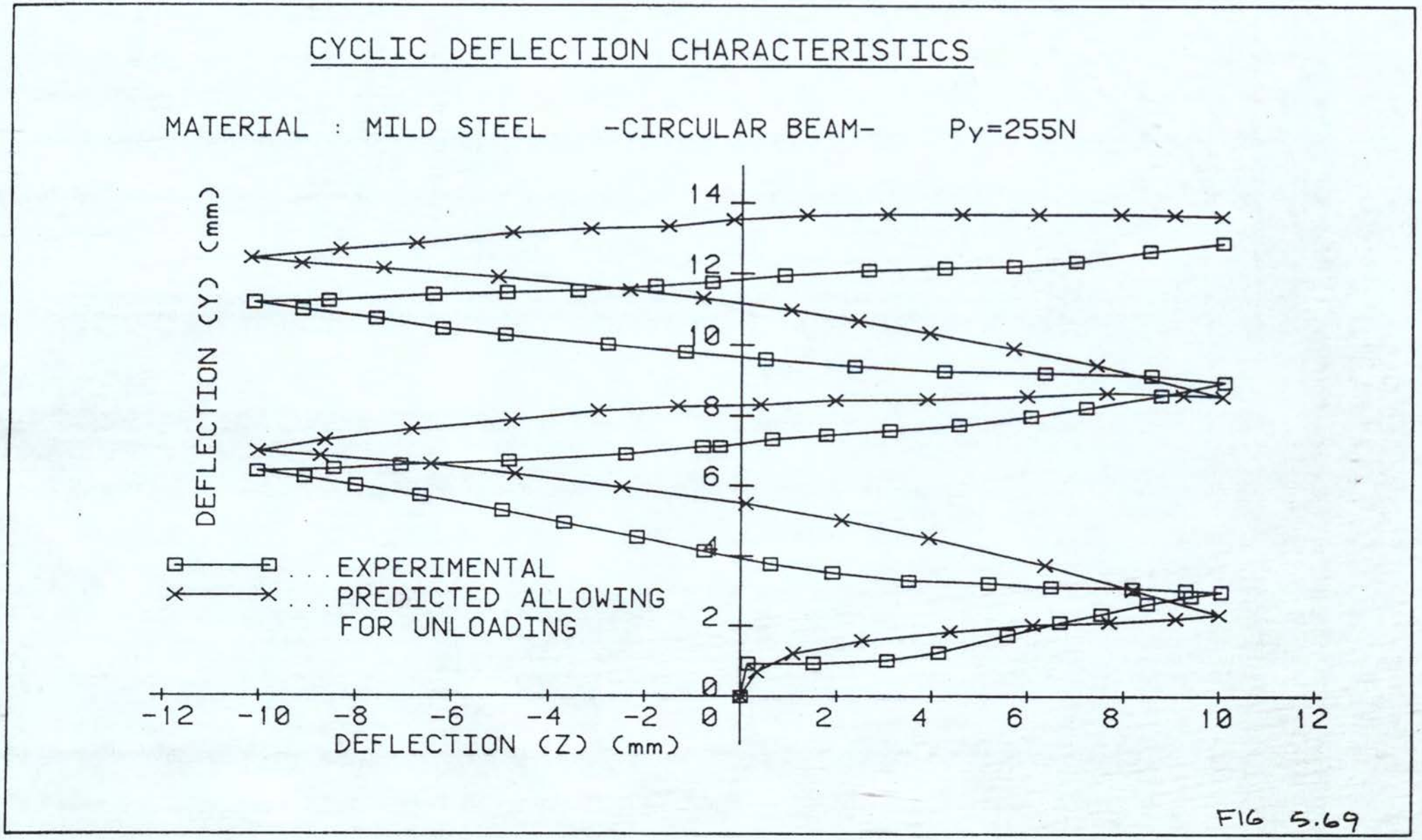
CYCLIC DEFLECTION CHARACTERISTICS
MATERIAL : MILD STEEL -CIRCULAR BEAM- Py=255N
DEFLECTION (Y) (mm)
14
12
10
8
6
4
2
0
. . . EXPERIMENTAL
. . . PREDICTED ALLOWING FOR UNLOADING
-12 -10 -8 -6 -4 -2 0 2 4 6 8 10 12
DEFLECTION (Z) (mm)

FIG 5.69

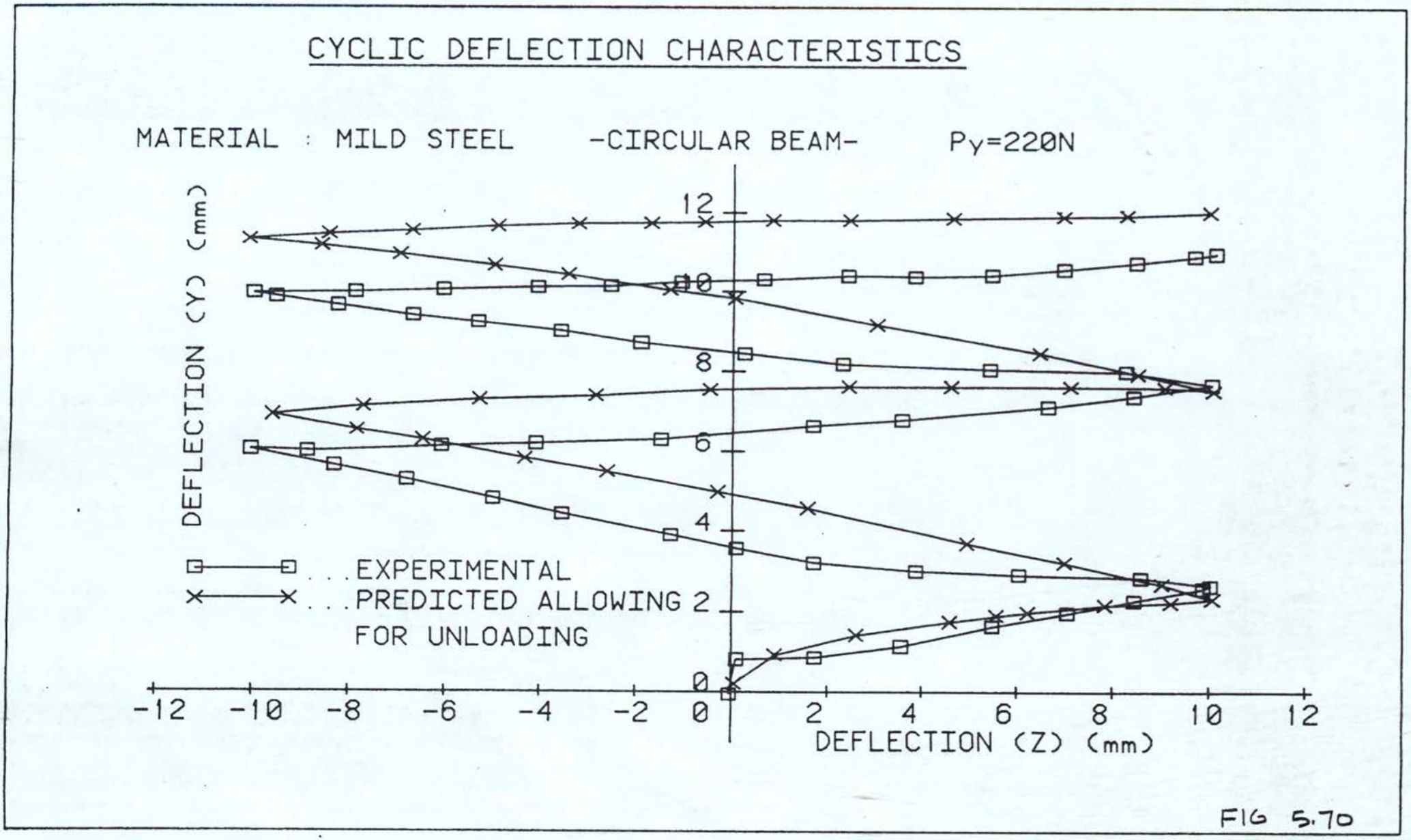
CYCLIC DEFLECTION CHARACTERISTICS
MATERIAL : MILD STEEL -CIRCULAR BEAM- Py=220N
DEFLECTION (Y) (mm)
12
10
8
6
4
2
0
-12 -10 -8 -6 -4 -2 0 2 4 6 8 10 12
DEFLECTION (Z) (mm)
...EXPERIMENTAL
...PREDICTED ALLOWING FOR UNLOADING

FIG 5.70

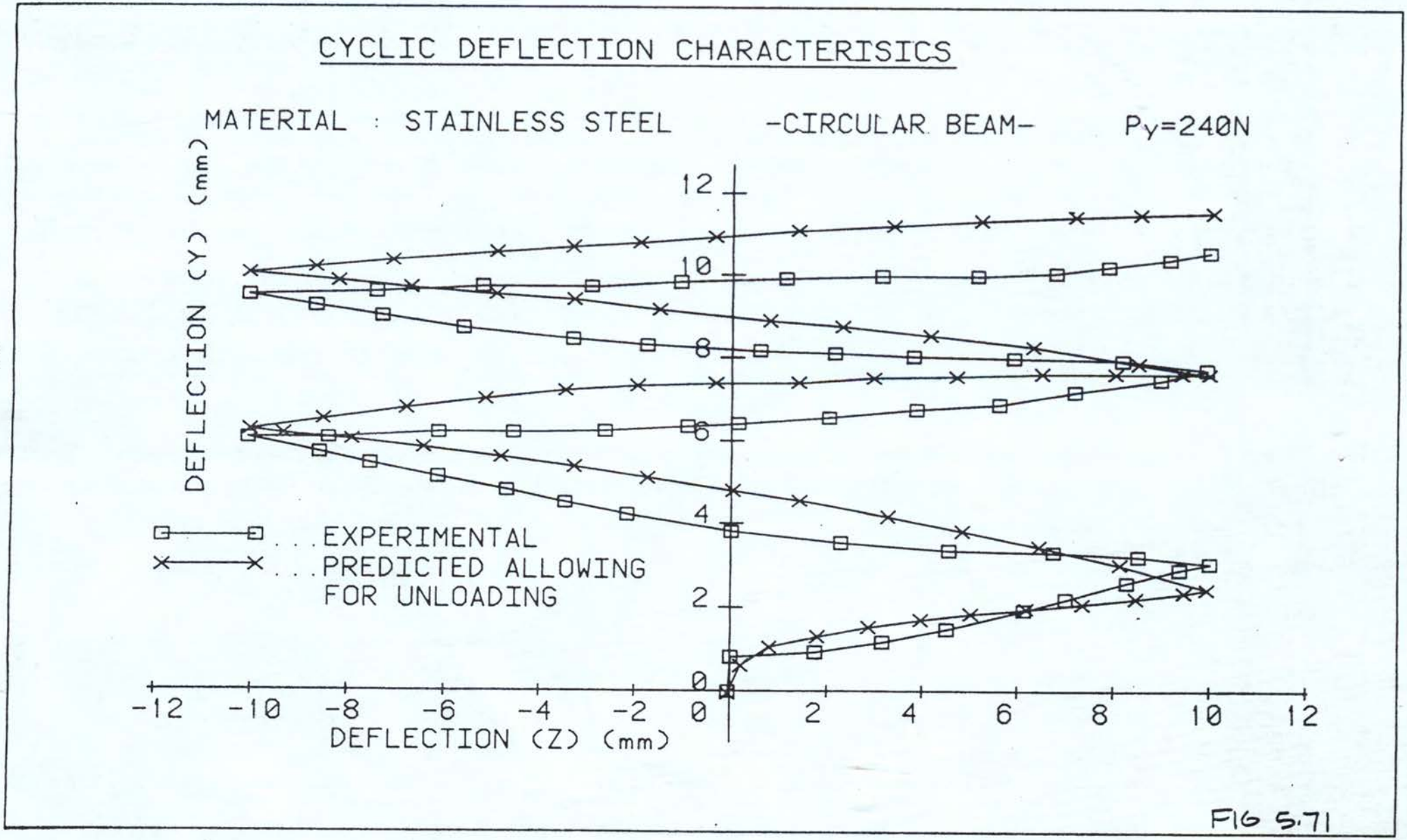
CYCLIC DEFLECTION CHARACTERISICS
MATERIAL : STAINLESS STEEL
-CIRCULAR BEAM-
Py=240N
DEFLECTION (Y) (mm)
12
10
8
6
4
2
0
. . . EXPERIMENTAL
. . . PREDICTED ALLOWING FOR UNLOADING
-12
-10
-8
-6
-4
-2
0
2
4
6
8
10
12
DEFLECTION (Z) (mm)

FIG 5.71

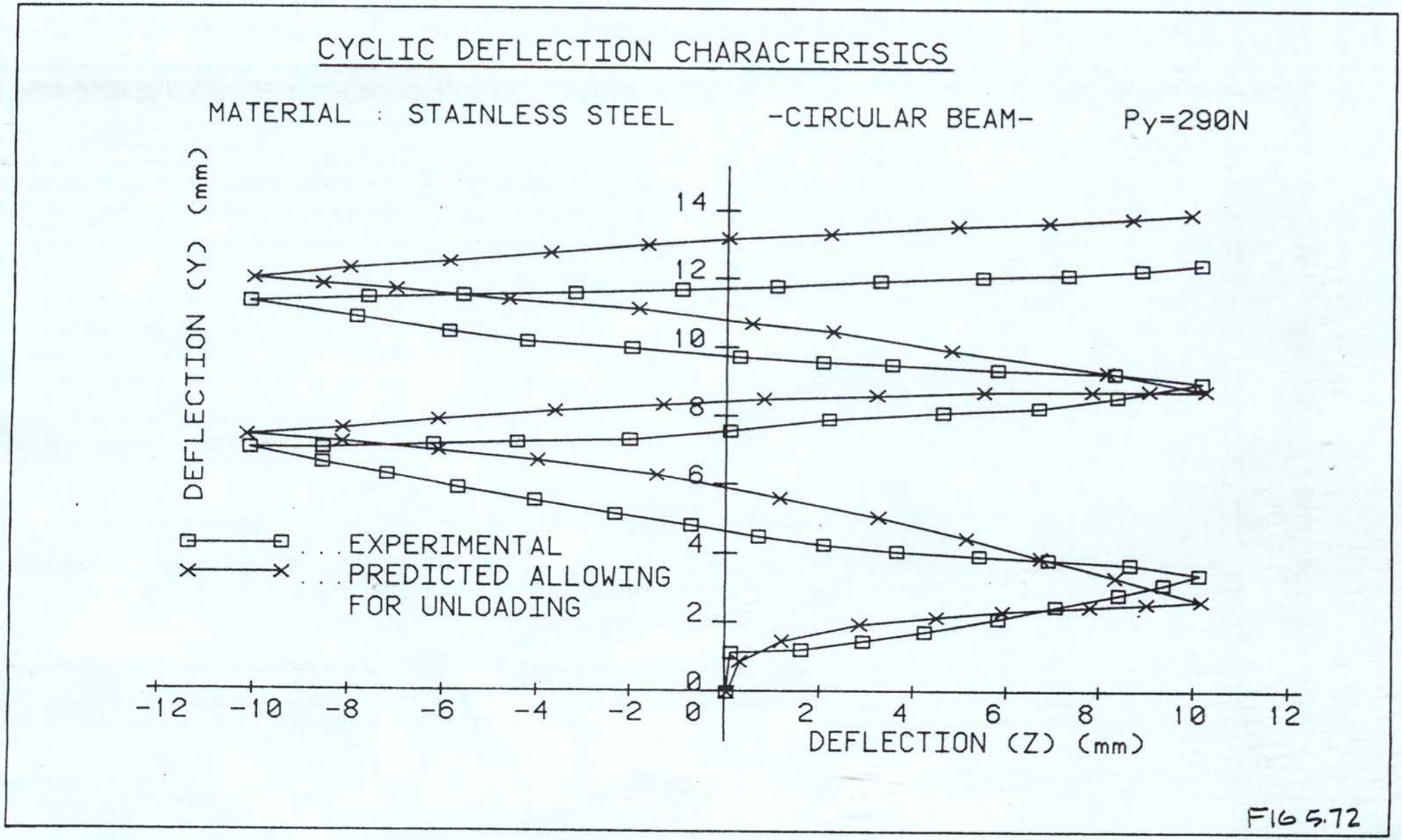
CYCLIC DEFLECTION CHARACTERISICS
MATERIAL : STAINLESS STEEL
-CIRCULAR BEAM-
Py=290N
DEFLECTION (Y) (mm)
14
12
10
8
6
4
2
0
-12
-10
-8
-6
-4
-2
0
2
4
6
8
10
12
DEFLECTION (Z) (mm)
. . .EXPERIMENTAL
. . .PREDICTED ALLOWING
FOR UNLOADING

FIG 5.72

5.2 THE EFFECT OF LOADING AND UNLOADING DURING BENDING

A major part of the research program was to develop the computer programme which allowed the stress-strain history of all elements within the beam to be determined throughout the cyclic bending process. Some results are now presented which show the stress-strain history of elements within the beam at various sections and a range of follow up vertical loads. In order to show this graphically three cross sections have been selected. The sections distance 'X' away from the free end of the beam are stationed at X = 50 mm, 95 mm and 110 mm.

Figs (5.72 to 5.73) show the cross section during the course of bi-axial loading. The output on all these figures is coded as follows

MAPP is the resultant moment due to application of loads Py and Pz.

X is the distance along the length of the beam, measured from the free end in mm.

THETA is the angle measured in degrees from Py axis to the line of the applied moment (Mapp).

The status of each element is coded using letters [A] through [X]. In order to explain the code let us consider Fig (5.72) [THETA = 0 X = 50].

The letter [A] indicates that these are the elements which have undergone plastic deformation and their current status on the stress-strain curve "1" as indicated on the right hand side of all these diagrams. Similarly the letter [F] indicates the elements current status is on curve "6". Figs (5.73 - 5.74) and (5.75) show the same cross section as the applied moment increase and, the neutral surface rotates due to increase of the horizontal load Pz.

On Fig (5.76) code [H] and [I] appears. This indicates that the elements concerned have undergone plastic deformation and, in the case of [H], the element moved from curve 1 to 6 during the course of last load increment. Similarly [I] indicates the element status has moved from 6 to 1. It must be appreciated that the nature of the material characteristics dictates that for element to move from curve 1 to 6 or vice-versa the unlaoding takes place from the elastic regions of these curves.

A more complex unloading can be seen on Fig (5.81) [X = 110 THETA = 45±]. The code [K] indicates the element has unloaded from a previous plastic state on curve 1, through curve 2 and onto its current position on curve 3. Similarly [M] indicates the elements have unloaded from plastic stae of curve 6, through curve 4 and onto its present status on curve 5.

Clearly on these selected figures some of the codes do not appear. During the course of analysis the elements at some stage or another were subjected to all the combinations of unloading listed by means of letters [A] through [X].

However the elements were rarely observed on curve 2 and 4. The unloading took place very rapidly and the maximum number of elements which simultaneously were in these regions of the stress-strain curve was two. This clearly demonstrates that the effect of neglecting the elements which were unloading is extremely small. This is certainly true for the range of plastic strains considered in the investigation but the unloading process could be significant at larger starins, where more elements would be unloaded by the rotation of the neutral surface. It is felt that the program developed is suitable for a wider range of problems involving larger strain but would require considerably more computer memory.

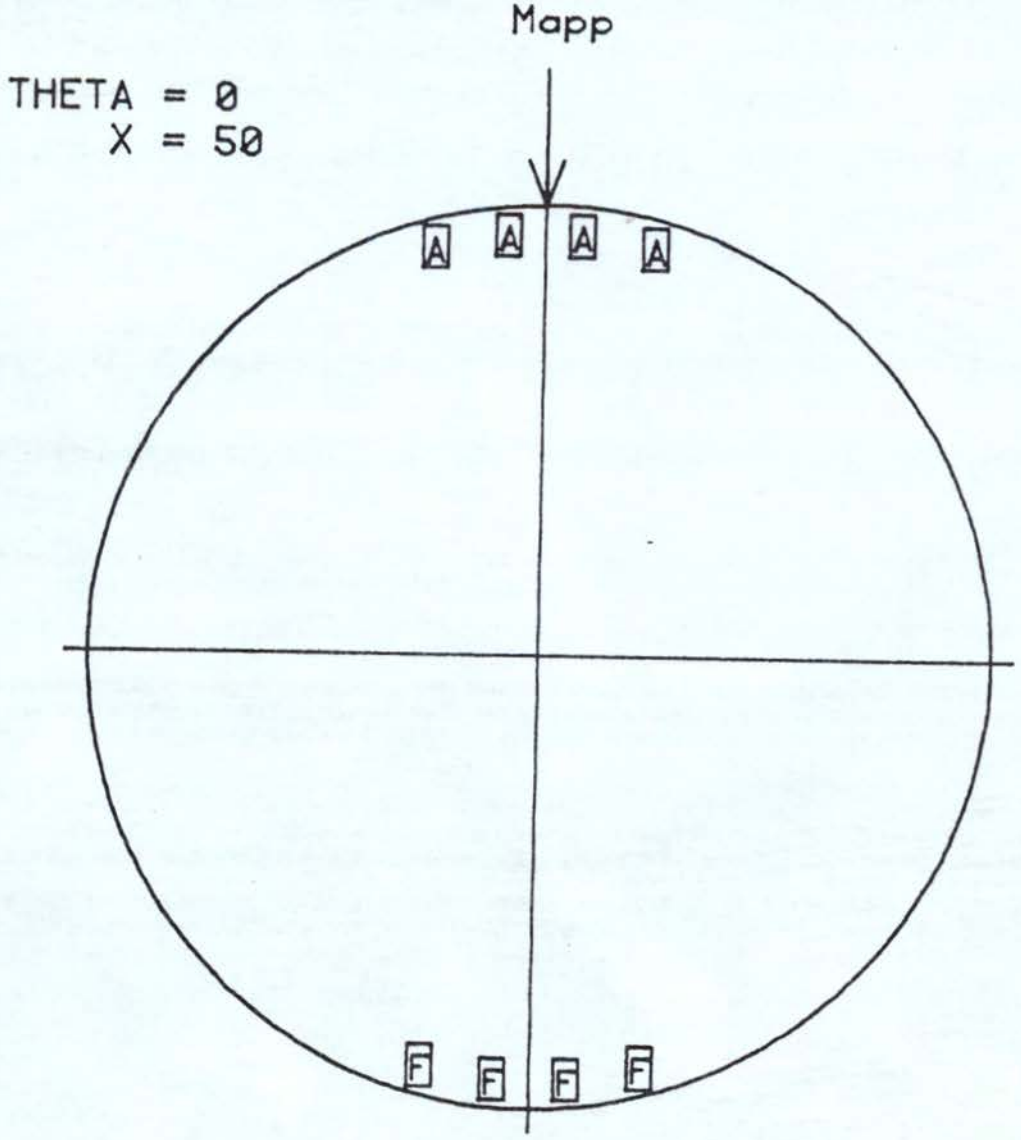

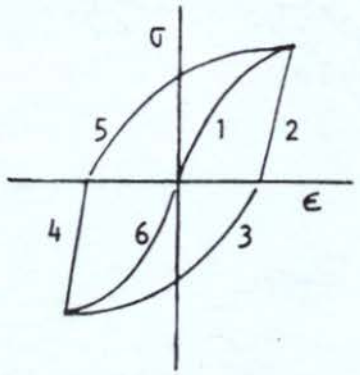

A	1
B	2
C	3
D	4
E	5
F	6
H	1 - 6
I	6 - 1
J	1 - 2
K	1 - 2 - 3
L	6 - 4
M	6 - 4 - 5
N	3 - 4
P	3 - 4 - 5
R	5 - 2
S	5 - 2 - 3
W	2 - 3
X	4 - 5

FIG 5.73.

THETA = 45
X = 50

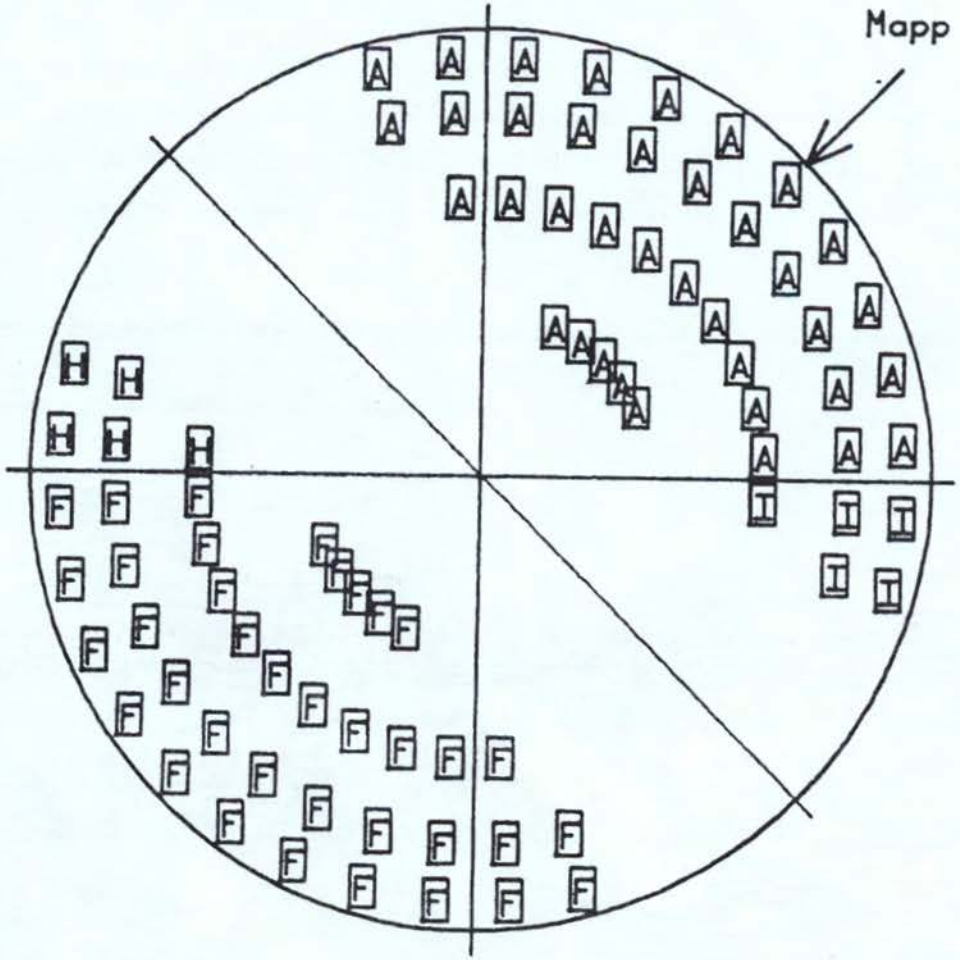

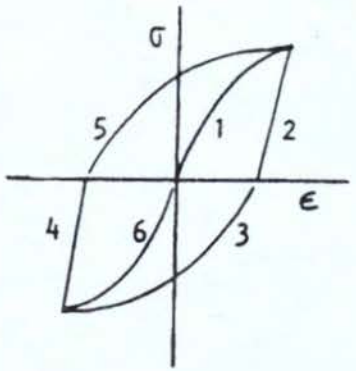

A	1
B	2
C	3
D	4
E	5
F	6
H	1 - 6
I	6 - 1
J	1 - 2
K	1 - 2 - 3
L	6 - 4
M	6 - 4 - 5
N	3 - 4
P	3 - 4 - 5
R	5 - 2
S	5 - 2 - 3
W	2 - 3
X	4 - 5

FIG 5.74

THETA = 46.4
X = 50

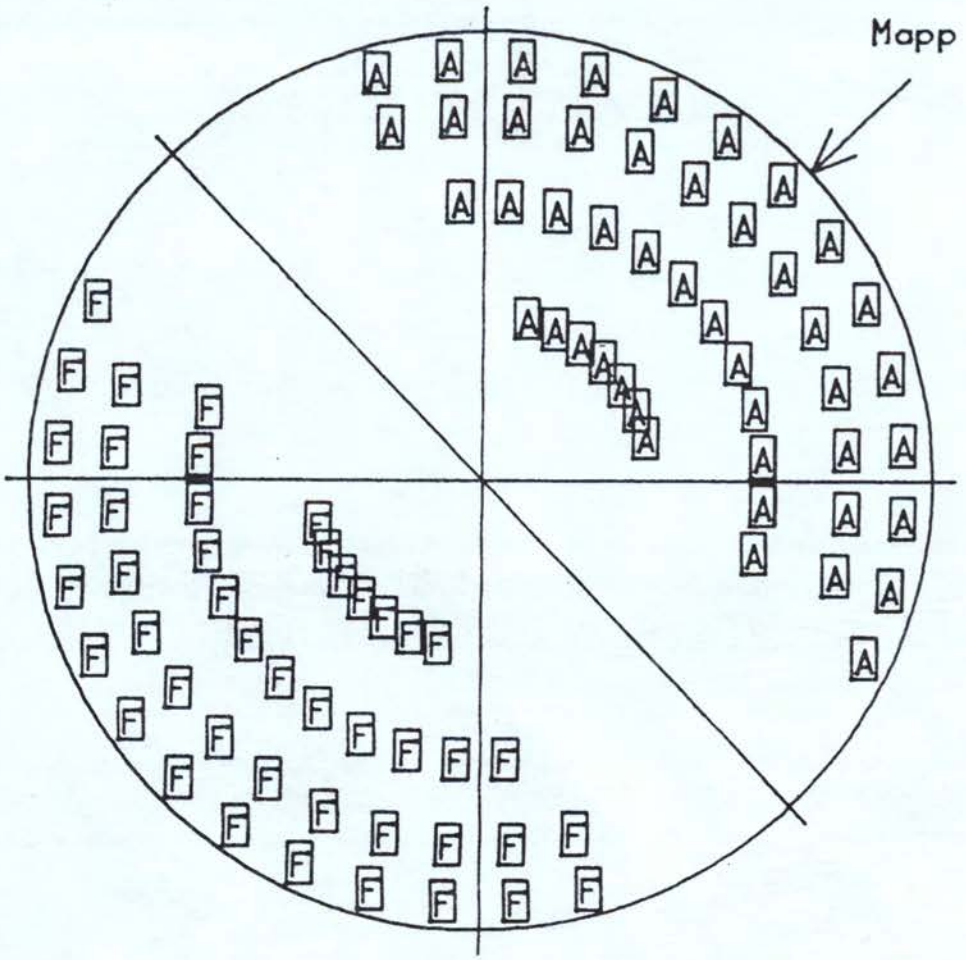

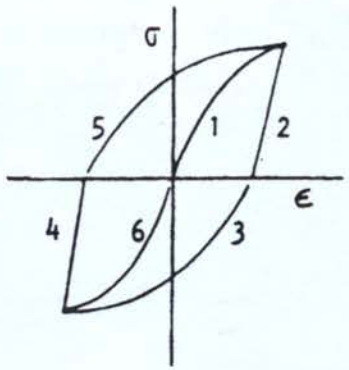

A	1
B	2
C	3
D	4
E	5
F	6
H	1 - 6
I	6 - 1
J	1 - 2
K	1 - 2 - 3
L	6 - 4
M	6 - 4 - 5
N	3 - 4
P	3 - 4 - 5
R	5 - 2
S	5 - 2 - 3
W	2 - 3
X	4 - 5

FIG 5.75

THETA = 47.9
X = 50

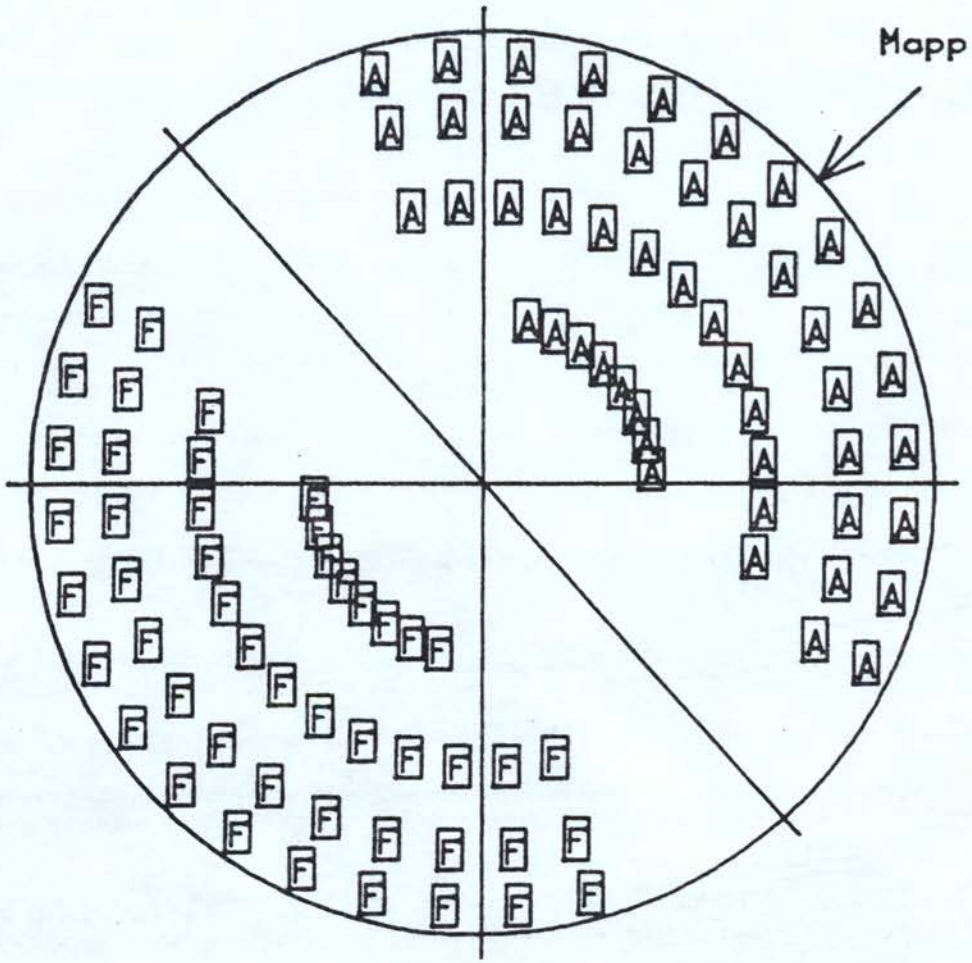

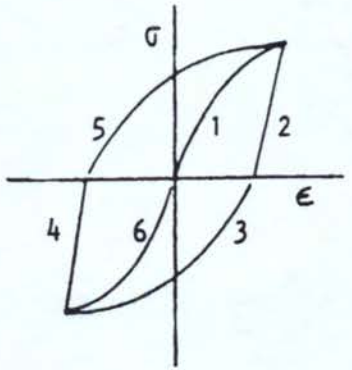

A	1
B	2
C	3
D	4
E	5
F	6
H	1 - 6
I	6 - 1
J	1 - 2
K	1 - 2 - 3
L	6 - 4
M	6 - 4 - 5
N	3 - 4
P	3 - 4 - 5
R	5 - 2
S	5 - 2 - 3
W	2 - 3
X	4 - 5

FIG. 5.76

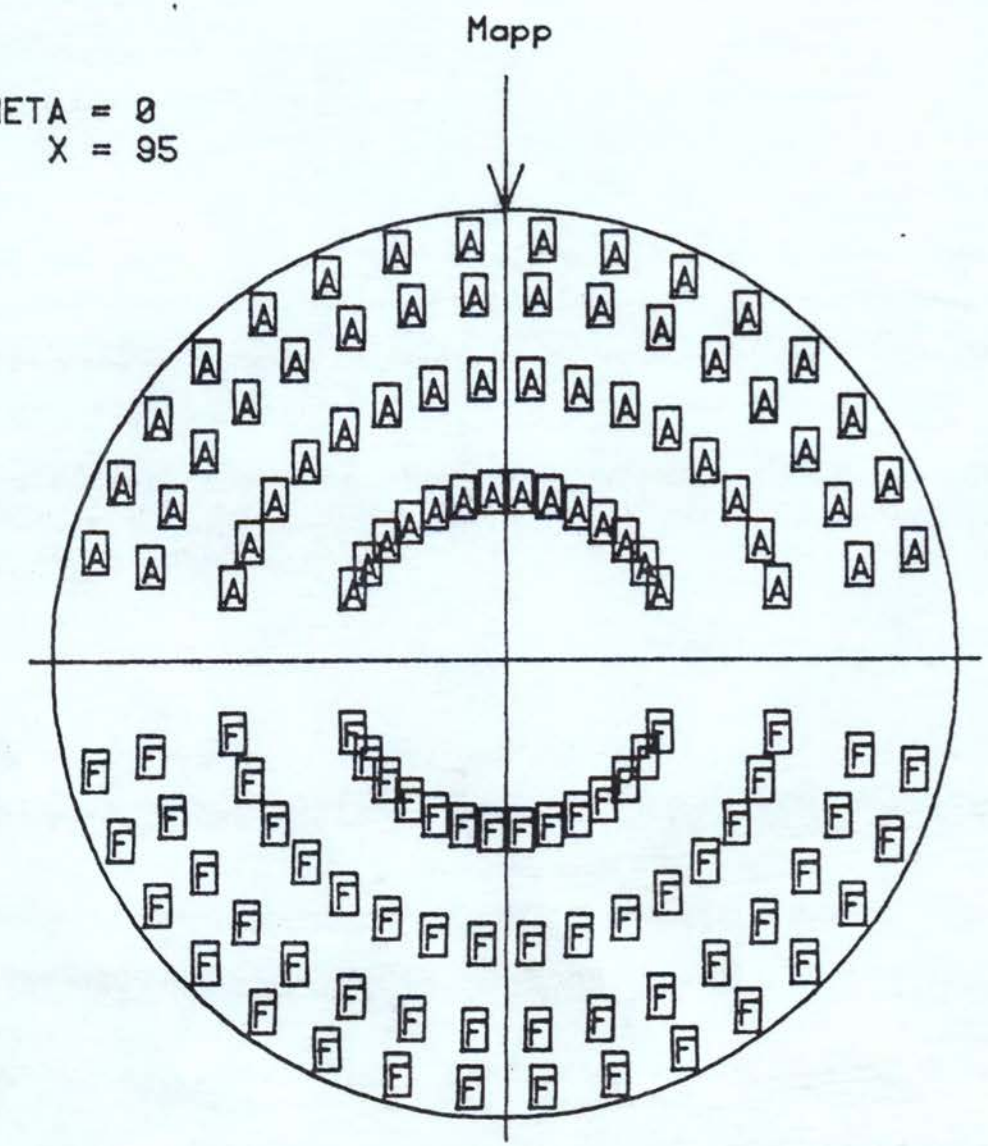

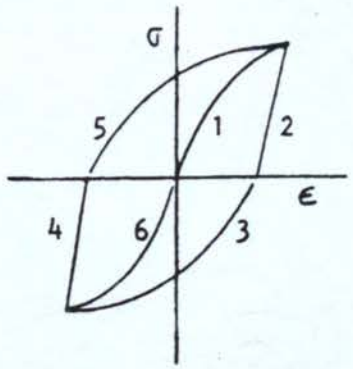

A	1
B	2
C	3
D	4
E	5
F	6
H	1 - 6
I	6 - 1
J	1 - 2
K	1 - 2 - 3
L	6 - 4
M	6 - 4 - 5
N	3 - 4
P	3 - 4 - 5
R	5 - 2
S	5 - 2 - 3
W	2 - 3
X	4 - 5

FIG 5.77

THETA = 45
X = 95

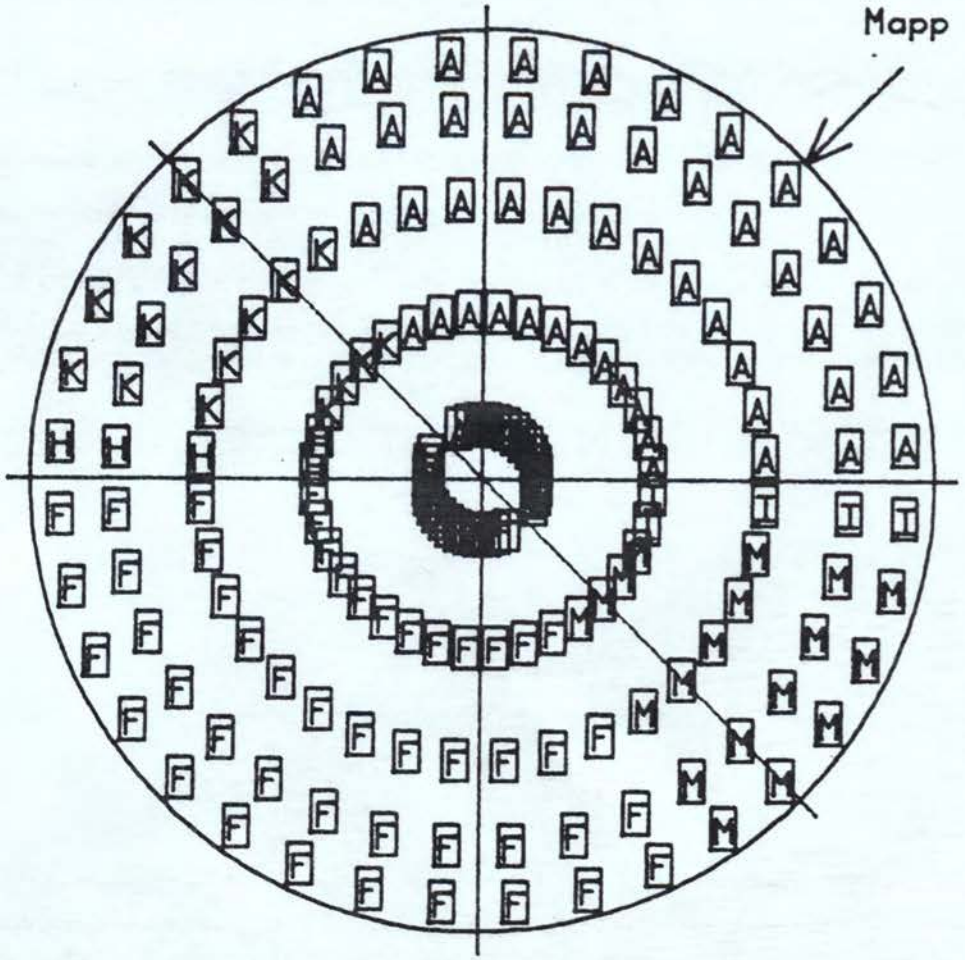

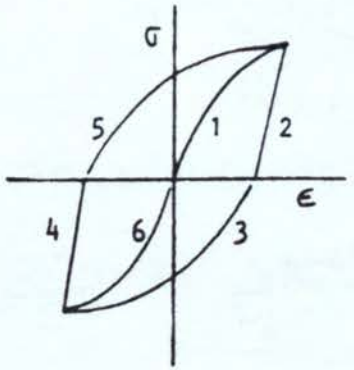

A	1
B	2
C	3
D	4
E	5
F	6
H	1 - 6
I	6 - 1
J	1 - 2
K	1 - 2 - 3
L	6 - 4
M	6 - 4 - 5
N	3 - 4
P	3 - 4 - 5
R	5 - 2
S	5 - 2 - 3
W	2 - 3
X	4 - 5

FIG 578

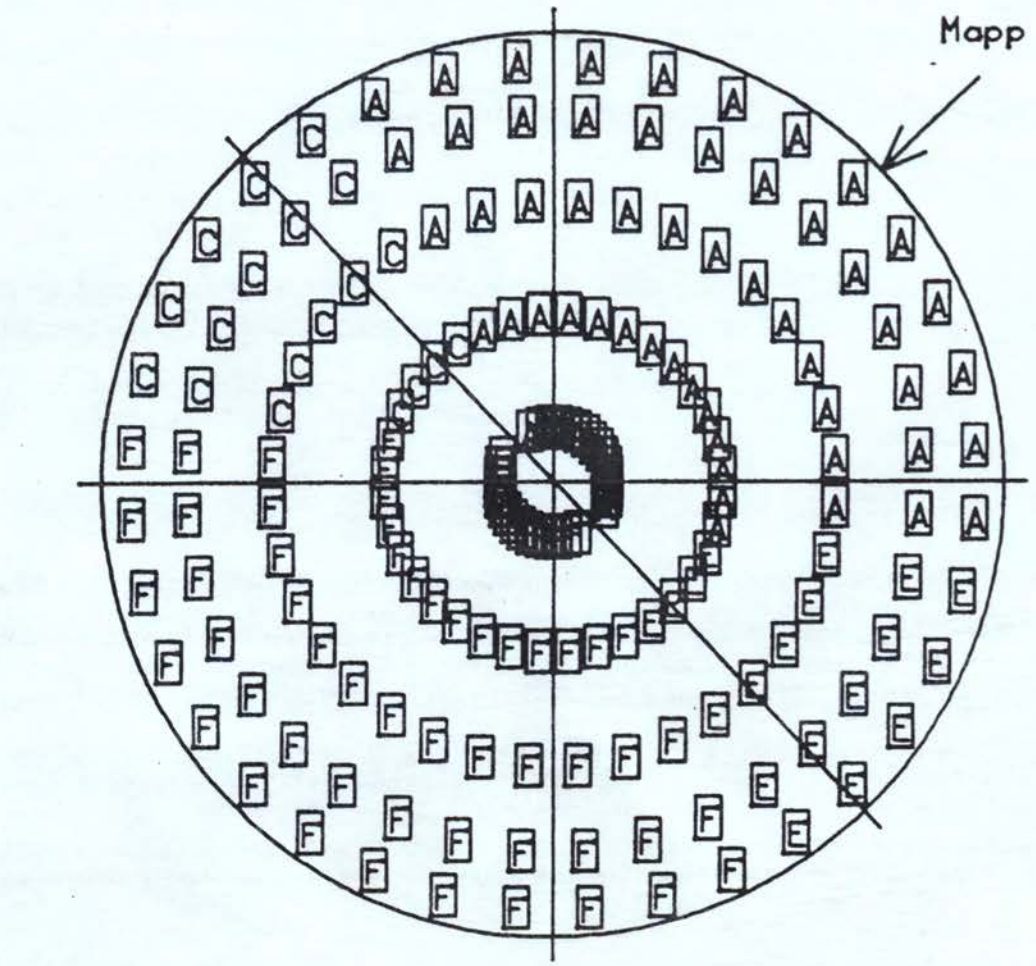

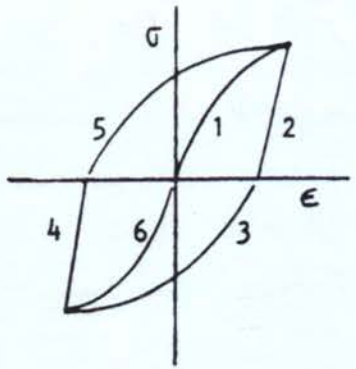

A	1
B	2
C	3
D	4
E	5
F	6
H	1 - 6
I	6 - 1
J	1 - 2
K	1 - 2 - 3
L	6 - 4
M	6 - 4 - 5
N	3 - 4
P	3 - 4 - 5
R	5 - 2
S	5 - 2 - 3
W	2 - 3
X	4 - 5

FIG 5.79

THETA = 47.9
X = 95

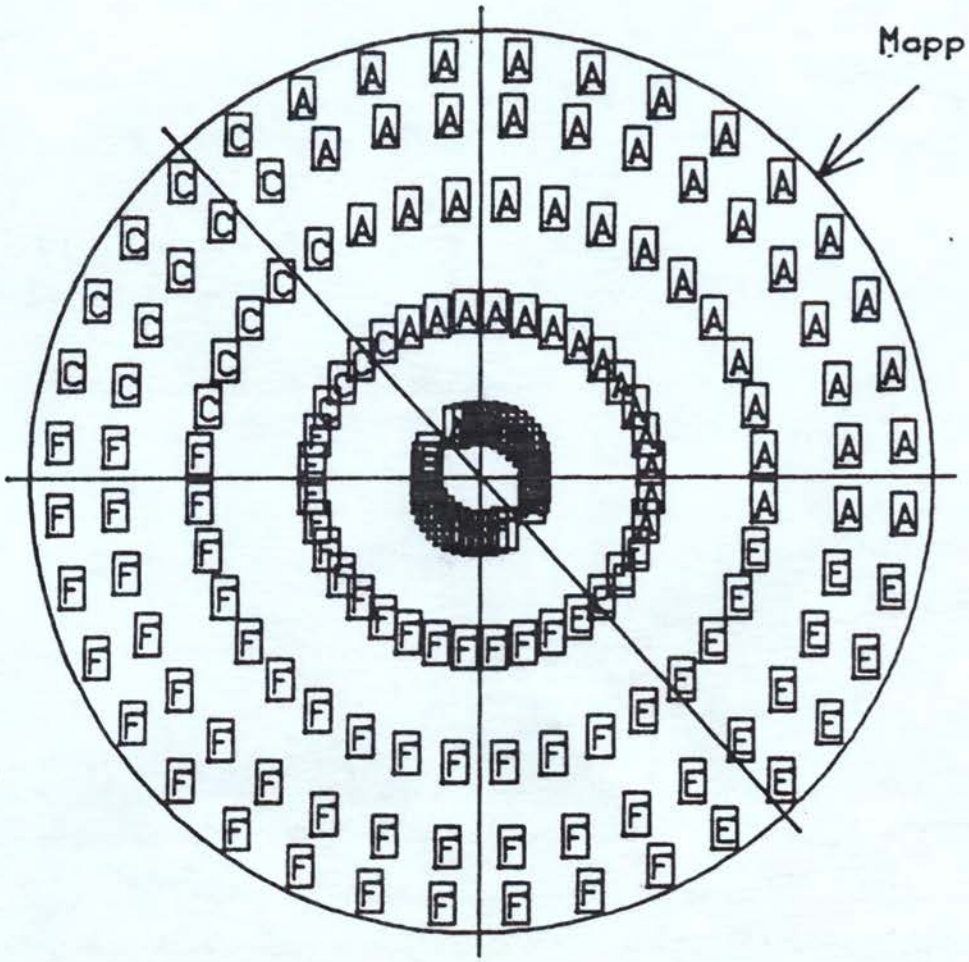

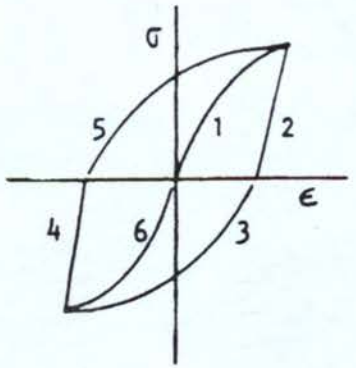

A	1
B	2
C	3
D	4
E	5
F	6
H	1 - 6
I	6 - 1
J	1 - 2
K	1 - 2 - 3
L	6 - 4
M	6 - 4 - 5
N	3 - 4
P	3 - 4 - 5
R	5 - 2
S	5 - 2 - 3
W	2 - 3
X	4 - 5

FIG 5.80

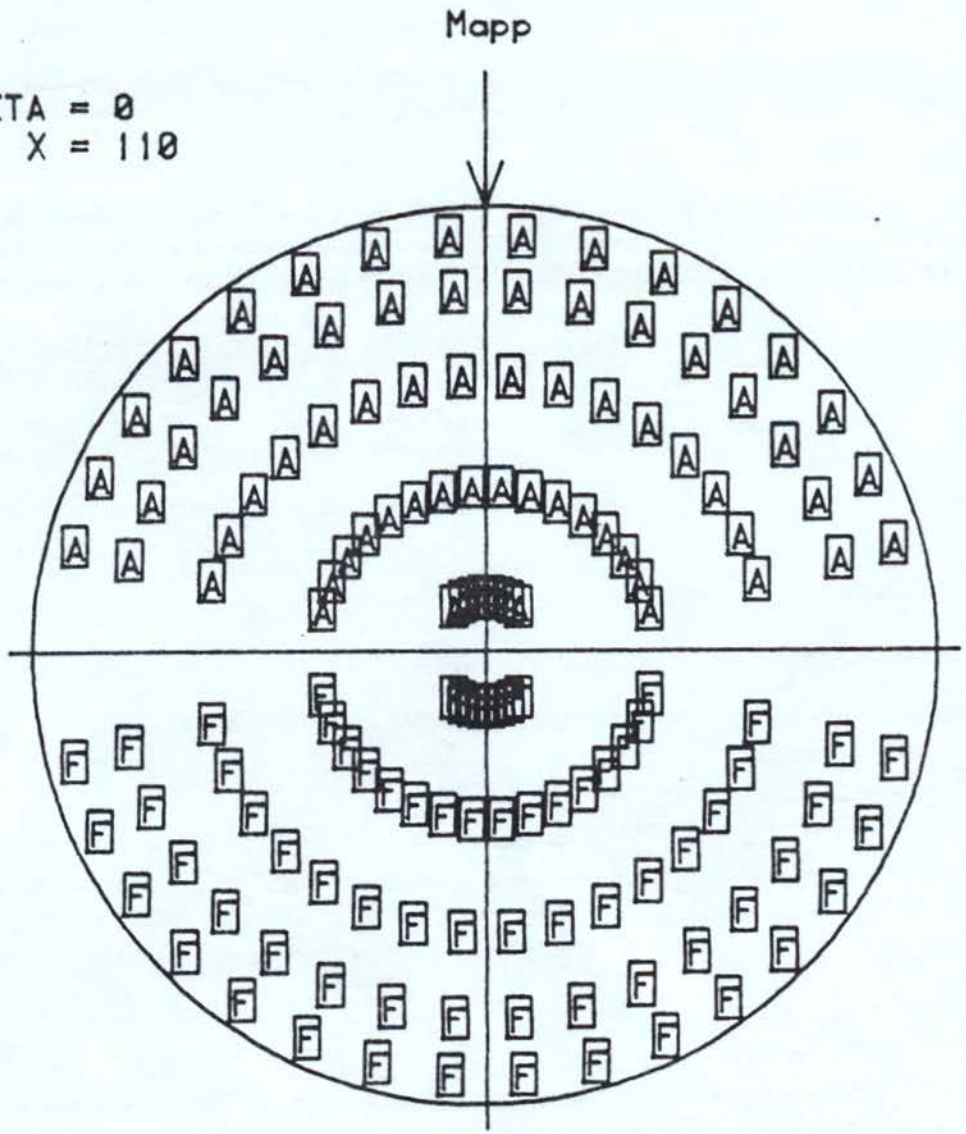

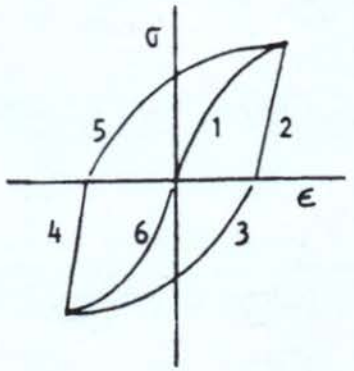

A	1
B	2
C	3
D	4
E	5
F	6
H	1 - 6
I	6 - 1
J	1 - 2
K	1 - 2 - 3
L	6 - 4
M	6 - 4 - 5
N	3 - 4
P	3 - 4 - 5
R	5 - 2
S	5 - 2 - 3
W	2 - 3
X	4 - 5

FIG 5.81

THETA = 45
X = 110

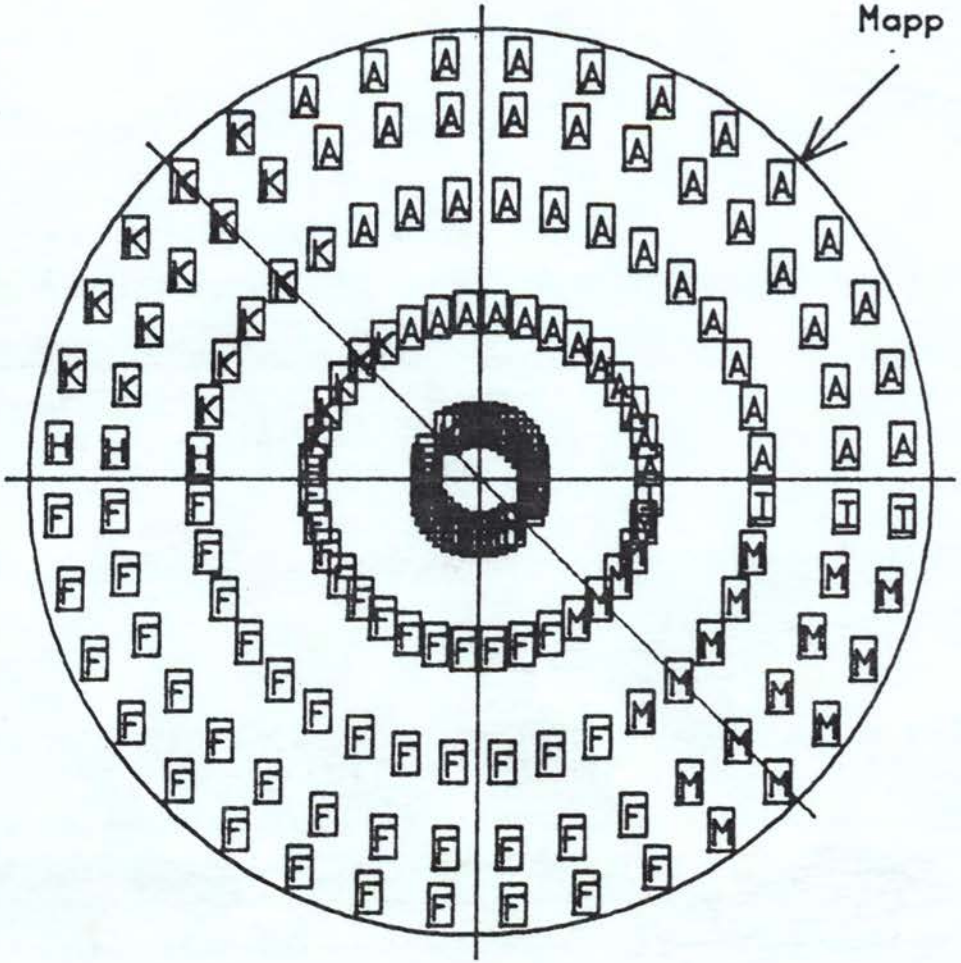

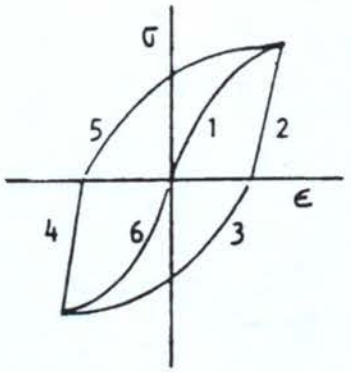

A	1
B	2
C	3
D	4
E	5
F	6
H	1 - 6
I	6 - 1
J	1 - 2
K	1 - 2 - 3
L	6 - 4
M	6 - 4 - 5
N	3 - 4
P	3 - 4 - 5
R	5 - 2
S	5 - 2 - 3
W	2 - 3
X	4 - 5

FIG 5.82

THETA = 46.4
X = 110

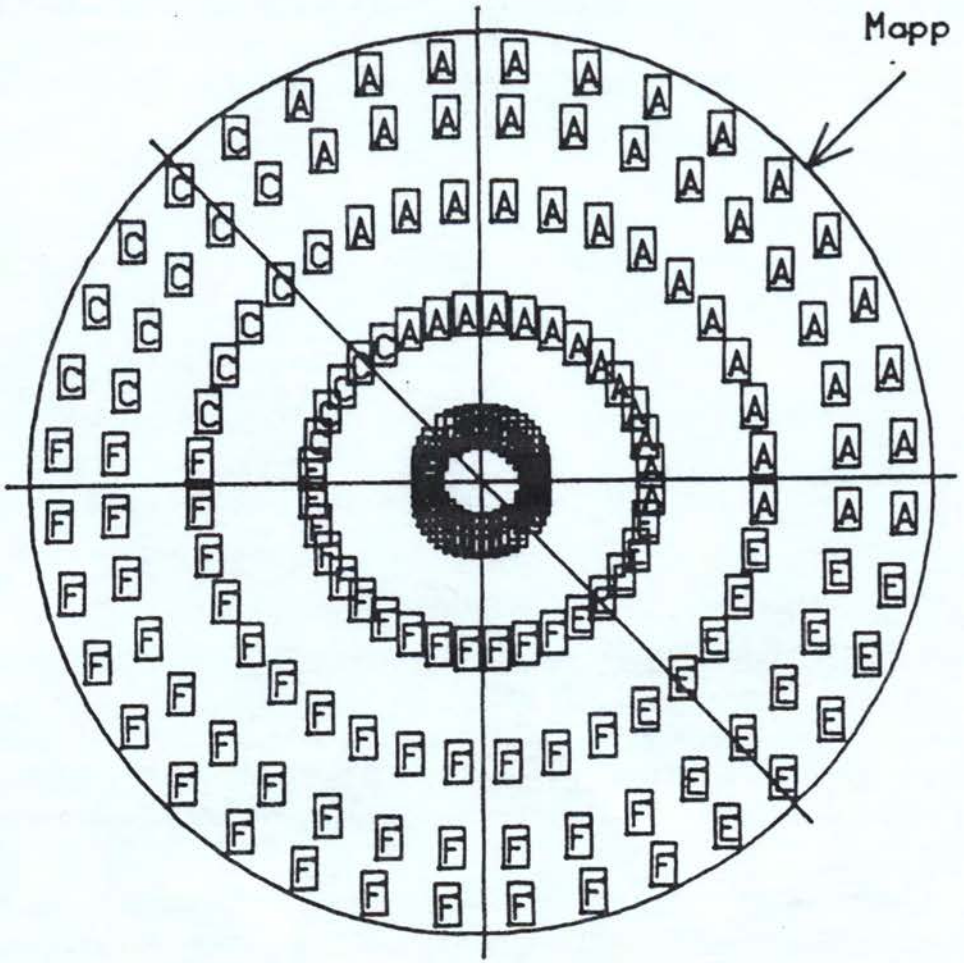

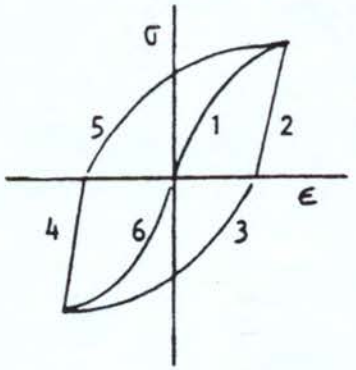

A	1
B	2
C	3
D	4
E	5
F	6
H	1 - 6
I	6 - 1
J	1 - 2
K	1 - 2 - 3
L	6 - 4
M	6 - 4 - 5
N	3 - 4
P	3 - 4 - 5
R	5 - 2
S	5 - 2 - 3
W	2 - 3
X	4 - 5

FIG 5.83

THETA = 47.9
X = 110

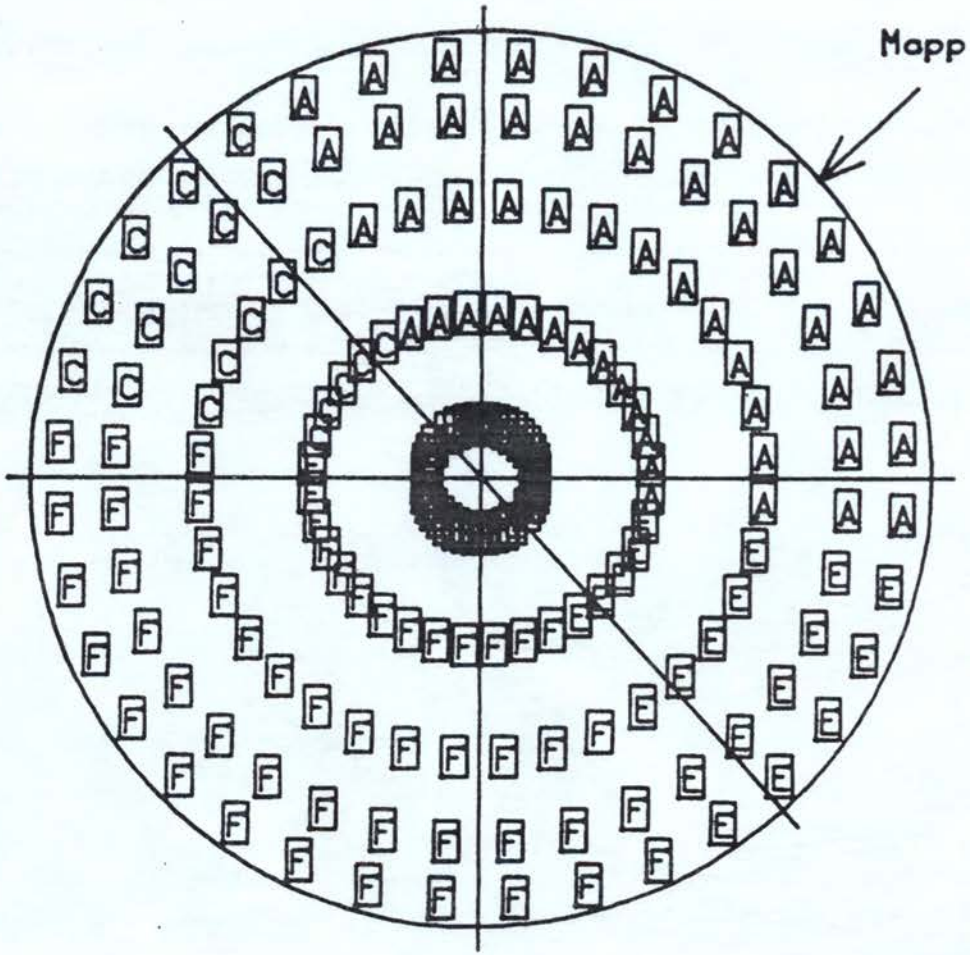

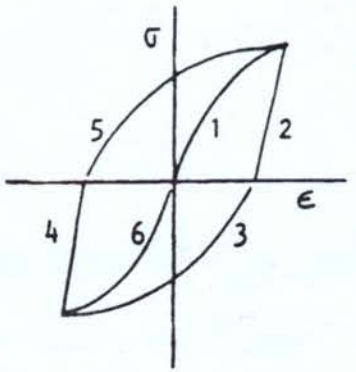

A	1
B	2
C	3
D	4
E	5
F	6
H	1 - 6
I	6 - 1
J	1 - 2
K	1 - 2 - 3
L	6 - 4
M	6 - 4 - 5
N	3 - 4
P	3 - 4 - 5
R	5 - 2
S	5 - 2 - 3
W	2 - 3
X	4 - 5

FIG 5.84

5.3 STRAIN DISTRIBUTION

There will be a distribution of outer fibre strain along the beam and also a distribution through the cross-section. The computer program monitored and updated these strains at all times in order to determine the current material properties. During the first quarter cycle the material data is the same for each section of the beam, but when we cycle the beam each element undergoes a different cyclic strain and therefore its properties are modified.

It is useful to examine the distribution of outer fibre strain along the beam and also to see how this strain distribution is modified by the cyclic process.

Some experimental data was obtained from a student project (45) and these results are compared with computer predictions in Fig (5.85) for the first quarter cycle. It can be seen that the results are quite good at the higher loads or strains and the agreement is less good at the small strain. This is consistent with previous results and reflects our lack of correlation in modelling the material behaviour accurately with the simple power law. The predicted strain distribution at the end of the first full cycle and the second cycle are shown in Fig (5.84). It can be seen that there is a redistribution of the strain, with a reduction in the maximum strain at the fixed end and a growth in the extent of the plastic zone along the beam.

Finally, although fatigue failure aspects were not investigated it was noted that on beams which were continually cycled that cracks, when they were developed, always started on the side of the beam which went into tension on the first quarter cycle. This is consistent with the findings of Tilley (48) who observed for several steels that fatigue life in push-pull specimens was reduced when the process was started with tension cycle.

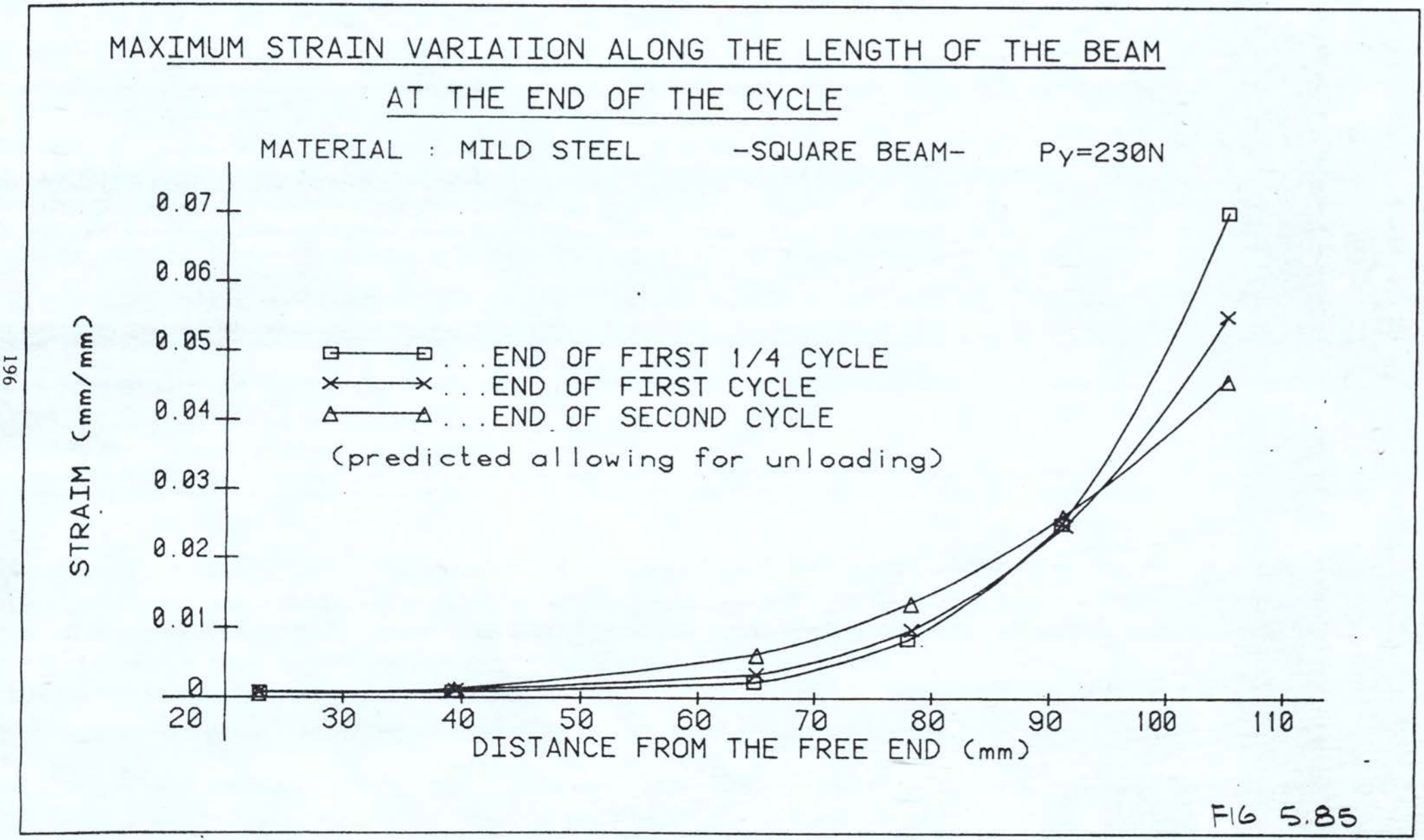
MAXIMUM STRAIN VARIATION ALONG THE LENGTH OF THE BEAM
AT THE END OF THE CYCLE
MATERIAL : MILD STEEL -SQUARE BEAM- Py=230N
STRAIM (mm/mm)
0.07
0.06
0.05
0.04
0.03
0.02
0.01
0
20
30
40
50
60
70
80
90
100
110
DISTANCE FROM THE FREE END (mm)
...END OF FIRST 1/4 CYCLE
...END OF FIRST CYCLE
...END OF SECOND CYCLE
(predicted allowing for unloading)

FIG 5.85

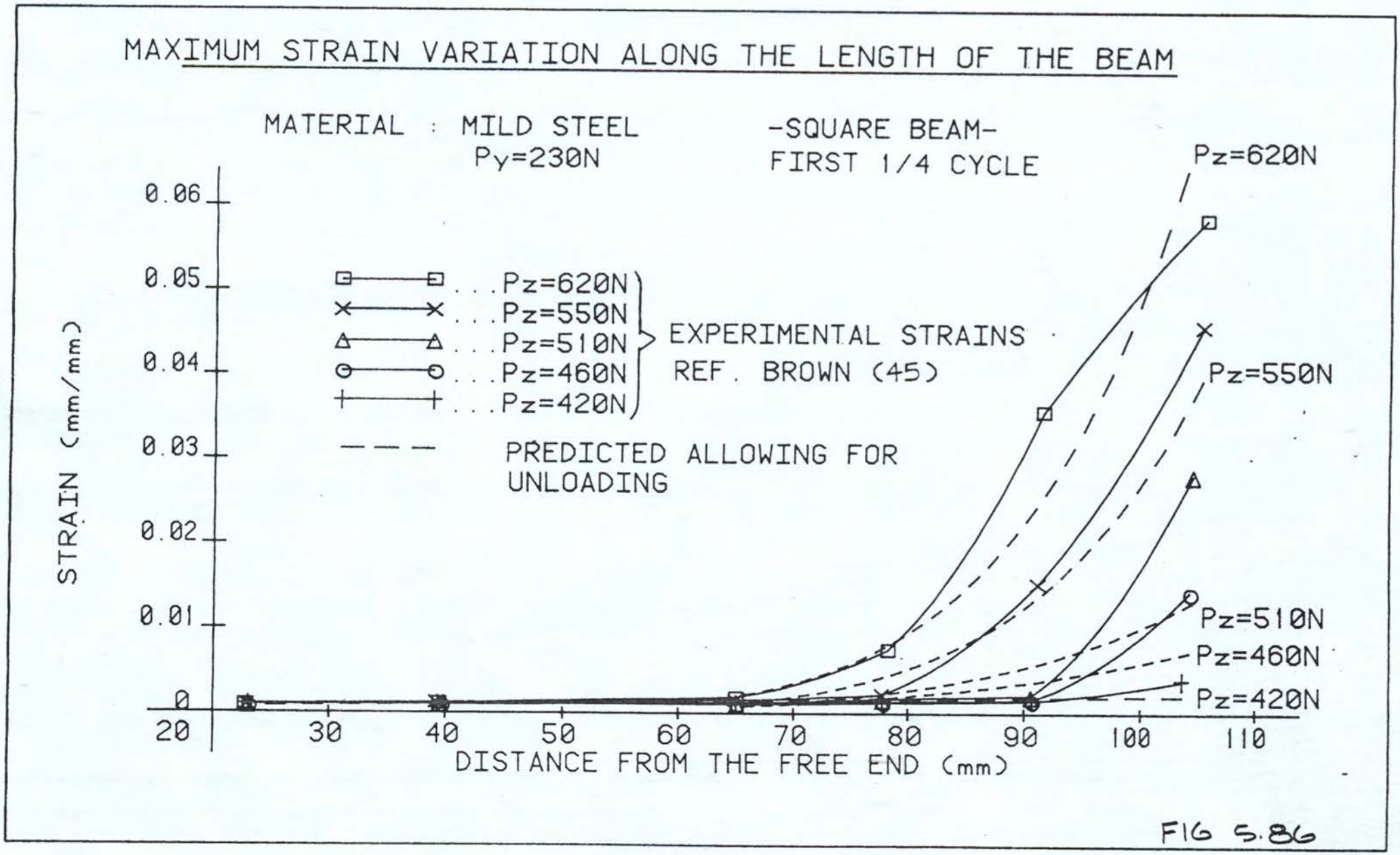
MAXIMUM STRAIN VARIATION ALONG THE LENGTH OF THE BEAM
MATERIAL : MILD STEEL
Py=230N
-SQUARE BEAM-
FIRST 1/4 CYCLE
Pz=620N
Pz=550N
Pz=510N
Pz=460N
Pz=420N
EXPERIMENTAL STRAINS
REF. BROWN (45)
PREDICTED ALLOWING FOR
UNLOADING
STRAIN (mm/mm)
0.06
0.05
0.04
0.03
0.02
0.01
0
20
30
40
50
60
70
80
90
100
110
DISTANCE FROM THE FREE END (mm)

FIG 5.86

5.4 GENERAL DISCUSSION

There are clearly problems in attempting to model material behaviour with a simple power law, particularly when the plastic strains are small and the elastic contribution cannot be neglected. A more complex mathematical description of the stress-strain curve could be developed but this would lead to computational problems and make the general problem less tractable. Clearly the discontinuity in the mild steel stress-strain curve creates particular difficulties and the results for this material in the first quarter cycle were not as good as those for the stainless steel. The lack of agreement between experimental and predicted load deflection characteristics could generally be explained by the errors in our modelling procedures. The more rounded and regular cyclic stress-strain curves could be modelled quite accurately with the simple power law and the predictions were accordingly better.

The lower yield point phenomenon of the mild steel caused particular difficulties. Generally in a tensile test Luders bands are developed progressively, starting at the most favourably orientated grains and the strain within the band is usually the full lower yield strain. There is the added problem of size effect, ie there is likely to be a higher yield point stress as the volume of stressed material is reduced, and this together with the fact that in bending there is a stress gradient which will affect the growth of the Luders band will obviously make analysis of the first quarter cycle difficult.

The lower yield point effect is a possible reason for the horizontal force-deflection relationship being displaced in the "forward" direction in the cyclic condition. This problem has been examined previously for cyclic push-pull tests for this type of material (47).

It has been shown that stress-strain curves are not always a good indication of material characteristics, such as anisotropy where a measure of the relative strains are often more revealing. The mode of vertical deflection in the first quarter cycle was not predictable, and although some perculiarities might have been expected for the mild steel, the results for the stainless steel were unexpected. However, there may be a plausible explanation for this behaviour. In determining the cycle stress-strain characteristics for this material the tests were always started in the tensile mode and it was assumed that the compressive characteristics would be the same. However, it has since been shown (4) that for this material the yield stress in compression was substantially lower in compression than tension and the material was therefore initially anisotropic.

The tensile and compression stress strain curves merged at higher strains and any initial differences were removed by the cyclic process. Now if we have a beam which has different properties in tension and compression then the neutral surface must be displaced towards the stronger side in order that equilibrium conditions are satisfied.

The outer fibre strain on the tensile side would be reduced and that on the compression side increased. The situation would be equivalent to applying a longitudinal compressive force to an isotropic beam and result in a shortening of the neutral surface. This compressive force would be reduced as the deformation proceeds and the tensile and compressive stresses approach one another, ie the neutral position. This may explain the observed behaviour of very little downward deflection during the early stages of deformation and then an accelerating rate afterwards.

However, the cyclic process itself appears to stabilise the material properties and this cyclic condition lends itself more readily to analysis.

In examining the distribution of strain along the beam we can see that the magnitude of the cyclic plastic strains are not large, and perhaps a more accurate mathematical model to describe the stress strain curve would have been justified even though it would have led to mathematical complexities and increased computational requirements. Also, the low level of cyclic strain developed may also account for some of the observed phenomenon. For example it is probably that for the mild steel that the strains within the Luders band was not the full yield point strain at the end of the first quarter cycle and this would lead to complications when the strain was reversed. Strain cycling within the lower yield point range has not generally been investigated, but the results obtained in bending would indicate that it may take several cycles before a stable condition is reached and a uniform hardening behaviour is observed.

The testing conditions were such that the cyclic strains were not dominant with respect to the "follow-up" vertical strains which can occur in some ratchetting problems.

The stainless steel was chosen because it was thought that its work hardening properties would result in different cyclic stress-strain characteristics compared with mild steel. It was an austenite-martensite transforming steel. The high toughness and ductility associated with this type of steel is attributed to a stress or strain induced transformation of metastable austenite to martensite with a resulting volume change. This volume change would be inhibited in bending due to the presence of adjacent non-transformed elastic material and would have resulted in residual stresses being developed. This would have led to a more searching test of the "finite element" approach adopted in this research. However, because of the low level of strain very little transformation occured, if any. In fact, there appears to be a cyclic strain range below which the transformation does not occur and the cyclic strain hardening which occurs is of the conventional type, ie by movement and reversal of dislocations.

It is therefore possible for the austenite-martensite transforming steels to quickly cycle to a steady state without much hardening and little transformation at low cyclic plastic strains. This in fact has been observed (54) for T347 stainless steel where a stable hysteresis loop was rapidly developed after a few cycles for strains up to 2%. At strains above this considerable and rapid hardening occurred with each cycle. Similar effects were observed by Daz (9).

Finally, although it was felt that there was little to gain from developing yield surfaces for this problem, some comments may be pertinent. Recent work has shown (4) that for many cyclic stable materials that kinematic hardening is an appropriate condition in push-pull testing. It would follow from this that if the moment curvature relationship can be developed from push-pull data that it also would show kinematic hardening. This would require experimental confirmation. It was shown that a kinematic model (53) was not appropriate for ratchetting problems because it predicted shakedown to zero ratchetting strain. However, this was based on the normality rule and the non-rotational translation of the yield surface. The fairly linear ratchetting strains observed experimentally would indicate that the stress or moment vector is touching the yield surface at one point, or not moving far over the surface. Therefore, whilst normality of the strain or curvature vector could be assumed because of the large amount of experimental confirmation of the normality rule, some further consideration should be given to the question of the movement of the yield surface and its possible rotation.

CONCLUSIONS AND RECOMMENDATIONS

CONCLUSIONS AND RECOMMENDATIONS FOR FURTHER WORK

CONCLUSIONS

1 The work has shown that accurate material data is a pre-requisite to any analysis of bending problems and that accurate mathematical modelling of this data is also essential.

2 The simplified curvature equation would be adequate for most plastic bending problems but solutions are possible using the full curvature relationships.

3 The work has identified specific problems relating to section symmetry and the position of the neutral surface for plastic bending. Alternative solutions have been proposed for rectangular beams which allow the inclination of the neutral surface to the plane of bending to be determined without recourse to lengthy mathematical procedures.

4 The general problem of bi-axial bending has been analysed and it has been shown that the more practically important condition of non-radial loading presents many more difficulties than that of radial loading. In particular the movement of the neutral surface is the most important in plastic bending since this causes individual elements to unload and re-load during a cycle of bending.

5 A direct mathematical solution to the problem is not possible and an iterative "finite element" method was developed which followed the hiearchy of loading of each individual element within the beam. This allowed material properties to be updated with each increment of strain and the position of the neutral surface to be located.

6 The cyclic material properties of the test materials were obtained, and it was shown that they could be modelled mathematically from the initial condition to the steady state condition and these properties were incorporated into the material database in the "finite element" computer program.

7 The characteristics of the cyclic stress-strain curves, with a small elastic component on stress reversal, leads to accurate modelling with relatively simple equations. To accurately model the initial material properties, with an extensive elastic region requires more complex equations which results in a major increase in computer programming and memory requirements. However it is shown that if the plastic strains are of elastic order then this procedure would be preferable to less accurate modelling because of the resulting poor correlation with experimental results.

8 The iterative methods developed can be extended to a wider range of problems. The results have shown that the maximum strains can be identified and predicted from cycle to cycle. This forms the basis for solving most high strain fatigue problems.

A knowledge of the maximum strains and a cumlative damage law would provide sufficient data for design. For the bending problem the extent of the plastic zone is shown to grow with cycles and although the maximum strain is reduced its location remains the same.

RECOMMENDATIONS FOR FURTHER WORK

1 It would be useful to examine materials which are less cyclically stable and continue to work harden with cycles. Although this may lead to shakedown for small strain ranges it would further test our ability to model the changing material properties.

2 Tests at much higher plastic strains for both cyclic stable and unstable materials would be useful to determine if the more accurate modelling of material behaviour at high strains gives satisfactory results.

3 Bi-axial stress systems should be examined to see if the same elemental fibre approach can be extended to a wider range of problems. If the position of the principal stresses and strains can be identified in a system then it might be possible to follow the history of loading of that element to determine the strains and cycles to failure.

APPENDICES

APPENDIX 1

SIMPLE PLASTIC BENDING

APPENDIX 1

SIMPLE PLASTIC BENDING

CIRCULAR BEAM - DEVELOPMENT OF AN ANALYTICAL SOLUTION

In Chapter Four some equations were given (equation 4.12, 4.13 and 4.14). In this Appendix derivation of these equations is presented.

Consider the beam cross-section. Subjected to some moment M and assumming proportional loading

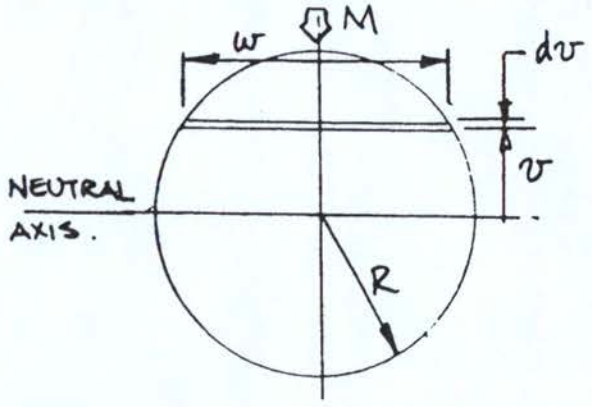

Strains at any distance 'v' away from neutral axis will be given by

$$\varepsilon = \frac{v}{R}\,\varepsilon_{max} \qquad - \quad A1.1$$

where ε_{max} is the maximum outer fibre strain at v = R

R is the radius of the beam.

Using the non linear stress-strain relationship $\sigma = \sigma_0 \varepsilon^n$ as previously defined in equation (4.6) and substituting for ε in equation A1.1 gives

$$\sigma = \sigma_0 \left(\frac{v}{R} \varepsilon_{max} \right)^n \qquad - \quad A1.2$$

For 'system' equilibrium the moment about the neutral surface must be zero. So equating the applied moment M with the internal moments, we have

$$M = 2 \int_0^R \sigma w \, v \, dv \qquad - \quad A1.3$$

substituting for σ from equation A1.2, gives

$$M = 2 \frac{\sigma_0 \varepsilon_{max}^n}{R^n} \int_0^R v^{n+1} \, w \, dv \qquad - \quad A1.4$$

from the diagram of the cross section it can be seen that

$$w = 2\sqrt{R^2 - v^2} \qquad - \quad A1.5$$

$$\text{therefore} \quad M = \frac{2\sigma\varepsilon_{max}^n}{R^n} \int_0^R v^{n+1} \, 2\sqrt{R^2 - v2} \, dv \qquad - \quad A1.6$$

Considering the integral part of A1.6

let $v = R\sin\alpha$

then $dv = R\cos\alpha \, d\alpha$

limits are when $v = R$ then $\alpha = \pi/2$

and when $v = 0$ then $\alpha = 0$

So $$\int_0^R v^{n+1} \, 2\sqrt{R^2 - v^2} \, dv = \int_0^{\pi/2} 2\sqrt{R^2 - R^2 \sin^2\alpha} \; R^{n+1} \sin^{n+1}\alpha \; R\cos\alpha \, d\alpha$$

$$= 2 \int_0^{\Pi/2} R^{n+3} \sin^{n+1}\alpha \cos^2\alpha \, d\alpha$$

$$= 2 R^{n+3} J$$

where $$J = \int_0^{\Pi/2} \cos^2\alpha \sin^{n+1}\alpha \, d\alpha$$ } A1.7 (Equation 4.14)

Replacing the integral part of equation A1.6 we have

$$M = 4\sigma_0 \varepsilon_{max}^{n} R^3 J \qquad - \quad A1.8$$

rearranging

$$\varepsilon_{max} = \left[\frac{M}{4\sigma_0 R^3 J} \right]^{1/n} \qquad - \quad A1.9$$

from equation (4.1) we have

$$\varepsilon = vk$$

at $\varepsilon = \varepsilon_{max}$ $v = R$

$$\varepsilon_{max} = RK$$

Substituting for εmax in equation A1.9 gives

$$K = \left[\frac{M}{4\sigma_0 R^{n+3} J} \right]^{1/n} \qquad - \quad A1.10$$

(Equation 4.14)

APPENDIX 2

"MOMENT"- COMPUTER PROGRAM LISTINGS

```
GO TO 100
REM SAVE "MOMENT"
CLOSE
OPEN "ESAVE";3,"U",A$
RUN 1010
INIT
DATA 0.005,0.007,0.009,0.013,0.018,0.02
DATA 12403,5920,3964,3256,2957,2634
DATA 0.6689,0.5545,0.4922,0.4674,0.4582,0.4361
DATA 50,75,95,105,110
DATA 0,1,2,3,3.5,4
GOSUB 4360
SET DEGREES
DIM A1(41)
DEF FNA(Esig)=Ssig0*Esig^Nn0
DEF FNB(Enew)=Ssig*Enew^Nn
DEF FNC(Esig)=-(172663*Esig-350)
DEF FND(Enew)=Sma*(Enew-Eadjust)/(Ec-Eadjust)
Msl=172000
Nu=6
Ssig0=3035
Nn0=0.4026
R0ads=5
A0ngle=10
R0adius=4
Ne=360/A0ngle*R0ads
PRINT "ENTER Py (STEADY LOAD) :";
INPUT Py
PRINT "ENTER Px (MAX VALUE FOR VARIABLE LOAD) :";
INPUT Pmax
Px=0
PRINT "ENTER Eplastic (Strain =H__ initial plastic deformation) :";
INPUT Eplastic
PAGE
Lths=5
REM INITIAL ESTIMATION OF E1
Ev=0
J=0
R0=0
FOR I=0 TO R0adius STEP R0adius/40
   J=J+1
   A1(J)=2*SQR(R0adius^2-I^2)*I^(Nn0+1)
NEXT I
FOR I=2 TO 40 STEP 2
   Ev=A1(I)+Ev
   IF I=40 THEN 530
   R0=A1(I+1)+R0
NEXT I
J1=R0adius/40/3*(A1(1)+A1(41)+4*Ev+2*R0)
REM CALCULATION OF ESTIMATED E1 SEE LATER
DIM A0rea(Ne),Emax(Ne),Start(Lths),S0(Nu),E0(Nu),N0(Nu),Z(Lths)
DIM Dx(Ne),Dy(Ne),R(R0ads+1),Esave(Lths),X0(2),A0(2,2),Y0(2)
DIM Alpa(Ne),Nrec(Ne),Emax1(Ne),Emax2(Ne),Nrec2(Ne),X(100),Y(100)
RESTORE 140
READ Z
RESTORE 110
READ E0,S0,N0
Start=1
```

```
0 X=0
0 Y=0
0 Emax=0
0 OPEN "ESAVE";3,"F",A$
0 I0=0
0 RESTORE 150
0 READ R
0 I0=0
0 FOR I=1 TO R0ads
0    Ae=PI*(R(I+1)^2-R(I)^2)*A0ngle/360
0    FOR J=0 TO 350 STEP A0ngle
0       I0=I0+1
0       A0rea(I0)=Ae
0    NEXT J
0 NEXT I
0 I0=0
0 FOR J=1 TO R0ads
0    FOR I=A0ngle/2 TO 360-A0ngle/2 STEP A0ngle
0       I0=I0+1
0       Alpa(I0)=I
0    NEXT I
0 NEXT J
0 DIM A1(2),M1(2)
0 GO TO 960
0 REM *********  UPDATE Px **********************
0 IF Px=0 THEN 950
0 T=ATN(Px/Py)+(ATN(Pmax/Py)-45)/6
0 Px=Py*TAN(T)
0 GO TO 990
0 Px=Py
0 REMcal
0 T=ATN(Px/Py)
0 PRINT @40:"J_J_J_        Mx          My          Mapp <---> Mcal   ";
00 PRINT @40:"    Strain      Z      OH_-=";INT(10*T)/10;"J_"
10 FOR K2=1 TO Lths
20    E1=R0adius*(Z(K2)*SQR(Px^2+Py^2)/(2*Ssig0*J1))^(1/Nn0)
30    T=ATN(Px/Py)
40    Eadjust=0
50    Ec=0
60    M1=0
70    A1=0
80    F=E1*0.5
90    Mapp=Z(K2)*SQR(Px^2+Py^2)
00    GOSUB Start(K2) OF 2710,2830
10    GOSUB 1390
20    GOSUB 1730
30    FOR I=1 TO Ne
40       Emax1(I)=Dy(I)*E1/R0adius
50    NEXT I
60    GOSUB Start(K2) OF 2750,2740
70    Mcal=0
80    Nrec2=Nrec
90    FOR I=1 TO Ne
00       GOSUB 1840
10       Mcal=S0tress*A0rea(I)*ABS(Dy(I))+Mcal
20    NEXT I
30    IF Mcal*1.0006=>Mapp AND Mcal*0.9994<=Mapp THEN 1260
40    GOSUB 3190
```

```
50 GO TO 1130
60 GOSUB 3560
70 PRINT @40: USING 1380:Px*Z(K2),Py*Z(K2),Mapp,Mcal,E1,Z(K2)
80 PRINT @40:"J_"
90 Esave(K2)=E1
00 GOSUB 2540
10 NEXT K2
20 WRITE #3:Esave,Px,Py
30 IF Px+1=>Pmax THEN 1350
40 GO TO 880
50 CLOSE
60 GO TO 3350
70 END
80 IMAGE 6D.3D,2X,6D.3D,2X,6D.3D,2X,6D.3D,2X,1D.6D,2X,3D.1D
90 REM*************** DRAW BEAM ********************
00 IF K0=7 THEN 1440
10 VIEWPORT 20,110,5,95
20 IF I$="A" THEN 1470
30 GO TO 1450
40 VIEWPORT 10,90,0,75
50 PRINT "^_HIT RETURN TO PROCEEDG_G_ ";
60 INPUT I$
70 PAGE
80 WINDOW -R0adius*1.3,R0adius*1.3,-R0adius*1.3,R0adius*1.3
90 MOVE @K0:-R0adius*1.2,R0adius*1.2
00 PRINT @K0:"THETA = ";INT(T*10)/10
10 MOVE @K0:-R0adius*1.2,R0adius*1.2
20 PRINT @K0:"J_";
30 PRINT @K0:"    Z = ";Z(K2)
40 MOVE @K0:0,R0adius
50 FOR L=0 TO 360
60    DRAW @K0:R0adius*SIN(L),R0adius*COS(L)
70 NEXT L
80 MOVE @K0:0,1.05*R0adius
90 DRAW @K0:0,-1.05*R0adius
00 MOVE @K0:-1.05*R0adius,0
10 DRAW @K0:1.05*R0adius,0
20 MOVE @K0:1.05*R0adius*SIN(T-90),1.05*R0adius*COS(T-90)
30 DRAW @K0:-1.05*R0adius*SIN(T-90),-1.05*R0adius*COS(T-90)
40 MOVE @K0:R0adius*SIN(T),R0adius*COS(T)
50 DRAW @K0:1.3*R0adius*SIN(T),1.3*R0adius*COS(T)
60 RMOVE @K0:-0.08*R0adius,0.08*R0adius
70 PRINT @K0:"Mapp"
80 MOVE @K0:R0adius*SIN(T),R0adius*COS(T)
90 DRAW @K0:1.1*R0adius*SIN(T+2),1.1*R0adius*COS(T+2)
00 MOVE @K0:R0adius*SIN(T),R0adius*COS(T)
10 DRAW @K0:1.1*R0adius*SIN(T-2),1.1*R0adius*COS(T-2)
20 RETURN
30 REM ***** CALCULATIONS OF NEW X AND Y *******
40 I=0
50 FOR J=1 TO R0ads
60    Rm=(R(J)+R(J+1))/2
70    FOR I0=A0ngle/2 TO 360-A0ngle/2 STEP A0ngle
80       I=I+1
90       Dx(I)=Rm*COS(Alpa(I)+T)
00       Dy(I)=Rm*SIN(Alpa(I)+T)
10    NEXT I0
20 NEXT J
30 RETURN
```

```
1940 REM ********  STRESS CALCULATION ************
1950 GOSUB Nrec2(I) OF 1880,1980,2020,2070,2110,2160
1960 GOSUB Nrec2(I) OF 2260,2290,2330,2370,2410,2260
1970 RETURN
1980 IF Emax2(I)<=Emax1(I) THEN 1970
1990 Ec=Emax(I) MAX ABS(Emax1(I))
2000 IF Emax2(I)<Eplastic AND SGN(Emax1(I))<>SGN(Emax2(I)) THEN 1960
2010 IF Ec<Eplastic AND Emax1(I)<0 THEN 1960
2020 IF Ec>Eplastic THEN 1940
2030 GO TO 1970
2040 Nrec2(I)=2
2050 GO TO 1980
2060 Nrec2(I)=6
2070 RETURN
2080 GOSUB 2460
2090 IF Emax1(I)=>Eadjust THEN 2010
2100 Nrec2(I)=3
2110 RETURN
2120 GOSUB 2460
2130 IF Eadjust-Emax2(I)>Eadjust-Emax1(I) THEN 2050
2140 RETURN
2150 Nrec2(I)=4
2160 GO TO 2080
2170 GOSUB 2460
2180 IF Emax1(I)<=-Eadjust THEN 2100
2190 Nrec2(I)=5
2100 RETURN
2110 GOSUB 2460
2120 IF Emax2(I)<=Emax1(I) THEN 2150
2130 Nrec2(I)=2
2140 GO TO 1990
2150 RETURN
2160 IF Emax1(I)<=Emax2(I) THEN 2210
2170 Ec=Emax(I) MAX ABS(Emax1(I))
2180 IF ABS(Emax2(I))<Eplastic AND SGN(Emax1(I))<>SGN(Emax2(I)) THEN
     2240
2190 IF Ec>Eplastic THEN 2220
2200 IF Ec<Eplastic AND Emax1(I)>0 THEN 2240
2210 RETURN
2220 Nrec2(I)=4
2230 GO TO 2070
2240 Nrec2(I)=1
2250 RETURN
2260 Enew=ABS(Emax1(I))
2270 Stress=FNA(Enew)
2280 RETURN
2290 REM Ci=FNC(Eadjust+Ec)
2300 REM Enew=Eadjust+Emax1(I)
2310 Stress=FND(Emax1(I))
2320 RETURN
2330 Enew=Eadjust-Emax1(I)
2340 GOSUB 2920
2350 Stress=FNB(Enew)
2360 RETURN
2370 REM Ci=FNC(Eadjust+Ec)
2380 REM Enew=Eadjust-Emax1(I)
2390 Stress=FND(Emax(I))
2400 RETURN
2410 Enew=Eadjust+Emax1(I)
```

```
20 GOSUB 2920
30 Stress=FNB(Enew)
40 REM
50 RETURN
60 REM******   CALCULATION OF Eadjust *******
70 IF Nrec2(I)<>Nrec(I) THEN 2500
80 Ec=Emax(I)
90 GO TO 2510
00 Ec=Emax(I) MAX ABS(Emax1(I))
10 Sma=FNA(Ec)
20 Eadjust=Ec-Sma/Msl
30 RETURN
40 REM ******  SUB UPDATE   ********
50 U$=STR(K2)
60 L=LEN(U$)
70 U$=SEG(U$,2,L)
80 U$="ELELMENT"&U$
90 OPEN U$;1,"F",A$
00 REM***************SAVE DATA FOR THIS ITERATION
10 Emax2=Emax1
20 FOR I=1 TO Ne
30    IF Nrec2(I)=1 OR Nrec2(I)=6 THEN 2660
40    IF Nrec2(I)<>Nrec(I) THEN 2660
50    GO TO 2670
60    Emax(I)=Emax(I) MAX ABS(Emax1(I))
70 NEXT I
80 WRITE #1:E1,Emax,Emax1,Nrec2
90 CLOSE 1
00 RETURN
10 REM  ************  SET INITIAL VARIABLES **********
20 Emax2=0
30 Emax=0
40 RETURN
50 REM ************* SET INITIAL RECORDS*****
60 Start(K2)=2
70 Nrec=1
80 FOR L=1 TO Ne
90    IF SGN(Emax1(L))=1 THEN 2810
00    Nrec(L)=6
10 NEXT L
20 RETURN
30 REM************** READ DATA LAST ITERATION
40 U$=STR(K2)
50 L=LEN(U$)
60 U$=SEG(U$,2,L)
70 U$="ELELMENT"&U$
80 OPEN U$;1,"R",A$
90 READ #1:Ev,Emax,Emax2,Nrec
00 CLOSE 1
10 RETURN
20 REM *********** CALCULATION OF CONSTANTS FOR CYCLIC CURVES
30 Esig=Ec+Eadjust
40 IF Esig<E0(1) THEN 2990
50 IF Esig>E0(Nu) THEN 3010
60 FOR L=1 TO Nu
70    IF Esig=>E0(L) AND Esig<=E0(L+1) THEN 3020
80 NEXT L
90 L=1
00 GO TO 3020
```

```
10 L=Nu-1
20 A0=1
30 A0(1,1)=E0(L)
40 A0(2,1)=E0(L+1)
50 Y0(1)=S0(L)
60 Y0(2)=S0(L+1)
70 A0=INV(A0)
80 X0=A0 MPY Y0
90 Ssig=X0(1)*Esig+X0(2)
00 A0=1
10 A0(1,1)=E0(L)
20 A0(2,1)=E0(L+1)
30 Y0(1)=N0(L)
40 Y0(2)=N0(L+1)
50 A0=INV(A0)
60 X0=A0 MPY Y0
70 Nn=X0(1)*Esig+X0(2)
80 RETURN
90 REMcal ************ INCREMENT OF E1 ****************
00 M1(2)=Mcal
10 A1(2)=E1
20 IF Mapp-M1(1)<0 AND Mapp-Mcal<0 THEN 3260
30 IF Mapp-M1(1)>0 AND Mapp-Mcal>0 THEN 3280
40 IF Mapp-M1(1)>0 AND Mapp-Mcal<0 THEN 3320
50 IF Mapp-M1(1)<0 AND Mapp-Mcal>0 THEN 3320
60 E1=E1-F
70 GO TO 3290
80 E1=E1+F
90 A1(1)=A1(2)
00 M1(1)=M1(2)
10 RETURN
20 E1=A1(1)-(Mapp-M1(1))*((A1(2)-A1(1))/(Mapp-M1(2)-(Mapp-M1(1))))
30 F=ABS(A1(1)-A1(2))/5
40 RETURN
50 REM ************** CONVERT STRAIN TO DEFLECTIONS *********
60 OPEN "ESAVE";2,"R",A$
70 ON EOF (2) THEN 3510
80 J=0
90 READ #2:Esave,Px,Py
00 T=ATN(Px/Py)
10 J=J+1
20 FOR I=1 TO Lths
30    IF I=1 THEN 3460
40    Dz=Dz+(Esave(I)+Esave(I-1))*(Z(I)-Z(I-1))^2/2/R0adius
50    GO TO 3470
60    Dz=Esave(I)*Z(I)^2/2/R0adius
70 NEXT I
80 X(J)=Dz*SIN(T)
90 Y(J)=Dz*COS(T)
00 GO TO 3390
10 CLOSE
20 OPEN "XYDEF";2,"F",A$
30 WRITE #2:X,Y
40 CLOSE
50 END
60 REM ***********  KEY ********************
70 T=0
80 GOSUB 1730
```

```
90 FOR I=1 TO Ne
00     W1=-R0adius*2.1
10     W2=R0adius*2.1
20     W3=W1*1.1
30     W4=W2*1.1
40     Ec=Emax(I) MAX ABS(Emax1(I))
50     IF Ec=>Eplastic THEN 3680
60     IF Nrec(I)=Nrec2(I) AND Ec<Eplastic THEN 3870
70     GO TO 3870
80     GOSUB 3890
90     IF Nrec(I)=1 AND Nrec2(I)=6 THEN 4000
00     IF Nrec(I)=6 AND Nrec2(I)=1 THEN 4020
10     IF Nrec(I)=1 AND Nrec2(I)=1 THEN 4040
20     IF Nrec(I)=6 AND Nrec2(I)=6 THEN 4060
30     IF Nrec(I)=2 AND Nrec2(I)=2 THEN 4080
40     IF Nrec(I)=3 AND Nrec2(I)=3 THEN 4100
50     IF Nrec(I)=4 AND Nrec2(I)=4 THEN 4120
60     IF Nrec(I)=5 AND Nrec2(I)=5 THEN 4140
70     IF Nrec(I)=1 AND Nrec2(I)=2 THEN 4160
80     IF Nrec(I)=1 AND Nrec2(I)=3 THEN 4180
90     IF Nrec(I)=6 AND Nrec2(I)=4 THEN 4200
00     IF Nrec(I)=2 AND Nrec2(I)=3 THEN 4220
10     IF Nrec(I)=6 AND Nrec2(I)=5 THEN 4240
20     IF Nrec(I)=3 AND Nrec2(I)=4 THEN 4260
30     IF Nrec(I)=3 AND Nrec2(I)=5 THEN 4280
40     IF Nrec(I)=4 AND Nrec2(I)=5 THEN 4300
50     IF Nrec(I)=5 AND Nrec2(I)=2 THEN 4320
60     IF Nrec(I)=5 AND Nrec2(I)=3 THEN 4340
70 NEXT I
80 RETURN
90 REM ********************SQUARE************************
00 MOVE @K0:Dx(I),Dy(I)
10 RMOVE @K0:-0.0067*(W2-W1),-0.01*(W4-W3)
20 RDRAW @K0:0.0067*2*(W2-W1),0
30 RDRAW @K0:0,0.02*(W4-W3)
40 RDRAW @K0:-0.0067*2*(W2-W1),0
50 RDRAW @K0:0,-0.02*(W4-W3)
60 MOVE @K0:Dx(I),Dy(I)
70 RMOVE @K0:-0.0035*(W2-W1),-0.007*(W4-W3)
80 PRINT @7,17:1.5,2.5
90 RETURN
00 PRINT @K0:"H"
10 GO TO 3870
20 PRINT @K0:"I"
30 GO TO 3870
40 PRINT @K0:"A"
50 GO TO 3870
60 PRINT @K0:"F"
70 GO TO 3870
80 PRINT @K0:"B"
90 GO TO 3870
00 PRINT @K0:"C"
10 GO TO 3870
20 PRINT @K0:"D"
30 GO TO 3870
40 PRINT @K0:"E"
50 GO TO 3870
60 PRINT @K0:"J"
```

```
70 GO TO 3870
80 PRINT @K0:"K"
90 GO TO 3870
00 PRINT @K0:"L"
10 GO TO 3870
20 PRINT @K0:"W"
30 GO TO 3870
40 PRINT @K0:"M"
50 GO TO 3870
60 PRINT @K0:"N"
70 GO TO 3870
80 PRINT @K0:"P"
90 GO TO 3870
00 PRINT @K0:"X"
10 GO TO 3870
20 PRINT @K0:"R"
30 GO TO 3870
40 PRINT @K0:"S"
50 GO TO 3870
60 PRINT "L_Plotter , Screen OR Auto-page G_G_:";
70 INPUT I$
80 IF I$="P" THEN 4430
90 IF I$="A" THEN 4410
00 IF I$<>"S" THEN 4360
10 K0=32
20 GO TO 4440
30 K0=7
40 REM
50 RETURN
```

APPENDIX 3

"CONTROL" - COMPUTER PROGRAM LISTINGS

```
10 POKE 59459,255
20 POKE 59471,255
25 DIM A(1000,3),OU(3),IV(3),RE(6)
30 SS=0
100 REM INPUT ROUTINE
105 PRINT"ENTER DATA FILE NUMBER STDATA?"
106 INPUT D$
107 D$="STDATA"+D$
108 PRINT D$
109 PRINT"ENTER C TO CONTINUE":INPUT X$:IF X$<>"C"THEN 109
110 PRINT"■■NUMBER OF CYCLES";
115 INPUT KK
120 PRINT"■WHAT IS THE DISPLACEMENT LIMIT IN M.M."
125 PRINT"LIMIT ?";:INPUT DI
126 DI=DI/3.3684:DJ=-DI
130 FOR S=0 TO 6
135 PRINT"■■NUMBER OF READ POINTS IN ELEMENT"S;:INPUT RE(S)
140 NEXT S
200 GOSUB 500
225 GOSUB 600
300 FOR J=1 TO KK
310 FOR I=1 TO 6
315 PRINT "ELEMENT NUMBER"I
320 ON I GOTO 330,340,350,360,370,380
330 REM EL.1
331 K=2
332 GOSUB 1250
333 GOSUB 800
335 GOTO 400
340 REM EL.2
341 K=1
343 GOSUB 800
345 GOTO 400
350 REM EL.3
351 K=1
353 GOSUB 1000
355 GOTO 400
360 REM EL.4
361 K=2
362 GOSUB  1250
363 GOSUB 850
365 GOTO 400
370 REM EL.5
371 K=1
373 GOSUB 850
375 GOTO 400
380 REM EL.6
381 K=1
383 GOSUB 900
385 GOTO 400
400 NEXT I
410 NEXT J
420 POKE 59471,255
425 GOSUB 1500
430 GOSUB 1400
450 PRINT"FIN."
460 STOP
```

```
500 REM CALCULATE THE OFFSETS
505 PRINT"FINDING OFFSETS"
510 Y=PEEK(59471) AND 192
512 Y=Y+63
515 FOR P=0 TO 2
520 POKE 59471,Y
530 POKE 59471,Y-21^P
550 OPEN1,12
555 PRINT#1,"ZF1R5"
560 INPUT#1,H:IF ST=2 GOTO 560
565 IV(P+1)=H
570 CLOSE 1
575 NEXT P
580 POKE 59471,Y
585 PRINT"VALUES ARE"
586 PRINT"TRAN 1="IV(1)
587 PRINT"TRAN 2="IV(2)
588 PRINT"TRAN 3="IV(3)
590 PRINT"ENTER GO";:INPUT G$
592 IF G$<>"GO" GOTO 500
595 RETURN
600 REM CONTROL FOR EL.0
605 PRINT"■■■■■ELEMENT ZERO"
610 GOSUB 1200
615 GOSUB 1250
620 GOSUB 1100
622 PRINT"CHECKING TO SEE IF LIMIT +VE"
623 PRINT"■LIMIT="OU(1)
625 IF OU(1)<(-DI/100) GOTO 638
630 IF OU(1)<(DI/100) GOTO 620
633 GOSUB 1300
635 GOTO 660
638 GOSUB 1240
640 PRINT"■■■■■■■■■■■■■■■■ERROR"
642 PRINT"■■MOTOR DIRECTION INCORRECT"
645 PRINT"■■CHANGE THE CONNECTIONS"
648 PRINT"IF READY TYPE Y"
650 INPUT S$
652 IF S$<>"Y" GOTO 645
655 GOTO 610
660 IT=0
662 SL=DI/RE(0)
665 IT=IT+SL
668 GOSUB 1100
670 IF OU(1)>=DI GOTO 690
673 IF OU(1)<IT GOTO 668
675 GOSUB 1300
678 GOTO 665
690 GOSUB 1240
692 GOSUB 1100
694 GOSUB 1300
695 GOSUB 1220
696 GOSUB 1100
697 GOSUB 1300
698 GOSUB 1100
699 GOSUB 1300
700 RETURN
800 REM CONTROL FOR EL. 1&2
```

```
810 SL=OU(K)/RE(I)
815 IT=OU(K)
820 GOSUB 1100
825 IF OU(K)>=(IT-SL) GOTO 820
830 GOSUB 1300
835 IF OU(K)<= 0 THEN RETURN
840 IT=OU(K)
845 GOTO 820
850 REM CONTROL FOR EL. 4&5
860 SL=OU(K)/RE(I)
865 IT=OU(K)
870 GOSUB 1100
875 IF OU(K)<=(IT-SL) GOTO 870
880 GOSUB 1300
885 IF OU(K)>= 0 THEN RETURN
890 IT=OU(K)
895 GOTO 870
900 REM CONTROL FOR EL.6
910 SL=DI/RE(I)
915 IT=OU(K)+SL
920 GOSUB 1100
925 IF OU(K)>=DI GOTO 950
930 IF OU(K)<=IT GOTO 920
935 GOSUB 1300
940 IT=OU(K)+SL
945 GOTO 920
950 GOSUB 1240
955 GOSUB 1100
960 GOSUB 1300
965 GOSUB 1220
970 GOSUB 1100
975 GOSUB 1300
980 GOSUB 1100
985 GOSUB 1300
990 RETURN
1000 REM CONTROL FOR EL.3
1010 SL=DJ/RE(I)
1015 IT=OU(K)+SL
1020 GOSUB 1100
1025 IF OU(K)<= DJ GOTO 1050
1030 IF OU(K)>=IT GOTO 1020
1035 GOSUB 1300
1040 IT=OU(K)+SL
1045 GOTO 1020
1050 GOSUB 1240
1055 GOSUB 1100
1060 GOSUB 1300
1065 GOSUB 1200
1070 GOSUB 1100
1075 GOSUB 1300
1080 GOSUB 1100
1085 GOSUB 1300
1090 RETURN
1100 REM READ SUB.
1120 Y=PEEK(59471) AND 192
1122 Y=Y+63
1125 FOR P=0 TO 2
1135 POKE 59471,Y-21P
```

```
1150 OPEN 1,12
1155 PRINT#1,"ZI1F1R5"
1160 INPUT#1,H:IF ST=2 THEN 1160
1170 OU(P+1)=H-IV(P+1)
1180 CLOSE 1
1185 NEXT P
1187 POKE 59471,Y
1190 RETURN
1200 REM FORWARD
1205 F=PEEK(59471) AND 191
1210 POKE 59471,F
1215 RETURN
1220 REM REVERSE
1225 F=PEEK(59471) AND 191
1230 POKE 59471,(F+64)
1235 RETURN
1240 REM STOP
1245 F=PEEK(59471) AND 127
1246 POKE 59471,(F+128)
1248 RETURN
1250 REM START
1252 F=PEEK(59471) AND 127
1254 POKE 59471,F
1258 RETURN
1300 REM STORE SUBROUTINE
1305 SS=SS+1
1310 FOR ZZ=1TO 3
1315 A(SS,ZZ)=OU(ZZ)
1320 NEXT ZZ
1350 RETURN
1400 H=0
1405 FOR F=1TO 3
1410 PRINT"TRAN"F"="A(H,F)
1415 NEXT F
1420 PRINT"ENTER  N";:INPUTN$:IF N$<>"N"GOTO1430
1425 H=H+1:GOTO 1405
1430 RETURN
1500 DOPEN#1,(D$),W
1505 FOR I=1TOSS
1510 FOR J=1TO3
1520 A$=STR$(A(I,J))
1530 PRINT#1,A$
1535 NEXT J
1540 NEXT I
1550 DCLOSE#1
1560 RETURN
```

REFERENCES

REFERENCES

1 HILL, R

"The Mathematical Theory of Plasticity" Oxford University Press (1950)

2 PHILLIPS, A

"Journal of Applied Mechanics" 18 (1951) p 353

3 TIMIOSHENKO, S

"Strength of Materials Part II" p 277 3rd Edition Van Nostrand

4 ADKIN, P

"PhD Thesis - to be submitted Coventry (Lanchester) Polytechnic (1986)

5 MENDLESON, A

"Plasticity" Macmillan, New York

6 COZZONE, F P

"Journal of Aeronautical Sciences" 14 (1947) p 422

7 PHILLIPS, A

"Introduction to Plasticity" Ronald, New York (1956)

8 JOHNSON W AND MELLOR, P B

"Engineering Plasticity" Von Nostrand Reinhold Company Ltd (1973)

REFERENCES CONTINUED

9 DAS, P K

"The Plastic Bending of Beams and the Effect of Strain Concentration on their Failure by High Strain Fatigue" PhD Thesis, Rugby College of Engineering Technology (1968)

10 LIN TH, ITO, M

"Theoretical Plastic Stree-Strain Relationships of a Polycrystal and the Comparison with the Von Mises and Tresca Plasticity Theories" Int Journal Engineering Sciences Vol 4 (1966)

11 PAUL, B

" Microscopic Criteria for Plastic Flow and Brittle Fracture" Fracture Vol II Ed Liebowitz, H (1968)

12 PRAGER, W and HODGE, P G

"Theory of Perfectly Plastic Solids" John Wiley, London (1951)

13 MANSON, S S

"Thermal Stress and Low-Cycle Fatigue" McGraw-Hill Book Company (1966)

14 GREEN, A P

" The Plastic Yielding of Notched Bars Due to Bending" Quart. & Mech 6 223 (1953)

REFERENCES CONTINUED

15 MILLER, K J

"Fatigue Under Multiaxial Stress-Strain Conditions" Sheffield University (1982)

16 ZYCZKOWSKI, M

"Combined Loading in the Theory of Plasticity" PWN - Polish Scientific Publishers (1981)

17 NEAL, B G

"The Plastic Method of Structural Analysis" Chapman and Hall London (1956)

18 HEYMAN, J

"Plastic Design of Frames" Parts I and II Cambridge University Press (1969)

19 BARRETT, A J

"Unsymmetrical Bending and Bending Combined with Axial Loading of a Beam with Rectangular Cross Section into the Plastic Range" Journal of the Royal Aeronautical Society Vol 57 1953 p 503

20 BROWN, E A

"Plastic Asymmetrical Bending of Beams" International Journal of Mechanical Sciences Vol 9 pp 77 - 82 (1967)

21 HARRISON, H B

"The Plastic Behaviour of Mild Steel Beam of Rectangular Section Bent about both Principal Axis" Struct Engr; Vol 41 p 231 (1963).

22 BROOKS, D S

"The Elastic-Plastic Behaviour Rectangular Section Carrying Biaxial Bending" Civil Engineering Transactions, The Institution of Engineers Australia (1964).

23 HEYMAN, J

"The Simple Plastic Bending of Beams", Proc Inst Civil Engineers Vol 41 p 757 - 759 (1968).

24 WEIL, N A and RAPASKY, F S

"Experience with Vessels of Delayed Coking Units" American Petroleun Institute Los Angles, California (1958).

25 COFFIN, L F

"The Resistance of Material to Cyclic Strain" Paper No 57 ASME Meeting A286 (1959).

26 MORETON, D N and MOFFAT, D G

"Shakedown of Three Stainless Steel Pressure Vessel Components" 3rd Int Conf on P V Technology Tokoyo (1971).

27 NEAL, B G

"The Plastic Method of Structural Analysis" 3rd Edition Chapman and Hall (1977).

28 LECKIE, F A

"Limit and Shakedown Loads in the Creep Range" Procedings of the International Conference, Berkly Castle, England, (1969) Ed D J Little.

29 PARKS, W

"Wings under Repeated Thermal Stresses" Aircraft Engineering Vol 26 (1954).

30 EDMOUNDS and BEER

"Notes on Incremental Collapse in Pressure Vessels" Journal of Mechanical Engrs Sciences Vol 3 (1961).

31 BREE, J

"Elastic-Plastic Behaviour of Thin Tubes Subjected to Internal Pressure and Intermittent High Heat Fluxes with Application to Fast Nuclear Reactor Fuel Elements" Journal of Strain Analysis (Vol 1, 2, 3) (1967).

32 MANSON, S S, HALFORD, G R and HIRSCHBERG, M H

"Creep-Fatigue Analysis by Strain Range Partitioning" ASME 1st Nat Press Vessel and Piping Conference.

REFERENCES CONTINUED

33 COFFIN, L F

"A review of Predictive Methods in the Regime where Inelastic Strains Dominate" Methods for Predicting Material Life in Fatigue ASME Meeting 1979.

34 LIANIS, G and FORD, H

"The yielding of Notched Bars due to Bending" 9th Int. Congress of Applied Mechanics (1957).

35 ROYALS, R

"Fatigue of Ductile Structures in Reverse Bending" PhD Thesis Cambridge University (1964).

36 ROYALS, R

"Low Cycle Endurance Behaviour of Mild Steel Beams in Reversed Bending" Journal of Strain Analysis Vol 1 No 3 (1966).

37 TOPPER, T H

"Cyclic Plastic Loading of Mild Steel" PhD Thesis Cambridge University (1962).

38 KRISHNASAMY, S, SHERBOURNE, A N and KHURANA, K K

"Deflection of Mild Steel Beams under Symmetrical Loads" 1972 SESA Spring Meeting, Cleveland, Ohio

39 PLAKOWSKI, N H and PALCHOUDHURI, A

"Softening of Certain Cold Worked Materials Under the Action of Fatigue Loads" Proc. of ASTM Vol 54 (1954).

40 DUGDALE, D S

"Stress-Strain Cycles of Large Amplitude" Journal of Mechanical and Physical Solids Vol 7 No 2 (1959).

41 MROZ, A

"An Attempt to Describe the Behaviour of Metals under Cyclic Using a More General Work Hardening Model" ACTA Mechanics Vol 7 (1967).

42 DAFALIAS, Y and POPOV, E

"A Model of Non-Linear Hardening Materials" ACTA Mechanics 21, (1975).

43 SIDEBOTTOM, O M and CHAN, C T

"Influence of Bauschinger Effect on Inelastic Bending of Beams" Proceding of the 1st U S National Congress of Applied Mechanics (1951).

44 PRAGER, W

"An Introduction to Plasticity" Addison Wesley Publication Ltd (1959).

45 BROWN, G A

"Bi-Plannar Bending" BSc - Final Year Project Report (1971) - Coventry (Lanchester) Polytechnic.

46 TOOR, A

"Graphplot - General Purpose Graph Plotting Program" Coventry (Lanchester) Polytechnic.

47 TAKADA, I and SUGIE, E

"Effect of Cyclic Straining on the Stress-Strain Behaviour of Line Pipe Steel" Tranactions ISIJ Vol 16 19766.

48 TILLEY, G P

"Strain and Rupture Behaviour Under High Stress Reversals" Jr of Strain Analysis Vol 2 No 3 (1967).

49 FRISCH-FAY, R

"Flexible Bars" Butterworth (1962).

50 RAMBERG, W and OSGOOD, W R

"Stress Strain Curves by Three Parameters" NACA Technical Note No 902 (National Advisory Committee on Aeronautics) (1943).

51 BAKER, J F and HORNE, M R and HEYMAN, J

"Plastic Behaviour and Design" The STeel Skeleton Vol 2 Cambridge (1956).

52 TUCKER, L E

"A Procedure for Designing Against Fatigue Failure of Notached Bars" SAE Paper No 720265 (1972).

53 HANCELL, P J and HARVEY, S J

"The Use of Kinematic Hardening Models in Multi-axial Cyclic Plasticity" Fatigue of Engineering Materials and Structures Vol 1 p 271 - 279 (1979).

54 COFFIN L F AND TAVERNELLI J F

"The Cyclic Straining and Fatigue of Metals". Trans.Met.Soc of AIME Vol 215 p794 - 807 (1959).